THE UNIVERSITY OF WARWICK

Library Declaration and Deposit Agreement

1. STUDENT DETAILS

Please complete the following:

Full name: ……

University ID number: ……

2. THESIS DEPOSIT

2.1 I understand that under my registration at the University, I am required to deposit my thesis with the University in BOTH hard copy and in digital format. The digital version should normally be saved as a single pdf file.

2.2 The hard copy will be housed in the University Library. The digital version will be deposited in the University's Institutional Repository (WRAP). Unless otherwise indicated (see 2.3 below) this will be made openly accessible on the Internet and will be supplied to the British Library to be made available online via its Electronic Theses Online Service (EThOS) service.
[At present, theses submitted for a Master's degree by Research (MA, MSc, LLM, MS or MMedSci) are not being deposited in WRAP and not being made available via EthOS. This may change in future.]

2.3 In exceptional circumstances, the Chair of the Board of Graduate Studies may grant permission for an embargo to be placed on public access to the hard copy thesis for a limited period. It is also possible to apply separately for an embargo on the digital version. (Further information is available in the *Guide to Examinations for Higher Degrees by Research*.)

2.4 *If you are depositing a thesis for a Master's degree by Research, please complete section (a) below. For all other research degrees, please complete both sections (a) and (b) below:*

(a) Hard Copy

I hereby deposit a hard copy of my thesis in the University Library to be made publicly available to readers (please delete as appropriate) EITHER immediately OR after an embargo period of ……..... months/years as agreed by the Chair of the Board of Graduate Studies.

I agree that my thesis may be photocopied. YES / NO (*Please delete as appropriate*)

(b) Digital Copy

I hereby deposit a digital copy of my thesis to be held in WRAP and made available via EThOS.

Please choose one of the following options:

EITHER My thesis can be made publicly available online. YES / NO (*Please delete as appropriate*)

OR My thesis can be made publicly available only after…..[date] (Please give date)
YES / NO (*Please delete as appropriate*)

OR My full thesis cannot be made publicly available online but I am submitting a separately identified additional, abridged version that can be made available online.
YES / NO (*Please delete as appropriate*)

OR My thesis cannot be made publicly available online. YES / NO (*Please delete as appropriate*)

3. GRANTING OF NON-EXCLUSIVE RIGHTS

Whether I deposit my Work personally or through an assistant or other agent, I agree to the following:

Rights granted to the University of Warwick and the British Library and the user of the thesis through this agreement are non-exclusive. I retain all rights in the thesis in its present version or future versions. I agree that the institutional repository administrators and the British Library or their agents may, without changing content, digitise and migrate the thesis to any medium or format for the purpose of future preservation and accessibility.

4. DECLARATIONS

(a) I DECLARE THAT:

- I am the author and owner of the copyright in the thesis and/or I have the authority of the authors and owners of the copyright in the thesis to make this agreement. Reproduction of any part of this thesis for teaching or in academic or other forms of publication is subject to the normal limitations on the use of copyrighted materials and to the proper and full acknowledgement of its source.

- The digital version of the thesis I am supplying is the same version as the final, hard-bound copy submitted in completion of my degree, once any minor corrections have been completed.

- I have exercised reasonable care to ensure that the thesis is original, and does not to the best of my knowledge break any UK law or other Intellectual Property Right, or contain any confidential material.

- I understand that, through the medium of the Internet, files will be available to automated agents, and may be searched and copied by, for example, text mining and plagiarism detection software.

(b) IF I HAVE AGREED (in Section 2 above) TO MAKE MY THESIS PUBLICLY AVAILABLE DIGITALLY, I ALSO DECLARE THAT:

- I grant the University of Warwick and the British Library a licence to make available on the Internet the thesis in digitised format through the Institutional Repository and through the British Library via the EThOS service.

- If my thesis does include any substantial subsidiary material owned by third-party copyright holders, I have sought and obtained permission to include it in any version of my thesis available in digital format and that this permission encompasses the rights that I have granted to the University of Warwick and to the British Library.

5. LEGAL INFRINGEMENTS

I understand that neither the University of Warwick nor the British Library have any obligation to take legal action on behalf of myself, or other rights holders, in the event of infringement of intellectual property rights, breach of contract or of any other right, in the thesis.

Please sign this agreement and return it to the Graduate School Office when you submit your thesis.

Student's signature: .....…… Date: .....

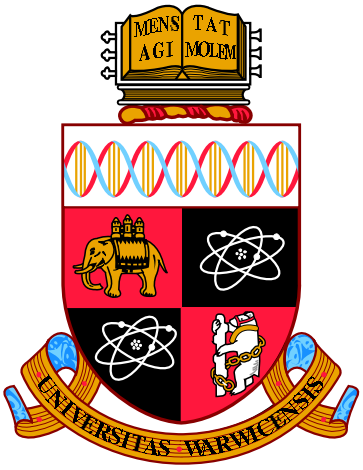

Computational surface partial differential equations

by

Thomas Ranner

Thesis

Submitted to the University of Warwick

for the degree of

Doctor of Philosophy

Mathematics Department

July 2013

THE UNIVERSITY OF
WARWICK

Contents

List of Tables

List of Figures

Acknowledgments

First, I would like to thank my Ph.D. supervisor, Professor Charles M. Elliott. He has introduced me into this field of research and provided me with the knowledge and skills to be able write this thesis. It is an honour to work with not only a world renowned academic but also a genuinely thoughtful, generous and kind person.

I would also like to thank Björn Stinner and Andreas Dedner for providing their expertise in scientific computing, especially for their help with the ALBERTA and DUNE software libraries. I have been lucky to have Andrew Stuart to mentor my progress which has provided helpful and alternative perspectives on my work and career. Scientific discussions with Klaus Deckelnick and Gerhard Dziuk have proved also to be incredibly useful: The opportunity to speak with original investigators of numerical methods for surface partial differential equations has proven to be extremely beneficial. I am also grateful for the comments of my examiners, Andrew Stuart and Endre Süli, which have greatly improved my thesis.

On a practical level, I wish to give thanks to the EPSRC for funding my studies and the Centre for Scientific Computing for providing the necessary computational facilities for my work. In addition I wish to thank the European Science Foundation, the Isaac Newton Institute, the London Mathematical Society, the Mathematisches Forschungsinstitut Oberwolfach, the Oxford Centre for Collaborative Applied Mathematics, the Society for Industrial and Applied Mathematics and the Wales Institute of Mathematical and Computational Sciences for various travel and conference grants. I would also like to thank Martin Rumpf at Universität Bonn and the Hausdorff Center for Mathematics for hosting my visits to Bonn.

Personally, I must thank Sergios Agapiou, Simon Cotter, Andrew Duncan,

Damon McDougall, Dave Moxey and Sebastian Vollmer for contributing to a lively and enjoyable atmosphere in B2.39, making it a pleasant space to work. It is fair to say that I would not have been able to perform any of the computations in this thesis without their help. I also wish to thank Andrew and Damon, along with Andrew Lam and David McCormick, for taking on the intimidating task of proofreading my work. A special thanks go to my various housemates and people I have played hockey with over the last four years.

I must thank my parents, and the rest of my family, for their unconditional support, love and encouragement: it has meant a great deal to me. Although, they will always say they do not really understand what I do, I hope they at least enjoy the pictures. The final, and most important, thanks goes to my girlfriend, Victoria: I would not be able to get anywhere without her.

For Grandad John

Declarations

I declare that this thesis contains entirely my own research, conducted under the supervision of Charles Elliott, except where otherwise stated. It has not been submitted for a degree at any other university. It has not been submitted for award at any other institution or for any other qualification. The material in chapter two is from a paper published in the IMA Journal of Numerical Analysis (Elliott and Ranner 2013). The material in chapter three is joint work with Charles Elliott and chapter four is joint work with Charles Elliott and Klaus Deckelnick. Much of the introductory material is taken from the work of Dziuk and Elliott (2013b): This forms the basis of the introduction and appendix.

Abstract

Surface partial differential equations model several natural phenomena; for example in fluid mechanics, cell biology and material science. The domain of the equations can often have complex and changing morphology. This implies analytic techniques are unavailable, hence numerical methods are required. The aim of this thesis is to design and analyse three methods for solving different problems with surface partial differential equations at their core.

First, we define a new finite element method for numerically approximating solutions of partial differential equations in a bulk region coupled to surface partial differential equations posed on the boundary of this domain. The key idea is to take a polyhedral approximation of the bulk region consisting of a union of simplices, and to use piecewise polynomial boundary faces as an approximation of the surface and solve using isoparametric finite element spaces. We study this method in the context of a model elliptic problem. The main result in this chapter is an optimal order error estimate which is confirmed in numerical experiments.

Second, we use the evolving surface finite element method to solve a Cahn-Hilliard equation on an evolving surface with prescribed velocity. We start by deriving the equation using a conservation law and appropriate transport formulae and provide the necessary functional analytic setting. The finite element method relies on evolving an initial triangulation by moving the nodes according to the prescribed velocity. We go on to show a rigorous well-posedness result for the continuous equations by showing convergence, along a subsequence, of the finite element scheme. We conclude the chapter by deriving error estimates and present various numerical examples.

Finally, we stray from surface finite element method to consider new unfitted finite element methods for surface partial differential equations. The idea is to use a fixed bulk triangulation and approximate the surface using a discrete approximation of the distance function. We describe and analyse two methods using a sharp interface and narrow band approximation of the surface for a Poisson equation. Error estimates are described and numerical computations indicate very good convergence and stability properties.

Chapter 1

Introduction

1.1 What is a surface partial differential equation?

Surface partial differential equations arise in a variety of natural applications. In this thesis we will study partial differential equations posed on both stationary and evolving surfaces both mathematically and numerically. The framework will be geometric since the domains in which these equations are posed will be curved.

A surface partial differential equation is a partial differential equation whose domain is an n-dimensional curved surface Γ living in $\mathbb{R}^{n+1}$. We contrast this with geometric partial differential equations which are partial differential equations for the evolution of a surface.

This means replacing the regular Cartesian derivatives with tangential gradients which are intrinsic to the surface; see Appendix A for full definitions. As an example, we consider the surface Poisson equation:

$$-\Delta_\Gamma u = f \quad \text{on } \Gamma. \tag{1.1.1}$$

Here Δ_Γ is the Laplace-Beltrami operator, the surface equivalent to the Laplace operator. This will be the simplest model equation we consider. We may also consider a more general elliptic equation on a surface:

$$-\nabla_\Gamma \cdot (\mathcal{A}\nabla_\Gamma u) + \mathcal{B} \cdot \nabla_\Gamma u + \mathcal{C}u = f \quad \text{on } \Gamma. \tag{1.1.2}$$

Here ∇_Γ is the tangential gradient and $\nabla_\Gamma \cdot$ the tangential divergence. This equation is elliptic if the diffusion tensor $\mathcal{A}$ is positive definite on the tangent space to Γ. In general, this means that $\mathcal{A}$ will vary in space, although the scalar matrix $\mathcal{A} = \alpha\,\mathrm{Id}$ is also allowed. We also allow time dependent equations such as the surface heat

equation:

$$\begin{aligned} u_t &= \Delta_\Gamma u \quad \text{on } \Gamma \\ u(\cdot,0) &= u_0 \quad \text{on } \Gamma. \end{aligned} \tag{1.1.3}$$

Throughout this thesis, we will assume that the boundary of Γ is empty, although this is not a restriction on our methods. In the case that $\partial\Gamma$ is not empty, we may consider standard boundary conditions alongside (1.1.2) or (1.1.3); for example:

$$u = g \text{ on } \partial\Gamma \quad \text{or} \quad \frac{\partial u}{\partial \mu} = g \quad \text{on } \partial\Gamma. \tag{1.1.4}$$

Here μ is the outward pointing unit conormal to $\partial\Gamma$ — normal to $\partial\Gamma$ but tangent to Γ. See Appendix A for more precise definitions.

Alternatively, one can also consider partial differential equations on an evolving n-dimensional surface $\{\Gamma(t)\}$ for $t \in [0,T]$. A prototypical example is the evolving surface heat equation:

$$\begin{aligned} \partial^\bullet u + u\nabla_\Gamma \cdot \mathbf{v} - \Delta_\Gamma u = 0 \quad &\text{on } \Gamma(t) \\ u(\cdot,0) = u_0 \quad &\text{on } \Gamma(0). \end{aligned} \tag{1.1.5}$$

Here, $\partial^\bullet$ is the material derivative and $\mathbf{v}$ the material velocity of $\Gamma(t)$. The material derivative, $\partial^\bullet u$, is an intrinsic derivative on the space-time domain of the equation measuring the rate of change of u along the flow of the surface; see Section 3.2.1 for more precise details. The evolution of the surface may be given or need to be computed as the solution of a geometric partial differential equation, which may depend on the evolution of the field u on the surface:

$$\mathbf{v} = g(x, \nu, H, u) \quad \text{on } \Gamma(t).$$

Here ν is the unit normal vector field to $\Gamma(t)$ and H is the mean curvature of $\Gamma(t)$. A simple example is given by forced mean curvature flow:

$$\mathbf{v} = V\nu \qquad V = -H + u \quad \text{on } \Gamma(t).$$

For a review of computational methods for geometric partial differential equations see Deckelnick, Dziuk and Elliott (2005).

Often in applications, domains have complex evolving morphology so analytic methods are unavailable. In this thesis, we derive and analyse computational methods to solve surface partial differential equations. In practice, this means finding a computable approximation of the equations. We are motivated by examples

which are of this fully coupled evolving form. In the problems presented in this thesis, we will assume either a given velocity or no velocity. Analysis of methods for surface partial differential equations coupled to geometric evolution laws is beyond the scope of current research methods.

1.2 Computational methods for surface partial differential equations

There are several methods designed to solve partial differential equations given in the literature. They fall into two broad categories: either using an explicit or implicit representation of the surface. The first approach uses a parametric viewpoint and approximates the surface using a triangulated surface and performs calculations on the discrete surface. The second category embeds the surface into Cartesian space and uses implicit representations of geometric quantities. In this section, we give a summary of a selection of these methods. As well as the given references, the review of Dziuk and Elliott (2013b) gives more details on many of these methods and their motivation.

The history of triangulated surfaces, and perhaps finite element methods in general, can be traced back to the work of Schellbach (1851) who proposed using a triangulated surface to solve Plateau's problem of determining the surface of a minimum area enclosed by a given closed curve. The first modern work to use a polyhedral approximation of a surface is due to Nedelec (1976) who considered a problem involving a surface integral. He constructed an exact triangulation of the surface consisting of curved simplices. To calculate the surface integral he used a high order quadrature rule to approximate the area element using a parameterisation of the surface. Baumgardner and Frederickson (1985) looked at ways to construct such exact triangulations.

The seminal work of Dziuk (1988) introduced what is now known as the surface finite element method. This method uses a polyhedral approximation of the surface consisting of planar triangles and then solves variational forms of partial differential equations using a finite element method. Integrals on each element can be performed exactly since elements in the mesh are no longer curved, however errors arising from approximating the surface in this way are of the same order as the standard planar interpolation error. This means the error is of optimal order with respect to the dimension of the surface. The method allows conventional software to be easily adapted for solving surface problems: The only difference is now that nodes live in one space dimension higher; see Figure 1.2.1 for an example.

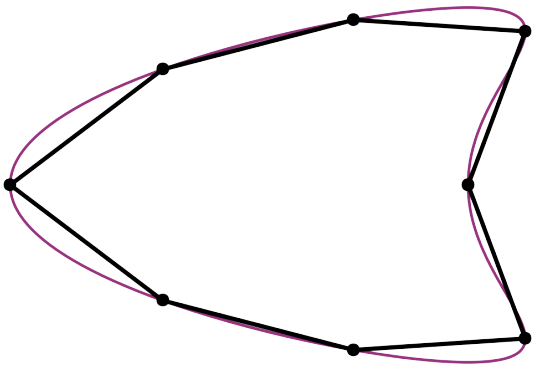

Figure 1.2.1: An example of a triangulated surface approximation of a curve $\Gamma = \{x \in \mathbb{R}^2 : \Phi(x) = 0\}$ with $\Phi(x_1, x_2) = \sqrt{(x_1 - x_2^2)^2 + x_2^2} - 1$.

Higher order surface approximations have been developed by others including Heine (2005) and Demlow (2009). A reliable and efficient error estimator for adaptive calculations is given by Demlow and Dziuk (2007). The surface finite element method was extended to linear and non-linear parabolic equations by Dziuk and Elliott (2007b). This approach was used by Barreira (2009) to solve a variety of non-linear problems on surfaces and Du, Ju and Tian (2011) have given an analysis of a fully discrete approximation of a Cahn-Hilliard equation posed on a triangulated surface.

Other discretisations of surface partial differential equations on stationary surfaces have used a triangulated surface as the computational domain. Dedner, Madhavan and Stinner (2013) have studied a discontinuous Galerkin method for solving a Poisson equation on a surface. Finite volume methods have been developed and analysed by Ju and Du (2009) and Ju, Tian and Wang (2009). Calhoun and Helzel (2010) have used a similar approach using logically Cartesian grids. Conservation laws on a sphere have been considered by Berger, Calhoun, Helzel and LeVeque (2009).

The evolving surface finite element method was introduced by Dziuk and Elliott (2007a), with further analysis given by: Dziuk, Lubich and Mansor (2012b); Dziuk and Elliott (2012); Lubich, Mansour and Venkataraman (2013); and Dziuk and Elliott (2013a). The idea is to construct an evolving discrete surface by moving the nodes of a triangulated surface according to the underlying surface evolution. Many of the properties from the stationary case, including optimal order errors, carry over to this case. One key problem with this method is that, in the case of large deformations, elements may become distorted. This can lead to large errors and poorly conditioned systems of linear equations to solve at each time step. Re-

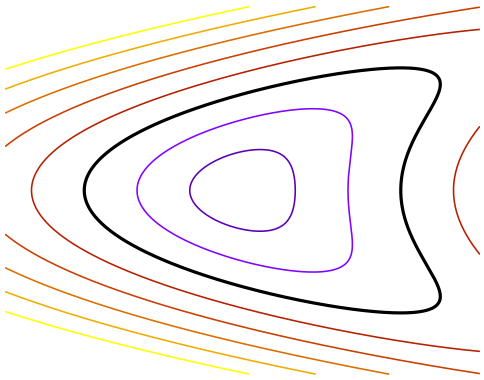

Figure 1.2.2: The level lines of a level set function for $\Phi(x_1, x_2) = \sqrt{(x_1 - x_2^2)^2 + x_2^2} - 1$. Highlighted in bold is the zero level line.

meshing strategies using conformal maps have been successfully used by Dziuk and Clarenz (2003) for spheres and by Eilks and Elliott (2008) for tori, but a more recent approach is to use an Arbitrary Lagrangian-Eulerian surface finite element method (Elliott and Styles 2012). The idea is to introduce an artificial tangential velocity to the nodes on the triangulated surface, and update the equations accordingly, in order to ensure good mesh quality. The authors Barrett, Garcke and Nürnberg (2008a,b,c,d) have developed novel discretisations of several geometric partial differential equations which introduce an artificial tangential velocity which leads to near equi-distribution of nodes.

Similar ideas have also been used by Dziuk, Kröner and Müller (2012a) in a finite volume scheme to solve scalar conservation laws on evolving surfaces. A second order wave equation on an evolving surface, the Jenner equation (Dziuk and Elliott 2013b), has been analysed by Lubich and Mansour (2012). The Jenner equation is derived from Hamilton's principle of stationary action and is the natural analogue of the classical acoustic wave equation on a given evolving surface.

The level set method is a very popular method for calculating solutions to surface partial differential equations using an implicit representation of the surface; see Sethian (1999) and Osher and Fedkiw (2002) for a review mainly focused on geometric partial differential equations. In this methodology, the surface is represented as the zero level set of a smooth function Φ defined on $\mathbb{R}^{n+1}$, i.e. $\Gamma = \{x \in \mathbb{R}^{n+1} : \Phi(x) = 0\}$; see Figure 1.2.2 for example. We can use this representation to reformulate surface partial differential equations as equations on $\mathbb{R}^{n+1}$ and solve using well established discretisation schemes. For example, we can translate

the heat equation on a given surface to Eulerian form given by

$$\begin{aligned} u_t &= \frac{1}{|\nabla\Phi|}\nabla\cdot(P\nabla u\,|\nabla\Phi|) \quad && \text{on } \mathbb{R}^{n+1}\times(0,T) \\ u(\cdot,0) &= u_0^e && \text{on } \mathbb{R}^{n+1}, \end{aligned} \tag{1.2.1}$$

where u_0^e is an extension of u_0 to $\mathbb{R}^{n+1}$ and

$$P(x) = \mathrm{Id} - \nu(x)\otimes\nu(x) \qquad \nu(x) = \frac{\nabla\Phi(x)}{|\nabla\Phi(x)|} \quad \text{for } x\in\mathbb{R}^{n+1}.$$

Here $\otimes$ denotes the outer product ($(a\otimes b)_{ij} = a_i b_j$). This equation can now be solved using standard computational methods. This is a degenerate parabolic equation since no diffusion can occur in the direction normal to the surface, and we now seek a solution u on all of $\mathbb{R}^{n+1}$. Both of these difficulties will have to be overcome in computational approximations of (1.2.1).

The work of Bertalmío, Cheng, Osher and Sapiro (2001) uses both an energetic and variational formulation to derive the Eulerian form of a variety of different parabolic surface partial differential equations. These embedded equations are solved using finite differences on a Cartesian grid in space and an explicit time stepping strategy. The authors say that this approach allows the use of "well-studied numerical techniques, with accurate error, stability and robustness measures; the topology of the underlying surface is not an issue; and we can derive simple, accurate, robust, and elegant implementations." This method is extended by Greer, Bertozzi and Sapiro (2006) to fourth-order equations including a Cahn-Hilliard equation and a fully non-linear thin film model both posed on surfaces. Furthermore, finite differences have been used to solve advection-diffusion equations on evolving surfaces in Eulerian form; see Adalsteinsson and Sethian (2003) and Xu and Zhao (2003), for example.

The problem of having (1.2.1) posed on a domain one dimension higher than (1.1.5) can be overcome by considering (1.2.1) on a narrow band around the surface $U = \{|\Phi(x)| < c : x \in \mathbb{R}^{n+1}\}$; see the method developed by Schwartz, Adalsteinsson, Colella, Arkin and Onsum (2005) for example. However, this introduces further difficulties in the approximation of artificial boundary conditions imposed on the boundary of U. Any implicit time stepping scheme must overcome the degeneracy of the Eulerian approximation of the Laplace-Beltrami operator. Some of these issues are resolved in Greer et al. (2006) using convexity splitting, alternating direction implicit methods and iterative solvers. Recent works by Greer (2006) and Chernyshenko and Olshanskii (2013) have suggested different non-degenerate forms

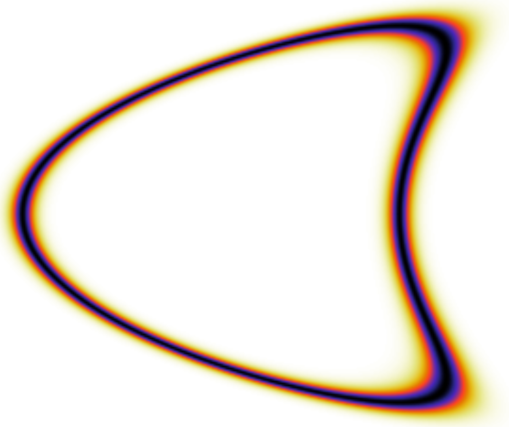

Figure 1.2.3: An example of a phase field representation of the curve $\Gamma = \{x \in \mathbb{R}^2 : \Phi(x) = 0\}$ with $\Phi(x_1, x_2) = \sqrt{(x_1 - x_2^2)^2 + x_2^2} - 1$. The plot is an isocolour plot of $\rho_\varepsilon(x) = 1/\cosh^2(\Phi(x)/\varepsilon)$ for $\varepsilon = 0.05$.

of the projection operator P.

The level set methodology has also been applied using the finite element method. Burger (2009) formulated an elliptic problem on a surface using an Eulerian formulation, and then used a finite element method based on a polyhedral narrow band about the surface. The parabolic case, including the Allen-Cahn equation and fourth order Cahn-Hilliard equation, was studied by Dziuk and Elliott (2008). Finally, the same authors have extended this work to evolving surfaces (Dziuk and Elliott 2010).

A different implicit representation of the surface comes from using phase field methods (Caginalp 1989; Deckelnick et al. 2005). The idea is to thicken the surface to a narrow band Γ_ε about the surface involving a small parameter ε related to the thickness of the band. To do this we consider a family of non-negative smooth functions ρ_ε that when scaled with $1/\varepsilon$ approximate the delta distribution of Γ as $\varepsilon \to 0$. We define Γ_ε to be the support of ρ_ε; see Figure 1.2.3 for example. The heat equation (1.1.5) in this formulation becomes

$$\begin{aligned} \partial_t(\rho u) &= \nabla \cdot (\rho \nabla u) \quad && \text{on } \Gamma_\varepsilon \times (0, t) \\ u(\cdot, 0) &= u_0^e && \text{on } \Gamma_\varepsilon. \end{aligned} \tag{1.2.2}$$

If we assume the surface is given by a level set function $\Phi\colon \mathbb{R}^{n+1} \to \mathbb{R}$, we may take

$$\rho_\varepsilon(x) = \sigma\left(\frac{\Phi(x)}{\varepsilon}\right).$$

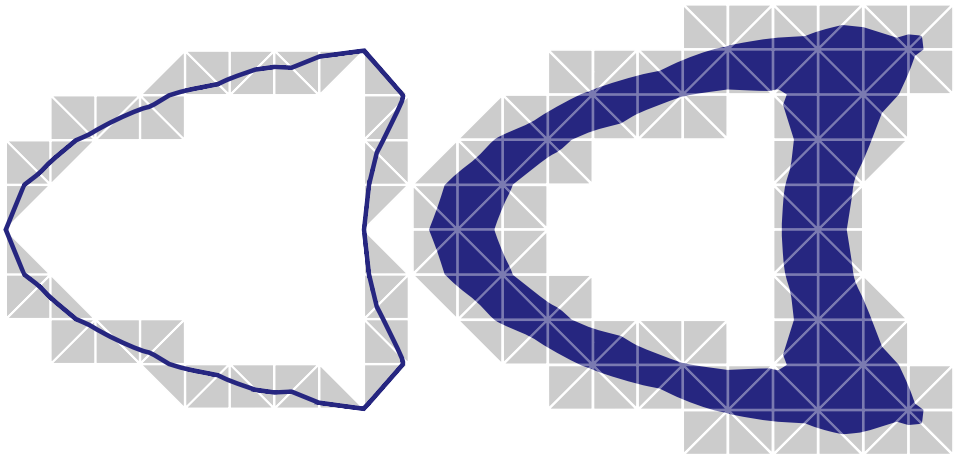

Figure 1.2.4: An example of the computational domains Γ_h and D_h for unfitted finite element methods.

where $\sigma(r) > 0$ if $|r| < \alpha_\omega$ and $\sigma(r) = 0$ if $|r| \geq \alpha_\omega$ for some constant $\alpha_\omega > 0$.

In the phase field methodology, one often solves for an unknown interface (surface) represented by a phase field variable φ which has a step transition from the bulk values $\approx \pm 1$ on either side of the interface. We can construct a phase field variable with compact support (i.e. the width of the interface is finite) with use of a double obstacle phase field model (Blowey and Elliott 1991, 1992). In this context, we form a diffuse interface with

$$\rho_\varepsilon = \sigma(\varphi), \qquad \text{where } \sigma(r) = 1 - r^2.$$

In this approach φ can be considered as a level set function for Γ.

Such a formulation was originally developed by Cahn, Fife and Penrose (1997) for a complex moving boundary problem. Numerical methods were proposed by Deckelnick, Elliott and Styles (2001) using a finite element method. The approach was generalised to different equations in the work of Rätz and Voigt (2006) on stationary surfaces and extended to evolving surfaces by Elliott, Stinner, Styles and Welford (2011). The formulation is based on an arbitrary triangulation of a background region. To remain efficient, in practice, this is adaptively refined to resolve the interface. This approach has been used successfully to solve the Cahn-Hilliard-Navier-Stokes system by Kay, Styles and Welford (2008).

To ensure the efficiency of level set methods, it has been suggested (Deckelnick, Dziuk, Elliott and Heine 2010; Olshanskii, Reusken and Grande 2009) to use unfitted finite element methods. The idea is to solve variational forms of surface equations by integrating over partial elements, also known as cut cells, of a back-

ground, fixed triangulation. The method has been successfully used for equations in planar domains with curved boundaries using finite element methods (Barrett and Elliott 1982, 1984, 1985, 1987a,b, 1988) and using discontinuous Galerkin methods (Bastian and Engwer 2009; Engwer and Heimann 2012), as well as for an interface problem (Hansbo and Hansbo 2002).

We describe these methods for a Poisson equation (1.1.1) on a surface Γ which is the zero level set of a smooth level set function Φ. This approach uses the Eulerian formulation of surface partial differential equations. The work of Deckelnick et al. (2010) considers an approximation of a surface Poisson equation using a bulk finite element space V_h defined over a union of elements which intersect $D_h := \{x \in \mathbb{R}^{n+1} : |\Phi_h(x)| < \varepsilon\}$; see Figure 1.2.4 for example. To ensure optimal order errors, the authors couple $\varepsilon = \beta h$, for $\beta > 0$, and solved:

$$\int_{D_h} P_h \nabla u_h \cdot \nabla \phi_h \, |\nabla \Phi_h| + u_h \phi_h \, |\nabla \Phi_h| \, \mathrm{d}x = \int_{D_h} f^e \phi_h \, |\nabla \Phi_h| \, \mathrm{d}x, \quad \text{for all } \phi_h \in V_h,$$

where Φ_h is a numerical approximation of Φ (for example, the nodal interpolant), P_h element-wise projection given by

$$P_h(x) = \mathrm{Id} - \nu_h(x) \otimes \nu_h(x), \qquad \nu_h(x) = \frac{\nabla \Phi_h(x)}{|\nabla \Phi_h(x)|}, \quad \text{for } x \in D_h.$$

One may also consider the limit of these equations as $\beta \to 0$ to derive a sharp interface approximation. We set $\Gamma_h := \{x \in \mathbb{R}^{n+1} : \Phi_h(x) = 0\}$ (see Figure 1.2.4), and V_h is a bulk finite element space over elements which intersect Γ_h (plus some technical details). This is the method of Olshanskii et al. (2009) who solve:

$$\int_{\Gamma_h} \nabla_{\Gamma_h} u_h \cdot \nabla_{\Gamma_h} \phi_h + u_h \phi_h \, \mathrm{d}\sigma_h = \int_{\Gamma_h} f^e \phi_h \, \mathrm{d}\sigma_h, \quad \text{for all } \phi_h \in V_h.$$

This finite element scheme is not initially well-posed unless we restrict the problem to finite element functions with $\nabla \phi_h \cdot \nu_h = 0$ where ν_h is the element-wise normal to Γ_h. This does not cause any problems numerically since solutions can be computed with the usual finite element basis functions used as a spanning set via the conjugate gradient method. The induced triangulation, the underlying triangulation restricted to the computational domain, may have arbitrarily small elements, hence the resulting system of linear equations may be extremely badly conditioned. Analysis and numerical tests by Olshanskii and Reusken (2010) show that a simple Jacobi preconditioner overcomes this problem. Recent work by Olshanskii, Reusken and Xu (2012) shows that the induced triangulation will satisfy a maximum angle

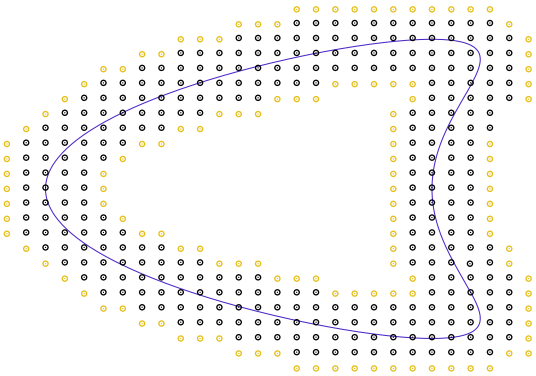

Figure 1.2.5: An example of the computational domain for the closest point method. The black nodes represent the nodes at which we calculate the solution of the partial differential equation. In addition the yellow nodes show the extra ghost nodes at which we must find the extended (interpolated) solution.

condition if the bulk triangulation satisfies a minimum angle condition.

An adaptive finite element method using the sharp interface approximation has been studied by Demlow and Olshanskii (2012) and an advection dominated problem is considered by Olshanskii, Reusken and Xu (2013). More details on these methods are given in Chapter 4.

The final method we mention is the closest point method. The idea is to create a very simple method by embedding a surface partial differential equation into a narrow band about the surface using the closest point operator (A.2.2) and then using Cartesian differential operators. The original method, proposed by Ruuth and Merriman (2008), proposes a two step method to construct solutions to (1.1.3) at each time step. First, one extends the solution off the surface to the computational domain using the closest point operator, replacing u by $u(p(\cdot))$. This step requires computation of the closest point operator and nodal interpolation to find the solution away from nodal values. Then, one computes the solution to the embedded partial differential equation — the surface partial differential equation with tangential surface operators replaced with their Cartesian counterparts — using standard finite differences on a Cartesian mesh in the computational domain for one time step. The computational domain is a narrow band about the surface defined by the nodes required to compute the finite difference stencil at each of the interpolation nodes; see Figure 1.2.5 for example. In effect, the method approximates solutions to

$$\partial_t\big(u(p)\big) - \Delta\big(u(p)\big) = 0.$$

The method relies on the fact that

$$\nabla u(p(x)) = \nabla_\Gamma u(x) \quad \text{for } x \in \Gamma.$$

This method has been generalised using different interpolation operators (Macdonald and Ruuth 2008), using implicit time stepping (Macdonald and Ruuth 2009), and using more general closest point operators (März and Macdonald 2012). It has been applied to a wide variety of problems including eigenvalue problems on surfaces (Macdonald, Brandman and Ruuth 2011). This method is incredibly cheap and simple to use although it currently lacks rigorous analysis.

1.3 Applications of surface partial differential equations

Surface partial differential equations arise in a wide variety of applications. We give details of a few here as motivation for the methods that follow. Many more applications have been studied. See Dziuk and Elliott (2007b) for a more detailed list.

Surface active agents

A strong motivating example for many of the methods listed above is that of advection and diffusion of a surface active agent (surfactant) on a fluid interface. Surfactants have an important role in many industrial and biological applications. We mention in particular plastic production (Grace 1982), oil recovery (Morrow and Mason 2001) and pulmonary function (Goerke 1998). Surfactants have the property of changing (normally reducing) the surface tension of the interface to which they are bound.

We consider a situation with two immiscible viscous fluids, of equal densities, with a drop of one fluid inside another separated by an energetic interface. We suppose that there is a surfactant which is insoluble in either of the fluids and hence is confined to the interfacial region. We assume that the surface energy depends on the concentration of surfactant and thus leads to a concentration dependent surface tension and the Marangoni effect.

We describe a model presented by Elliott et al. (2011). The mathematical formulation consists of a moving interface problem of Navier-Stokes form coupled to an advection-diffusion equation on the interface. The problem is to find an interface $\Gamma(t)$ separating two fluid domains $\Omega_1(t)$ and $\Omega_2(t)$, a fluid velocity $\mathbf{v}$, pressure p, and a surfactant concentration u. Within the bulk domains $\Omega_j(t)$, we have the

Navier-Stokes system:

$$\partial_t \mathbf{v} + (\mathbf{v} \cdot \nabla)\mathbf{v} = -\nabla p + \frac{1}{\mathrm{Re}}\Delta \mathbf{v}$$
$$\nabla \cdot \mathbf{v} = 0,$$

and on the unknown evolving surface $\Gamma(t)$ we have mass and momentum balances:

$$[\mathbf{v}]_2^1 = 0 \qquad \mathbf{v} \cdot \nu = V_\Gamma$$
$$\left[-p\mathrm{Id} + \frac{2}{\mathrm{Re}} D(\mathbf{v})\right]_2^1 = -\frac{1}{\mathrm{Re}\,\mathrm{Ca}}\big(\sigma(u)H + \nabla_\Gamma \sigma(u)\big).$$

Here ν is the unit normal vector field pointing into $\Omega_1(t)$, H is the mean curvature of $\Gamma(t)$, $\sigma(u)$ is the concentration dependent surface tension, Re and Ca are the Reynolds and capillary numbers (dimensionless numbers derived from physical quantities), V_Γ is the normal velocity of $\Gamma(t)$ and $D(\mathbf{v}) = \frac{1}{2}\big(\nabla \mathbf{v} + (\nabla \mathbf{v})^{\mathrm{t}}\big)$ is a deformation tensor. Finally, $[\eta]_2^1$ represents the jump of η between Ω_1 and Ω_2. The concentration u satisfies the conservation equation

$$\partial^\bullet u + u\nabla_\Gamma \cdot \mathbf{v} - \nabla_\Gamma \cdot q = 0 \quad \text{ on } \Gamma(t),$$

where $q = q(u)$ is the flux by which u is driven.

Several numerical approaches have been taken to solve similar problems. We mention the work of Xu, Li, Lowengrub and Zhao (2006), Lowengrub, Xu and Voigt (2007), and Xu, Yang and Lowengrub (2012) based on the level set method of Xu and Zhao (2003); the authors of Ganesan and Tobiska (2009) and Ganesan, Hahn, Held and Tobiska (2012) used an Arbitrary Lagrangian-Eulerian surface finite element method; and Elliott et al. (2011) who took a phase field approach. The study of James and Lowengrub (2004), who considered a conservative volume of fluid method, and the work of Lai, Tseng and Huang (2008), who used the immersed boundary method of Peskin (1972), pursue the same problem from a more physical point of view.

In other situations, we may drop the assumption that the surfactant only exists on the interface between the two fluids (Defay and Prigogine 1966). In this case, we will model soluble surfactants which may live on the interface $\Gamma(t)$ or in one of the bulk phases $\Omega_2(t)$. Typically, we extend the previous model by assuming that the surfactant has concentration u on the interface $\Gamma(t)$ and w in $\Omega_2(t)$ and

satisfying:

$$\begin{aligned} \partial_t w + \mathbf{v} \cdot \nabla w - \nabla \cdot q_w &= 0 && \text{in } \Omega_2(t) \\ \partial^\bullet u + u \nabla_\Gamma \cdot \mathbf{v} - \nabla_\Gamma \cdot q_u &= \frac{\partial w}{\partial \nu} && \text{on } \Gamma(t), \end{aligned}$$

where q_u and q_w are the fluxes for the surfactant in $\Omega_2(t)$ and $\Gamma(t)$ respectively. The system is completed by prescribing the flux of surfactant between bulk and interface phases:

$$\frac{\partial w}{\partial \nu} + L(w, u) = 0,$$

or assuming instantaneous transport between the phases:

$$u = \gamma(w|_{\Gamma(t)}).$$

This model is similar to that derived by Bothe, Prüss and Simonett (2005) and Bothe and Prüss (2010). The precise form of L or γ will be determined by an adsorption/desorption model governed by Langmuir kinetics. Modelling using Langmuir kinetics can be found in work by Novak, Gao, Choi, Resasco, Schaff and Slepchenko (2007); Kwon and Derby (2001); Booty and Siegel (2010); Medvedev and Stuchebrukhov (2011); and Rätz and Röger (2012) in a variety of different applications.

Numerical methods have been derived for this extension, extending the previous works for insoluble surfactants. We mention in particular the work of Garcke, Lam and Stinner (2013) and Teigen, Li, Lowengrub, Wang and Voigt (2009) both using a phase field method. The review of Li and Kim (2012) is also a useful reference.

Pattern formation on biological surfaces

The classical work of Turing (1952) showed that many different patterns in nature can be modelled by a simple system of reaction-diffusion equations. The review of Baker, Gaffney and Maini (2008) gives more modern biological applications of what are now called Turing patterns. Numerical examples suggest that similar reaction-diffusion systems posed on growing biological surfaces exhibit diffusion-driven instability of spatially uniform structures and thus lead to spatial patterns.

An example of such a model comes from the growth of solid tumours. The evolution of the solid bulk tumour is determined by a concentration of growth promoting factor on the surface. The mathematical problem is to find the tumour surface $\Gamma(t)$, evolving with velocity $\mathbf{v} = V\nu$ and scalar functions u, w which are

surface concentrations satisfying an evolution equation

$$V = -\varepsilon H + \delta u,$$

and a system of reaction-diffusion equations

$$\partial^\bullet u + u\nabla_\Gamma \cdot \mathbf{v} = \Delta_\Gamma u + f_1(u,w)$$
$$\partial^\bullet w + w\nabla_\Gamma \cdot \mathbf{v} = D_w \Delta_\Gamma w + f_2(u,w).$$

In the first equation ε and δ are positive parameters. The εH is a regularising term ensuring smoothness of the surface and the δu reflects the promotion of growth of the surface by the concentration of u. In the reaction-diffusion system, D_w is the positive diffusion coefficient of the species w and f_1, f_2 model the interactions between the two surface concentrations. An example is the activator-depleted substrate model (Schnakenberg 1979), known as the Brusselator model, in which

$$f_1(u,w) = \gamma(a - u + u^2 w) \quad \text{and} \quad f_2(u,w) = \gamma(b - u^2 w),$$

with $\gamma, a, b > 0$ constants. This model is a combination of ideas from the work of Crampin, Gaffney and Maini (1999) and Chaplain, Ganesh and Graham (2001).

Numerical studies of this model are given by Barreira, Elliott and Madzvamuse (2011) using a surface finite element method and by Bergdorf, Sbalzarini and Koumoutsakos (2010) using a Lagrangian particle method based on the level set methodology.

A similar model for brain growth was studied numerically by Lefevre and Mangin (2010). Further numerical studies can be found in Varea, Aragón and Barrio (1999) and Plaza, Sánchez-Garduño, Padilla, Barrio and Maini (2004). Other authors have considered problems where one of the chemical species may also live in the interior bulk phase. For example, Rätz and Röger (2012) consider a Turing-type model for Guanine-tri-phosphate (GTP) binding proteins in biological cells which can exist in either cytosolic volume or membrane surface using ideas from Langmuir kinetics similar to the models for soluble surfactants.

Both Neilson, Mackenzie, Webb and Insall (2011) and Elliott, Stinner and Venkataraman (2012) consider problems in cell motility using a reaction-diffusion system called the Meinhardt model (Gierer and Meinhardt 1972). This is coupled to a fourth order geometric equation for the cell membrane coming from a Helfrich energy.

Phase separation on surfaces

The final example we consider comes from a model for the etching of silver in a silver-gold alloy whose surface is immersed in an electrolyte. It is an example where coupling surface evolution with a surface process leads to highly complex morphology. The following model was developed by Erlebacher, Aziz, Karma, Dimitrov and Sieradzki (2001) and Eilks and Elliott (2008).

The goal is to find a surface $\Gamma(t)$, evolving with velocity $\mathbf{v} = V\nu$, representing a surface monolayer, and a surface concentration u, of gold atoms in the binary mixture of gold and electrolyte adatoms in the surface monolayer, satisfying the geometric law

$$V = -J_{\text{diss}} = v_0(1 - \delta H),$$

and the conservation law

$$\partial^\bullet u + u\nabla_\Gamma \cdot \mathbf{v} - \nabla_\Gamma \cdot q = VC_0,$$

with C_0 the bulk gold concentration and q the diffusive surface flux of adatoms given by

$$q = -J_{\text{diff}} = -b(u)\nabla_\Gamma w \qquad w = -\gamma\Delta_\Gamma u + \psi'(u),$$

where w is the chemical potential, $b(u)$ is a concentration dependent mobility and ψ is the double well free energy occurring in Cahn-Hilliard theory. The free energy of regular solution ψ is given by the logarithmic functional

$$\psi(u) = \frac{\theta_{\text{cr}}}{2}u(1-u) + \frac{\theta}{4}\big(u\log u + (1-u)\log(1-u)\big). \tag{1.3.1}$$

The parameter θ represents the temperature of the system and θ_{cr} the critical temperature. We assume $\theta < \theta_{\text{cr}}$ so that ψ has a double well form and phase separation occurs. A typical form of b is $b(c) = \frac{B}{2}(1-u^2)$. Computations based on the surface finite element method can be found in Eilks and Elliott (2008).

Analysis of a surface finite element method for a Cahn-Hilliard equation on a stationary surface is given by Du et al. (2011). Further computations can be found in Schoenborn and Desai (1999) and Marenduzzo and Orlandini (2013). Mercker, Ptashnyk, Kühnle, Hartmann, Weiss and Jäger (2012) considered a Cahn-Hilliard type equation forced by terms depending on the curvature of the surface, again on a fixed surface.

Models of phase separation in biology have also been developed. Elliott et al. (2012) considered a problem in cell motility and Elliott and Stinner (2010a,b, 2013)

studied a problem on biomembranes.

We conclude this section by summarising the challenges these particular applications bring.

Curved surfaces: The underlying domain of the partial differential equations lives in curved space. Our numerical methods will have to find a way to capture the essential geometric aspects of the surface. We wish to make no assumptions with respect to symmetry.

Evolving surfaces: The domains we consider may also be time dependent. The methods we design must have a way to track this change. Ideally, we wish to try to use as many features of simpler systems as possible. This means we wish to use a time stepping procedure that results in solving a sequence of problems each on a different stationary surface.

Large deformations: We wish to be able to make no restrictions on the size of the deformation of the surface. Large deformations and topology changes will restrict the type of representation used for the surface.

Unknown evolutions: In most of the applications above the surface, and its evolution, is a priori unknown. This means we must combine our methods with computational techniques which can determine the motion of the surface.

Bulk effects: The surface effects we are modelling may be physically coupled to systems living in a volume region about the surface. Our numerical methods should be able to be combined with other methods for these equations.

Non-linear effects: The equations in this thesis are meant as model problems for the complicated systems presented above. As such, we should always have these applications in mind when making assumptions.

1.4 Outline of thesis

The original content of this thesis consists of three chapters. The first extends the surface finite element method to problems where a diffusion on a surface is coupled to diffusion in a bulk domain. The second studies an evolving surface finite element method applied to a Cahn-Hilliard equation. Finally, the third looks at new unfitted finite element methods for surface partial differential equations.

The first problem we tackle, shown in Chapter 2, is a coupled bulk-surface equation. Often, applications of the surface finite element method consider problems where the evolution of surface concentrations depend on 'bulk effects'. These effects fall into two broad categories. In each, we assume a surface is embedded in a volumetric domain. In the first case, the substance which lives on the surface may also live in parts of the volumetric region. The second case considers an evolution of the surface forced by some underlying equations for motion in the surrounding volume. Of course, both effects can occur in the same model.

To develop a method for these applications, we consider the following model problem. Given a domain Ω with closed boundary Γ, we seek a solution pair $u\colon \Omega \to \mathbb{R}$ and $v\colon \Gamma \to \mathbb{R}$ satisfying

$$-\Delta u + u = f \quad \text{in } \Omega \tag{1.4.1a}$$

$$(\alpha u - \beta v) + \frac{\partial u}{\partial \nu} = 0 \quad \text{on } \Gamma \tag{1.4.1b}$$

$$-\Delta_\Gamma v + v + \frac{\partial u}{\partial \nu} = g \quad \text{on } \Gamma. \tag{1.4.1c}$$

We assume $f\colon \Omega \to \mathbb{R}$ and $g\colon \Gamma \to \mathbb{R}$ are given functions and α, β are positive constants. Equations (1.4.1a) and (1.4.1c) represent diffusion equation in the bulk and on the surface, and (1.4.1b) represents the exchange of concentration between the bulk and surface phases. This particular choice of coupling on the surface has been used by Novak et al. (2007). It can be viewed as a linearisation of the more general equation

$$L(u, v) + \frac{\partial u}{\partial \nu} = 0,$$

where $\partial_u L(u, v) > 0$ and $\partial_v L(u, v) < 0$, which has been used by: Kwon and Derby (2001); Booty and Siegel (2010); Medvedev and Stuchebrukhov (2011); and Rätz and Röger (2012), for example. We leave the numerical analysis of more general couplings, the parabolic case and evolving domains to future work.

Our method works by taking a polyhedral approximation Ω_h of Ω and using the boundary faces of Ω_h, which we will call Γ_h, as an approximation of Γ. We then use a finite element method to solve a variational form of the above equations. This work also includes the use of higher order isoparametric finite elements. We show well-posedness for these equations and derive optimal order error estimates for the finite element method. This chapter also includes details of a numerical implementation and examples to demonstrate the rates of convergence.

In Chapter 3, we consider our second problem looking at a Cahn-Hilliard equation on an evolving surface. The Cahn-Hilliard equation (Cahn and Hilliard

1958) can be used to model several natural phenomena; applications using a Cahn-Hilliard equation can be found in Section 1.3. Analysis of the Cahn-Hilliard equation, in planar domains, started in the 1980's with the work of Elliott and Songmu (1986) and numerical work of Elliott and French (1987, 1989) and Elliott, French and Milner (1989), which was extended to stationary surfaces by Du et al. (2011). A review of the behaviour of the Cahn-Hilliard equation in the planar case is given by Elliott (1989).

We will study the following problem mathematically. We assume we are given an evolving surface $\{\Gamma(t)\}$, for $t \in [0,T]$, with prescribed velocity v. We seek a solution u of

$$\partial^\bullet u + u\nabla_\Gamma \cdot v = \Delta_\Gamma \left(-\varepsilon \Delta_\Gamma u + \frac{1}{\varepsilon}\psi'(u) \right) \qquad \text{on } \Gamma(t), \tag{1.4.2}$$

subject to the initial condition $u(\cdot,0) = u_0$ on $\Gamma(0) = \Gamma_0$. This is a fourth-order non-linear equation posed on an evolving domain. We will look for solutions via a second-order splitting method. We assume that ε is a small, but fixed, positive parameter and ψ is the quartic double-well potential given by

$$\psi(z) = \frac{1}{4}(z^2-1)^2.$$

This is taken as a simplification of the logarithmic potential (1.3.1). We note that for general surface evolutions the Ginzburg-Landau functional will not decrease along solutions of this equation and (1.4.2) is not a gradient flow. One can enforce energy decrease by imposing extra assumptions on v. Alternatively, one can calculate a coupled gradient flow equation for u and v using techniques from Elliott and Stinner (2010a).

This chapter is broken into four sections. In the first we derive the continuous equation above (1.4.2). This comes from a simple conservation law on a surface and applying a generalisation of the Reynolds transport theorem to curved surfaces. Next, we derive our evolving surface finite element method. This is based on the original method of Dziuk and Elliott (2007a). In section four, the discrete solution is shown to satisfy an energy bound, hence we can use weak convergence results, along with domain perturbation arguments, to show that the continuous equations have a solution. The fifth section then shows that the finite element method converges with optimal order errors in appropriate surface norms. The chapter finishes with various numerical examples confirming the analytical results.

The final problem we consider, shown in Chapter 4, studies unfitted finite element methods for surface partial differential equations. We suppose we are given

a level set function describing the surface which may have been obtained using a level set or phase field method for a geometric partial differential equation. This method has the possibility of use in a large variety of applications where volumetric forces determine the position and geometry of an evolving interface. We would like a method with the efficiency of the parametric approach of the surface finite element method, but without worrying about constructing a good triangulation from an implicit representation of the surface. Our starting points are the sharp interface method of Olshanskii et al. (2009) and the narrow band method of Deckelnick et al. (2010). We extend these methods by using the full Cartesian gradient of basis functions instead of projecting onto the tangential directions to the surface.

Given a smooth level set function Φ with $\Gamma = \{x \in \mathbb{R}^{n+1} : \Phi(x) = 0\}$, we wish to solve the surface elliptic problem:

$$-\Delta_\Gamma u + u = f \quad \text{on } \Gamma. \tag{1.4.3}$$

We assume we have a fixed bulk triangulation $\mathscr{T}_h$ of a neighbourhood of Γ and Φ_h is some approximation of Φ (the nodal interpolant, for example). We define $\Gamma_h := \{x \in \mathbb{R}^{n+1} : \Phi_h(x) = 0\}$ and $D_h := \{x \in \mathbb{R}^{n+1} : |\Phi_h(x)| < h\}$, which both consist of partial elements. For the sharp interface method, we set V_h to be the space of piecewise linear finite element functions over the set of elements in $\mathscr{T}_h$ which intersect Γ_h (plus some technical assumptions) and solve

$$\int_{\Gamma_h} \nabla u_h \cdot \nabla \phi_h + u_h \phi_h \,\mathrm{d}\sigma_h = \int_{\Gamma_h} f^e \phi_h \,\mathrm{d}\sigma_h \quad \text{for all } \phi_h \in V_h. \tag{1.4.4}$$

Alternatively, for the narrow band method, we set V_h to be the space of piecewise linear finite element functions over the set of elements in $\mathscr{T}_h$ which intersects D_h and solve

$$\frac{1}{2h}\int_{D_h} \nabla u_h \cdot \nabla \phi_h + u_h \phi_h \,\mathrm{d}x = \frac{1}{2h}\int_{D_h} f^e \phi_h \,\mathrm{d}x \quad \text{for all } \phi_h \in V_h. \tag{1.4.5}$$

The use of full gradients means we no longer have degenerate equations to solve and gives us control over the error of our finite element method away from the surface since we can bound the gradient of the error in the normal direction to the surface. The properties of these new methods are explored both analytically and numerically for a surface Poisson equation (1.4.3) and are shown to give comparable results to the surface finite element method.

The thesis is completed by Appendix A which sets up our notation and assumptions. This preliminary material describes the surface finite element method

as proposed by Dziuk (1988). Many of the proofs from main chapters are given in full detail here taken from Dziuk and Elliott (2013b). This section also includes details of numerical experiments which will be used as a basis for comparison for the other chapters.

Chapter 2

A finite element analysis of a coupled bulk-surface equation

2.1 Introduction

In this chapter, we will describe and analyse a method for solving equations arising from models with both bulk and surface effects taken into account. The key idea is to take a polyhedral approximation of the bulk region, consisting of a union of simplices, and to use its boundary faces as an approximation of the surface. Using the boundary faces in our calculations allows us to use the surface finite element method, as described in Appendix A, to calculate and analyse the surface terms in our equations. The novelty of this work is to combine these ideas with previous studies of Lenoir (1986), Bernardi (1989) and Dubois (1990) to account for the errors coming from the bulk terms.

We will restrict the presentation to a sample linear elliptic problem. Given a sufficiently smooth boundary, we will show error bounds of order h^k in the H^1 norm and order h^{k+1} in the L^2 norm, where k is the polynomial degree of the underlying finite element space and h is the mesh size. This coincides with both error estimates for planar domains (for example, Brenner and Scott 2002) and elliptic equations on surfaces (Demlow 2009). This is because any errors introduced by the approximation of the geometry are of the same order as interpolation errors.

2.1.1 The coupled system

For a bounded domain $\Omega \subset \mathbb{R}^n$ with boundary Γ, we seek solutions $u\colon \Omega \to \mathbb{R}$ and $v\colon \Gamma \to \mathbb{R}$ of the system

$$-\Delta u + u = f \quad \text{in } \Omega \tag{2.1.1a}$$

$$(\alpha u - \beta v) + \frac{\partial u}{\partial \nu} = 0 \quad \text{on } \Gamma \tag{2.1.1b}$$

$$-\Delta_\Gamma v + v + \frac{\partial u}{\partial \nu} = g \quad \text{on } \Gamma. \tag{2.1.1c}$$

Here we assume that f and g are known functions on Ω and Γ, respectively, and $\alpha, \beta > 0$ are positive constants. We can think of α and β as constants coming from non-dimensionalising a physical model. We denote by Δ_Γ the Laplace-Beltrami operator on Γ and by ν the outward pointing unit normal to Γ.

2.1.2 Outline of chapter

The chapter proceeds as follows. In the second section we will derive a variational form for the equations and explore existence, uniqueness and regularity of solutions. The third section focuses on how to construct our computational domain and the errors this introduces into our method. In the fourth section we develop the finite element method and in the fifth section we will look for error bounds for this method. In the final section we will show some numerical results.

Throughout, we will use the notation of Deckelnick et al. (2005) introduced in Appendix A.

2.2 Well-posedness of the continuous problem

In this section, we introduce the variational form that the method is based on. We go on to prove an existence and uniqueness result using the Lax-Milgram theorem (Evans 1998) and then show a regularity result by considering the bulk and surface equations separately. Throughout this chapter, we will make the same assumptions on the domain as in Appendix A, except now since $\Omega \subset \mathbb{R}^n$, we assume that Γ is an $(n-1)$-dimensional hypersurface.

2.2.1 Variational form

We take functions $\eta\colon \Omega \to \mathbb{R}$ and $\xi\colon \Gamma \to \mathbb{R}$ in a suitable space of test functions, multiply (2.1.1a) by η and (2.1.1c) by ξ. Applying integration by parts (A.2.8) gives

$$\int_\Omega \nabla u \cdot \nabla \eta + u\eta \,\mathrm{d}x - \int_\Gamma \eta \frac{\partial u}{\partial \nu} \,\mathrm{d}\sigma = \int_\Omega f\eta \,\mathrm{d}x, \tag{2.2.1a}$$

$$\int_\Gamma \nabla_\Gamma v \cdot \nabla_\Gamma \xi + v\xi \,\mathrm{d}\sigma + \int_\Gamma \frac{\partial u}{\partial \nu}\xi \,\mathrm{d}\sigma = \int_\Gamma g\xi \,\mathrm{d}\sigma. \tag{2.2.1b}$$

The boundary condition (2.1.1b) tells us that

$$-\int_\Gamma \eta \frac{\partial u}{\partial \nu} \,\mathrm{d}\sigma = \int_\Gamma (\alpha u - \beta v)\eta \,\mathrm{d}\sigma \quad \text{and} \quad \int_\Gamma \frac{\partial u}{\partial \nu}\xi \,\mathrm{d}\sigma = -\int_\Gamma (\alpha u - \beta v)\xi \,\mathrm{d}\sigma. \tag{2.2.2}$$

We substitute these into (2.2.1) to get

$$\int_\Omega \nabla u \cdot \nabla \eta + u\eta \,\mathrm{d}x + \int_\Gamma (\alpha u - \beta v)\eta \,\mathrm{d}\sigma = \int_\Omega f\eta \,\mathrm{d}x, \tag{2.2.3a}$$

$$\int_\Gamma \nabla_\Gamma v \cdot \nabla_\Gamma \xi + v\xi \,\mathrm{d}\sigma - \int_\Gamma (\alpha u - \beta v)\xi \,\mathrm{d}\sigma = \int_\Gamma g\eta \,\mathrm{d}\sigma. \tag{2.2.3b}$$

We now take a weighted sum of (2.2.3a) and (2.2.3b) to obtain the variational form

$$\begin{aligned} \alpha \int_\Omega \nabla u \cdot \nabla \eta + u\eta \,\mathrm{d}x + \beta \int_\Gamma \nabla_\Gamma v \cdot \nabla_\Gamma \xi + v\xi \,\mathrm{d}\sigma \\ + \int_\Gamma (\alpha u - \beta v)(\alpha \eta - \beta \xi) \,\mathrm{d}\sigma = \alpha \int_\Omega f\eta \,\mathrm{d}x + \beta \int_\Gamma g\xi \,\mathrm{d}\sigma. \end{aligned} \tag{2.2.4}$$

We will test this variational form over the space $H^1(\Omega) \times H^1(\Gamma)$, which we define to be the product space

$$H^1(\Omega) \times H^1(\Gamma) := \{(\eta, \xi) : \eta \in H^1(\Omega) \text{ and } \xi \in H^1(\Gamma)\}.$$

We equip this space with the inner product

$$\langle (\eta_1, \xi_1), (\eta_2, \xi_2) \rangle_{H^1(\Omega)\times H^1(\Gamma)} := \langle \eta_1, \eta_2 \rangle_{H^1(\Omega)} + \langle \xi_1, \xi_2 \rangle_{H^1(\Gamma)},$$

and induced norm given by

$$\|(\eta, \xi)\|_{H^1(\Omega)\times H^1(\Gamma)} := \left(\|\eta\|^2_{H^1(\Omega)} + \|\xi\|^2_{H^1(\Gamma)} \right)^{\frac{1}{2}}.$$

It is clear that $H^1(\Omega) \times H^1(\Gamma)$ is a Hilbert space with this inner product. Details of how to define the surface Sobolev space $H^1(\Gamma)$, and higher order spaces, can be found in Appendix A. Using a Sobolev space formulation requires us to interpret $u|_\Gamma$ in the trace sense:

Theorem 2.2.1 (Trace Theorem)**.** *Assume Ω is bounded and $\Gamma = \partial\Omega$ is C^1 and $1 \leq p < \infty$. Then there exists a bounded linear operator*

$$T\colon W^{1,p}(\Omega) \to L^p(\Gamma) \tag{2.2.5}$$

such that $Tw = w|_\Gamma$ if $w \in W^{1,p}(\Omega) \cap C(\bar{\Omega})$. Furthermore there exists a constant c_T, depending only on p and Ω such that

$$\|Tw\|_{L^p(\Gamma)} \leq c_T \|w\|_{W^{1,p}(\Omega)}, \tag{2.2.6}$$

for each $w \in W^{1,p}(\Omega)$. We call Tw the trace of w on Γ.

Proof. A proof is given is by Evans (1998, Chapter 5.5, Theorem 1). □

Throughout, we will write u for Tu on Γ.

We will approximate solutions of the weak from of (2.1.1): Find $(u, v) \in H^1(\Omega) \times H^1(\Gamma)$ such that

$$\begin{aligned} \alpha \int_\Omega \nabla u \cdot \nabla \eta + u\eta \,\mathrm{d}x + \beta \int_\Gamma \nabla_\Gamma v \cdot \nabla_\Gamma \xi + v\xi \,\mathrm{d}\sigma \\ + \int_\Gamma (\alpha u - \beta v)(\alpha\eta - \beta\xi) \,\mathrm{d}\sigma = \alpha \int_\Omega f\eta \,\mathrm{d}x + \beta \int_\Gamma g\xi \,\mathrm{d}\sigma \\ \text{for all } (\eta, \xi) \in H^1(\Omega) \times H^1(\Gamma). \end{aligned} \tag{2.2.7}$$

To help with the notations later, we will write $a\big((u, v), (\eta, \xi)\big)$ for the left-hand side of this equation and $l\big((\eta, \xi)\big)$ for the right-hand side. In this way, we can rewrite (2.2.7) as

$$a\big((u, v), (\eta, \xi)\big) = l\big((\eta, \xi)\big) \quad \text{for all } (\eta, \xi) \in H^1(\Omega) \times H^1(\Gamma). \tag{2.2.8}$$

2.2.2 Existence, uniqueness and regularity

To apply the standard Lax-Milgram techniques, we must show that a is bounded and coercive and l is bounded over $H^1(\Omega) \times H^1(\Gamma)$.

To see that a is bounded, we notice that for $(w,y),(\eta,\xi)\in H^1(\Omega)\times H^1(\Gamma)$,

$$\begin{aligned} a\big((w,y),(\eta,\xi)\big) &\le \alpha\,\|w\|_{H^1(\Omega)}\,\|\eta\|_{H^1(\Omega)} + \beta\,\|y\|_{H^1(\Gamma)}\,\|\xi\|_{H^1(\Gamma)} \\ &\quad + \int_\Gamma (\alpha w - \beta y)(\alpha\eta - \beta\xi)\,\mathrm{d}\sigma \\ &\le \sqrt{2}\max\{\alpha,\beta\}\,\|(w,y)\|_{H^1(\Omega)\times H^1(\Gamma)}\,\|(\eta,\xi)\|_{H^1(\Omega)\times H^1(\Gamma)} \\ &\quad + 2c_T^2\max\{\alpha,\beta\}^2\,\|(w,y)\|_{H^1(\Omega)\times H^1(\Gamma)}\,\|(\eta,\xi)\|_{H^1(\Omega)\times H^1(\Gamma)} \\ &\le c\,\|(w,y)\|_{H^1(\Omega)\times H^1(\Gamma)}\,\|(\eta,\xi)\|_{H^1(\Omega)\times H^1(\Gamma)}\,. \end{aligned} \tag{2.2.9}$$

Here c_T is the constant from the Trace Theorem (Theorem 2.2.1). Coercivity of a is immediate since we have for $(\eta,\xi)\in H^1(\Omega)\times H^1(\Gamma)$,

$$\begin{aligned} a\big((\eta,\xi),(\eta,\xi)\big) &= \alpha\,\|\eta\|^2_{H^1(\Omega)} + \beta\,\|\xi\|^2_{H^1(\Gamma)} + \|\alpha\eta - \beta\xi\|^2_{L^2(\Gamma)} \\ &\ge \sqrt{2}\min\{\alpha,\beta\}\,\|(\eta,\xi)\|^2_{H^1(\Omega)\times H^1(\Gamma)}\,. \end{aligned} \tag{2.2.10}$$

Hence a is coercive on $H^1(\Omega)\times H^1(\Gamma)$ as $\alpha,\beta>0$.

It is clear that l is bounded under the assumption that $f\in H^{-1}(\Omega)$ and $g\in H^{-1}(\Gamma)$.

Theorem 2.2.2 (Existence and uniqueness)**.** *Given $\alpha,\beta>0$, $f\in H^{-1}(\Omega)$ and $g\in H^{-1}(\Gamma)$ there exists a unique pair $(u,v)\in H^1(\Omega)\times H^1(\Gamma)$ such that*

$$a\big((u,v),(\eta,\xi)\big) = l\big((\eta,\xi)\big) \quad \textit{for all } (\eta,\xi)\in H^1(\Omega)\times H^1(\Gamma). \tag{2.2.11}$$

Furthermore, if Γ is C^3, we can achieve bounds in the H^2-norm by considering restricting the bilinear form a by setting η and ξ equal to zero in turn.

For $\eta=0$, we get

$$\beta\int_\Gamma \big(\nabla_\Gamma v\cdot\nabla_\Gamma\xi + v\xi\big)\,\mathrm{d}\sigma + \beta^2\int_\Gamma v\xi\,\mathrm{d}\sigma = \beta\int_\Gamma g\xi + \alpha\beta\int_\Gamma u\xi\,\mathrm{d}\sigma \quad \text{for all } \xi\in H^1(\Gamma).$$

This is exactly the variational form of the equation

$$-\beta\Delta_\Gamma v + (\beta+\beta^2)v = \beta g + \alpha\beta u \quad \text{on } \Gamma.$$

By the Trace Theorem (Theorem 2.2.1) and Theorem 2.2.2, we know that $u\in L^2(\Gamma)$. Hence by surface elliptic theory (Aubin 1982), similarly to Theorem A.2.5, we have that $v\in H^2(\Gamma)$ and have the bound

$$\|v\|_{H^2(\Gamma)} \le c\big(\,\|g\|_{L^2(\Gamma)} + \|v\|_{L^2(\Gamma)} + \|u\|_{H^1(\Omega)}\,\big). \tag{2.2.12}$$

For $\xi = 0$, we get

$$\alpha \int_\Omega \big(\nabla u \cdot \nabla \eta + u\eta\big)\,\mathrm{d}x + \alpha^2 u\eta\,\mathrm{d}\sigma = \alpha \int_\Omega f\eta\,\mathrm{d}x + \alpha\beta \int_\Gamma v\eta\,\mathrm{d}\sigma \quad \text{for all } \eta \in H^1(\Omega).$$

This equation arises as the variational form of the equation

$$\begin{aligned} -\alpha\Delta u + \alpha u &= \alpha f \text{ in } \Omega \\ \frac{\partial u}{\partial \nu} + \alpha u &= \beta v \text{ on } \Gamma. \end{aligned}$$

By regularity theory of elliptic problems with Robin boundary data (see Ladyzhenskaia and Uraltseva (1968) or Gilbarg and Trudinger (2001)), if Γ is C^3, we have that $u \in H^2(\Omega)$ with the bound

$$\|u\|_{H^2(\Omega)} \leq c\big(\,\|f\|_{L^2(\Omega)} + \|v\|_{H^{1/2}(\Gamma)}\,\big). \tag{2.2.13}$$

Combining (2.2.12) and (2.2.13) gives the following regularity result:

Theorem 2.2.3 (Regularity)**.** *Let Γ be C^3, $f \in L^2(\Omega)$, $g \in L^2(\Gamma)$ and $\alpha, \beta > 0$. If (u, v) solves the variational problem (2.2.7) then $(u, v) \in H^2(\Omega) \times H^2(\Gamma)$ and*

$$\|(u, v)\|_{H^2(\Omega)\times H^2(\Gamma)} \leq c\big(\,\|f\|_{L^2(\Omega)} + \|g\|_{L^2(\Omega)}\,\big). \tag{2.2.14}$$

2.3 Domain perturbation

The first step we take in discretising the system (2.1.1) is to create a polyhedral domain $\check{\Omega}_h$ with boundary $\check{\Gamma}_h$ and then describe higher order approximations $\Omega_h^{(k)}$ and $\Gamma_h^{(k)}$. Our finite element method will be based on these domains. In this section, we will explain how to construct such a domain and provide estimates for the errors introduced by approximating the domain. To prove the results in this section, we will assume Γ is C^{k+1}.

2.3.1 Domain approximation

We follow ideas taken from the work of Lenoir (1986), Bernardi (1989) and Dubois (1990) in order to define the triangulation of our bulk domain and results of Dziuk (1988), Dziuk and Elliott (2007a) and Demlow (2009) to make estimates about the perturbation of the boundary of this domain. The higher order surface finite element space, used here, are described in Heine (2005).

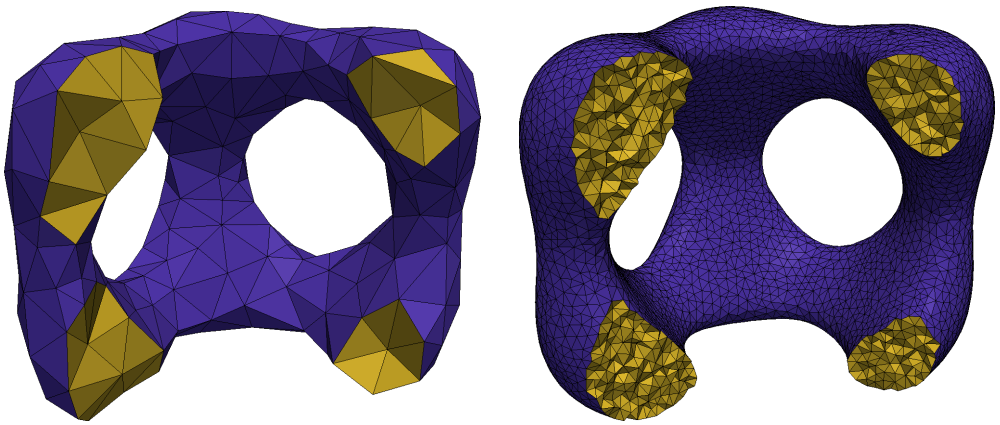

Figure 2.3.1: An example of a triangulated domains $\check{\Omega}_h$ in $\mathbb{R}^3$, cut open to see the interior simplices. These have been created using the CGAL package's 3D Mesh Generation demos. See Alliez et al. (2012) for details. These polyhedra are approximations of $\Omega = \{x : \Phi(x) < 0\}$ with Φ from (2.6.1)

.

Let $\check{\Omega}_h$ be a polyhedral approximation of Ω and set $\check{\Gamma}_h := \partial\check{\Omega}_h$. We suppose that the faces of $\check{\Gamma}_h$ are $(N-1)$ simplices whose vertices lie on Γ so that $\check{\Gamma}_h$ is a discrete approximation of Γ in the sense of Section A.3.1. We assume this is given at the start of the procedure; see for example Figure 2.3.1. We take a quasi-uniform triangulation $\check{\mathscr{T}}_h$ of $\check{\Omega}_h$ (Definition A.3.1) consisting of closed simplices, either triangles in $\mathbb{R}^2$ or tetrahedra in $\mathbb{R}^3$.

We define $h := \max\{\operatorname{diam}(T) : T \in \check{\mathscr{T}}_h\}$ and assume that h is sufficiently small so that $\check{\Gamma}_h \subseteq U$ so that for all $x \in \check{\Gamma}_h$, there exists a unique point $p = p(x) \in \Gamma$ defined by (A.2.2). Finally, we assume that for each $T \in \check{\mathscr{T}}_h$, $T \cap \check{\Gamma}_h$ has at most one face of T.

Exact triangulation

In order to define our computational domains, we first define an exact triangulation of Ω. An exact triangulation is made up of 'curved simplices' which together cover all of Ω exactly.

The unit reference n-simplex is defined to be the unit simplex with vertices at $(0,\dots,0)$, $(1,0,\dots,0)$, $(0,1,0,\dots,0)$, $\dots$, $(0,\dots,0,1)$. For each simplex $T \in \check{\mathscr{T}}_h$, we define an affine function $F_T\colon \mathbb{R}^n \to \mathbb{R}^n$ which maps the unit reference n-simplex $\hat{T}$ onto T (mapping the vertices of $\hat{T}$ onto the vertices of T) which we write as

$$F_T(\hat{x}) = A_T\hat{x} + b_T \quad \text{for } \hat{x} \in \hat{T}. \tag{2.3.1}$$

We say that a closed set T^e is a curved n-simplex if there exists a C^1-mapping F_T^e that maps $\hat{T}$ onto T^e that is of the form

$$F_T^e = F_T + \Phi_T, \tag{2.3.2}$$

where F_T is the affine map from (2.3.1) and Φ_T is a C^1-mapping from $\hat{T}$ to $\mathbb{R}^n$ satisfying

$$C_T := \sup_{\hat{x}\in\hat{T}} \left| D\Phi_T(\hat{x}) A_T^{-1} \right| < 1. \tag{2.3.3}$$

From this definition, we immediately have the following result:

Proposition 2.3.1. *If the F_T^e exists, then it is a C^1-diffeomorphism from $\hat{T}$ onto T^e and satisfies*

$$\sup_{\hat{x}\in\hat{T}} |DF_T^e(\hat{x})| \leq (1 + C_T) |A_T|, \tag{2.3.4a}$$

$$\sup_{x\in T^e} \left| D(F_T^e)^{-1}(x) \right| \leq (1 - C_T)^{-1} |A_T|^{-1}, \tag{2.3.4b}$$

$$(1 - C_T)^n |\det A_T| \leq |\det DF_T^e(\hat{x})| \leq (1 + C_T)^n |\det A_T| \quad \text{for all } \hat{x} \in \hat{T}. \tag{2.3.4c}$$

We define an exact triangulation of a domain as a set of curved simplices $\mathscr{T}_h^e$ such that

$$\bigcup_{T^e\in\mathscr{T}_h^e} T^e = \bar{\Omega} \qquad \text{and} \qquad \sup_{T\in\check{\mathscr{T}}_h} C_T \leq C < 1.$$

There are several ways of defining such a Φ_T given in the literature. Zlamal (1973, 1974) and Scott (1973) considered problems with finite element spaces defined over curved spaces. Scott gives an explicit construction of an exact triangulation in two space dimensions which was generalised by Lenoir (1986) to arbitrary dimensions. Here, we will use a construction based on work by Dubois (1990) which uses the normal projection operator (A.2.2). We will adopt the notation used by Bänsch and Deckelnick (1999) and Deckelnick, Günther and Hinze (2009).

Bearing in mind our assumption on the triangulation, each $T \in \check{\mathscr{T}}_h$ is either an internal simplex, with at most one node on $\check{\Gamma}_h$, in which case we set $\Phi_T = 0$; or T has more than one node on the boundary. If T is not an internal simplex, we denote by $l \geq 2$ the number of nodes of T that lie on $\check{\Gamma}_h$ and denote by $\psi_1, \ldots, \psi_{n+1}$ the vertices of T, ordered so that $\psi_1, \ldots, \psi_l$ lie on $\check{\Gamma}_h$. For each point $x \in T$, we define barycentric coordinates by

$$x = \sum_{j=1}^{n+1} \lambda_j \psi_j$$

and write $\hat{x} = (\lambda_1, \lambda_2, \ldots, \ldots, \lambda_n)$. We next introduce

$$\lambda^* = \lambda^*(\hat{x}) = \sum_{j=1}^{l} \lambda_j \quad \text{and} \quad \hat{\sigma} = \{\hat{x} \in \hat{X} : \lambda^*(\hat{x}) = 0\}.$$

In three dimensions, $\hat{\sigma}$ falls into the following cases:

1. If $T \cap \check{\Gamma}_h$ is an edge of a tetrahedron ($l = 2$), then $\hat{\sigma}$ is the inverse image of the edge spanned by ψ_3, ψ_4 under F_T;
2. If $T \cap \check{\Gamma}_h$ is a face of a tetrahedron ($l = 3$), then $\hat{\sigma}$ is the point $F_T^{-1}(\psi_4)$.

For $\hat{x} \notin \hat{\sigma}$, we denote the projection of x onto $\tau = T \cap \check{\Gamma}_h$ by $y = y(\hat{x})$ defined by

$$y = \sum_{j=1}^{l} \frac{\lambda_j}{\lambda^*} \psi_j \in \tau. \tag{2.3.5}$$

Then using the normal projection $p(y) \in \Gamma$ of y given by (A.2.2), we define Φ_T.

Definition 2.3.2. Given $k \in \mathbb{N}$, we define $\Phi_T \colon \hat{T} \to \mathbb{R}^n$ by

$$\Phi_T(\hat{x}) := \begin{cases} (\lambda^*)^{k+2}(p(y) - y) & \text{if } \hat{x} \notin \hat{\sigma} \\ 0 & \text{if } \hat{x} \in \hat{\sigma}. \end{cases} \tag{2.3.6}$$

We now follow a sequence of lemmas from Bernardi (1989) to show that Φ_T is C^1 and satisfies (2.3.3).

Lemma 2.3.3. *The mapping y is C^{k+1} on $\hat{T} \setminus \hat{\sigma}$ and satisfies*

$$\|D_{\hat{x}}^m y\|_{L^\infty(\hat{T}\setminus\hat{\sigma})} \leq \frac{ch}{(\lambda^*)^m} \quad \textit{for } 1 \leq m \leq k+1. \tag{2.3.7}$$

Proof. The proof is given in Lemma 6.2 by Bernardi (1989). □

Lemma 2.3.4. *The mapping $p(y)$ is of class C^{k+1} on $\hat{T} \setminus \hat{\sigma}$ and we have the bound*

$$\|D_{\hat{x}}^m (p(y) - y)\|_{L^\infty(\hat{T}\setminus\hat{\sigma})} \leq \frac{ch^2}{(\lambda^*)^m} \quad \textit{for } 1 \leq m \leq k+1. \tag{2.3.8}$$

Proof. Using Equation 2.9 from Bernardi (1989),

$$D^m(f \circ g) = \sum_{r=1}^{m} D^r f \left(\sum_{\underline{i} \in E(m,r)} c_{\underline{i}} \prod_{q=1}^{m} (D^q g)^{i_q} \right)$$

where

$$E(m,r) = \left\{ \underline{i} = (i_1, \dots, i_m) \in \mathbb{N}^m : \sum_{q=1}^{m} i_q = r \text{ and } \sum_{q=1}^{m} q\, i_q = m \right\},$$

we remark that

$$\|D^m_{\hat{x}}(p(y)-y)\|_{L^\infty(\hat{T}\setminus\hat{\sigma})} \leq c \sum_{r=1}^{m} \left(\left\|D^r_y(p(y)-y)\right\|_{L^\infty(\tau)} \prod_{q=1}^{m} \left\|D^q_{\hat{x}} y\right\|^{i_q}_{L^\infty(\hat{T}\setminus\hat{\sigma})} \right).$$

We notice that $p(y) = y$ if $y = \psi_j$ for any $0 \leq j \leq l$ – that is if y is a corner of T lying on $\tau = T \cap \check{\Gamma}_h$ – so $y|_\tau$ can be seen as a linear interpolant of $p(y)$ on τ. Hence from our geometric assumptions on Γ, $\left\|D^r_y(p(y)-y)\right\|_{L^\infty(\tau)} \leq ch^{2-r}$ for $0 \leq r \leq 2$.

Using (2.3.7), we see if $m \leq 2$,

$$\|D^m_{\hat{x}}(p(y)-y)\|_{L^\infty(\hat{T}\setminus\hat{\sigma})} \leq c \sum_{r=1}^{m} \frac{h^{2-r} h^{(\sum_{q=1}^m i_q)}}{(\lambda^*)^{(\sum_{q=1}^m q\, i_q)}} \leq \frac{ch^2}{(\lambda^*)^m},$$

and if $m > 2$,

$$\|D^m_{\hat{x}}(p(y)-y)\|_{L^\infty(\hat{T}\setminus\hat{\sigma})} \leq c \left(\sum_{r=1}^{2} \frac{h^{2-r} h^{(\sum_{q=1}^m i_q)}}{(\lambda^*)^{(\sum_{q=1}^m q\, i_q)}} + \sum_{r=3}^{m} \frac{h^{(\sum_{q=1}^m i_q)}}{(\lambda^*)^{(\sum_{q=1}^m q\, i_q)}} \right) \leq \frac{ch^2}{(\lambda^*)^m}. \square$$

Proposition 2.3.5. *The mapping Φ_T is C^{k+1} on $\hat{T}$ and we have the bound*

$$\|D^m \Phi_T\|_{L^\infty(\hat{T})} \leq ch^2 \quad \text{for } 0 \leq m \leq k+1. \tag{2.3.9}$$

Furthermore, Φ_T satisfies (2.3.3).

Proof. Using the Leibniz formula, we have for any $\hat{x} \in \hat{T} \setminus \hat{\sigma}$,

$$\begin{aligned} D^m \Phi_T(\hat{x}) &= D^m_{\hat{x}}\big((\lambda^*)^{k+2}(p(y)-y)\big) \\ &= \sum_{r=0}^{m} \binom{m}{r} (k+2)\dots(k+3-r)(\lambda^*)^{k+2-r} (D_{\hat{x}}\lambda^*)^r D^{m-r}_{\hat{x}}(p(y)-y). \end{aligned}$$

Applying (2.3.8) gives

$$\left\|D^m_{\hat{x}}\big((\lambda^*)^{k+2}(p(y)-y)\big)\right\|_{L^\infty(\hat{T}\setminus\hat{\sigma})} \leq c \sum_{r=0}^{m} (\lambda^*)^{k+2-r} \frac{ch^2}{(\lambda^*)^{m-r}} \leq ch^2 (\lambda^*)^{k+2-m}.$$

The mapping Φ_T is C^{k+1} on $\hat{T} \setminus \hat{\sigma}$ with derivatives of order less than or equal to

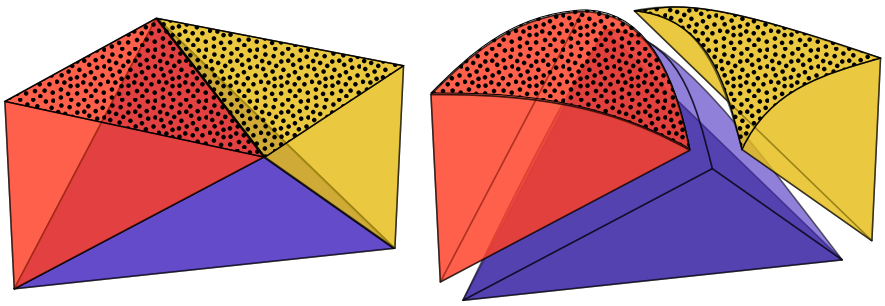

Figure 2.3.2: A plot of two sections of triangulation. The left shows three tetrahedra in $\check{\mathscr{T}}_h$ and the right shows the corresponding three tetrahedra in $\mathscr{T}_h^e$. The surface is shown by spots on both sides. The red and yellow tetrahedra (left and right in each image) share a face with the boundary ($l = 3$) and the blue tetrahedron (centre in each image) shares an edge with the boundary ($l = 2$). This means the red and yellow curved tetrahedra have four curved faces and the blue tetrahedron has two curved faces.

$k+1$ tending to zero when $\hat{x}$ tends to a point in $\hat{\sigma}$, since $\lambda^* = 0$ for $\hat{x} \in \hat{\sigma}$. Hence, Φ_T is a C^{k+1} mapping on $\hat{T}$ (Gilbarg and Trudinger 2001, p. 10) which satisfies (2.3.9).

Since $|\partial \hat{x}_l / \partial x_j| \leq ch$, (Ciarlet and Raviart 1972a, p. 239), we know that

$$\left|A_T^{-1}\right| = \frac{c}{h} \quad \text{and} \quad C_T \leq \sup_{\hat{x}\in\hat{T}} \left(|D\Phi_T \hat{x}| \, |A_T|^{-1} \right) \leq ch.$$

Hence Φ_T satisfies (2.3.3) for h small enough. □

We will call the exact triangulation, defined by F_T^e above, $\mathscr{T}_h^e$. Note that under this construction, in three dimensions, simplices in $\mathscr{T}_h^e$, which have more than one vertex on the boundary, can have more than one curved face. See Figure 2.3.2 for example.

Remark 2.3.6. Note that we could have chosen $\Phi_T(\hat{x}) = \lambda^*(p(y) - y)$. This would define an exact triangulation of Ω however this function is not $C^1(T)$, since the first derivatives are not continuous at $\lambda^* = 0$. This would mean the interpolation theory of Bernardi (1989) would not be available. Our construction combines the ideas of Lenoir (1986) and Dubois (1990).

Computational domain

We are now in a position to define our computational domains $\Omega_h^{(k)}$ and $\Gamma_h^{(k)}$. Given $T \in \check{\mathscr{T}}_h$, let $\phi_1^k, \ldots, \phi_{n_k}^k$ be a Lagrangian basis of degree k on $\hat{T}$ corresponding to the nodal points $\hat{x}^1, \ldots, \hat{x}^{n_k}$ (see Figure 2.4.1). Then for $\hat{x} \in \hat{T}$, we can define a

parametrisation of a polynomial simplex $T^{(k)}$ by

$$F_T^{(k)}(\hat{x}) = \sum_{j=1}^{n_k} F_T^e(\hat{x}^j)\phi_j^k(\hat{x}). \tag{2.3.10}$$

We can carry out this procedure for each simplex $T \in \check{\mathscr{T}}_h$. Since the basis functions $\{\phi_j^k\}$ are unisolvent, $F_T^{(k)}$ is also a diffeomorphism on each simplex. We define $\Omega_h^{(k)}$ as the union of elements $\mathscr{T}_h^{(k)}$ given by

$$T^{(k)} := \{F_T^{(k)}(\hat{x}) : \hat{x} \in \hat{T}\}, \qquad \mathscr{T}_h^{(k)} := \{T^{(k)} : T \in \check{\mathscr{T}}_h\}.$$

Then $\Gamma_h^{(k)}$ is defined to be the boundary of the domain $\Omega_h^{(k)}$ with triangulation $\mathscr{T}_h^{(k)}\Big|_{\Gamma_h^{(k)}}$. The choice of Lagrangian basis ensures that the nodes of $\Gamma_h^{(k)}$ lie on Γ. This construction admits quasi-uniform triangulations $\mathscr{T}_h^{(k)}$ and $\mathscr{T}_h^{(k)}\Big|_{\Gamma_h^{(k)}}$ for $\Omega_h^{(k)}$ and $\Gamma_h^{(k)}$, respectively. Note that, like the exact simplices in $\mathscr{T}_h^e$, the simplices in $\mathscr{T}_h^{(k)}$ can have curved (polynomial) faces.

2.3.2 Bulk estimates

In this section, we will bound the difference between the exact and computational domains using the fact that $F_T^{(k)}$ is an interpolant of the parametrisation F_T^e.

We define a function $G_h \colon \Omega_h^{(k)} \to \Omega$ locally by $G_h|_{T^{(k)}} := F_T^e \circ (F_T^{(k)})^{-1}$ for each $T^{(k)} \in \mathscr{T}_h^{(k)}$. This is a homeomorphism, which when restricted to interior simplices (those with at most one vertex on the boundary) is the identity map. We use the notation DG_h for the gradient of G_h, where $(DG_h)_{ij} = (\partial/\partial x_j)(G_h)_i$ and DG_h^{t} for its transpose. We will also write DG_h^{-1} for $D(G_h^{-1}) = (DG_h)^{-1}$. We denote by $J_h|_T$ the absolute value of the determinant of $DG_h|_T$.

We denote by B_h the union of elements in $\mathscr{T}_h^{(k)}$ which have more than one vertex on the boundary $\Gamma_h^{(k)}$ and $B_h^\ell = G_h(B_h)$ the associated exact elements in $\mathscr{T}_h^e$. Note that B_h is the region where G_h is different from the identity.

Let us use the notation that for a fixed $\hat{x} \in \hat{T}$, we denote $F_T^{(k)}(\hat{x}) = x$, then one may write that

$$G_h(x) = F_T^e\big((F_T^{(k)})^{-1}(x)\big) = F_T^e(\hat{x}) = x + \big(F_T^e(\hat{x}) - F_T^{(k)}(\hat{x})\big). \tag{2.3.11}$$

Lemma 2.3.7. *If Γ is C^{k+1}, then $G_h|_{T^{(k)}}$ is $C^{k+1}(T^{(k)})$ for each $T^{(k)} \in \mathscr{T}_h^{(k)}$ and we have that $\|G_h\|_{W^{k+1,\infty}(T^{(k)})}$ is bounded independently of h.*

Proof. Using (2.3.11), we can write G_h as

$$G_h(x) = F_T(\hat{x}) + \Phi_T(\hat{x}).$$

Since $x \mapsto \hat{x}$ is smooth on each element, G_h is the sum of an affine function and a C^{k+1} function, so G_h is of class C^{k+1} on $T^{(k)}$. To achieve the bound independently of h, we use (2.3.3). □

The next proposition is the main result in this section. It gives bounds on the geometric errors between Ω and Ω_h. We show this bound for boundary simplices only since for interior simplices $DG_h^t|_T = \mathrm{Id}$ and $J_h|_T = 1$.

Proposition 2.3.8 (Geometric bulk estimates)**.** *Let $T \in \mathscr{T}_h^{(k)}$ be a boundary simplex and T^e the associated exact simplex in $\mathscr{T}_h^e$. Under the assumption that $\mathscr{T}_h$ is quasi-uniform, for sufficiently small h, we have that*

$$\left\| DG_h^t|_T - \mathrm{Id} \right\|_{L^\infty(T)} \leq ch^k \tag{2.3.12a}$$

$$\left\| J_h|_T - 1 \right\|_{L^\infty(T)} \leq ch^k. \tag{2.3.12b}$$

Proof. We will show that

$$\left| \frac{\partial}{\partial x_j} (G_h)_i - \delta_{ij} \right| \leq ch^k,$$

which will show the required bounds. The first result follows a simple calculations and the second is shown by Ipsen and Rehman (2008).

We start by taking the x_j derivative of G_h to get

$$\frac{\partial}{\partial x_j} (G_h)_i = \sum_l \frac{\partial (F_T^{(k)})^{-1}(x)_l}{\partial x_j} \frac{\partial \big(F_T^e(\hat{x})\big)_i}{\partial \hat{x}_l},$$

where we have used the substitution $F_T^{(k)}(\hat{x}) = x$. Similarly, we have

$$\delta_{ij} = \frac{\partial (F_T^{(k)})^{-1}(x)_i}{\partial x_j} = \sum_l \frac{\partial (F_T^{(k)})^{-1}(x)_l}{\partial x_j} \frac{\partial \big(F_T^{(k)}(\hat{x})\big)_i}{\partial \hat{x}_l}.$$

Hence

$$\frac{\partial}{\partial x_j} (G_h)_i - \delta_{ij} = \sum_l \frac{\partial (F_T^{(k)})^{-1}(x)_l}{\partial x_j} \frac{\partial}{\partial \hat{x}_l} \big(F_T^e(\hat{x}) - F_T^{(k)}(\hat{x})\big)_i.$$

It is classical (Ciarlet and Raviart 1972a, Lemma 7, p. 238) that

$$\left|\frac{\partial\left((F_T^{(k)})^{-1}(\hat{x})\right)_l}{\partial x_j}\right| = \left|\frac{\partial \hat{x}_l}{\partial x_j}\right| \leq \frac{c}{h},$$

and from standard interpolation theory, we see that

$$\left|\frac{\partial}{\partial \hat{x}_l}\left(F_T^e(\hat{x}) - F_T^{(k)}(\hat{x})\right)_i\right| \leq c\left\|D_{\hat{x}}^{k+1}(F_T^e)\right\|_{L^\infty(\hat{T})}.$$

However we may use the fact that $\left|D_{\hat{x}}^{m+1}x_j\right| \leq ch^m$ (Ciarlet and Raviart 1972a, p. 239) and change coordinates to see

$$\left\|D_{\hat{x}}^{k+1}(F_T^e)\right\|_{L^\infty(\hat{T})} \leq ch^{k+1}\left\|F_T^e \circ (F_T^{(k)})^{-1}\right\|_{W^{k+1,\infty}(T^{(k)})} = ch^{k+1}\left\|G_h\right\|_{W^{k+1,\infty}(T^{(k)})}.$$

From Lemma 2.3.7, we know $\|G_h\|_{W^{k+1,\infty}(T^{(k)})}$ is bounded independently of h, this shows that

$$\left|\frac{\partial}{\partial x_j}(G_h)_i - \delta_{ij}\right| \leq ch^k. \qquad \square$$

We next show how we can relate functions defined on the exact and computational domains. We do this through a 'lifting' process.

Definition 2.3.9. For a function $\eta_h \colon \Omega_h^{(k)} \to \mathbb{R}$, we define its lift $\eta_h^\ell \colon \Omega \to \mathbb{R}$ by

$$\eta_h^\ell := \eta_h \circ G_h^{-1}. \tag{2.3.13}$$

For a function $\eta \colon \Omega \to \mathbb{R}$, we can define its inverse lift $\eta^{-\ell} \colon \Omega_h^{(k)} \to \mathbb{R}$ by

$$\eta^{-\ell} := \eta \circ G_h. \tag{2.3.14}$$

From this definition, it follows that $(\eta^{-\ell})^\ell = \eta$. We can show that norms on Ω and $\Omega_h^{(k)}$ are equivalent using this process:

Proposition 2.3.10. *Let $\eta_h \colon \Omega_h^{(k)} \to \mathbb{R}$ and let $\eta_h^\ell \colon \Omega \to \mathbb{R}$ be its lift. Then there exists constants $c_1, c_2 > 0$, independent of h, such that*

$$c_1\left\|\eta_h^\ell\right\|_{L^2(\Omega)} \leq \|\eta_h\|_{L^2(\Omega_h^{(k)})} \leq c_2\left\|\eta_h^\ell\right\|_{L^2(\Omega)}, \tag{2.3.15a}$$

$$c_1\left\|\nabla\eta_h^\ell\right\|_{L^2(\Omega)} \leq \|\nabla\eta_h\|_{L^2(\Omega_h^{(k)})} \leq c_2\left\|\nabla\eta_h^\ell\right\|_{L^2(\Omega)}. \tag{2.3.15b}$$

Proof. Using the transformation $y = G_h(x)$, we can write integrals over $\Omega_h^{(k)}$ as

$$\int_{\Omega_h^{(k)}} \eta_h(x)\,\mathrm{d}x = \int_\Omega \eta_h^\ell(y)(J_h^\ell(y))^{-1}\,\mathrm{d}y,$$

and the gradient of $\Omega_h^{(k)}$ as

$$\nabla_x \eta_h(x) = DG_h^{\mathrm{t}}(y)\nabla_y \eta_h^\ell(y).$$

The two results then simply follow by applying the previous proposition. □

In the following error analysis, we will require the following narrow band trace inequality.

Lemma 2.3.11. *Let $\mathcal{N}_\delta \subseteq U$ be the band of width δ, given by*

$$\mathcal{N}_\delta = \{x \in \Omega : -\delta < d(x) < 0\}, \tag{2.3.16}$$

where d is the signed distance function to Γ. Assuming that $\delta > 0$ is sufficiently small so that $\mathcal{N}_\delta \subset U$, it holds that for $\eta \in H^1(\Omega)$

$$\|\eta\|_{L^2(\mathcal{N}_\delta)} \leq c\delta^{\frac{1}{2}} \|\eta\|_{H^1(\Omega)}. \tag{2.3.17}$$

Proof. After this proof was written, the author was informed that this result was given by Oganesyan and Rukhovets (1979).

First, we may assume that $\eta \in C^1(\Omega)$, since the more general result will follow by a density argument. Note that $d \in C^2(\mathcal{N}_\delta)$ and $|\nabla d| = 1$ on $\mathcal{N}_\delta$. We can apply the co-area formula to integrals over $\mathcal{N}_\delta$ as follows:

$$\int_{\mathcal{N}_\delta} \eta(y)^2\,\mathrm{d}y = \int_{\mathcal{N}_\delta} \eta(y)^2\,|\nabla d(y)|\,\mathrm{d}y = \int_{-\delta}^0 \left(\int_{\Gamma_s} \eta^2|_{\Gamma_s}\,\mathrm{d}\sigma \right) \mathrm{d}s. \tag{2.3.18}$$

Here Γ_s denotes the C^2 hypersurface which is the inverse images of s under d, namely $\Gamma_s = \{x \in \mathcal{N}_\delta : d(x) = s\}$.

Next, we wish to apply a trace inequality type argument to bound the right-hand side of this equation. We follow the proof of the trace inequality from Grisvard (2011, Theorem 1.5.1.10). Let the vector field $D\colon \bar{\Omega} \to \mathbb{R}^n$ be an extension of ∇d in $C^1(\bar{\Omega})$, equal to ∇d on $\mathcal{N}_\delta$, with the bound $\|D\|_{C^1(\bar{\Omega})} \leq c\,\|d\|_{C^2(\mathcal{N}_\delta)}$. Setting $\Omega_s = \{x \in \Omega : d(x) < s\}$, we have that

$$\int_{\Omega_s} \nabla(\eta^2) \cdot D\,\mathrm{d}x = 2\int_{\Omega_s} \eta\nabla\eta \cdot D\,\mathrm{d}x.$$

On the other hand, applying Green's theorem, using the notation ν_s for the normal to Γ_s, we obtain

$$\int_{\Omega_s} \nabla(\eta^2) \cdot D \,\mathrm{d}x = \int_{\Gamma_s} \eta^2 \, D \cdot \nu_s \,\mathrm{d}\sigma - \int_{\Omega_s} \eta^2 \, \nabla \cdot D \,\mathrm{d}x.$$

Since $D \cdot \nu_s = 1$ on Γ_s, combining these two equations we have that

$$\int_{\Gamma_s} \eta^2 \, D \cdot \nu_s \,\mathrm{d}\sigma = 2 \int_{\Omega_s} \eta \, \nabla\eta \cdot D \,\mathrm{d}x + \int_{\Omega_s} \eta \, \nabla \cdot D \,\mathrm{d}x,$$

which means that

$$\int_{\Gamma_s} \eta^2 \,\mathrm{d}\sigma \leq 2 \max_{\bar{\Omega}_s} |D| \int_{\Omega_s} |\eta| \, |\nabla\eta| \,\mathrm{d}x + \max_{\bar{\Omega}_s} |\nabla \cdot D| \int_{\Omega_s} \eta^2 \,\mathrm{d}x.$$

Since we have that $\Omega_s \subseteq \Omega$, applying a Young's inequality gives

$$\int_{\Gamma_s} \eta^2 \,\mathrm{d}\sigma \leq c \, \|D\|_{C^1(\bar{\Omega})} \int_{\Omega} \left(|\nabla\eta|^2 + \eta^2 \right) \mathrm{d}x.$$

Hence, using (2.3.18), we have that

$$\|\eta\|^2_{L^2(\mathcal{N}_\delta)} \leq c\delta \, \|\eta\|^2_{H^1(\Omega)} \,. \qquad \square$$

2.3.3 Surface estimates

In this section, we will recall results for the approximation of the surface. These follow since $\Gamma_h^{(k)}$ can be viewed an an interpolant of Γ. Proofs of these results for $k = 1$ are given in Appendix A. Proofs for $k \geq 1$ are given by Demlow (2009).

We remark that these proofs are available since $G_h|_{\Gamma_h^{(k)}} = p|_{\Gamma_h^{(k)}}$, the closest point operator.

Proposition 2.3.12 (Geometric surface estimates)**.** *Under our assumptions on* Γ *and* $\Gamma_h^{(k)}$*, we have that*

$$\|d\|_{L^\infty(\Gamma_h^{(k)})} \leq ch^{k+1}. \tag{2.3.19}$$

Let μ_h *be the quotient of measures on the surface and approximate surface, so that* $\mathrm{d}\sigma = \mu_h \,\mathrm{d}\sigma_h$*. Then we have the estimate*

$$\sup_{\Gamma_h^{(k)}} |1 - \mu_h| \leq ch^{k+1}. \tag{2.3.20}$$

Let P *and* P_h *denote projections onto the tangent space of* Γ *and* Γ_h *respectively.*

We introduce the notation

$$\mathcal{Q}_h = \frac{1}{\mu_h}(\mathrm{Id} - d\mathcal{H})PP_hP(\mathrm{Id} - d\mathcal{H}), \tag{2.3.21}$$

then we have the estimate

$$|P - \mathcal{Q}_h| \leq ch^{k+1}. \tag{2.3.22}$$

We use the closest point operator (A.2.2) to define the lift of surface functions.

Definition 2.3.13. Given $\xi_h \colon \Gamma_h^{(k)} \to \mathbb{R}$, we define its lift, denoted by $\xi_h^\ell \colon \Gamma \to \mathbb{R}$, (implicitly) by

$$\xi_h^\ell(p(x)) := \xi_h(x). \tag{2.3.23}$$

Similarly, for a function $\xi \colon \Gamma \to \mathbb{R}$, we define its inverse lift, written $\xi^{-\ell} \colon \Gamma_h^{(k)} \to \mathbb{R}$, by

$$\xi^{-\ell}(x) := \xi(p(x)). \tag{2.3.24}$$

Similarly to Proposition 2.3.10, we have a result equating norms on Γ and $\Gamma_h^{(k)}$.

Proposition 2.3.14. *Let $\xi_h \colon \Gamma_h^{(k)} \to \mathbb{R}$ and let $\xi_h^\ell \colon \Gamma \to \mathbb{R}$ be its lift. Then there exists constants $c_1, c_2 > 0$, independent of h, such that*

$$c_1 \left\| \xi_h^\ell \right\|_{L^2(\Gamma)} \leq \|\xi_h\|_{L^2(\Gamma_h^{(k)})} \leq c_2 \left\| \xi_h^\ell \right\|_{L^2(\Gamma)}, \tag{2.3.25a}$$

$$c_1 \left\| \nabla_\Gamma \xi_h^\ell \right\|_{L^2(\Gamma)} \leq \|\nabla_{\Gamma_h} \xi_h\|_{L^2(\Gamma_h^{(k)})} \leq c_2 \left\| \nabla_\Gamma \xi_h^\ell \right\|_{L^2(\Gamma)}. \tag{2.3.25b}$$

2.4 Finite element method

This section describes our finite element method. In this chapter, we will use piecewise polynomial finite element functions of the same degree as the approximation of the domain. This leads to so-called isoparametric elements which will give the optimal rate of convergence. One could also implement this method with different order finite element functions, although this would lead to a suboptimal order error.

2.4.1 Isoparametric finite element spaces

We use this section to define finite element spaces $V_h^{(k)}$ and $S_h^{(k)}$ used in our finite element method. We recall that the computational domains $\Omega_h^{(k)}$ and $\Gamma_h^{(k)}$ are defined by element-wise parametrisations $F_T^{(k)} \colon \hat{T} \to T^{(k)} \subseteq \Omega_h^{(k)}$ (2.3.10). In both the bulk and surface cases, we define the finite element functions to be continuous functions which are piecewise polynomials of degree k with respect to the barycentric

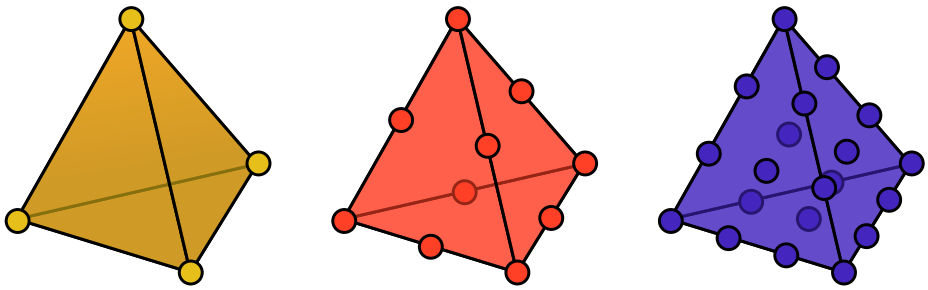

(a) $k = 1$, 4 nodes (b) $k = 2$, 10 nodes (c) $k = 3$, 20 nodes

Figure 2.4.1: The locations of the order k Lagrangian nodes in three space dimensions on a tetrahedron.

coordinates of the reference element in dimensions n and $n-1$. An important part of the construction is that the trace of a finite element function from $V_h^{(k)}$ on $\Gamma_h^{(k)}$ lies in $S_h^{(k)}$.

More precisely, for the bulk finite element functions, we define

$$V_h^{(k)} := \{\eta_h \in C(\Omega_h^{(k)}) : \eta_h|_T = \hat{\eta}_h \circ (F_T^{(k)})^{-1} \text{ with } \hat{\eta}_h \in P_k(\hat{T}) \text{ for all } T \in \mathscr{T}_h^{(k)}\}. \tag{2.4.1}$$

For the surface finite element functions, we introduce

$$S_h^{(k)} := \{\xi_h \in C(\Gamma_h^{(k)}) : \xi_h|_\tau = \hat{\xi}_h \circ (F_T^{(k)})^{-1} \text{ with } \hat{\xi}_h \in P_k(\hat{\tau}) \text{ and } \tau \subset T \in \mathscr{T}_h^{(k)} \text{ for all } \tau \in \mathscr{T}_h^{(k)}|_{\Gamma_h^{(k)}}\}. \tag{2.4.2}$$

We have used the notation $\hat{\tau} = (F_T^{(k)})^{-1}(\tau)$ for the face of the reference element $\hat{T}$ corresponding to τ and $P_k(\omega)$ for the space of Lagrangian polynomials of degree k on ω; see Figure 2.4.1 for the location of Lagrangian nodes in three dimensions.

We will write ν_h for the element-wise defined outward normal to $\Gamma_h^{(k)}$. This lets us define the tangential gradient of a finite element function $\xi_h \in S_h^{(k)}$ by

$$\nabla_{\Gamma_h} \xi_h := \nabla \widetilde{\xi}_h - (\nabla \widetilde{\xi}_h \cdot \nu_h)\nu_h = P_h \nabla \widetilde{\xi}_h.$$

From now on we will assume k is fixed and write $\Omega_h, \Gamma_h, \mathscr{T}_h, V_h$ and S_h for $\Omega_h^{(k)}, \Gamma_h^{(k)}, \mathscr{T}_h^{(k)}, V_h^{(k)}$ and $S_h^{(k)}$ without ambiguity.

2.4.2 Description of the method

We define approximations, f_h and g_h, of the data, f and g, using the appropriate inverse lifts. That is:

$$f_h = f^{-\ell} J_h, \qquad g_h = g^{-\ell} \mu_h. \tag{2.4.3}$$

The discrete problem is: Find $(u_h, v_h) \in V_h \times S_h$ such that

$$\begin{aligned} \alpha \int_{\Omega_h} \left(\nabla u_h \cdot \nabla \eta_h + u_h \eta_h \right) \mathrm{d}x + \beta \int_{\Gamma_h} \left(\nabla_{\Gamma_h} v_h \cdot \nabla_{\Gamma_h} \xi_h + v_h \xi_h \right) \mathrm{d}\sigma_h \\ + \int_{\Gamma_h} (\alpha u_h - \beta v_h)(\alpha \eta_h - \beta \xi_h) \, \mathrm{d}\sigma_h = \alpha \int_{\Omega_h} f_h \eta_h \, \mathrm{d}x + \beta \int_{\Gamma_h} g_h \xi_h \, \mathrm{d}\sigma_h, \\ \text{for all } (\eta_h, \xi_h) \in V_h \times S_h. \end{aligned} \tag{2.4.4}$$

Remark 2.4.1. This choice of f_h and g_h is not fully practical for arbitrary $(f, g) \in L^2(\Omega) \times L^2(\Gamma)$ as the right-hand side integrals would need to be calculated via some numerical integration rule. We are not concerned with analysing such errors in this chapter and will assume that it is possible to calculate these integrals exactly; for general results on numerical integration in the context of curved domains, see Ciarlet and Raviart (1972b) and Barrett and Elliott (1987a).

Remark 2.4.2. To implement this method, we use exact integration to calculate mass and stiffness matrices on reference elements using the transformation (2.3.10).

We introduce the following functionals on $V_h \times S_h$ to describe the finite element method more succinctly:

$$\begin{aligned} a_h\big((w_h, y_h)(\eta_h, \xi_h)\big) &:= \alpha \int_{\Omega_h} \left(\nabla w_h \cdot \nabla \eta_h + w_h \eta_h \right) \mathrm{d}x \\ &\quad + \beta \int_{\Gamma_h} \left(\nabla_{\Gamma_h} y_h \cdot \nabla_{\Gamma_h} \xi_h + y_h \xi_h \right) \mathrm{d}\sigma_h \\ &\quad + \int_{\Gamma_h} (\alpha w_h - \beta y_h)(\alpha \eta_h - \beta \xi_h) \, \mathrm{d}\sigma_h, \\ l_h\big((\eta_h, \xi_h)\big) &:= \alpha \int_{\Omega_h} f_h \eta_h \, \mathrm{d}x + \beta \int_{\Gamma_h} g_h \xi_h \, \mathrm{d}\sigma_h, \end{aligned}$$

so that we can write (2.4.4) as: Find $(u_h, v_h) \in V_h \times S_h$ such that

$$a_h\big((u_h, v_h), (\eta_h, \xi_h)\big) = l_h\big((\eta_h, \xi_h)\big) \quad \text{for all } (\eta_h, \xi_h) \in V_h \times S_h. \tag{2.4.5}$$

Theorem 2.4.3. *The finite element method defined in* (2.4.4) *has a unique solution*

$(u_h, v_h) \in V_h \times S_h$ *for* h *small enough, which satisfies the bound*

$$\|(u_h, v_h)\|_{H^1(\Omega_h)\times H^1(\Gamma_h)} \leq c\,\|(f, g)\|_{L^2(\Omega)\times L^2(\Gamma)}\,. \tag{2.4.6}$$

Proof. It is clear that the equations have a unique solution since a_h is also coercive — this follows from the same reasoning as (2.2.10). To show the bound, we use the coercivity of a_h, the equivalence of norms shown in Proposition 2.3.10 and Proposition 2.3.14, and equations (2.3.12b) and (2.3.20) to see that for h small enough:

$$\|(u_h, v_h)\|_{H^1(\Omega)\times H^1(\Gamma)} \leq c\,\|(f_h, g_h)\|_{L^2(\Omega_h)\times L^2(\Gamma_h)} \leq c\,\|(f, g)\|_{L^2(\Omega)\times L^2(\Gamma)}\,. \qquad \square$$

2.4.3 Lifted finite element spaces

In order to estimate the errors introduced in our finite element method, we define the lifted finite element space that lifts of finite element functions live in. In particular, this allows us to define (u_h^ℓ, v_h^ℓ); the lifts of the finite element solution defined on the same domains – in fact, in the same spaces – as the solutions of the continuous problem. We define the lifted finite element spaces as

$$\begin{aligned} V_h^\ell &:= \{\eta_h^\ell : \eta_h \in V_h\} \subseteq H^1(\Omega), \\ S_h^\ell &:= \{\xi_h^\ell : \xi_h \in S_h\} \subseteq H^1(\Gamma). \end{aligned} \tag{2.4.7}$$

It is important to note that the trace on Γ of functions in V_h^ℓ lives in S_h^ℓ.

Proposition 2.4.4 (Approximation property)**.** *For the lifted finite element spaces* V_h^ℓ *and* S_h^ℓ *defined above, there exists an interpolation operator* $I_h \colon H^{k+1}(\Omega) \times H^{k+1}(\Gamma) \to V_h^\ell \times S_h^\ell$ *such that for* $2 \leq m \leq k+1$*,*

$$\begin{aligned} \|(w, y) - I_h(w, y)\|_{L^2(\Omega)\times L^2(\Gamma)} + h\,\|(w, y) - I_h(w, y)\|_{H^1(\Omega)\times H^1(\Gamma)} \\ \leq c h^m\,\|(w, y)\|_{H^m(\Omega)\times H^m(\Gamma)}\,, \end{aligned} \tag{2.4.8}$$

for all $(w, y) \in H^2(\Omega) \times H^2(\Gamma)$*.*

Proof. We start by defining the interpolation operator $\widetilde{I}_h \colon H^2(\Omega)\times H^2(\Gamma) \to V_h \times S_h$ so that (w, y) and $\widetilde{I}_h(w, y)$ agree at the nodes of Ω_h and Γ_h. This defines a $\widetilde{I}_h(w, y)$ uniquely since the Lagrangian basis is unisolvent on each element. We use both lifts to define $I_h(w, y) = (\widetilde{I}_h(w, y))^\ell$. The error bounds follow from previously studied interpolation theory; see Bernardi (1989) for the bulk and Demlow (2009) for the surface. The result for surface terms with $k = 1$ is given in Proposition A.6.2. $\square$

Using the fact that, for $(w_h, y_h) \in V_h \times S_h$,

$$\nabla(w_h^\ell) = \nabla(w_h \circ G_h^{-1}) = DG_h^{-\mathrm{t}}(\nabla w_h)^\ell,$$

(writing $DG_h^{-\mathrm{t}}$ for $(DG_h^{-1})^{\mathrm{t}}$) and from Dziuk (1988),

$$(P_h(\mathrm{Id} - d\mathcal{H}))\nabla_\Gamma(y_h^\ell) = (\nabla_{\Gamma_h} y_h)^\ell,$$

we have that

$$\begin{aligned} a_h\big((w_h, y_h), (\eta_h, \xi_h)\big) &= \alpha \int_\Omega \big(DG_h^{\mathrm{t}} \nabla w_h^\ell \cdot DG_h^{\mathrm{t}} \nabla \eta_h^\ell + w_h \ell \eta_h^\ell\big)(J_h^\ell)^{-1} \,\mathrm{d}x \\ &\quad + \beta \int_\Gamma \big(\mathcal{Q}_h \nabla_\Gamma y_h^\ell \cdot \nabla_\Gamma \xi_h^\ell + y_h^\ell \xi_h^\ell\big)(\mu_h^\ell)^{-1} \,\mathrm{d}\sigma \\ &\quad + \int_\Gamma (\alpha w_h^\ell - \beta y_h^\ell)(\alpha \eta_h^\ell - \beta \xi_h^\ell)(\mu_h^\ell)^{-1} \,\mathrm{d}\sigma \\ &=: a_h^\ell\big((w_h^\ell, y_h^\ell), (\eta_h^\ell, \xi_h^\ell)\big). \end{aligned}$$

Whereas for the right-hand side, we immediately have that $l_h\big((\eta_h, \xi_h)\big) = l\big((\eta_h^\ell, \xi_h^\ell)\big)$ since

$$\begin{aligned} \int_{\Omega_h} f_h \eta_h \,\mathrm{d}x &= \int_{\Omega_h} (f^{-\ell} J_h)\eta_h \,\mathrm{d}x = \int_\Omega (f^{-\ell} J_h)^\ell \eta_h^\ell (J_h^\ell)^{-1} \,\mathrm{d}x \\ &= \int_\Omega f \, J_h^\ell \, \eta_h^\ell (J_h^\ell)^{-1} \,\mathrm{d}x = \int_\Omega f \eta_h^\ell \,\mathrm{d}x, \end{aligned}$$

and

$$\begin{aligned} \int_{\Gamma_h} g_h \xi_h \,\mathrm{d}\sigma_h &= \int_{\Gamma_h} (g^{-\ell} \mu_h)\xi_h \,\mathrm{d}\sigma_h = \int_\Gamma (g^{-\ell} \mu_h)^\ell \xi_h^\ell (\mu_h^\ell)^{-1} \,\mathrm{d}\sigma \\ &= \int_\Gamma g \, \mu_h^\ell \, \xi_h^\ell (\mu_h^\ell)^{-1} \,\mathrm{d}\sigma = \int_\Gamma g \xi_h^\ell \,\mathrm{d}\sigma. \end{aligned}$$

Hence, we may rewrite (2.4.4) as: Find $(u_h^\ell, v_h^\ell) \in V_h^\ell \times S_h^\ell$

$$a_h^\ell\big((u_h^\ell, v_h^\ell), (\eta_h^\ell, \xi_h^\ell)\big) = l\big((\eta_h^\ell, \xi_h^\ell)\big) \quad \text{for all } (\eta_h^\ell, \xi_h^\ell) \in V_h^\ell \times S_h^\ell. \tag{2.4.9}$$

We will make use of the fact that a_h^ℓ now makes sense for all function pairs in $H^1(\Omega) \times H^1(\Gamma)$ in the following.

2.5 Error analysis

In this section, we wish to compare the error between the solutions (u, v) of the continuous problem (2.1.1) and the solutions (u_h, v_h) of the discrete problem (2.4.4) defined in Section 2.4.

One of the problems we have to overcome is the fact that the two problems are posed over different domains. However, the lift operators and the estimates from Section 2.3 will help us. The proof follows a similar route to the abstract error bounds from Section A.4.

In order to derive optimal order error estimates for $k > 1$, we must assume higher regularity of the smooth solution (u, v) and the surface Γ. We require $(u, v) \in H^{k+1}(\Omega) \times H^{k+1}(\Gamma)$ which, in turn, forces Γ to be C^{k+2}.

Theorem 2.5.1. *Let $(u, v) \in H^{k+1}(\Omega) \times H^{k+1}(\Gamma)$ be the solution of the variational problem (2.2.7) and let $(u_h, v_h) \in V_h \times S_h$ be the solution of the finite element scheme given by (2.4.4). Denote by u_h^ℓ and v_h^ℓ the lifts of u_h and v_h, respectively. Then we have the following error bounds:*

$$\left\|(u - u_h^\ell, v - v_h^\ell)\right\|_{H^1(\Omega)\times H^1(\Gamma)} \leq C_1 h^k, \tag{2.5.1}$$

and

$$\left\|(u - u_h^\ell, v - v_h^\ell)\right\|_{L^2(\Omega)\times L^2(\Gamma)} \leq C_1 h^{k+1}, \tag{2.5.2}$$

where

$$C_1 = c\big(\,\|(u, v)\|_{H^{k+1}(\Omega)\times H^{k+1}(\Gamma)} + \|(f, g)\|_{L^2(\Omega)\times L^2(\Gamma)}\,\big).$$

The proof of this result will be shown at the end of this section.

2.5.1 Geometric errors

As with the surface finite element method detailed in Appendix A, part of the error of the finite element method comes from the fact that there is a so-called 'variational crime', that is we are using different bilinear forms in the exact and approximate formulations and $V_h \not\subseteq H^1(\Omega)$ and $S_h \not\subseteq H^1(\Gamma)$. These errors come from the change in geometry of the computational domain. This error is encapsulated in the difference between the bilinear forms a and a_h^ℓ.

Lemma 2.5.2. *For $(w,y),(\eta,\xi) \in V_h^\ell \times S_h^\ell$, we have*

$$\begin{aligned}&\Big|a\big((w,y),(\eta,\xi)\big) - a_h^\ell\big((w,y),(\eta,\xi)\big)\Big| \\ &\qquad \le ch^k \|w\|_{H^1(B_h^\ell)} \|\eta\|_{H^1(B_h^\ell)} + ch^{k+1} \|(w,y)\|_{H^1(\Omega)\times H^1(\Gamma)} \|(\eta,\xi)\|_{H^1(\Omega)\times H^1(\Gamma)}.\end{aligned} \tag{2.5.3}$$

Proof. To prove this lemma, we split the forms a and a_h^ℓ into bulk, surface and cross terms:

$$\begin{aligned} a^{(\Omega)}(w,\eta) &= \alpha \int_\Omega \nabla w \cdot \nabla \eta + w\eta \,\mathrm{d}x \\ a^{(\Gamma)}(y,\xi) &= \beta \int_\Gamma \nabla_\Gamma y \cdot \nabla_\Gamma \xi + y\xi \,\mathrm{d}\sigma \\ a^{(\times)}\big((w,y),(\eta,\xi)\big) &= \int_\Gamma (\alpha w - \beta y)(\alpha\eta - \beta\xi) \,\mathrm{d}\sigma. \end{aligned}$$

We define $a_h^{(\Omega)}, a_h^{(\Gamma)}$ and $a_h^{(\times)}$ and $a_h^{(\Omega)\ell}, a_h^{(\Gamma)\ell}$ and $a_h^{(\times)\ell}$ similarly.

Given $w,\eta \in V_h^\ell$, we split the bulk term further:

$$\begin{aligned}&\Big|a_h^{(\Omega)\ell}(w,\eta) - a^{(\Omega)}(w,\eta)\Big| \\ &\quad = \alpha \left| \int_{\Omega_h} \nabla w^{-\ell} \cdot \nabla \eta^{-\ell} + w^{-\ell}\eta^{-\ell} \,\mathrm{d}x - \int_\Omega \nabla w \cdot \nabla \eta + w\eta \,\mathrm{d}x \right| \\ &\quad \le \alpha \left| \int_{\Omega_h} \nabla w^{-\ell} \cdot \nabla \eta^{-\ell} \,\mathrm{d}x - \int_\Omega \nabla w \cdot \nabla \eta \,\mathrm{d}x \right| + \alpha \left| \int_{\Omega_h} w^{-\ell}\eta^{-\ell} \,\mathrm{d}x - \int_\Omega w\eta \,\mathrm{d}x \right| \\ &\quad \le \alpha \,|\mathcal{A}_1 + \mathcal{A}_2 + \mathcal{A}_3| + \alpha \left| \int_{\Omega_h} w^{-\ell}\eta^{-\ell} \,\mathrm{d}x - \int_\Omega w\eta \,\mathrm{d}x \right|,\end{aligned}$$

with

$$\begin{aligned} \mathcal{A}_1 &= \int_\Omega (DG_h^{\mathrm{t}} - \mathrm{Id}) \nabla w \cdot DG_h^{\mathrm{t}} \nabla \eta \frac{1}{J_h^\ell} \,\mathrm{d}x \\ \mathcal{A}_2 &= \int_\Omega \nabla w \cdot (DG_h^{\mathrm{t}} - \mathrm{Id}) \nabla \eta \frac{1}{J_h^\ell} \,\mathrm{d}x \\ \mathcal{A}_3 &= \int_\Omega \nabla w \cdot \nabla \eta \left(\frac{1}{J_h^\ell} - 1 \right) \mathrm{d}x. \end{aligned}$$

Making use of the fact that

$$\frac{1}{J_h^\ell} - 1 = 0 \quad \text{and} \quad DG_h^{\mathrm{t}} - \mathrm{Id} = 0 \quad \text{in } \Omega \setminus B_h^\ell,$$

we actually have

$$\begin{aligned}\mathcal{A}_1 &= \int_{B_h^\ell} (DG_h^{\mathrm{t}} - \mathrm{Id})\nabla w \cdot DG_h^{\mathrm{t}} \nabla\eta \frac{1}{J_h^\ell}\,\mathrm{d}x \\ \mathcal{A}_2 &= \int_{B_h^\ell} \nabla w \cdot (DG_h^{\mathrm{t}} - \mathrm{Id})\nabla\eta \frac{1}{J_h^\ell}\,\mathrm{d}x \\ \mathcal{A}_3 &= \int_{B_h^\ell} \nabla w \cdot \nabla\eta \left(\frac{1}{J_h^\ell} - 1\right)\,\mathrm{d}x.\end{aligned}$$

Using Proposition 2.3.8, we see that the three terms $\mathcal{A}_j$ are bounded by

$$|\mathcal{A}_j| \leq ch^k \|\nabla w\|_{L^2(B_h^\ell)} \|\nabla\eta\|_{L^2(B_h^\ell)}.$$

Similarly, we obtain

$$\left|\int_{\Omega_h} w^{-\ell}\eta^{-\ell}\,\mathrm{d}x - \int_\Omega w\eta\,\mathrm{d}x\right| = \left|\int_\Omega w\eta\left(\frac{1}{J_h^\ell} - 1\right)\,\mathrm{d}x\right| \leq ch^k \|w\|_{L^2(B_h^\ell)} \|\eta\|_{L^2(B_h^\ell)}.$$

For the surface terms, given $y, \xi \in S_h^\ell$, we have

$$\begin{aligned}&\left|a_h^{(\Gamma)\ell}(y,\xi) - a^{(\Gamma)}(y,\xi)\right| \\ &= \beta\left|\int_{\Gamma_h} \nabla_{\Gamma_h} y^{-\ell}\cdot\nabla_{\Gamma_h}\xi^{-\ell} + y^{-\ell}\xi^{-\ell}\,\mathrm{d}\sigma_h - \int_\Gamma \nabla_\Gamma y\cdot\nabla_\Gamma\xi + y\xi\,\mathrm{d}\sigma\right| \\ &\leq \beta\left|\int_{\Gamma_h} \nabla_{\Gamma_h} y^{-\ell}\cdot\nabla_{\Gamma_h}\xi^{-\ell}\,\mathrm{d}\sigma_h - \int_\Gamma \nabla_\Gamma y\cdot\nabla_\Gamma\xi\,\mathrm{d}\sigma\right| + \beta\left|\int_{\Gamma_h} y^{-\ell}\xi^{-\ell}\,\mathrm{d}\sigma_h - \int_\Gamma y\xi\,\mathrm{d}\sigma\right|.\end{aligned}$$

Then using Proposition 2.3.12, we see that

$$\begin{aligned}&\left|\int_{\Gamma_h} \nabla_{\Gamma_h} y^{-\ell}\cdot\nabla_{\Gamma_h}\xi^{-\ell}\,\mathrm{d}\sigma_h - \int_\Gamma \nabla_\Gamma y\cdot\nabla_\Gamma\xi\,\mathrm{d}\sigma\right| \\ &\qquad = \left|\int_\Gamma (\mathrm{Id} - \mu_h^\ell\mathcal{Q}_h^\ell)\nabla_\Gamma y\cdot\nabla_\Gamma\xi\,\mathrm{d}\sigma\right| \leq ch^{k+1}\|\nabla_\Gamma y\|_{L^2(\Gamma)}\|\nabla_\Gamma\xi\|_{L^2(\Gamma)},\end{aligned}$$

and

$$\left|\int_{\Gamma_h} y^{-\ell}\xi^{-\ell}\,\mathrm{d}\sigma_h - \int_\Gamma y\xi\,\mathrm{d}\sigma\right| = \left|\int_\Gamma y\xi\left(\frac{1}{\mu_h} - 1\right)\,\mathrm{d}\sigma\right| \leq ch^{k+1}\|y\|_{L^2(\Gamma)}\|\xi\|_{L^2(\Gamma)}.$$

This is the same reasoning as Lemma A.6.3.

Using the previous result, we also have that

$$\begin{aligned}
&\Big|a_h^{(\times)\ell}\big((w,y)(\eta,\xi)\big) - a^{(\times)}\big((w,y)(\eta,\xi)\big)\Big| \\
&\quad= \left|\int_{\Gamma_h} (\alpha w^{-\ell} - \beta y^{-\ell})(\alpha\eta^{-\ell} - \beta\xi^{-\ell})\,\mathrm{d}\sigma_h - \int_\Gamma (\alpha w - \beta y)(\alpha\eta - \beta\xi)\,\mathrm{d}\sigma\right| \\
&\quad= \left|\int_\Gamma (\alpha w - \beta y)(\alpha\eta - \beta\xi)\left(\frac{1}{\mu_h^\ell} - 1\right)\,\mathrm{d}\sigma\right| \\
&\quad\le ch^{k+1}\,\|(w,y)\|_{L^2(\Gamma)\times L^2(\Gamma)}\,\|(\eta,\xi)\|_{L^2(\Gamma)\times L^2(\Gamma)} \\
&\quad\le ch^{k+1}\,\|(w,y)\|_{H^1(\Omega)\times H^1(\Gamma)}\,\|(\eta,\xi)\|_{H^1(\Omega)\times H^1(\Gamma)}\,.
\end{aligned}$$

This shows (2.5.3). □

We remark briefly that since $\mathcal{B}_h^\ell$ is contained in Ω, we also have for functions $(\eta,\xi) \in V_h^\ell \times S_h^\ell$ that

$$\begin{aligned}
&\Big|a\big((w,y),(\eta,\xi)\big) - a_h^\ell\big((w,y),(\eta,\xi)\big)\Big| \\
&\qquad\le ch^k\,\|(w,y)\|_{H^1(\Omega)\times H^1(\Gamma)}\,\|(\eta,\xi)\|_{H^1(\Omega)\times H^1(\Gamma)}\,.
\end{aligned} \tag{2.5.4}$$

However, we can also use Lemma 2.3.11, for integrals over $\mathcal{B}_h^\ell$:

Lemma 2.5.3. *For $\eta \in H^1(\Omega)$,*

$$\|\eta\|_{L^2(B_h^\ell)} \le ch^{1/2}\,\|\eta\|_{H^1(\Omega)}\,. \tag{2.5.5}$$

Proof. We may apply Lemma 2.3.11 to a domain $\mathcal{N}_\delta$. We can choose $\delta > 0$ such that $\delta_\Gamma > ch > \delta > h > 0$, so that $\mathcal{B}_h^\ell \subseteq \mathcal{N}_\delta \subseteq U$ since the width of $\mathcal{B}_h^\ell$ is just one element. Hence, we infer

$$\|\eta\|_{L^2(\mathcal{B}_h^\ell)} \le \|\eta\|_{L^2(\mathcal{N}_\delta)} \le c\delta^{1/2}\,\|\eta\|_{H^1(\Omega)} \le ch^{1/2}\,\|\eta\|_{H^1(\Omega)}\,.$$ □

2.5.2 Proof of error bounds (2.5.1) and (2.5.2)

Let $(u,v) \in H^{k+1}(\Omega) \times H^{k+1}(\Gamma)$ be the solution of the variational problem (2.2.7) and let $(u_h, v_h) \in V_h \times S_h$ be the solution of the finite element scheme given by (2.4.4). Denote by u_h^ℓ and v_h^ℓ the lifts of u_h and v_h, respectively. Define $F_h\colon H^1(\Omega)\times H^1(\Gamma) \to \mathbb{R}$ by

$$F_h\big((\eta,\xi)\big) := a\big((u - u_h^\ell, v - v_h),(\eta,\xi)\big). \tag{2.5.6}$$

Lemma 2.5.4. *If $(\eta,\xi) = (\eta_h^\ell, \xi_h^\ell) \in V_h^\ell \times S_h^\ell$, then F_h is bounded by*

$$\left|F_h\big((\eta_h^\ell,\xi_h^\ell)\big)\right| \leq ch^k \left\|(u_h^\ell, v_h^\ell)\right\|_{H^1(\Omega)\times H^1(\Gamma)} \left\|(\eta_h^\ell,\xi_h^\ell)\right\|_{H^1(\Omega)\times H^1(\Gamma)}. \tag{2.5.7}$$

If $(\eta,\xi) \in H^2(\Omega)\times H^2(\Gamma)$, then we can improve the bound on F_h to

$$\begin{aligned}\left|F_h\big((\eta,\xi)\big)\right| \leq \big(ch^{k+1} \left\|(u_h^\ell, v_h^\ell)\right\|_{H^1(\Omega)\times H^1(\Gamma)} + ch \left\|(u_h^\ell - u, v_h^\ell - v)\right\|_{H^1(\Omega)\times H^1(\Gamma)} \\ + ch^{k+1} \|(u,v)\|_{H^2(\Omega)\times H^2(\Gamma)}\big) \|(\eta,\xi)\|_{H^2(\Omega)\times H^2(\Gamma)}.\end{aligned} \tag{2.5.8}$$

Proof. First, we notice that if $(\eta,\xi) = (\eta_h^\ell,\xi_h^\ell) \in V_h^\ell \times S_h^\ell$, using the fact that (u,v) satisfies (2.2.7) and (u_h^ℓ, v_h^ℓ) satisfies (2.4.9), F_h can be written as

$$\begin{aligned}F_h\big((\eta_h^\ell,\xi_h^\ell)\big) &= a\big((u-u_h^\ell, v-v_h^\ell), (\eta_h^\ell,\xi_h^\ell)\big) \\ &= l\big((\eta_h^\ell,\xi_h^\ell)\big) - a\big((u_h^\ell,v_h^\ell),(\eta_h^\ell,\xi_h^\ell)\big) \\ &= \Big(l\big((\eta_h^\ell,\xi_h^\ell)\big) - l\big((\eta_h^\ell,\xi_h^\ell)\big)\Big) \\ &\qquad - \Big(a\big((u_h^\ell,v_h^\ell),(\eta_h^\ell,\xi_h^\ell)\big) - a_h^\ell\big((u_h^\ell,v_h^\ell),(\eta_h^\ell,\xi_h^\ell)\big)\Big) \\ &= -\Big(a\big((u_h^\ell,v_h^\ell),(\eta_h^\ell,\xi_h^\ell)\big) - a_h^\ell\big((u_h^\ell,v_h^\ell),(\eta_h^\ell,\xi_h^\ell)\big)\Big).\end{aligned}$$

Applying the result from (2.5.4) gives (2.5.7).

To show the second result, we assume $(\eta,\xi) \in H^2(\Omega)\times H^2(\Gamma)$ and introduce the interpolant $I_h(\eta,\xi) \in V_h^\ell \times S_h^\ell$ of (η,ξ), so that

$$\begin{aligned}F_h\big((\eta,\xi)\big) &= a\big((u-u_h^\ell, v-v_h^\ell),(\eta,\xi)\big) \\ &= a\big((u-u_h^\ell, v-v_h^\ell),(\eta,\xi) - I_h(\eta,\xi)\big) + a\big((u-u_h^\ell, v-v_h^\ell), I_h(\eta,\xi)\big).\end{aligned}$$

Then, again we can use the fact that (u,v) satisfies (2.2.7) and (u_h^ℓ,v_h^ℓ) satisfies (2.4.9), so that

$$\begin{aligned}F_h\big((\eta,\xi)\big) = a\big((u-u_h^\ell, v-v_h^\ell),(\eta,\xi) - I_h(\eta,\xi)\big) \\ + \Big(a_h^\ell\big((u_h^\ell,v_h^\ell), I_h(\eta,\xi)\big) - a\big((u_h^\ell,v_h^\ell), I_h(\eta,\xi)\big)\Big).\end{aligned}$$

Hence, we have that

$$\begin{aligned} F_h\big((\eta,\xi)\big) = a\big((u-u_h^\ell, v-v_h^\ell),(\eta,\xi) - I_h(\eta,\xi)\big) \\ + \Big(a_h^\ell\big((u_h^\ell, v_h^\ell), I_h(\eta,\xi)-(\eta,\xi)\big) - a\big((u_h^\ell, v_h^\ell), I_h(\eta,\xi)-(\eta,\xi)\big)\Big) \\ + \Big(a_h^\ell\big((u_h^\ell - u, v_h^\ell - v),(\eta,\xi)\big) - a\big((u_h^\ell - u, v_h^\ell - v),(\eta,\xi)\big)\Big) \\ + \Big(a_h^\ell\big((u,v),(\eta,\xi)\big) - a\big((u,v),(\eta,\xi)\big)\Big). \end{aligned} \tag{2.5.9}$$

We bound each of the terms on the right hand side of (2.5.9) in turn. For the first term we apply the approximation property (Proposition 2.4.4) to see

$$\begin{aligned} &\Big|a\big((u-u_h^\ell, v-v_h^\ell),(\eta,\xi) - I_h(\eta,\xi)\big)\Big| \\ &\qquad \leq c\left\|(u-u_h^\ell, v-v_h^\ell)\right\|_{H^1(\Omega)\times H^1(\Gamma)} ch\,\|(\eta,\xi)\|_{H^2(\Omega)\times H^2(\Gamma)}. \end{aligned}$$

For the second term, we use the geometric bound (2.5.4), again, with the approximation property (Proposition 2.4.4) to obtain

$$\begin{aligned} &\Big|a_h^\ell\big((u_h^\ell, v_h^\ell), I_h(\eta,\xi)-(\eta,\xi)\big) - a\big((u_h^\ell, v_h^\ell), I_h(\eta,\xi)-(\eta,\xi)\big)\Big| \\ &\qquad \leq ch^k\left\|(u_h^\ell, v_h^\ell)\right\|_{H^1(\Omega)\times H^1(\Gamma)} ch\,\|(\eta,\xi)\|_{H^2(\Omega)\times H^2(\Gamma)}. \end{aligned}$$

A bound for the third term follows by applying the geometric bound (2.5.4)

$$\begin{aligned} &\Big|a_h^\ell\big((u_h^\ell - u, v_h^\ell - v),(\eta,\xi)\big) - a\big((u_h^\ell - u, v_h^\ell - v),(\eta,\xi)\big)\Big| \\ &\qquad \leq ch^k\left\|(u_h^\ell - u, v_h^\ell - v)\right\|_{H^1(\Omega)\times H^1(\Gamma)} \|(\eta,\xi)\|_{H^1(\Omega)\times H^1(\Gamma)}. \end{aligned}$$

Finally, for the fourth term, we simply apply (2.5.5) followed by the result from Lemma 2.5.3 to see

$$\begin{aligned} &\Big|a_h^\ell\big((u,v),(\eta,\xi)\big) - a\big((u,v),(\eta,\xi)\big)\Big| \\ &\qquad \leq ch^k\,\|u\|_{H^1(B_h^\ell)}\,\|\eta\|_{H^1(B_h^\ell)} + ch^{k+1}\,\|(u,v)\|_{H^1(\Omega)\times H^1(\Gamma)}\,\|(\eta,\xi)\|_{H^1(\Omega)\times H^1(\Gamma)} \\ &\qquad \leq ch^{k+1}\,\|(u,v)\|_{H^2(\Omega)\times H^2(\Gamma)}\,\|(\eta,\xi)\|_{H^2(\Omega)\times H^2(\Gamma)}. \end{aligned}$$

Adding together the previous four results in (2.5.9) gives (2.5.7). □

Remark 2.5.5. Note that in the absence of domain perturbation that

$$F_h\big((\eta_h,\xi_h)\big) = 0,$$

where this is simply Galerkin orthogonality, whereas in the absence of the bulk equations then the bound would be of order h^{k+1} (Demlow 2009).

Proof of Theorem 2.5.1. The H^1 error estimate (2.5.1) follows simply by combining the approximation property (Proposition 2.4.4) with the bound on F_h from (2.5.7). We rewrite the error as

$$\begin{aligned}
&a\big((u-u_h^\ell, v-v_h^\ell), (u-u_h^\ell, v-v_h^\ell)\big)\\
&\qquad = a\big((u-u_h^\ell, v-v_h^\ell), (u,v) - I_h(u,v)\big)\\
&\qquad\qquad - a\big((u-u_h^\ell, v-v_h^\ell), I_h(u,v) - (u_h^\ell, v_h^\ell)\big)\\
&\qquad = a\big((u-u_h^\ell, v-v_h^\ell), (u,v) - I_h(u,v)\big) + F_h\big(I_h(u,v) - (u_h^\ell, v_h^\ell)\big).
\end{aligned}$$

The result follows from application of a Cauchy inequality and the coercivity of the bilinear form a (2.2.10). To show that the given value of C_1, we use (2.4.6) from Theorem 2.4.3 and (2.3.15a, 2.3.25a) to bound $\big\|(u_h^\ell, v_h^\ell)\big\|_{H^1(\Omega)\times H^1(\Gamma)}$.

We will use an Aubin–Nitsche duality argument to show the L^2 bound. For $\zeta = (\zeta_1, \zeta_2) \in L^2(\Omega) \times L^2(\Gamma)$, we define the dual problem: Find $z_\zeta \in H^1(\Omega) \times H^1(\Gamma)$ such that

$$a\big((\eta,\xi), z_\zeta\big) = \langle \zeta, (\eta,\xi)\rangle_{L^2(\Omega)\times L^2(\Gamma)} \quad \text{for all } (\eta,\xi) \in H^1(\Omega) \times H^1(\Gamma). \tag{2.5.10}$$

Here $\langle (w,y), (\eta,\xi)\rangle_{L^2(\Omega)\times L^2(\Gamma)}$ denotes the sum of the L^2 inner products between w and η on Ω and y and ξ on Γ. Similarly to Theorem 2.2.3, one can show the following regularity result for the dual problem:

$$\|z_\zeta\|_{H^2(\Omega)\times H^2(\Gamma)} \le c\,\|\zeta\|_{L^2(\Omega)\times L^2(\Gamma)}\,. \tag{2.5.11}$$

We write the error,

$$e = (u-u_h^\ell, v-v_h^\ell) \in L^2(\Omega) \times L^2(\Gamma),$$

as the data for the dual problem and test with $(\eta,\xi) = e$ so that

$$\|e\|^2_{L^2(\Omega)\times L^2(\Gamma)} = a(e, z_e) = F_h(z_e).$$

Hence, using (2.5.8) combined with the H^1 error bound (2.5.1) and the dual regularity result (2.5.11), we have

$$\|e\|^2_{L^2(\Omega)\times L^2(\Gamma)} = F_h(z_e) \le C_1 h^{k+1}\,\|e\|_{L^2(\Omega)\times L^2(\Gamma)}\,. \qquad \square$$

2.6 Numerical experiments

The method was implemented using the ALBERTA finite element toolbox (Schmidt, Siebert, Köster and Heine 2005). We solve the linear system using a block Jacobi iteration: Given (u_h^0, v_h^0), for $k = 0, 1, \ldots$, find (u_h^{k+1}, v_h^{k+1}) as the solution of:

$$\begin{aligned} a_h\big((u_h^{k+1}, v_h^k), (\eta_h, 0)\big) &= l_h\big((\eta_h, 0)\big) && \text{for all } \eta_h \in V_h \\ a_h\big((u_h^{k+1}, v_h^{k+1}), (0, \xi_h)\big) &= l_h\big((0, \xi_h)\big) && \text{for all } \xi_h \in S_h, \end{aligned}$$

until $\alpha \left\| u_h^{k+1} - u_h^k \right\|_{L^\infty(\Omega_h)} + \beta \left\| v_h^{k+1} - v_h^{k+1} \right\|_{L^\infty(\Gamma_h)} \leq 10^{-10}$. Two linear solves are performed at each iteration using an direct sparse solver. One could also use a (preconditioned) conjugate gradient method.

The first problem we consider has $\alpha = \beta = 1$ and Ω is the unit ball in $\mathbb{R}^3$. The data is chosen so that the exact solution is

$$\begin{aligned} u(x_1, x_2, x_3) &= \beta \exp\big(- x_1(x_1 - 1)x_2(x_2 - 1)\big) \\ v(x_1, x_2, x_3) &= \big(\alpha + x_1(1 - 2x_1) + x_2(1 - 2x_2)\big) \exp\big(- x_1(x_1 - 1)x_2(x_2 - 1)\big). \end{aligned}$$

We calculate the the right hand side by setting (f_h, g_h) to be an interpolant of (f, g) into $V_h \times S_h$. We ran two simulations: one with $k = 1$, and one with $k = 2$. We present the error calculated after solving the matrix system at each mesh size in Table 2.1 for $k = 1$ and Table 2.2 for $k = 2$. The experimental order of convergence (eoc) is calculated through formula (A.7.1). This experiment demonstrates the expected theoretical order of convergence showing that this bound is tight.

We take a second example from Deckelnick et al. (2010). We take $\Omega = \{x \in \mathbb{R}^3 : \Phi(x) < 0\}$ for Φ given by

$$\begin{aligned} \Phi(x_1, x_2, x_3) = (1 - x_1^2)^2 + (1 - x_2^2)^2 + (1 - x_3^2)^2 \\ + (4 - x_1^2 - x_2^2)^2 + (4 - x_2^2 - x_3^2)^2 + (4 - x_1^2 - x_3^2)^2 - 15. \end{aligned} \tag{2.6.1}$$

We consider the problem with $f = 0$ and g given by

$$g(x) = 100 \exp\left(- \sum_{j=1}^{4} |x - x_j|^2 \right),$$

h	L^2 error	(eoc)	H^1 error	(eoc)
1.000000	$1.556084 \cdot 10^{-1}$	-	$8.412952 \cdot 10^{-1}$	
$8.201523 \cdot 10^{-1}$	$6.945582 \cdot 10^{-2}$	4.068547	$6.031542 \cdot 10^{-1}$	1.678406
$4.799888 \cdot 10^{-1}$	$2.375760 \cdot 10^{-2}$	2.002490	$3.485974 \cdot 10^{-1}$	1.023385
$2.555341 \cdot 10^{-1}$	$6.692238 \cdot 10^{-3}$	2.009740	$1.831428 \cdot 10^{-1}$	1.021009
$1.321787 \cdot 10^{-1}$	$1.744647 \cdot 10^{-3}$	2.039433	$9.301660 \cdot 10^{-2}$	1.027742
$6.736035 \cdot 10^{-2}$	$4.427043 \cdot 10^{-4}$	2.034429	$4.672631 \cdot 10^{-2}$	1.021320
$3.399254 \cdot 10^{-2}$	$1.112504 \cdot 10^{-4}$	2.019429	$2.339324 \cdot 10^{-2}$	1.011617

h	L^2 error	(eoc)	H^1 error	(eoc)
1.000000	$5.080238 \cdot 10^{-1}$	-	2.908569	
$8.201523 \cdot 10^{-1}$	$1.591067 \cdot 10^{-1}$	5.855554	1.607240	2.991664
$4.799888 \cdot 10^{-1}$	$4.342084 \cdot 10^{-2}$	2.424061	$8.413412 \cdot 10^{-1}$	1.208220
$2.555341 \cdot 10^{-1}$	$1.108272 \cdot 10^{-2}$	2.166144	$4.247143 \cdot 10^{-1}$	1.084348
$1.321787 \cdot 10^{-1}$	$2.785873 \cdot 10^{-3}$	2.094697	$2.128454 \cdot 10^{-1}$	1.048012
$6.736035 \cdot 10^{-2}$	$6.973524 \cdot 10^{-4}$	2.054635	$1.064757 \cdot 10^{-1}$	1.027520
$3.399254 \cdot 10^{-2}$	$1.743772 \cdot 10^{-4}$	2.026669	$5.324210 \cdot 10^{-2}$	1.013381

Table 2.1: Error table for the case $k = 1$, Problem 1 - bulk errors, $\|u - u_h\|$, (top) and surface errors, $\|v - v_h\|$, (bottom).

h	L^2 error	(eoc)	H^1 error	(eoc)
1.000000	$3.894207 \cdot 10^{-2}$	-	$3.511490 \cdot 10^{-1}$	
$8.172473 \cdot 10^{-1}$	$1.034114 \cdot 10^{-2}$	6.570149	$1.476235 \cdot 10^{-1}$	4.293793
$5.060717 \cdot 10^{-1}$	$1.304277 \cdot 10^{-3}$	4.320133	$4.026584 \cdot 10^{-2}$	2.710747
$2.773996 \cdot 10^{-1}$	$1.737998 \cdot 10^{-4}$	3.352355	$1.061322 \cdot 10^{-2}$	2.217832
$1.447909 \cdot 10^{-1}$	$2.259868 \cdot 10^{-5}$	3.137667	$2.723960 \cdot 10^{-3}$	2.091786
$7.391824 \cdot 10^{-2}$	$2.882693 \cdot 10^{-6}$	3.062727	$6.894787 \cdot 10^{-4}$	2.043497

h	L^2 error	(eoc)	H^1 error	(eoc)
1.000000	$1.538024 \cdot 10^{-1}$	-	1.258018	
$8.172473 \cdot 10^{-1}$	$2.188515 \cdot 10^{-2}$	9.661695	$3.745396 \cdot 10^{-1}$	6.003538
$5.060717 \cdot 10^{-1}$	$3.332406 \cdot 10^{-3}$	3.927097	$1.052173 \cdot 10^{-1}$	2.649211
$2.773996 \cdot 10^{-1}$	$4.516347 \cdot 10^{-4}$	3.324205	$2.718041 \cdot 10^{-2}$	2.251310
$1.447909 \cdot 10^{-1}$	$5.816879 \cdot 10^{-5}$	3.152298	$6.874227 \cdot 10^{-3}$	2.114402
$7.391824 \cdot 10^{-2}$	$7.342240 \cdot 10^{-6}$	3.078402	$1.725037 \cdot 10^{-3}$	2.056324

Table 2.2: Error table for the case $k = 2$, Problem 1 - bulk errors, $\|u - u_h\|$, (top) and surface errors, $\|v - v_h\|$, (bottom).

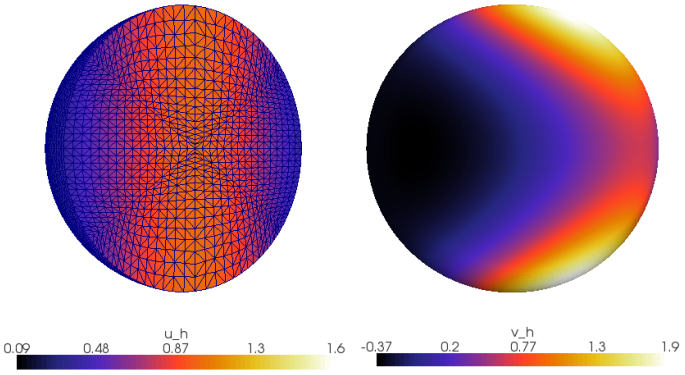

Figure 2.6.1: Plot of the solution of the finite element scheme at $h \approx .2$, Problem 1, using quadratic elements, along the plane $x = y$ in Ω, with mesh shown, (left) and on the surface Γ (right).

with

$$x_1 = (-1, 1, 2.04), \quad x_2 = (1, 2.04, 1),$$
$$x_3 = (2.04, 0, 1), \quad x_4 = (-0.5, -1.0, -2.04).$$

We have used $k = 1$ in this example. The results are shown in Figure 2.6.2. This shows that this method is very flexible with respect to the geometry of the underlying domain and remains accurate despite large variations the curvature of the boundary surface.

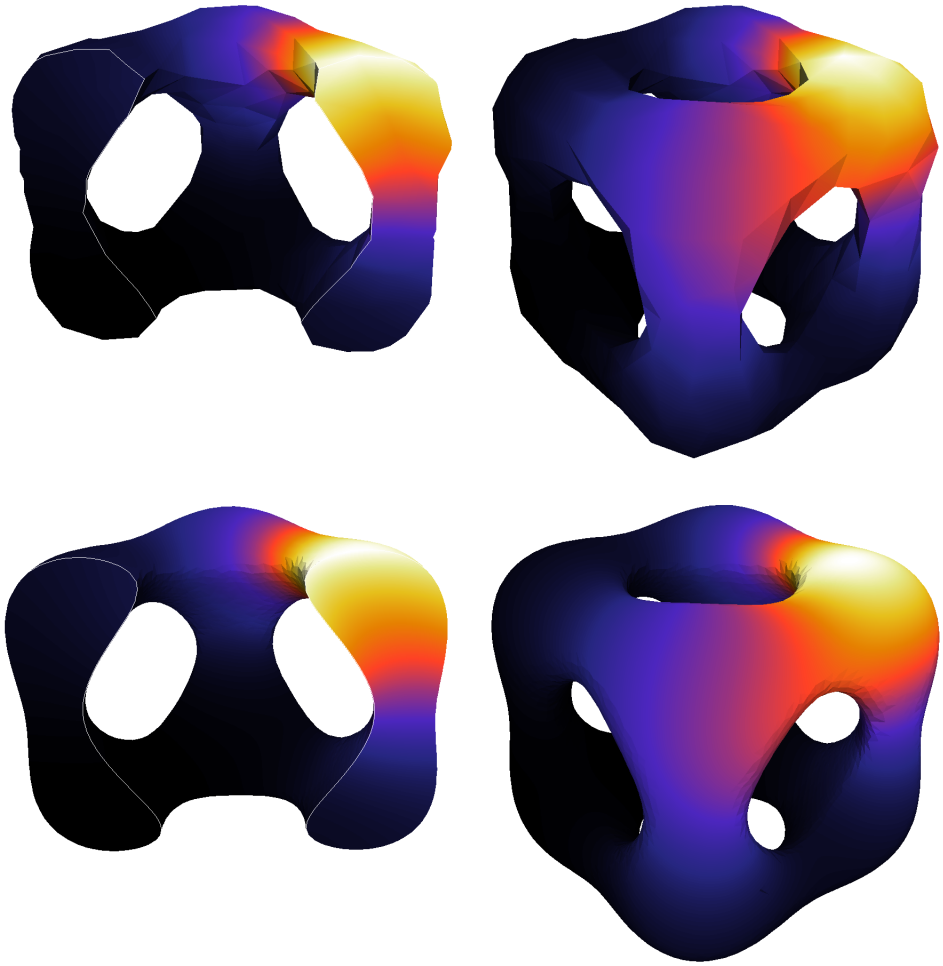

Figure 2.6.2: Plot of solutions of the finite element scheme for the second problem. The top line is the calculations on a coarse mesh and the lower line has a finer mesh. The left images show the bulk solution u_h on a part of the domain and the right images show the surface solution v_h. The bulk solutions have been cut open.

Chapter 3

Analysis of a Cahn-Hilliard equation on an evolving surface

3.1 Introduction

In this chapter, we will study a Cahn-Hilliard equation posed on an evolving surface with prescribed velocity. The key methodology in the chapter is to use the evolving surface finite element method originally proposed by Dziuk and Elliott (2007a) for a surface heat equation. The idea is to take a triangulation of the initial surface and evolving the nodes along the velocity field. This leads to a family of discrete surfaces on which we can pose a variational form of the Cahn-Hilliard equation.

There are two key results in this chapter: first, we show well-posedness of the continuous scheme and, second, we show convergence of a finite element scheme. The well-posedness result is proven rigorously by showing convergence, along a subsequence, of the discrete scheme. In contrast to the planar setting, there are extra difficulties in this work since the classical Bochner space set-up is unavailable to us. The finite element method is analysed under the assumption of higher regularity of the solution and shown to converge to the true solution quadratically with respect to the mesh size in an L^2 norm. The chapter concludes with some numerical examples to show various properties of the methodology.

3.1.1 The Cahn-Hilliard equations

We assume we are given an evolving surface $\{\Gamma(t)\}$, for $t \in [0,T]$, which evolves according to a given underlying velocity field v which can be decomposed into normal

(v_ν) and tangential components (v_τ) so that $v = v_\nu + v_\tau$. We seek a solution u of

$$\partial^\bullet u + u\nabla_\Gamma \cdot v = \Delta_\Gamma \left(-\varepsilon \Delta_\Gamma u + \frac{1}{\varepsilon}\psi'(u) \right) \quad \text{on} \bigcup_{t\in(0,T)} \Gamma(t) \times \{t\} \tag{3.1.1}$$

subject to the initial condition

$$u(\cdot, 0) = u_0 \quad \text{on } \Gamma(0) = \Gamma_0. \tag{3.1.2}$$

Here $\partial^\bullet u$ denotes the material derivative of u and $\Delta_\Gamma u$ the Laplace-Beltrami operator of u. The function ψ is a double well potential, which we will take to be given by

$$\psi(z) = \frac{1}{4}(z^2 - 1)^2. \tag{3.1.3}$$

The behaviour of the Cahn-Hilliard equation in the planar case is well studied; see the review of Elliott (1989). Extra effects such as spatial or concentration dependent mobilities or more physically realistic potentials could also be solved with similar methods to those suggested in this chapter. Such considerations are left for future work.

This Cahn-Hilliard equation is a simplification of the model for surface dissolution set out in Section 1.3. We have chosen not to consider the geometric terms which would come from taking a gradient-flow of a Ginzburg-Landau functional. From a modelling view point, we consider these terms as forcing a geometric evolution law for the surface; see Elliott and Stinner (2010a) for example. The model of Mercker et al. (2012) takes a different approach and considers terms coming from a Helfrich energy forcing the Cahn-Hilliard equation but on a stationary surface. The aim of this work is to analyse a model equation of this form.

The results in this chapter can be seen as a generalisation of the work of Du et al. (2011) to evolving surfaces. They consider a fully discrete approximation of a Cahn-Hilliard equation posed on a two-dimensional stationary surface with boundary (with a zero Dirichlet boundary condition) under the assumption $u_0 \in H_0^1(\Gamma) \cap H^2(\Gamma)$ and $\Delta_\Gamma u_0 \in H_0^1(\Gamma) \cap W^{1,2+\gamma}(\Gamma)$ for $\gamma \in (0, 1)$. They show an error estimate of the form

$$\max_m \left\| u_h^m - u^{-\ell}(t_m) \right\|_{L^2(\Gamma_h)} \leq c(h^2 + \tau^2),$$

where $0 = t_0 < t_1 < \ldots < t_m < \ldots < t_M = T$ is a partition of time with fixed time step τ and $u^{-\ell}$ is the inverse lift (3.3.24) of the continuous solution u.

3.1.2 Outline of chapter

The chapter is laid out as follows. In section two, we will derive a Cahn-Hilliard equation on an evolving surface using a local conservation law. We introduce the notation for partial differential equations on evolving surfaces following Deckelnick et al. (2005) and state any assumptions on the smoothness of the surfaces and its evolution we require in later chapters. The third section introduces a finite element discretisation of the continuous equations. We describe the process of triangulating an evolving surface and how we formulate the space discrete-time continuous problem as a system of ordinary differential equations. This section is completed by showing some domain perturbation results relating geometric quantities on the discrete and smooth surfaces. Well-posedness of the continuous equations is addressed in the fourth section. An existence result is achieved by showing convergence, along a subsequence, of the discrete solutions as the mesh size tends to zero. In section five, we analyse the errors introduced by our finite element scheme and go on to show an optimal order error estimate. Some numerical experiments are shown in the sixth section backing up the analytical results.

We will use a Gronwall inequality as a standard tool in this chapter which leads to exponential dependence on ε in most bounds. We are not interested in taking $\varepsilon \to 0$ in this work so will simply write c_ε for a generic constant which depends on ε.

3.2 Derivation of continuous equations

In this section we will derive a Cahn-Hilliard equation on an evolving surface. We start by listing all assumptions on the surface and its evolution in time. Included in these assumptions is the notation we will use to describe evolving surfaces. The notation is taken from Deckelnick et al. (2005) and extends our description of stationary surfaces introduced in Appendix A; in particular, the material derivative is introduced in detail. The main content of this chapter is the derivation of our Cahn-Hilliard equation via a conservation law and the definition of solution we will use.

3.2.1 Assumptions on the evolving surface

Given a final time $T > 0$, for each time $t \in [0, T]$, we write $\Gamma(t)$ for a compact, smooth, connected n-dimensional hypersurface in $\mathbb{R}^{n+1}$ for $n = 1, 2$ or 3 and $\Gamma_0 = \Gamma(0)$. We assume that $\Gamma(t)$ is the boundary of an open, bounded domain $\Omega(t)$.

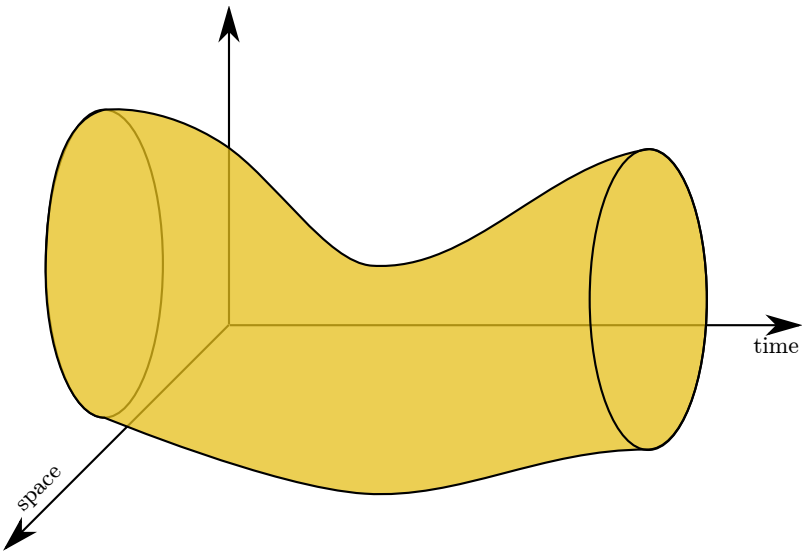

Figure 3.2.1: A sketch of the space-time domain $\mathcal{G}_T$.

It follows that $\Gamma(t)$ admits a description as the zero level set of a signed distance function $d(\cdot,t)\colon \mathbb{R}^{n+1} \to \mathbb{R}$ so that $d(\cdot,t) < 0$ in $\Omega(t)$ and $d(\cdot,t) > 0$ in $\bar{\Omega}(t)^c$. We denote by $\mathcal{G}_T$ for the space-time domain given by

$$\mathcal{G}_T = \bigcup_{t\in[0,T]} \Gamma(t) \times \{t\}. \tag{3.2.1}$$

For our analysis, it is sufficient to consider $d(\cdot,t)$ locally to $\Gamma(t)$. We restrict our thoughts to $\mathcal{N}(t)$, an open neighbourhood of $\Gamma(t)$. We choose $\mathcal{N}(t)$ so that $|\nabla d(x,t)| \neq 0$ for $x \in \mathcal{N}(t)$ and assume that

$$d, d_t, d_{x_i}, d_{x_i x_j} \in C^2(\mathcal{N}_T) \quad \text{for } i,j = 1,\dots,n+1;$$

here $\mathcal{N}_T = \bigcup_{t\in[0,T]} \mathcal{N}(t) \times \{t\}$. The orientation of $\Gamma(t)$ is fixed by choosing $\nu(x,t) = \nabla d(x,t)$. For $(x,t) \in \mathcal{G}_T$, we denote $P = P(x,t)$ the projection operator onto the tangent space $T_x\Gamma(t)$, given by $P_{ij}(x,t) = \delta_{ij} - \nu_i(x,t)\nu_j(x,t)$ and by $\mathcal{H} = \mathcal{H}(x,t)$ the (extended) Weingarten map (or shape operator),

$$\mathcal{H}_{ij}(x,t) = (\nu_i(x,t))_{x_j} = d_{x_i x_j}(x,t).$$

We will use the fact that $P\mathcal{H} = \mathcal{H}P = \mathcal{H}$.

The same notation as described in Appendix A will be used to describe tangential gradients and define Sobolev spaces over time dependent surfaces, $H^s(\Gamma(t))$. We will make use of the following Sobolev embeddings:

Lemma 3.2.1. *For $\Gamma(t)$ as above, we have*

$$W^{1,q}(\Gamma(t)) \subset \begin{cases} L^{nq/(n-q)}(\Gamma(t)) & \text{for } q < n \\ C^0(\Gamma(t)) & \text{for } q > n. \end{cases} \tag{3.2.2}$$

Furthermore there exists a constant $c = c(n, q)$, independent of t, such that for any $\eta \in W^{1,q}(\Gamma(t))$,

$$\|\eta\|_{L^{nq/(n-q)}(\Gamma(t))} \leq c \|\eta\|_{W^{1,q}(\Gamma(t))} \qquad \text{for } q < n \tag{3.2.3a}$$

$$\|\eta\|_{L^{\infty}(\Gamma(t))} \leq c \|\eta\|_{W^{1,q}(\Gamma(t))} \qquad \text{for } q > n. \tag{3.2.3b}$$

Proof. A proof for a fixed surface is given by Hebey (2000) in Theorems 2.5 and 2.6. The constant in the bound is independent of time since we only consider a compact interval of time. □

In particular, this allows us to embed $H^1(\Gamma(t))$ in $L^6(\Gamma(t))$ for dimensions $n = 1, 2, 3$ so that $\|\psi'(\eta)\|_{L^2(\Gamma(t))} \leq c \|\eta\|_{H^1(\Gamma(t))}$.

Further, we require that for each $(x, t) \in \mathcal{N}_T$ there exists a unique $p = p(x, t) \in \Gamma(t)$, such that

$$x = p(x, t) + d(x, t)\nu(p(x, t), t). \tag{3.2.4}$$

This exists by the same reasoning as in Lemma A.2.2. As before, we extend ν, P and $\mathcal{H}$ to functions on $\mathcal{N}_T$ by setting

$$\nu(x, t) = \nu(p(x, t), t) = \nabla d(x, t),$$

and similarly $P(x, t) = P(p(x, t), t) = \mathrm{Id} - \nu(x) \otimes \nu(x)$ and $\mathcal{H}(x, t) = \nabla^2 d(x, t)$ for $(x, t) \in \mathcal{N}_T$.

Although it is sufficient to describe the evolution of the surface through a normal velocity, we wish to consider material surfaces for which a material particle, at $X(t)$ on $\Gamma(t)$, has a velocity $\dot{X}(t)$ not necessarily only in the normal direction. Hence, we assume that we are given a global velocity field v so that points $X(t)$ evolve with the velocity $\dot{X}(t) = v(X(t), t)$. We will assume that $v \in C^2(\mathcal{N}_T)$.

We can calculate the normal velocity v_ν of $\Gamma(t)$, at a point x, by considering a curve $\gamma(s) \in \Gamma(s)$ for $s \in (t - \delta, t + \delta)$, with $\gamma(t) = x$ and $\gamma'(t) = v_\nu(x, t)$, the velocity of the surface, then $d(\gamma(s), s) = 0$ and

$$0 = \frac{d}{ds} d(\gamma(s), s) = \nabla d(\gamma(s), s) \cdot \gamma'(s) + d_t(\gamma(s), s),$$

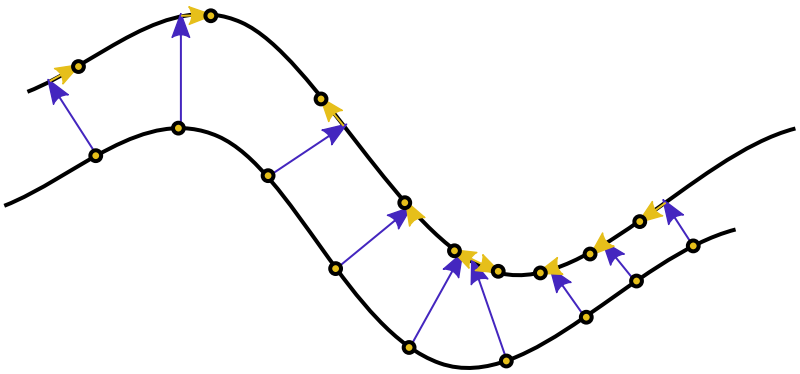

Figure 3.2.2: A sketch of a surface evolving with a material velocity $v = v_\tau + v_\nu$. The normal velocity, indicated in blue, describes the evolution of the surface. The tangential velocity, indicated in yellow, describes the evolution of material points along the surface.

hence

$$v_\nu(x,t) = -d_t(x,t)\nu(x,t) \quad \text{for } x \in \Gamma(t).$$

We say v_τ is a tangential velocity field if $v_\tau \cdot \nu = 0$ in $\mathcal{N}_T$. Given a tangential velocity field v_τ, we call

$$v := v_\tau + v_\nu$$

a material velocity field. We considering the surface $\Gamma(t)$ as a composite of material points which move within the surface $\Gamma(t)$ according to the material velocity v. See Figure 3.2.2 for an example.

Remark 3.2.2. The normal velocity describes the geometric evolution of the surface and the tangential velocity is often thought of as an advective term. From a modelling point of view it is common to only think about a normal velocity. The Marangoni effect, a force driven by surface tension gradient, is an example leading to a tangential velocity.

3.2.2 Material derivative and transport formulae

Given a family of surfaces $\{\Gamma(t)\}$ evolving in time with normal velocity field v_ν, we define the normal time derivative ∂° of a function $\eta\colon \mathcal{G}_T \to \mathbb{R}$ by

$$\partial^\circ \eta := \frac{\partial \widetilde{\eta}}{\partial t} + v_\nu \cdot \nabla \widetilde{\eta}. \tag{3.2.5}$$

Here, $\widetilde{\eta}$ denotes a smooth extension of η to $\mathcal{N}_T$. This derivative describes how a quantity η evolves in time with respect to the evolution of $\Gamma(t)$. It can be shown that this definition is an intrinsic surface derivative, independent of the choice of

extension: for any $(x,t) \in \mathcal{G}_T$, define the curve $\gamma(s) \in \Gamma(s)$ for $s \in (t-\delta, t+\delta)$ with $\gamma(t) = x$ and $\gamma'(t) = v_\nu(\gamma(t), t)$, then

$$\frac{\mathrm{d}}{\mathrm{d}s}\eta(\gamma(s), s) = \partial^\circ \eta(\gamma(s), s).$$

Given a tangential vector field v_τ, we define the material derivative of a scalar function $\eta \colon \mathcal{G}_T \to \mathbb{R}$, by

$$\partial^\bullet \eta := \partial^\circ \eta + v_\tau \cdot \nabla_\Gamma \eta = \frac{\partial \widetilde{\eta}}{\partial t} + v \cdot \nabla \widetilde{\eta}.$$

The following formula shows the significance of the material derivative. The result is a generalisation of the classical Reynolds' Transport Formula to curved domains.

Lemma 3.2.3 (Transport formula)**.** *Let $\mathcal{M}(t)$ be an evolving surface with normal velocity v_ν. Let v_τ be a tangential velocity field on $\mathcal{M}(t)$. Let the boundary $\partial\mathcal{M}(t)$ evolve with velocity $v = v_\nu + v_\tau$. Assume that η is a function such that all the following quantities exist. Then, we obtain the identity*

$$\frac{\mathrm{d}}{\mathrm{d}t}\int_{\mathcal{M}(t)} \eta \,\mathrm{d}\sigma = \int_{\mathcal{M}(t)} \partial^\bullet \eta + \eta \nabla_\Gamma \cdot v \,\mathrm{d}\sigma. \tag{3.2.6}$$

Proof. A proof can be found in Dziuk and Elliott (2007a, Lemma 2.2). □

As a consequence of this result, we have the following relations for the time derivatives of the L^2 and Dirichlet inner products on $\{\Gamma(t)\}$.

Corollary 3.2.4. *Using the same notation as in Lemma 3.2.3, assume that η, φ are functions such that the following quantities exist. We have*

$$\frac{\mathrm{d}}{\mathrm{d}t}\int_{\mathcal{M}(t)} \eta\varphi \,\mathrm{d}\sigma = \int_{\mathcal{M}(t)} \partial^\bullet \eta\, \varphi + \eta\, \partial^\bullet \varphi + \eta\varphi\, \nabla_\Gamma \cdot v \,\mathrm{d}\sigma. \tag{3.2.7}$$

Denote by $D(v)$ the rate of deformation tensor given by

$$D(v)_{ij} = \frac{1}{2}\sum_{k=1}^{n+1} \left(\mathcal{A}_{ik}\underline{D}_k v_j + \mathcal{A}_{jk}\underline{D}_k v_i\right) \quad \text{for } i,j = 1,\dots,n+1, \tag{3.2.8}$$

and by $\mathcal{B}(v)$ the tensor

$$\mathcal{B}(v) := \partial^\bullet \mathcal{A} + \nabla_\Gamma \cdot v\mathcal{A} - 2D(v). \tag{3.2.9}$$

For any matrix $\mathcal{A} = \mathcal{A}(x,t)$ which is positive definite on the tangent space to $\Gamma(t)$, we have the formula

$$\begin{aligned}\frac{\mathrm{d}}{\mathrm{d}t}\int_{\mathcal{M}(t)} \mathcal{A}\nabla_\Gamma\eta\cdot\nabla_\Gamma\varphi\,\mathrm{d}\sigma = \int_{\mathcal{M}(t)} \mathcal{A}\nabla_\Gamma\partial^\bullet\eta\cdot\nabla_\Gamma\varphi + \mathcal{A}\nabla_\Gamma\eta\cdot\nabla_\Gamma\partial^\bullet\varphi\,\mathrm{d}\sigma \\ + \int_{\mathcal{M}(t)} \mathcal{B}(v)\nabla_\Gamma\eta\cdot\nabla_\Gamma\varphi\,\mathrm{d}\sigma.\end{aligned} \tag{3.2.10}$$

Proof. Equation (3.2.7) follows from the product rule $\partial^\bullet(\eta\varphi) = \partial^\bullet\eta\,\varphi + \eta\,\partial^\bullet\varphi$. The result of (3.2.10) is given in detail for $\eta = \varphi$ by Dziuk and Elliott (2007a, Lemma 2.2) and the polarised form ($\eta \neq \varphi$) is given by Dziuk and Elliott (2013a, Lemma 2.1). □

We conclude this subsection with a result allowing us to extend functions defined on one surface to the whole space-time domain.

Lemma 3.2.5. *Fix $t \in [0,T]$ and let $\eta \in H^1(\Gamma(t))$, respectively $C^1(\Gamma(t))$. Then there exists an extension $\widetilde{\eta}\colon \mathcal{G}_T \to \mathbb{R}$ such that $\widetilde{\eta}|_t = \eta$ and $\widetilde{\eta} \in H^1(\Gamma(s))$, resp. $C^1(\Gamma(s))$, for all times $s \in [0,T]$ and $\partial^\bullet\widetilde{\eta} = 0$.*

Proof. The ordinary differential equation:

$$\frac{\mathrm{d}}{\mathrm{d}s}X(s) = v(X(s),s) \quad \text{for } s\in[0,T], \qquad X(t) = x,$$

determines a flow $\phi_s(x)$ on $\mathcal{G}_T$ for $x \in \Gamma(t)$ such that

$$\phi_s(x) \in \Gamma(s) \quad \text{for all } s\in[0,T] \quad \text{and } \phi_t(x) = x.$$

Our assumptions on v imply that $\phi_s\colon \Gamma(t)\to\Gamma(s)$ and $(\phi_s)^{-1}\colon \Gamma(s)\to\Gamma(t)$ are both C^1 mappings; see Hartman (2002, Theorem 3.1).

We define the extension $\widetilde{\eta}$ by

$$\widetilde{\eta}(x,s) := \eta((\phi_s)^{-1}(x)) \quad \text{for } (x,s)\in\mathcal{G}_T.$$

It is clear that since $(\phi_s)^{-1} \in C^1(\Gamma(t);\Gamma(s))$, we have $\widetilde{\eta}\in H^1(\Gamma(s))$ (resp. $C^1(\Gamma(s))$) for all times $s\in[0,T]$.

Finally, we can calculate for $y = (\phi_s)^{-1}(x)$,

$$\partial^\bullet\widetilde{\eta}(x,s) = \frac{\mathrm{d}}{\mathrm{d}s}\widetilde{\eta}(\phi_s(y),s) = \frac{\mathrm{d}}{\mathrm{d}s}\eta(y) = 0 \quad \text{for } (x,s)\in\mathcal{G}_T.$$ □

3.2.3 Derivation of Cahn-Hilliard equations

For the Cahn-Hilliard equation posed in a Cartesian domain, first studied by Cahn and Hilliard (1958), one can derive the equations as an H^{-1} gradient flow of the Ginzburg-Landau functional

$$E_{\mathrm{GL}}(u) = \int_\Omega \frac{\varepsilon}{2} |\nabla u|^2 + \frac{1}{\varepsilon}\psi(u) \,\mathrm{d}x.$$

This allows one to show well-posedness of solutions using gradient flow techniques since E_{GL} is a Lyapunov function (Elliott 1989). Although this functional can be easily extended to surfaces:

$$E^\Gamma_{\mathrm{GL}}(u) = \int_\Gamma \frac{\varepsilon}{2} |\nabla_\Gamma u|^2 + \frac{1}{\varepsilon}\psi(u) \,\mathrm{d}\sigma, \tag{3.2.11}$$

this approach does not make sense in the context of evolving surfaces since the variation of the surface version of E^Γ_{GL} is not defined for $\Gamma = \{\Gamma(t)\}$. Alternatively, we can consider the non-autonomous function $E^{\Gamma(t)}_{\mathrm{GL}}$, then, using the transport formulae (3.2.6) and (3.2.10), we have:

$$\begin{aligned}
&\frac{\mathrm{d}}{\mathrm{d}t}\left(\int_{\Gamma(t)} \frac{\varepsilon}{2} |\nabla_\Gamma u|^2 + \frac{1}{\varepsilon}\psi(u) \,\mathrm{d}\sigma\right) \\
&\quad = \int_{\Gamma(t)} \varepsilon \nabla_\Gamma u \cdot \nabla_\Gamma \partial^\bullet u + \frac{1}{\varepsilon}\psi'(u)\partial^\bullet u \,\mathrm{d}\sigma + \int_{\Gamma(t)} \frac{\varepsilon}{2}\mathcal{B}(v)\nabla_\Gamma u \cdot \nabla_\Gamma u + \frac{1}{\varepsilon}\psi(u)\nabla_\Gamma \cdot v \,\mathrm{d}\sigma.
\end{aligned}$$

To obtain a gradient flow there would need to be a model for v and which would lead to a coupled system for u and v. In terms of modelling, we feel these extra terms are geometric terms determining an evolution equation for the surface, which we assume is given. Therefore, we do not consider such terms in this work.

In place of the gradient flow approach, we will consider a conservation law on an evolving surface with a diffusive flux driven by a chemical potential. This is the approach taken by Erlebacher et al. (2001) in the derivation of the model presented in Section 1.3. In general, the energy $E^{\Gamma(t)}_{\mathrm{GL}}(u)$ will not decrease along the trajectory of solutions. Any long term results will be dependent on assumptions on the long term behaviour of the surface.

Conservation law

Let u represent a density of a scalar quantity on $\Gamma(t)$. For an arbitrary portion $\mathcal{M}(t)$ of $\Gamma(t)$ (which is the image of a portion $\mathcal{M}_0$ of Γ_0 under the velocity flow $v = v_\nu$),

we will assume a conservation law of the form

$$\frac{\mathrm{d}}{\mathrm{d}t}\int_{\mathcal{M}(t)} u \,\mathrm{d}\sigma = \int_{\partial\mathcal{M}(t)} q \cdot \mu \,\mathrm{d}\sigma. \tag{3.2.12}$$

Here q represents the tangential flux of u on $\{\Gamma(t)\}$. For the left hand side of (3.2.12), we use the transport formula (3.2.6):

$$\frac{\mathrm{d}}{\mathrm{d}t}\int_{\mathcal{M}(t)} u \,\mathrm{d}\sigma = \int_{\mathcal{M}(t)} \partial^\circ u + u\nabla_\Gamma \cdot v_\nu \,\mathrm{d}\sigma,$$

and for the right hand side, we use integration by parts (A.2.8):

$$\int_{\partial\mathcal{M}(t)} q \,\mathrm{d}\sigma = -\int_{\mathcal{M}(t)} \nabla_\Gamma \cdot q \,\mathrm{d}\sigma.$$

Equating the two previous equations leads to the pointwise conservation law

$$\partial^\circ u + u\nabla_\Gamma \cdot v_\nu + \nabla_\Gamma \cdot q = 0. \tag{3.2.13}$$

Remark 3.2.6. One has the choice to model the surface as either a set evolving with purely normal velocity, and that any tangential motion can be described via an advective flux, or consisting of material points. The second approach, used by Dziuk and Elliott (2007a), leads to a conservation law of the form:

$$\partial^\bullet u + u\nabla_\Gamma \cdot v + \nabla_\Gamma \cdot q = 0.$$

The second approach can be seen as equivalent to the first, with the addition of an advective flux driven by the tangential velocity of the surface. This is the approach taken in this work.

Cahn-Hilliard equation

We will assume that the flux q is the sum of a diffusive flux q_d and an advective flux q_a:

$$q_d = -\nabla_\Gamma w \quad \text{and} \quad q_a = uv_\tau.$$

The diffusive flux is driven by the gradient of chemical potential w given by

$$w = -\varepsilon\Delta_\Gamma u + \frac{1}{\varepsilon}\psi'(u).$$

This leads to the fourth order Cahn-Hilliard equation on $\mathcal{G}_T$:

$$\partial^\bullet u + u\nabla_\Gamma \cdot v = \Delta_\Gamma \left(-\varepsilon \Delta_\Gamma u + \frac{1}{\varepsilon}\psi'(u) \right). \tag{3.2.14}$$

Alternatively, following Elliott et al. (1989), we can write this equation as a system of second order equations:

$$\partial^\bullet u + u\nabla_\Gamma \cdot v - \Delta_\Gamma w = 0 \tag{3.2.15a}$$

$$-\varepsilon \Delta_\Gamma u + \frac{1}{\varepsilon}\psi'(u) - w = 0. \tag{3.2.15b}$$

We close the system with the initial condition

$$u(\cdot, 0) = u_0 \quad \text{on } \Gamma_0. \tag{3.2.16}$$

There are no boundary conditions since the boundary of $\Gamma(t)$ is empty.

3.2.4 Solution spaces

In standard parabolic theory one looks for solutions in Bochner spaces. Considering our Cahn-Hilliard equation on a Cartesian domain Ω (Elliott 1989), one would expect solutions to live in the spaces

$$u \in L^\infty(0, T; H^1(\Omega)), u' \in L^2(0, T; H^{-1}(\Omega)), w \in L^2(0, T; H^1(\Omega)).$$

These spaces are constructed by considering u as a function from $(0, T)$ into the Hilbert space $H^1(\Omega)$. We would like to extend this definition so that $u(t)$ is in the now time-dependent Hilbert space $H^1(\Gamma(t))$. The following definitions are this generalisation. We consider Sobolev spaces over the space-time domain $\mathcal{G}_T$. We will write $\nabla_{\mathcal{G}_T}$ for the space-time gradient and $\mathrm{d}\sigma_T$ for the space-time measure on $\mathcal{G}_T$. We contrast our approach with that of Vierling (2011), who proposed using an equivalent formulation using a reference domain.

We start by presenting the space-time domains $L^2(\mathcal{G}_T)$ and $H^1(\mathcal{G}_T)$ defined by

$$L^2(\mathcal{G}_T) := \left\{ \eta \in L^1_{\mathrm{loc}}(\mathcal{G}_T) : \int_{\mathcal{G}_T} \eta^2 \, \mathrm{d}\sigma_T < +\infty \right\}$$

$$H^1(\mathcal{G}_T) := \left\{ \eta \in L^2(\mathcal{G}_T) : \nabla_{\mathcal{G}_T} \eta \in L^2(\mathcal{G}_T) \right\}.$$

with norms

$$\|\eta\|_{L^2(\mathcal{G}_T)} := \left(\int_{\mathcal{G}_T} \eta^2 \,\mathrm{d}\sigma_T\right)^{\frac{1}{2}}$$
$$\|\eta\|_{H^1(\mathcal{G}_T)} := \left(\|\eta\|^2_{L^2(\mathcal{G}_T)} + \|\nabla_{\mathcal{G}_T}\eta\|^2_{L^2(\mathcal{G}_T)}\right)^{\frac{1}{2}}.$$

Proposition 3.2.7. *The space $H^1(\mathcal{G}_T)$ is compactly embedded into $L^2(\mathcal{G}_T)$.*

Proof. The result follows from the Rellich-Kondrakov theorem for manifolds shown in Hebey (2000, Theorem 2.9) □

Using the identities,

$$\int_0^T \int_{\Gamma(t)} \eta \,\mathrm{d}\sigma \,\mathrm{d}t = \int_{\mathcal{G}_T} \frac{\eta}{\sqrt{1+|v_\nu|^2}} \,\mathrm{d}\sigma_T,$$

and

$$\nabla_{\mathcal{G}_T}\eta = \left(\nabla_\Gamma \eta + \frac{\partial^\circ \eta \, v_\nu}{1+|v_\nu|^2}, \frac{\partial^\circ \eta}{1+|v_\nu|^2}\right),$$

our assumptions on v imply that the space-time norms can be replaced with the equivalent norms

$$\|\eta\|'_{L^2(\mathcal{G}_T)} := \left(\int_0^T \int_{\Gamma(t)} \eta^2 \,\mathrm{d}\sigma \,\mathrm{d}t\right)^{\frac{1}{2}}$$
$$\|\eta\|'_{H^1(\mathcal{G}_T)} := \left(\int_0^T \int_{\Gamma(t)} \eta^2 + |\nabla_\Gamma \eta|^2 + (\partial^\circ \eta)^2 \,\mathrm{d}\sigma \,\mathrm{d}t\right)^{\frac{1}{2}}.$$

We will use the equivalent primed norms (dropping the prime) on $L^2(\mathcal{G}_T)$ and $H^1(\mathcal{G}_T)$ in the following.

We define the space $L^2_{L^2}$ by

$$L^2_{L^2} := \left\{\eta \in L^1_{\mathrm{loc}}(\mathcal{G}_T) : \int_0^T \int_{\Gamma(t)} \eta \,\mathrm{d}\sigma \,\mathrm{d}t < +\infty\right\},$$

with the inner product

$$(\eta, \xi)_{L^2_{L^2}} := \int_0^T \int_{\Gamma(t)} \eta\xi \,\mathrm{d}\sigma \,\mathrm{d}t.$$

It is clear that $L^2_{L^2}$ is equivalent to $L^2(\mathcal{G}_T)$ and hence is a Hilbert space.

Next, we define the space $L^2_{H^1}$ as

$$L^2_{H^1} := \left\{\eta\colon \mathcal{G}_T \to \mathbb{R} : \eta \in L^2_{L^2} \text{ and } \nabla_\Gamma \eta \in (L^2_{L^2})^{n+1}\right\},$$

with the inner product

$$(\eta, \xi)_{L^2_{H^1}} := \int_0^T \int_{\Gamma(t)} \nabla_\Gamma \eta \cdot \nabla_\Gamma \xi + \eta\xi \,\mathrm{d}\sigma \,\mathrm{d}t,$$

where $\nabla_\Gamma \eta$ should be interpreted in the weak sense. Notice that elements of this space are weakly differentiable at almost every time.

Lemma 3.2.8. *The space $L^2_{H^1}$ is a Hilbert space.*

Proof. It is clear that this is an inner product space and we are left to show completeness. Suppose that η_k is a Cauchy sequence in $L^2_{H^1}$. This implies that η_k and $\nabla_\Gamma \eta_k$ are Cauchy sequences in $L^2(\mathcal{G}_T)$ and $(L^2(\mathcal{G}_T))^{n+1}$. This means that there exists $\eta \in L^2(\mathcal{G}_T), \xi \in (L^2(\mathcal{G}_T))^{n+1}$ such that

$$\|\eta_k - \eta\|_{L^2(\mathcal{G}_T)} + \|\nabla_\Gamma \eta_k - \xi\|_{L^2(\mathcal{G}_T)} \to 0 \quad \text{as } k \to \infty.$$

Fix $t^* \in (0,T)$ and let $\varphi \in C^1(\Gamma(t^*))$ and $\alpha \in C(0,T)$. Using Lemma 3.2.5, we can construct $\widetilde{\varphi}\colon \mathcal{G}_T \to \mathbb{R}$ such that $\widetilde{\varphi}(\cdot, t) = \varphi$ and $\widetilde{\varphi} \in C^1(\Gamma(t))$ for each time $t \in (0,T)$. Then, for $j = 1, \dots, n+1$, we obtain

$$\begin{aligned}
&\int_0^T \int_{\Gamma(t)} \eta \underline{D}_j(\alpha\widetilde{\varphi}) + \xi_j(\alpha\widetilde{\varphi}) \,\mathrm{d}\sigma \,\mathrm{d}t \\
&\quad = \int_0^T \int_{\Gamma(t)} (\eta - \eta_k)\underline{D}_j(\alpha\widetilde{\varphi}) + \left(\eta_k \underline{D}_j(\alpha\widetilde{\varphi}) + \xi_j(\alpha\widetilde{\varphi})\right) \mathrm{d}\sigma \,\mathrm{d}t \\
&\quad = \int_0^T \int_{\Gamma(t)} (\eta - \eta_k)\underline{D}_j(\alpha\widetilde{\varphi}) + (-\underline{D}_j\eta_k + \xi_j)(\alpha\widetilde{\varphi}) \,\mathrm{d}\sigma \,\mathrm{d}t,
\end{aligned}$$

where we have used the fact that η_k is weakly differentiable at almost every time. Taking the limit $k \to \infty$, we infer

$$\int_0^T \alpha \left(\int_{\Gamma(t)} \eta \underline{D}_j \widetilde{\varphi} + \xi_j \widetilde{\varphi} \,\mathrm{d}\sigma \right) \mathrm{d}t = 0.$$

Since this holds for all $\alpha \in C(0,T)$, by the Fundamental Lemma of the Calculus of

Variations, at $t = t^*$, we have

$$\int_{\Gamma(t^*)} \eta \underline{D}_j \varphi + \xi_j \varphi \, \mathrm{d}\sigma = 0 \quad \text{for all } \varphi \in C^1(\Gamma(t^*)).$$

Since the choice of t^* was arbitrary, we infer that ξ is the weak gradient of η for almost every time $t \in (0, T)$ and the proof is complete. □

The equivalence of norms implies that $\eta \in L^2_{H^1}$ with $\partial^\bullet u \in L^2_{L^2}$ if, and only if, $\eta \in H^1(\mathcal{G}_T)$.

For $1 \leq q \leq \infty$, we will define the space $L^q_{H^1}$ by

$$L^q_{H^1} := \left\{ \eta \in L^q(\mathcal{G}_T) : \|\eta\|_{L^q_{H^1}} < +\infty \right\},$$

with norm

$$\|\eta\|_{L^q_{H^1}} := \begin{cases} \left(\displaystyle\int_0^T \|\eta\|^q_{H^1(\Gamma(t))} \, \mathrm{d}t \right)^{\frac{1}{q}} & \text{for } q < \infty, \\ \operatorname*{ess\,sup}_{t \in (0,T)} \|\eta\|_{H^1(\Gamma(t))} & \text{for } q = \infty. \end{cases}$$

It is clear that $L^\infty_{H^1} \subset L^2_{H^1}$ and that

$$\|\eta\|_{L^2_{H^1}} \leq \sqrt{T} \, \|\eta\|_{L^\infty_{H^1}} \quad \text{for all } \eta \in L^\infty_{H^1}.$$

Finally, we define $L^\infty_{H^2}$ and $L^2_{H^2}$ by

$$L^\infty_{H^2} := \left\{ \eta \in L^2(\mathcal{G}_T) : \operatorname*{ess\,sup}_{t \in (0,T)} \|\eta\|_{H^2(\Gamma(t))} < +\infty \right\}$$
$$L^2_{H^2} := \left\{ \eta \in L^2(\mathcal{G}_T) : \int_0^T \|\eta\|^2_{H^2(\Gamma(t))} \, \mathrm{d}t < +\infty \right\}.$$

Remark 3.2.9. As a restriction on our analysis we will only consider $\partial^\bullet u$ as a function in $L^2_{L^2}$ since we do not wish to consider a weak material derivative. Such considerations are left to future work.

We conclude this section with a result which will take an integral in time equality into an almost everywhere in time equality. The proof is the generalisation of a similar result given by in Robinson (2001, Lemma 7.4) for planar domains.

Lemma 3.2.10. *Let $\eta \in L^2_{H^1}$ with*

$$\int_0^T \int_{\Gamma(t)} \nabla_\Gamma \eta \cdot \nabla_\Gamma \xi + \eta \xi \, \mathrm{d}\sigma \, \mathrm{d}t = 0 \quad \textit{for all } \xi \in L^2_{H^1}. \tag{3.2.17}$$

Then for almost all times $t \in (0,T)$,

$$\int_{\Gamma(t)} \nabla_\Gamma \eta \cdot \nabla_\Gamma \varphi + \eta\varphi \,\mathrm{d}\sigma = 0 \quad \text{for all } \varphi \in L^2_{H^1}. \tag{3.2.18}$$

Proof. Fix $\varphi \in L^2_{H^1}$ and $\alpha \in C([0,T])$, then choosing $\xi = \alpha\varphi \in L^2_{H^1}$ and

$$0 = \int_0^T \int_{\Gamma(t)} \nabla_\Gamma \eta \cdot \nabla_\Gamma \xi + \eta\xi \,\mathrm{d}\sigma \,\mathrm{d}t = \int_0^T \alpha \left(\int_{\Gamma(t)} \nabla_\Gamma \eta \cdot \nabla_\Gamma \varphi + \eta\varphi \,\mathrm{d}\sigma \right) \mathrm{d}t.$$

Since the choice of α was arbitrary, the Fundamental Lemma of the Calculus of Variations implies the result. □

3.2.5 Weak and variational form

Our finite element method will be based on a variational form of (3.2.15). The standard approach of simply integrating by parts leads to a weak form, which although useful for analytic considerations, will still contain explicit reference to the velocity field v. We can remove this by using the transport formula (3.2.6), hiding this instead in the material derivative of a test function. The resulting equation will be called the variational form.

We start by multiplying (3.2.15a, 3.2.15b) by a test function φ and apply integration by parts to the Laplacian terms to give the weak form. This will be the definition of solution used throughout this chapter.

Definition 3.2.11 (Weak solution). We say that the pair $(u,w)\colon \mathcal{G}_T \to \mathbb{R}^2$, with $u \in L^\infty_{H^1} \cap H^1(\mathcal{G}_T)$ and $w \in L^2_{H^1}$, are a weak solution of the Cahn-Hilliard equation (3.2.14) if, for almost every time $t \in (0,T)$,

$$\int_{\Gamma(t)} \partial^\bullet u\varphi + u\varphi\nabla_\Gamma \cdot v + \nabla_\Gamma w \cdot \nabla_\Gamma \varphi \,\mathrm{d}\sigma = 0 \tag{3.2.19a}$$

$$\int_{\Gamma(t)} \varepsilon \nabla_\Gamma u \cdot \nabla_\Gamma \varphi + \frac{1}{\varepsilon}\psi'(u)\varphi - w\varphi \,\mathrm{d}\sigma = 0, \tag{3.2.19b}$$

$$\text{for all } \varphi \in L^2_{H^1},$$

and $u(\cdot,0) = u_0$ pointwise almost everywhere in Γ_0.

We will show well-posedness of a weak solution in Section 3.4 by showing convergence of a finite element method.

Restricting our thoughts to $\varphi \in H^1(\mathcal{G}_T)$, applying the transport formula to

the first two terms in (3.2.19a) gives

$$\int_{\Gamma(t)} \partial^\bullet u\varphi + u\varphi\nabla_\Gamma \cdot v \,\mathrm{d}\sigma = \frac{\mathrm{d}}{\mathrm{d}t}\left(\int_{\Gamma(t)} u\varphi \,\mathrm{d}\sigma\right) - \int_{\Gamma(t)} u\partial^\bullet\varphi \,\mathrm{d}\sigma.$$

This gives the variational formulation:

$$\frac{\mathrm{d}}{\mathrm{d}t}\left(\int_{\Gamma(t)} u\varphi \,\mathrm{d}\sigma\right) + \int_{\Gamma(t)} \nabla_\Gamma w \cdot \nabla_\Gamma\varphi \,\mathrm{d}\sigma = \int_{\Gamma(t)} u\partial^\bullet\varphi \,\mathrm{d}\sigma \tag{3.2.20a}$$

$$\int_{\Gamma(t)} \varepsilon\nabla_\Gamma u \cdot \nabla_\Gamma\varphi + \frac{1}{\varepsilon}\psi'(u)\varphi \,\mathrm{d}\sigma = \int_{\Gamma(t)} w\varphi \,\mathrm{d}\sigma. \tag{3.2.20b}$$

As with other chapters, it will be useful to write these equations using abstract bilinear forms. We define the following three to describe the above equations for $\eta, \varphi \in H^1(\Gamma(t))$:

$$\begin{aligned} m(\eta,\varphi) &= \int_{\Gamma(t)} \eta\varphi \,\mathrm{d}\sigma \\ a(\eta,\varphi) &= \int_{\Gamma(t)} \nabla_\Gamma\eta \cdot \nabla_\Gamma\varphi \,\mathrm{d}\sigma \\ g(v;\eta,\varphi) &= \int_{\Gamma(t)} \eta\varphi\nabla_\Gamma \cdot v \,\mathrm{d}\sigma. \end{aligned}$$

This lets us write (3.2.19) as

$$\begin{aligned} m(\partial^\bullet u,\varphi) + g(v;u,\varphi) + a(w,\varphi) &= 0 \\ \varepsilon a(u,\varphi) + \frac{1}{\varepsilon}m(\psi'(u),\varphi) - m(w,\varphi) &= 0, \end{aligned} \tag{3.2.21}$$

and (3.2.20) as

$$\begin{aligned} \frac{\mathrm{d}}{\mathrm{d}t}m(u,\varphi) + a(w,\varphi) &= m(u,\partial^\bullet\varphi) \\ \varepsilon a(u,\varphi) + \frac{1}{\varepsilon}m(\psi'(u),\varphi) &= m(w,\varphi). \end{aligned} \tag{3.2.22}$$

We may also write the results of Corollary 3.2.4 in this form:

$$\begin{aligned} \frac{\mathrm{d}}{\mathrm{d}t}m(\eta,\varphi) &= m(\partial^\bullet\eta,\varphi) + m(\eta,\partial^\bullet\varphi) + g(v;\eta,\varphi) \\ \frac{\mathrm{d}}{\mathrm{d}t}a(\eta,\varphi) &= a(\partial^\bullet\eta,\varphi) + a(\eta,\partial^\bullet\varphi) + b(v;\eta,\varphi), \end{aligned}$$

with the addition of

$$b(v;\eta,\varphi) = \int_{\Gamma(t)} \mathcal{B}(v)\nabla_\Gamma\eta \cdot \nabla_\Gamma\varphi \,\mathrm{d}\sigma,$$

using $\mathcal{A} = \mathrm{Id}$ in the definition of $\mathcal{B}(v)$.

3.3 Finite element approximation

In this section, we propose a finite element method for approximating solutions of the Cahn-Hilliard equation (3.2.14). It is based on the evolving surface finite element method of Dziuk and Elliott (2007a). Similarly to other chapters, we will use a discrete approximation of the family of surfaces $\{\Gamma(t)\}$ approximated at each time by a polyhedral surface $\Gamma_h(t)$ with nodes lying on $\Gamma(t)$. We impose, in addition, that the nodes of $\{\Gamma_h(t)\}$ evolve according to the smooth underlying velocity of the surface $\{\Gamma(t)\}$. Our time dependent finite element space will be based on this family of discrete surfaces.

From a practical view point, a key advantage of this methodology is that basis functions have zero discrete material velocity. We will see that this results in no mention of the velocity or curvature in the resulting finite element scheme.

3.3.1 Evolving triangulation and discrete material derivative

Let $\Gamma_{h,0}$ be a polyhedral approximation of the initial surface Γ_0 with the restriction that the nodes $\{X_j^0\}_{j=1}^N$ of $\Gamma_{h,0}$ lie on Γ_0. Ideas of how to construct this can be found in Section A.3.1. We evolve the nodes to form trajectories $\{X_j(t)\}_{j=1}^N$ by the smooth surface velocity:

$$\dot{X}_j(t) = v(X_j(t), t), \quad X_j(0) = X_j^0, \qquad \text{for } j = 1, \dots, N.$$

Interpolating between these nodes defines a family of discrete surfaces $\{\Gamma_h(t)\}$. At each time, we assume that we have a triangulation $\mathscr{T}_h(t)$ of $\Gamma_h(t)$, with h the maximum diameter of elements in $\mathscr{T}_h(t)$ uniformly in time:

$$h := \sup_{t\in(0,T)} \max_{E(t)\in\mathscr{T}_h(t)} \operatorname{diam} E(t). \tag{3.3.1}$$

We assume that $\mathscr{T}_h$ is quasi-uniform as in the sense defined in Definition A.3.1, uniformly in time.

Lemma 3.3.1. *Under our assumptions on $\{\Gamma_h(t)\}$, we have that*

$$\sup_{t\in[0,T]} \left(\|\nabla_{\Gamma_h} \cdot V_h\|_{L^\infty(\Gamma_h(t))} + \|\mathcal{B}_h(V_h)\|_{L^\infty(\Gamma_h(t))} \right) \leq c \sup_{t\in[0,T]} \|v\|_{C^2(\mathcal{N}_T)}. \tag{3.3.2}$$

Proof. The result follows from applying the geometric estimates (3.3.26) and (3.3.45) along with our assumption that $v \in C^2(\mathcal{N}_T)$. □

Remark 3.3.2. In practical situations, assuming a uniformly regular mesh may not be feasible. Large surface deformations can lead to poor quality triangulations with deformed elements. In such cases, re-meshing may be required; see Clarenz, Diewald, Dziuk and Rumpf (2004); Eilks and Elliott (2008), for example. Alternatively, one may use an arbitrary Lagrangian-Eulerian formulation by allowing extra tangential mesh motions; see Elliott and Styles (2012) and Elliott and Stinner (2013) for details.

We define ν_h element-wise as the unit outward pointing normal to $\Gamma_h(t)$ and denote by ∇_{Γ_h} the tangential gradient on $\Gamma_h(t)$ defined element-wise by

$$\nabla_{\Gamma_h}\eta_h := \nabla\widetilde{\eta}_h - (\nabla\widetilde{\eta}_h \cdot \nu_h)\nu_h = (\mathrm{Id} - \nu_h \otimes \nu_h)\nabla\widetilde{\eta}_h =: P_h\nabla\widetilde{\eta}_h.$$

This is a vector-valued quantity and we will denote its components by

$$\nabla_{\Gamma_h}\eta_h = \left(\underline{D}_{h,1}\eta_h, \ldots, \underline{D}_{h,n+1}\eta_h\right)$$

We define the finite element space of piecewise linear functions on $\Gamma_h(t)$ by

$$S_h(t) := \{\phi_h \in C(\Gamma_h(t)) : \phi_h|_{E(t)} \text{ is affine linear, for each } E(t) \in \mathscr{T}_h(t)\}. \quad (3.3.3)$$

We will write $\{\phi_j^N(\cdot,t)\}_{j=1}^N$ for the nodal basis of $S_h(t)$ given by $\phi_j^N(X_i(t),t) = \delta_{ij}$.

The definition of a basis of $S_h(t)$ allows us to characterise the velocity of the surface $\{\Gamma_h(t)\}$. An arbitrary point $X(t)$ on $\Gamma_h(t)$ evolves according to the discrete velocity V_h:

$$\dot{X}(t) = V_h(X(t),t) = \sum_{j=1}^N \dot{X}_j(t)\phi_j^N(X(t),t) = \sum_{j=1}^N v(X_j(t),t)\phi_j^N(X(t),t). \quad (3.3.4)$$

We will write $\mathcal{G}_{h,T}$ as the discrete equivalent to $\mathcal{G}_T$:

$$\mathcal{G}_{h,T} := \bigcup_{t\in(0,T)} \Gamma_h(t) \times \{t\}. \quad (3.3.5)$$

The discrete velocity V_h induces a discrete material derivative. For a scalar quantity η_h on $\mathcal{G}_{h,T}$, we define the discrete material derivative $\partial_h^\bullet\eta_h$ by

$$\partial_h^\bullet\eta_h := \partial_t\widetilde{\eta}_h + \nabla\widetilde{\eta}_h \cdot V_h, \quad (3.3.6)$$

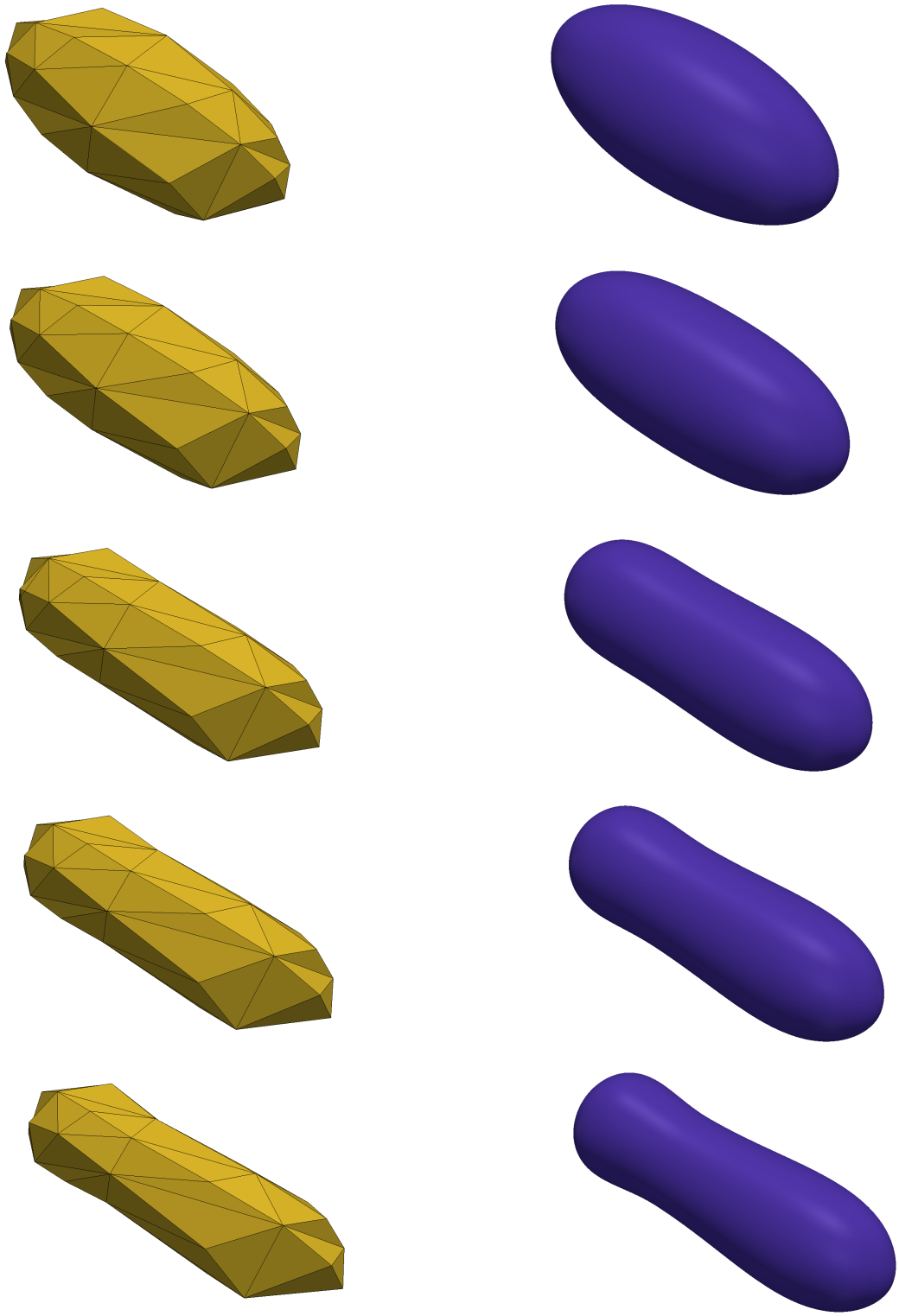

Figure 3.3.1: Example of an evolving triangulated surface. The left images (yellow) represent a course mesh and the right (blue) a more refined mesh.

where $\widetilde{\eta}_h$ is an arbitrary extension of η_h to $\mathcal{N}_T$. This leads to the remarkable transport property of the basis functions $\{\phi_j^N\}$.

Lemma 3.3.3 (Transport of basis functions)**.** *Let $\phi_j^N : \mathcal{G}_{h,T} \to \mathbb{R}$ be a nodal basis function as described above, then*

$$\partial_h^\bullet \phi_j^N = 0. \tag{3.3.7}$$

Proof. From $\phi_j^N(X_i(t), t) = \delta_{ij}$, we have

$$\begin{aligned} 0 = \frac{\mathrm{d}}{\mathrm{d}t}\phi_j^N(X_i(t),t) &= \phi_{j,t}^N(X_i(t),t) + \nabla\phi_j^N(X_i(t),t)\cdot\dot{X}_i(t) \\ &= \phi_{j,t}^N(X_i(t),t) + \nabla\phi_j^N(X_i(t),t)\cdot V_h(X_i(t),t) = \partial_h^\bullet\phi_j^N(X_i(t),t). \end{aligned}$$

This implies that $\partial_h^\bullet\phi_j^N$ is zero at all vertices of $\Gamma_h(t)$, and hence $\partial_h^\bullet\phi_j^N = 0$. □

These discrete quantities also satisfy a variant of the transport formula from Lemma 3.2.3. We label the surface measure on $\Gamma_h(t)$ as $\mathrm{d}\sigma_h$.

Lemma 3.3.4 (Transport lemma for triangulated surfaces)**.** *Let $\{\Gamma_h(t)\}$ be a discrete family of triangulated surfaces evolving with velocity V_h. Let η_h, ϕ_h be time-dependent finite element functions such that the following quantities exist. Then, we have*

$$\frac{\mathrm{d}}{\mathrm{d}t}\int_{\Gamma_h(t)} \eta_h \,\mathrm{d}\sigma_h = \int_{\Gamma_h(t)} \partial_h^\bullet\eta_h + \eta_h\nabla_{\Gamma_h}\cdot V_h \,\mathrm{d}\sigma_h. \tag{3.3.8}$$

In particular, for the L^2 inner product this means that

$$\frac{\mathrm{d}}{\mathrm{d}t}\int_{\Gamma_h(t)} \eta_h\phi_h \,\mathrm{d}\sigma_h = \int_{\Gamma_h(t)} (\partial_h^\bullet\eta_h)\phi_h + \eta_h(\partial_h^\bullet\phi_h) + \eta_h\phi_h\nabla_{\Gamma_h}\cdot V_h \,\mathrm{d}\sigma_h, \tag{3.3.9}$$

and for the Dirichlet inner product, we obtain

$$\begin{aligned} \frac{\mathrm{d}}{\mathrm{d}t}\int_{\Gamma_h(t)} \nabla_{\Gamma_h}\eta_h\cdot\nabla_{\Gamma_h}\phi_h \,\mathrm{d}\sigma_h = &\int_{\Gamma_h(t)} \nabla_{\Gamma_h}(\partial_h^\bullet\eta_h)\cdot\nabla_{\Gamma_h}\phi_h + \nabla_{\Gamma_h}\eta_h\cdot\nabla_{\Gamma_h}(\partial_h^\bullet\phi_h)\,\mathrm{d}\sigma_h \\ &+ \sum_{E(t)\in\mathscr{T}_h(t)}\int_{E(t)} \mathcal{B}_h(V_h)\nabla_{\Gamma_h}\eta_h\cdot\nabla_{\Gamma_h}\phi_h \,\mathrm{d}\sigma_h, \end{aligned} \tag{3.3.10}$$

where

$$\mathcal{B}_h(V_h) = \frac{1}{2}(\nabla_{\Gamma_h}\cdot V_h)\mathrm{Id} - D_h(V_h) \quad \text{and} \quad D_h(V_h)_{ij} = \frac{1}{2}\big(\underline{D}_{h,i}V_{h,j} + \underline{D}_{h,j}V_{h,i}\big).$$

Proof. Following Dziuk and Elliott (2013a, Lemma 4.2), we write

$$\frac{\mathrm{d}}{\mathrm{d}t}\int_{\Gamma_h(t)}\eta_h\,\mathrm{d}\sigma_h=\sum_{E(t)\in\mathscr{T}_h}\frac{\mathrm{d}}{\mathrm{d}t}\int_{E(t)}\eta_h\,\mathrm{d}\sigma_h,$$

and apply the results transport formulae of Lemma 3.2.3 and Corollary 3.2.4 element-wise. □

3.3.2 Finite element scheme

Simply put, our finite element scheme for the approximate solutions of (3.2.14) is based on solving a discrete version of the variational form (3.2.20) on the surface $\{\Gamma_h(t)\}$ over the finite element space $S_h(t)$.

We will assume that the initial condition to our finite element method $U_0\in S_h(\Gamma_{h,0})$ satisfies

$$\int_{\Gamma_{h,0}}\varepsilon\left(|U_0|^2+|\nabla_{\Gamma_h}U_0|^2\right)+\frac{1}{\varepsilon}\psi(U_0)\,\mathrm{d}\sigma_h<+\infty. \tag{3.3.11}$$

Remark 3.3.5. One particular choice of initial condition will be to take U_0 as a suitable approximation (for example, $\Pi_h u_0$ defined in (3.3.48)) of u_0 with u_0 satisfying (3.4.8).

Our solution spaces will be

$$\begin{aligned}S_h^T&:=\{\phi_h\in C(\mathcal{G}_{h,T}):\phi_h(\cdot,t)\in S_h(t)\text{ for all }t\in[0,T],\text{ and }\partial_h^\bullet\phi_h\in C(\mathcal{G}_{h,T})\}\\ \widetilde{S}_h^T&:=\{\phi_h\in C(\mathcal{G}_{h,T}):\phi_h(\cdot,t)\in S_h(t)\text{ for all }t\in[0,T]\}.\end{aligned} \tag{3.3.12}$$

The finite element scheme is: Given U_0, find $U_h\in S_h^T$ and $W_h\in\widetilde{S}_h^T$ such that for almost every time $t\in(0,T)$

$$\frac{\mathrm{d}}{\mathrm{d}t}\left(\int_{\Gamma_h(t)}U_h\phi_h\,\mathrm{d}\sigma_h\right)+\int_{\Gamma_h(t)}\nabla_{\Gamma_h}W_h\cdot\nabla_{\Gamma_h}\phi_h\,\mathrm{d}\sigma_h=\int_{\Gamma_h(t)}U_h\partial_h^\bullet\phi_h\,\mathrm{d}\sigma_h \tag{3.3.13a}$$

$$\int_{\Gamma_h(t)}\varepsilon\nabla_{\Gamma_h}U_h\cdot\nabla_{\Gamma_h}\phi_h+\frac{1}{\varepsilon}\psi'(U_h)\phi_h\,\mathrm{d}\sigma_h=\int_{\Gamma_h(t)}W_h\phi_h\,\mathrm{d}\sigma_h \tag{3.3.13b}$$

$$\text{for all }\phi_h\in S_h(t),$$

subject to the initial condition

$$U_h(\cdot,0)=U_0. \tag{3.3.14}$$

The transport formula (3.3.9) implies that, for $\phi_h \in S_h^T$, (3.3.13a) is equivalent to

$$\int_{\Gamma_h(t)} \partial_h^\bullet U_h \phi_h + U_h \phi_h \nabla_{\Gamma_h} \cdot V_h + \nabla_{\Gamma_h} W_h \cdot \nabla_{\Gamma_h} \phi_h \, \mathrm{d}\sigma_h = 0. \tag{3.3.15}$$

We can write these equations in matrix form. First, we will introduce vectors $\alpha(t), \beta(t) \in \mathbb{R}^N$ for the nodal values of U_h and W_h by

$$U_h(x,t) = \sum_{j=1}^N \alpha_j(t) \phi_j^N(x,t), \quad W_h(x,t) = \sum_{j=1}^N \beta_j(t) \phi_j^N(x,t) \quad \text{for } (x,t) \in \mathcal{G}_{h,T}.$$

In place of the bilinear forms, we have the mass matrix $\mathcal{M}(t)$ and stiffness matrix $\mathcal{S}(t)$:

$$\mathcal{M}(t)_{ij} = \int_{\Gamma_h(t)} \phi_i^N \phi_j^N \, \mathrm{d}\sigma_h \qquad \mathcal{S}(t)_{ij} = \int_{\Gamma_h(t)} \nabla_{\Gamma_h} \phi_i^N \cdot \nabla_{\Gamma_h} \phi_j^N \, \mathrm{d}\sigma_h,$$

and in place of the non-linear term, we will write

$$\Psi(\alpha(t))_j = \int_{\Gamma_h(t)} \psi' \left(\sum_{i=1}^N \alpha_i(t) \phi_i^N \right) \phi_j^N \, \mathrm{d}\sigma_h.$$

Using the transport of basis property (Lemma 3.3.3), we can write (3.3.13) as

$$\frac{\mathrm{d}}{\mathrm{d}t} \left(\mathcal{M}(t)\alpha(t) \right) + \mathcal{S}(t)\beta(t) = 0 \tag{3.3.16a}$$

$$\varepsilon \mathcal{S}(t)\alpha(t) + \frac{1}{\varepsilon} \Psi(\alpha(t)) - \mathcal{M}(t)\beta(t) = 0. \tag{3.3.16b}$$

Alternatively, eliminating $\beta(t)$, this can be written as

$$\frac{\mathrm{d}}{\mathrm{d}t} \left(\mathcal{M}(t)\alpha(t) \right) + \mathcal{S}(t)\mathcal{M}(t)^{-1} \left(\varepsilon \mathcal{S}(t)\alpha(t) + \frac{1}{\varepsilon} \Psi(\alpha(t)) \right) = 0. \tag{3.3.17}$$

One could also use lumped mass integration (Thomée 2006, chapter 15) instead of the full mass matrix.

Notice that this is the same structure as a finite element discretisation of a Cahn-Hilliard equation posed on a planar domain. We now have time dependent matrices which need to be assembled each time step. Various time stepping schemes have been considered for second-order parabolic problems on evolving surfaces. We mention in particular the work of Dziuk et al. (2012b), Dziuk and Elliott (2012) and Lubich et al. (2013).

Next, we introduce abstract notation which permit a more compact writing of the analysis that follows:

$$\begin{aligned} m_h(\eta_h, \phi_h) &= \int_{\Gamma_h(t)} \eta_h \phi_h \,\mathrm{d}\sigma_h \\ a_h(\eta_h, \phi_h) &= \int_{\Gamma_h(t)} \nabla_{\Gamma_h} \eta_h \cdot \nabla_{\Gamma_h} \phi_h \,\mathrm{d}\sigma_h \\ g_h(V_h; \eta_h, \phi_h) &= \int_{\Gamma_h(t)} \eta_h \phi_h \nabla_{\Gamma_h} \cdot V_h \,\mathrm{d}\sigma_h. \end{aligned}$$

The lets us write (3.3.13) as

$$\begin{aligned} \frac{\mathrm{d}}{\mathrm{d}t} m_h(U_h, \phi_h) + a_h(W_h, \phi_h) &= m_h(U_h, \partial_h^\bullet \phi_h) \\ \varepsilon a_h(U_h, \phi_h) + \frac{1}{\varepsilon} m_h(\psi'(U_h), \phi_h) &= m_h(W_h, \phi_h), \end{aligned}$$

and (3.3.15) as

$$m_h(\partial_h^\bullet U_h, \phi_h) + g_h(V_h; U_h, \phi_h) + a_h(W_h, \phi_h) = 0.$$

The transport laws from Lemma 3.3.4 transfer to the abstract setting also:

$$\begin{aligned} \frac{\mathrm{d}}{\mathrm{d}t} m_h(\eta_h, \phi_h) &= m_h(\partial_h^\bullet \eta_h, \phi_h) + m_h(\eta_h, \partial_h^\bullet \phi_h) + g_h(V_h; \eta_h, \phi_h) \\ \frac{\mathrm{d}}{\mathrm{d}t} a_h(\eta_h, \phi_h) &= a_h(\partial_h^\bullet \eta_h, \phi_h) + a_h(\eta_h, \partial_h^\bullet \phi_h) + b_h(V_h; \eta_h, \phi_h), \end{aligned}$$

where

$$b_h(V_h; \eta_h, \phi_h) = \sum_{E(t) \in \mathscr{T}_h(t)} \int_{E(t)} \mathcal{B}_h(V_h) \nabla_{\Gamma_h} \eta_h \cdot \nabla_{\Gamma_h} \phi_h \,\mathrm{d}\sigma_h.$$

Under the above assumptions, the following estimates are possible.

Theorem 3.3.6 (Well-posedness of the finite element scheme (3.3.13))**.** *For any $T > 0$, under the above assumptions on U_0 and $\{\Gamma_h(t)\}$, there exists a unique solution pair $(U_h, W_h) \in S_h^T \times \widetilde{S}_h^T$, both with C^1 in time nodal values, to the finite element scheme (3.3.13). Furthermore, $\int_{\Gamma_h(t)} U_h \,\mathrm{d}\sigma_h$ is conserved:*

$$\int_{\Gamma_h(t)} U_h \,\mathrm{d}\sigma_h = \int_{\Gamma_{h,0}} U_0 \,\mathrm{d}\sigma_h \quad \text{for all } t \in (0, T), \tag{3.3.18}$$

and the following bound is satisfied:

$$\begin{aligned}\sup_{t\in(0,T)}\int_{\Gamma_h(t)}\frac{\varepsilon}{2}\left(|\nabla_{\Gamma_h}U_h|^2+U_h^2\right)+\frac{1}{\varepsilon}\psi(U_h)\,\mathrm{d}\sigma_h+\frac{1}{2}\int_0^T\|W_h\|^2_{H^1(\Gamma_h(t))}\,\mathrm{d}t\\ \leq c_\varepsilon\int_{\Gamma_{h,0}}\frac{\varepsilon}{2}\left(|\nabla_{\Gamma_h}U_0|^2+|U_0|^2\right)+\frac{1}{\varepsilon}\psi(U_0)\,\mathrm{d}\sigma_h.\end{aligned}\tag{3.3.19}$$

Proof. Considering (3.3.17), since $\mathcal{M}(t)$ is positive definite, $\mathcal{S}(t)$ positive semi-definite and Ψ is locally Lipschitz, standard theory of ordinary differential equations gives a unique short-time solution $\alpha\in C^1([0,T_0];\mathbb{R}^N)$ for some $T_0<T$. From (3.3.8), we know $\mathcal{S}(t)$ and $\mathcal{M}(t)$ are C^1 in time, and $\mathcal{M}(t)^{-1}\in C^1$ by the Inverse Function Theorem. Thus, we infer

$$\beta(t)=\mathcal{M}(t)^{-1}\mathcal{S}(t)\mathcal{M}(t)^{-1}(\varepsilon\mathcal{S}(t)\alpha(t)+\frac{1}{\varepsilon}\Psi(\alpha(t)))\in C^1([0,T_0];\mathbb{R}^N).$$

This is easily translated into solutions U_h,W_h in the appropriate spaces.

To extend to the long-term solution, we construct an energy bound. We start by testing (3.3.13a) with W_h and (3.3.13b) with $\partial_h^\bullet U_h$ and sum to see

$$\begin{aligned}&\varepsilon a_h(U_h,\partial_h^\bullet U_h)+\frac{1}{\varepsilon}m_h(\psi'(U_h),\partial_h^\bullet U_h)+a_h(W_h,W_h)\\&\quad=-\frac{\mathrm{d}}{\mathrm{d}t}m_h(U_h,W_h)+m_h(U_h,\partial_h^\bullet W_h)+m_h(\partial_h^\bullet U_h,W_h).\end{aligned}$$

Applying the transport formulae from Lemma 3.3.4, we obtain

$$\begin{aligned}&\frac{\mathrm{d}}{\mathrm{d}t}\left(\varepsilon a_h(U_h,U_h)+\frac{1}{\varepsilon}m_h(\psi(U_h),1)\right)+a_h(W_h,W_h)\\&\quad=\frac{\varepsilon}{2}b_h(V_h;U_h,U_h)+\frac{1}{\varepsilon}g_h(V_h;\psi(U_h),1)-g_h(V_h;U_h,W_h).\end{aligned}$$

Using Lemma 3.3.1, applying a Young's inequality with $\delta=1/4$ leads to

$$\begin{aligned}&\frac{\mathrm{d}}{\mathrm{d}t}\left(\int_{\Gamma_h(t)}\frac{\varepsilon}{2}|\nabla_{\Gamma_h}U_h|^2+\frac{1}{\varepsilon}\psi(U_h)\,\mathrm{d}\sigma_h\right)+\int_{\Gamma_h(t)}|\nabla_{\Gamma_h}W_h|^2\,\mathrm{d}\sigma_h\\&\quad\leq c\int_{\Gamma_h(t)}\frac{\varepsilon}{2}|\nabla_{\Gamma_h}U_h|^2+\frac{1}{\varepsilon}\psi(U_h)\,\mathrm{d}\sigma_h+c\,\|U_h\|^2_{L^2(\Gamma_h(t))}+\frac{1}{4}\,\|W_h\|^2_{L^2(\Gamma_h(t))}.\end{aligned}\tag{3.3.20}$$

We start again by testing (3.3.13a) with εU_h. This gives

$$\begin{aligned}&\varepsilon\frac{\mathrm{d}}{\mathrm{d}t}m_h(U_h,U_h)+\varepsilon a_h(W_h,U_h)-\varepsilon m_h(U_h,\partial_h^\bullet U_h)\\&\quad=\frac{\varepsilon}{2}\frac{\mathrm{d}}{\mathrm{d}t}m_h(U_h,U_h)+\varepsilon a_h(W_h,U_h)-\frac{\varepsilon}{2}g_h(V_h;U_h,U_h)=0.\end{aligned}$$

Subtracting (3.3.13b) tested with W_h leads to

$$\begin{aligned}\frac{\varepsilon}{2}\frac{\mathrm{d}}{\mathrm{d}t}\left(\|U_h\|^2_{L^2(\Gamma_h(t))}\right)+\|W_h\|^2_{L^2(\Gamma_h(t))}&=\frac{\varepsilon}{2}g_h(V_h;U_h,U_h)+\frac{1}{\varepsilon}m_h(\psi'(U_h),W_h)\\&\leq\left(\frac{c}{\varepsilon}+c\varepsilon\right)\|U_h\|^2_{H^1(\Gamma_h(t))}+\frac{1}{4}\|W_h\|^2_{L^2(\Gamma_h(t))},\end{aligned}\tag{3.3.21}$$

where in the last line we have used the assumptions on the discrete velocity and the Sobolev embedding $H^1(\Gamma_h(t))\hookrightarrow L^6(\Gamma_h(t))$ from Lemma 3.3.8. Taking the sum of (3.3.20) and (3.3.21) and using a Gronwall inequality gives

$$\begin{aligned}&\sup_{t\in(0,T_0)}\int_{\Gamma_h(t)}\frac{\varepsilon}{2}\left(|\nabla_{\Gamma_h}U_h|^2+U_h^2\right)+\frac{1}{\varepsilon}\psi(U_h)\,\mathrm{d}\sigma_h+\frac{1}{2}\int_0^{T_0}\|W_h\|^2_{H^1(\Gamma_h(t))}\,\mathrm{d}t\\&\quad\leq c_\varepsilon\int_{\Gamma_{h,0}}\frac{\varepsilon}{2}\left(|\nabla_{\Gamma_h}U_0|^2+|U_0|^2\right)+\frac{1}{\varepsilon}\psi(U_0)\,\mathrm{d}\sigma_h.\end{aligned}$$

Since the right-hand side of the energy bound can be bounded independent of T_0, we can turn the short-time result into a result for $(0,T)$, where T is arbitrary.

Finally, Since $\phi_h=1$ is an admissible test function in (3.3.13a), it is clear that $\int_{\Gamma_h(t)}U_h\,\mathrm{d}\sigma_h$ is conserved. □

3.3.3 Lifted finite elements

As with other sections, the following analysis will rely on lift operators defined using a time dependent closest point operator similar to (A.6.1). This lifting process will also be applied to the surface triangulation, as well as finite element functions. This will induce a further discrete material velocity v_h which will describe how the lifts of triangles on $\{\Gamma(t)\}$ evolve.

We recall that, on a neighbourhood $\mathcal{N}_T$ of $\mathcal{G}_T$, for each point $(x,t)\in\mathcal{N}_T$, there exists a unique point $p(x,t)\in\Gamma(t)$:

$$p(x,t)=x+d(x,t)\nu(p(x,t),t).\tag{3.3.22}$$

We will call $p=p(x,t)$ the (time dependent) closest point operator. It is clear that $p(\cdot,t)$ is a homeomorphism from $\Gamma_h(t)$ onto $\Gamma(t)$, for all $t\in[0,T]$.

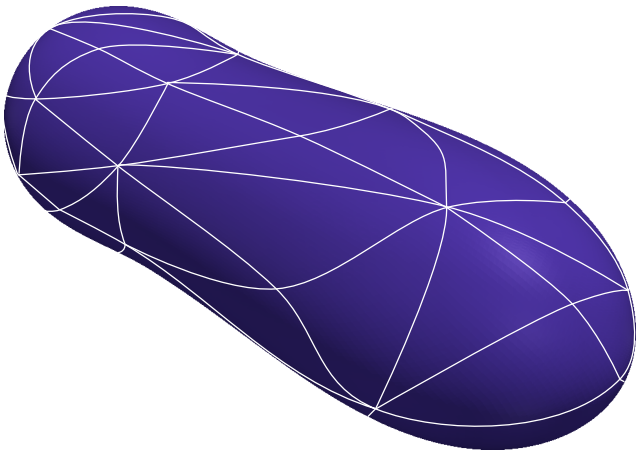

Figure 3.3.2: An example of a triangulation lifted onto a smooth surface.

First, for a function $\eta_h \colon \mathcal{G}_{h,T} \to \mathbb{R}$, we define its lift, $\eta_h^\ell \colon \mathcal{G}_T \to \mathbb{R}$, implicitly, by:

$$\eta_h^\ell(p(x,t),t) = \eta_h(x,t), \tag{3.3.23}$$

and, for a function $\eta \colon \mathcal{G}_T \to \mathbb{R}$, we define its inverse lift, $\eta^{-\ell} \colon \mathcal{G}_{h,T} \to \mathbb{R}$ by

$$\eta^{-\ell}(x,t) := \eta(p(x,t),t). \tag{3.3.24}$$

It is clear that these operations are inverses of each other

$$(\eta^{-\ell})^\ell = \eta \qquad \text{and} \qquad (\eta_h^\ell)^{-\ell} = \eta_h.$$

Furthermore, (3.3.22) allows us to define a lifted triangulation $\mathscr{T}_h^\ell(t)$ of $\Gamma(t)$ by

$$\mathscr{T}_h^\ell = \{e(t) = E^\ell(t) : E(t) \in \mathscr{T}_h(t)\}, \qquad E^\ell(t) := \{p(x,t) : x \in E(t)\}. \tag{3.3.25}$$

This defines an exact triangulation in the sense of Section 2.3.1; see Figure 3.3.2 for an example.

Similarly to Lemma A.6.1, we know that the lifting operation is stable:

Lemma 3.3.7 (Stability of lift)**.** *Let $\eta_h \colon \mathcal{G}_{h,T} \to \mathbb{R}$, with lift $\eta_h^\ell \colon \mathcal{G}_T \to \mathbb{R}$, be such that the following quantities exist. For $1 \leq q \leq +\infty$, there exist $c_1, c_2 > 0$, independent of h, but depending on q, such that for each time $t \in [0,T]$ and each element $E(t) \in \mathscr{T}_h(t)$ with associated lifted element $e(t) \in \mathscr{T}_h^\ell(t)$, the following hold:*

$$c_1 \left\| \eta_h^\ell \right\|_{L^q(e(t))} \leq \|\eta_h\|_{L^q(E(t))} \leq c_2 \left\| \eta_h^\ell \right\|_{L^q(e(t))} \tag{3.3.26a}$$

$$c_1 \left\| \nabla_\Gamma \eta_h^\ell \right\|_{L^q(e(t))} \leq \|\nabla_{\Gamma_h} \eta_h\|_{L^q(E(t))} \leq c_2 \left\| \nabla_\Gamma \eta_h^\ell \right\|_{L^q(e(t))} \tag{3.3.26b}$$

$$\left\| \nabla_{\Gamma_h}^2 \eta_h \right\|_{L^2(E(t))} \leq c \left(\left\| \nabla_\Gamma^2 \eta_h^\ell \right\|_{L^2(e(t))} + h \left\| \nabla_\Gamma \eta_h^\ell \right\|_{L^2(e(t))} \right). \tag{3.3.26c}$$

Proof. The result of Lemma A.6.1 (Dziuk 1988) can be easily extended to L^q norms and to the context of evolving surfaces (Dziuk and Elliott 2007a). □

This result allows us to give Sobolev embeddings for discrete surfaces:

Lemma 3.3.8. *For $\Gamma_h(t)$ as above,*

$$W^{1,q}(\Gamma_h(t)) \subset \begin{cases} L^{nq/(n-q)}(\Gamma_h(t)) & \text{for } q < n \\ L^\infty(\Gamma_h(t)) & \text{for } q > n. \end{cases} \tag{3.3.27}$$

Furthermore there exists a constant $c = c(n, q)$, independent of h, such that for any $\eta_h \in W^{1,q}(\Gamma_h(t))$

$$\|\eta_h\|_{L^{nq/(n-q)}(\Gamma_h(t))} \leq c \|\eta_h\|_{W^{1,q}(\Gamma_h(t))} \qquad \text{for } q < n \tag{3.3.28a}$$

$$\|\eta_h\|_{L^\infty(\Gamma_h(t))} \leq c \|\eta_h\|_{W^{1,q}(\Gamma_h(t))} \qquad \text{for } q > n. \tag{3.3.28b}$$

Proof. To see the embedding result, we apply Lemma 3.2.1. The bounds then follow using the stability of the lift (Lemma 3.3.7). □

As in other chapters, we will write $S_h^\ell(t)$ for the space of lifted finite element functions:

$$S_h^\ell(t) = \{\varphi_h = \phi_h^\ell : \phi_h \in S_h(t)\}.$$

This space comes with the standard approximation property:

Proposition 3.3.9 (Approximation property)**.** *The Lagrangian interpolation operator $I_h \colon C(\Gamma(t)) \to S_h^\ell(t)$ is well defined and, for $z \in H^2(\Gamma(t))$, satisfies the bound*

$$\|z - I_h z\|_{L^2(\Gamma(t))} + h \|\nabla_\Gamma (z - I_h z)\|_{L^2(\Gamma(t))} \leq c h^2 \|z\|_{H^2(\Gamma(t))}, \tag{3.3.29}$$

and

$$\|\nabla_\Gamma(z - I_h z)\|_{L^q(\Gamma(t))} \leq c h^{1+\min(0,n/q-n/2)} \|z\|_{H^2(\Gamma(t))} \quad \text{for} \begin{cases} 1 \leq q \leq \infty & \text{if } n = 1 \\ 1 \leq q < \infty & \text{if } n = 2 \\ 1 \leq q \leq 6 & \text{if } n = 3. \end{cases} \tag{3.3.30}$$

Proof. The proof follows in the same way as Proposition A.6.2 (Dziuk 1988). We give details of the proof for the L^q case, for q as listed above.

The linear interpolant $\widetilde{I}_h z \in S_h(t)$, given by

$$\widetilde{I}_h z(x) = \sum_{j=1}^{N} z(X_j(t)) \phi_j^N(x,t),$$

is well defined since z is continuous (Theorem 3.2.1). Consider one element $E(t) \in \mathscr{T}_h(t)$ with associated lifted element $e(t) \in \mathscr{T}_h^\ell(t)$. Then standard interpolation theory (Ciarlet 1978, Theorem 3.1.6) applies since we have the continuous embedding $H^1(\Gamma(t)) \hookrightarrow W^{1,q}(\Gamma(t))$:

$$\left\| z^{-\ell} - \widetilde{I}_h z \right\|_{W^{1,q}(E(t))} \leq c h^{1+min(0,n/q-n/2)} \left\| z^{-\ell} \right\|_{H^2(E(t))}.$$

The stability result in Lemma 3.3.7 implies that we can lift this result to the smooth surface. Summing over all elements, we see that

$$\|z - I_h z\|_{W^{1,q}(\Gamma(t))} \leq c h^{1+min(0,n/q-n/2)} \|z\|_{H^2(\Gamma(t))}. \qquad \square$$

Remark 3.3.10. For the remainder of this chapter, we will write lower case letters for the lift of finite element functions with capital letters (i.e. $U_h^\ell = u_h$ and $W_h^\ell = w_h$) and φ_h for the lift of ϕ_h.

The motion of the edges of the triangles in the triangulation $\{\mathscr{T}_h^\ell(t)\}$ defines a discrete material velocity for the surface $\{\Gamma(t)\}$. Let $X(t)$ be the trajectory of a point on $\{\Gamma_h(t)\}$ with velocity $V_h(X(t),t)$. We set $Y(t) = p(X(t),t)$, where p is the closest point operator (3.3.22), and then define v_h by

$$v_h(Y(t),t) := Y'(t) = \frac{\partial p}{\partial t}(X(t),t) + \nabla p(X(t),t) \cdot V_h(X(t),t), \tag{3.3.31}$$

so that for $x \in \Gamma_h(t)$, using (3.3.22), we have

$$v_h(p(x,t),t) = (P(x,t) - d(x,t)\mathcal{H}(x,t))V_h(x,t) - d_t(x,t)\nu(x) - d(x,t)\nu_t(x,t).$$

This defines another discrete material derivative for functions $\varphi_h(\cdot,t) \in S_h^\ell(t)$. We define the discrete material derivative on $\mathcal{G}_T$ element-wise by

$$\partial_h^\bullet \varphi_h := (\partial_t \varphi_h + v_h \cdot \nabla \varphi_h). \tag{3.3.32}$$

It can be shown, similarly to (3.3.7), that $\partial_h^\bullet (\phi_j^N)^\ell = 0$. A quick calculation (Dziuk and Elliott 2013a) shows that for all $\phi_h \in S_h(t)$, with lift $\varphi_h \in S_h^\ell(t)$,

$$\partial_h^\bullet \varphi_h = (\partial_h^\bullet \phi_h)^\ell, \tag{3.3.33}$$

We will write $S_h^{\ell,T}$ and $\widetilde{S}_h^{\ell,T}$ for the lifts of the spaces S_h^T and $\widetilde{S}_h^T$ defined by (3.3.12). It is clear that from Lemma 3.3.7 that

$$S_h^{\ell,T} \subset H^1(\mathcal{G}_T) \quad \text{and} \quad \widetilde{S}_h^{\ell,T} \subset L^2_{H^1}.$$

We remark that the continuous and discrete material velocities on $\{\Gamma(t)\}$ only differ in the tangential direction (which we will show to be bounded to second order in the mesh size). This implies that the difference between the two material derivatives on $\{\Gamma(t)\}$ only depends on the tangential gradient of the original function and not on any time derivatives.

These definitions also permit transport formulae:

Lemma 3.3.11 (Transport lemma for smooth triangulated surfaces)**.** *Let $\{\Gamma(t)\}$ be an evolving surface decomposed at each time into a family curved elements $\{\mathscr{T}_h^\ell(t)\}$ whose edges evolve with velocity v_h. Then the following relations hold for functions $\eta_h, \varphi_h \colon \mathcal{G}_T \to \mathbb{R}$ such that the following quantities exist:*

$$\frac{\mathrm{d}}{\mathrm{d}t} \int_{\Gamma(t)} \eta_h \,\mathrm{d}\sigma = \int_{\Gamma(t)} \partial_h^\bullet \eta_h + \eta_h \nabla_\Gamma \cdot v_h \,\mathrm{d}\sigma, \tag{3.3.34}$$

and

$$\frac{\mathrm{d}}{\mathrm{d}t} m(\eta_h, \varphi_h) = m(\partial_h^\bullet \eta_h, \varphi_h) + m(\eta_h, \partial_h^\bullet \varphi_h) + g(v_h; \eta_h, \varphi_h) \tag{3.3.35}$$

$$\frac{\mathrm{d}}{\mathrm{d}t} a(\eta_h, \varphi_h) = a(\partial_h^\bullet \eta_h, \varphi_h) + a(\eta_h, \partial_h^\bullet \varphi_h) + b(v_h; \eta_h, \varphi_h). \tag{3.3.36}$$

Finally, for a diffusion tensor $\mathcal{A}$ which is positive definite on the tangent space to

$\Gamma(t)$, *we have the formula for all* $e(t) \in \mathscr{T}_h^\ell(t)$,

$$\frac{\mathrm{d}}{\mathrm{d}t}\int_{e(t)} \mathcal{A}\nabla_\Gamma \eta_h \cdot \nabla_\Gamma \varphi_h \,\mathrm{d}\sigma = \int_{e(t)} \mathcal{A}\nabla_\Gamma(\partial_h^\bullet \eta_h)\cdot\nabla_\Gamma\varphi_h + \mathcal{A}\nabla_\Gamma\eta_h\cdot\nabla_\Gamma(\partial_h^\bullet\varphi_h)\,\mathrm{d}\sigma + \int_{e(t)} \mathcal{B}(v_h)\nabla_\Gamma\eta_h\cdot\nabla_\Gamma\varphi_h\,\mathrm{d}\sigma, \tag{3.3.37}$$

where

$$\mathcal{B}(v_h) = \partial_h^\bullet \mathcal{A} + \nabla_\Gamma \cdot v_h \mathcal{A} - 2D(v_h)$$
$$D(v_h)_{ij} = \frac{1}{2}\sum_{k=1}^{n+1}(\mathcal{A}_{ik}\underline{D}_k(v_h)_j + \mathcal{A}_{jk}\underline{D}_k(v_h)_i) \qquad \text{for } i,j = 1,\dots,n+1.$$

Proof. Following Dziuk and Elliott (2013a, Lemma 4.2), we again decompose $\Gamma(t)$ into lifted elements so that

$$\frac{\mathrm{d}}{\mathrm{d}t}\int_{\Gamma(t)}\eta_h\,\mathrm{d}\sigma = \sum_{e(t)\in\mathscr{T}_h^\ell(t)}\left(\frac{\mathrm{d}}{\mathrm{d}t}\int_{e(t)}\eta_h\,\mathrm{d}\sigma\right),$$

and apply the results of Lemma 3.2.3 and Corollary 3.2.4 element-wise. □

3.3.4 Geometric estimates

We next derive bounds on the difference between the continuous and discrete geometric quantities. We start by recalling some results about stationary surfaces which still hold in the evolving case and go on by relating these to differences in the bilinear forms.

Lemma 3.3.12. *For* $\{\Gamma(t)\}$ *and* $\{\Gamma_h(t)\}$ *as above, we have*

$$\sup_{t\in[0,T]} \|d(\cdot,t)\|_{L^\infty(\Gamma(t))} \le ch^2. \tag{3.3.38}$$

Let μ_h *denote the quotient of surface measures* $\mathrm{d}\sigma$ *on* $\Gamma(t)$ *and* $\mathrm{d}\sigma_h$ *on* $\Gamma_h(t)$ *such that* $\mu_h\,\mathrm{d}\sigma_h = \mathrm{d}\sigma$*; then*

$$\sup_{t\in[0,T]}\sup_{\Gamma_h(t)}|1-\mu_h| \le ch^2. \tag{3.3.39}$$

Let P *and* P_h *denote the projections onto the tangent spaces of* $\Gamma(t)$ *and* $\Gamma_h(t)$ *respectively; then*

$$\sup_{t\in[0,T]}\sup_{\Gamma_h(t)}|PP_hP - P| \le ch^2. \tag{3.3.40}$$

Proof. The proof of these results can be found in Lemma A.5.1 for the stationary case and easily extended to evolving surfaces (Dziuk and Elliott 2007a). □

We next look to bound time derivatives of these quantities. The following terms describe how close the evolutions of the surfaces are:

Lemma 3.3.13. *The discrete material velocity on* $\{\Gamma_h(t)\}$ *satisfies the following estimates:*

$$\sup_{t\in[0,T]} \|\partial_h^\bullet d\|_{L^\infty(\Gamma_h(t))} \leq ch^2 \tag{3.3.41a}$$

$$\sup_{t\in[0,T]} \|\partial_h^\bullet (\nu - \nu_h)\|_{L^\infty(\Gamma_h(t))} \leq ch \tag{3.3.41b}$$

$$\sup_{t\in[0,T]} \|\partial_h^\bullet (P_h\nu)\|_{L^\infty(\Gamma_h(t))} \leq ch^2 \tag{3.3.41c}$$

$$\sup_{t\in[0,T]} \|\partial_h^\bullet \mu_h\|_{L^\infty(\Gamma_h(t))} \leq ch^2. \tag{3.3.41d}$$

Proof. A proof is given by Dziuk and Elliott (2013a) for (3.3.41a, 3.3.41c, 3.3.41d). Equation (3.3.41b) follows by the same reasoning. Similar ideas to the proof of Lemma 3.3.12 are used. □

Next, we relate the results of these two lemmas to the bilinear forms introduced above.

Lemma 3.3.14. *Let* $Z_h, \phi_h \in S_h(t)$ *with lifts* $z_h, \varphi_h \in S_h^\ell(t)$*. Then the following estimates hold for the given bilinear forms:*

$$|m_h(Z_h,\phi_h) - m(z_h,\varphi_h)| \leq ch^2 \|Z_h\|_{L^2(\Gamma_h(t))} \|\phi_h\|_{L^2(\Gamma_h(t))} \tag{3.3.42a}$$

$$|a_h(Z_h,\phi_h) - a(z_h,\varphi_h)| \leq ch^2 \|\nabla_{\Gamma_h} Z_h\|_{L^2(\Gamma_h(t))} \|\nabla_{\Gamma_h}\phi_h\|_{L^2(\Gamma_h(t))} \tag{3.3.42b}$$

$$|g_h(V_h;Z_h,\phi_h) - g(v_h;z_h,\varphi_h)| \leq ch^2 \|Z_h\|_{L^2(\Gamma_h(t))} \|\phi_h\|_{L^2(\Gamma_h(t))} \tag{3.3.42c}$$

$$|b_h(V_h;Z_h,\phi_h) - b(v_h;z_h,\varphi_h)| \leq ch^2 \|\nabla_{\Gamma_h} Z_h\|_{L^2(\Gamma_h(t))} \|\nabla_{\Gamma_h}\phi_h\|_{L^2(\Gamma_h(t))}. \tag{3.3.42d}$$

Proof. The first two results are equivalent to Lemma A.6.3. It is left to show the third and fourth. It is worth remarking that Dziuk and Elliott (2013a) present a similar bound to (3.3.42c):

$$|g_h(V_h;Z_h,\phi_h) - g(v_h;z_h,\varphi_h)| \leq ch^2 \|Z_h\|_{H^1(\Gamma_h(t))} \|\phi_h\|_{H^1(\Gamma_h(t))}.$$

The following proof was found independently by Lubich and Mansour (2012).

To show (3.3.42c), we start by recalling that for $Z_h, \phi_h \in S_h^T$:

$$\int_{\Gamma_h(t)} Z_h \phi_h \,\mathrm{d}\sigma_h = \int_{\Gamma(t)} z_h \varphi_h \frac{1}{\mu_h^\ell} \,\mathrm{d}\sigma.$$

Then using the two discrete transport formulae (3.3.8) and (3.3.34), we see that

$$\begin{aligned}\frac{\mathrm{d}}{\mathrm{d}t}\int_{\Gamma_h(t)} Z_h \phi_h \,\mathrm{d}\sigma_h &= \int_{\Gamma_h(t)} \partial_h^\bullet Z_h \phi_h + Z_h \partial_h^\bullet \phi_h + Z_h \phi_h \nabla_{\Gamma_h} \cdot V_h \,\mathrm{d}\sigma_h \\ &= \int_{\Gamma(t)} \left(\partial_h^\bullet z_h \varphi_h + z_h \partial_h^\bullet \varphi_h\right) \frac{1}{\mu_h^\ell} \,\mathrm{d}\sigma + \int_{\Gamma_h(t)} Z_h \phi_h \nabla_{\Gamma_h} \cdot V_h \,\mathrm{d}\sigma_h,\end{aligned}$$

and

$$\begin{aligned}\frac{\mathrm{d}}{\mathrm{d}t}\int_{\Gamma(t)} z_h \varphi_h \frac{1}{\mu_h^\ell} \,\mathrm{d}\sigma &= \int_{\Gamma(t)} \left(\partial_h^\bullet z_h \varphi_h + z_h \partial_h^\bullet \varphi_h\right) \frac{1}{\mu_h^\ell} \,\mathrm{d}\sigma \\ &\quad + \int_{\Gamma(t)} z_h \varphi_h \partial_h^\bullet \left(\frac{1}{\mu_h^\ell}\right) + z_h \varphi_h \frac{1}{\mu_h^\ell} \nabla_\Gamma \cdot v_h \,\mathrm{d}\sigma.\end{aligned}$$

Equating terms, we see that

$$\begin{aligned}&\int_{\Gamma_h(t)} Z_h \phi_h \nabla_{\Gamma_h} \cdot V_h \,\mathrm{d}\sigma_h - \int_{\Gamma(t)} z_h \varphi_h \nabla_\Gamma \cdot v_h \,\mathrm{d}\sigma \\ &\qquad = \int_{\Gamma(t)} z_h \varphi_h \partial_h^\bullet \left(\frac{1}{\mu_h^\ell}\right) + z_h \varphi_h \left(\frac{1}{\mu_h^\ell} - 1\right) \nabla_\Gamma \cdot v_h \,\mathrm{d}\sigma.\end{aligned}$$

In particular, this holds for all basis functions and is linear in Z_h and ϕ_h so can be extended to all $Z_h, \phi_h \in S_h(t)$. Using (3.3.39) and (3.3.41d), we see that

$$\begin{aligned}|g(v_h; z_h, \varphi_h) - g_h(V_h; Z_h, \phi_h)| &\leq c\left(\left|\partial_h^\bullet\left(\frac{1}{\mu_h}\right)\right| + \left|1 - \frac{1}{\mu_h}\right|\right) \|z_h\|_{L^2(\Gamma(t))} \|\varphi_h\|_{L^2(\Gamma(t))} \\ &\leq ch^2 \|z_h\|_{L^2(\Gamma(t))} \|\varphi_h\|_{L^2(\Gamma(t))}.\end{aligned}$$

The estimate (3.3.26) finishes the proof.

Next, we apply similar ideas for the Dirichlet inner product. Starting once more with $Z_h, \phi_h \in S_h^T$. Let $E(t) \in \mathscr{T}_h(t)$ with associated lifted element $e(t) \in \mathscr{T}_h^\ell(t)$. Then, from (A.6.6), we have the identity

$$\int_{E(t)} \nabla_{\Gamma_h} Z_h \cdot \nabla_{\Gamma_h} \phi_h \,\mathrm{d}\sigma_h = \int_{e(t)} \mathcal{Q}_h^\ell \nabla_\Gamma z_h \cdot \nabla_\Gamma \varphi \,\mathrm{d}\sigma,$$

where

$$\mathcal{Q}_h = \frac{1}{\mu_h}(\mathrm{Id} - d\mathcal{H})PP_hP(\mathrm{Id} - d\mathcal{H}).$$

We remark that $\mathcal{Q}_h^\ell$ is positive definite on the tangent space to $\Gamma(t)$.

This implies using (3.3.10):

$$\begin{aligned}
&\frac{\mathrm{d}}{\mathrm{d}t}\int_{E(t)} \nabla_{\Gamma_h} Z_h \cdot \nabla_{\Gamma_h}\phi_h \,\mathrm{d}\sigma_h \\
&\quad= \int_{E(t)} \nabla_{\Gamma_h}\partial_h^\bullet Z_h \cdot \nabla_{\Gamma_h}\phi_h + \nabla_{\Gamma_h} Z_h \cdot \nabla_{\Gamma_h}\partial_h^\bullet\phi_h + \mathcal{B}_h(V_h)\nabla_{\Gamma_h} Z_h \cdot \nabla_{\Gamma_h}\phi_h \,\mathrm{d}\sigma_h \\
&\quad= \int_{e(t)} \mathcal{Q}_h^\ell \left(\nabla_\Gamma \partial_h^\bullet z_h \cdot \nabla_\Gamma \varphi_h + \nabla_\Gamma z_h \cdot \nabla_\Gamma \partial_h^\bullet \varphi_h\right) \mathrm{d}\sigma \\
&\qquad\quad + \int_{E(t)} \mathcal{B}_h(V_h)\nabla_{\Gamma_h} Z_h \cdot \nabla_{\Gamma_h}\phi_h \,\mathrm{d}\sigma_h,
\end{aligned}$$

and, using (3.3.37):

$$\begin{aligned}
\frac{\mathrm{d}}{\mathrm{d}t}\int_{E(t)} \nabla_{\Gamma_h} Z_h \cdot \nabla_{\Gamma_h}\phi_h \,\mathrm{d}\sigma_h &= \frac{\mathrm{d}}{\mathrm{d}t}\int_{e(t)} \mathcal{Q}_h^\ell \nabla_\Gamma z_h \cdot \nabla_\Gamma \varphi_h \,\mathrm{d}\sigma \\
&= \int_{e(t)} \mathcal{Q}_h^\ell \left(\nabla_\Gamma \partial_h^\bullet z_h \cdot \nabla_\Gamma \varphi_h + \nabla_\Gamma z_h \cdot \nabla_\Gamma \partial_h^\bullet \varphi_h\right) \mathrm{d}\sigma \\
&\quad + \int_{e(t)} \widetilde{\mathcal{B}}_h(v_h)\nabla_\Gamma z_h \cdot \nabla_\Gamma \varphi_h \,\mathrm{d}\sigma,
\end{aligned}$$

where

$$\widetilde{\mathcal{B}}_h(v_h) = \partial_h^\bullet\left(Q_h^\ell\right) + Q_h^\ell\big(\mathrm{Id}\nabla_\Gamma \cdot v_h - 2D(v_h)\big).$$

Equating terms, we see that

$$\int_{E(t)} \mathcal{B}_h(V_h)\nabla_{\Gamma_h} Z_h \cdot \nabla_{\Gamma_h}\phi_h \,\mathrm{d}\sigma_h = \int_{e(t)} \widetilde{\mathcal{B}}(v_h)\nabla_\Gamma z_h \cdot \nabla_\Gamma \varphi_h \,\mathrm{d}\sigma.$$

Again, since all basis functions are in S_h^T, and this relationship is linear with respect to Z_h and ϕ_h, this result can be extended to all $Z_h, \phi_h \in S_h(t)$.

Next, we notice that since $\nabla_\Gamma = P\nabla_\Gamma$, and P is positive definite on the tangent space to $\Gamma(t)$, we have that

$$\mathcal{B}(v_h) = \partial_h^\bullet P + P(\mathrm{Id}\nabla_\Gamma \cdot v_h - 2D(v_h)).$$

Using Lemmas 3.3.12, we have

$$\left|P - \mathcal{Q}_h^\ell\right| \leq |P - PP_hP| + ch^2 \leq ch^2.$$

We note that since $\partial^\bullet \nu \cdot \nu = 0$, we have $\partial_h^\bullet P = 0$. Using similar ideas to Lemma A.5.2,

with Lemma 3.3.13, we obtain

$$\begin{aligned}\left|\partial_h^\bullet(P-\mathcal{Q}_h^\ell)\right| &\leq |\partial_h^\bullet(P-PP_hP)| + ch^2 \\ &= |\partial_h^\bullet(P\nu_h \otimes P\nu_h)| + ch^2 \leq c\,|P(\partial_h^\bullet\nu_h)\otimes P\nu_h| + ch^2 \leq ch^2.\end{aligned}$$

This shows that

$$\begin{aligned}\left|\widetilde{\mathcal{B}}(v_h) - \mathcal{B}(v_h)\right| &= \left|\partial_h^\bullet(\mathcal{Q}_h^\ell - P) + (\mathcal{Q}_h^\ell - P)\big(\mathrm{Id}\nabla_\Gamma\cdot v_h - 2D(v_h)\big)\right| \\ &\leq \left|\partial_h^\bullet(\mathcal{Q}_h^\ell - P)\right| + c\left|\mathcal{Q}_h^\ell - P\right| \leq ch^2.\end{aligned}$$

This implies that

$$\begin{aligned}&\left|\int_{E(t)} \mathcal{B}_h(V_h)\nabla_{\Gamma_h} Z_h\cdot\nabla_{\Gamma_h}\phi_h\,\mathrm{d}\sigma_h - \int_{e(t)}\mathcal{B}(v_h)\nabla_\Gamma Z_h\cdot\nabla_\Gamma\varphi_h\,\mathrm{d}\sigma\right| \\ &\quad= \left|\int_{e(t)}\big(\widetilde{B}(v_h) - B(v_h)\big)\nabla_\Gamma Z_h\cdot\nabla_\Gamma\varphi_h\,\mathrm{d}\sigma\right| \\ &\quad\leq ch^2\,\|\nabla_\Gamma z_h\|_{L^2(e(t))}\,\|\nabla_\Gamma\varphi_h\|_{e(\Gamma(t))}\,.\end{aligned}$$

Summing this result over all elements gives the desired result. □

Using the same reasoning, it is also clear that

$$\left|m_h(\psi'(Z_h),\phi_h) - m(\psi'(z_h),\varphi_h)\right| \leq ch^2\left\|\psi'(Z_h)\right\|_{L^2(\Gamma_h(t))}\|\phi_h\|_{L^2(\Gamma_h(t))}\,. \tag{3.3.43}$$

Similar results apply if the first argument is the material derivative of a finite element function:

Lemma 3.3.15. *For $Z_h \in S_h^T, \phi_h \in \widetilde{S}_h^T$ with lifts $z_h, \varphi_h \in S_h^\ell(t)$ for each time, we have*

$$|m_h(\partial_h^\bullet Z_h,\varphi_h) - m(\partial_h^\bullet z_h,\phi_h)| \leq ch^2\,\|\partial_h^\bullet Z_h\|_{L^2(\Gamma_h(t))}\,\|\phi_h\|_{L^2(\Gamma_h(t))} \tag{3.3.44a}$$

$$|a_h(\partial_h^\bullet Z_h,\varphi_h) - a(\partial_h^\bullet z_h,\phi_h)| \leq ch^2\,\|\nabla_{\Gamma_h}(\partial_h^\bullet Z_h)\|_{L^2(\Gamma_h(t))}\,\|\nabla_{\Gamma_h}\phi_h\|_{L^2(\Gamma_h(t))}\,. \tag{3.3.44b}$$

Proof. Both results follow by using the fact, $(\partial_h^\bullet Z_h)^\ell = \partial_h^\bullet z_h$ and applying the results from Lemma 3.3.14. See also Dziuk and Elliott (2013a, Lemma 5.8). □

The next lemma bounds errors from the approximation of v by v_h.

Lemma 3.3.16. *The difference between the continuous velocity v and the discrete velocity v_h on $\Gamma(t)$ can be estimated by*

$$|v - v_h| + h\,|\nabla_\Gamma(v - v_h)| \leq ch^2\,\|v\|_{C^2(\mathcal{N}_T)} < ch^2. \tag{3.3.45}$$

Proof. See Dziuk and Elliott (2013a, Lemma 5.6). □

This allows us to bound the error between the material derivatives on $\Gamma(t)$:

Corollary 3.3.17. *Suppose that $\eta\colon \mathcal{G}_T \to \mathbb{R}$ and $\partial^\bullet\eta$ and $\partial_h^\bullet\eta$ exist. For $\eta \in H^1(\Gamma(t))$, we have the estimate*

$$\|\partial^\bullet\eta - \partial_h^\bullet\eta\|_{L^2(\Gamma(t))} \leq ch^2\,\|\nabla_\Gamma\eta\|_{L^2(\Gamma(t))}\,, \tag{3.3.46}$$

and for $\eta \in H^2(\Gamma(t))$, we obtain

$$\|\nabla_\Gamma(\partial^\bullet\eta - \partial_h^\bullet\eta)\|_{L^2(\Gamma(t))} \leq ch^2\,\|\eta\|_{H^2(\Gamma(t))}\,. \tag{3.3.47}$$

Proof. See Dziuk and Elliott (2013a, Corollary 5.7). □

3.3.5 Ritz projection

We conclude this section by constructing a discrete projection operator, similar to an interpolation operator. We define the Ritz projection operator $\Pi_h\colon H^1(\Gamma(t)) \to S_h(t)$ as the unique solution of

$$a_h(\Pi_h z, \phi_h) = a(z, \varphi_h) \quad \text{for all } \phi_h \in S_h(t), \text{ with lift } \varphi_h \in S_h^\ell(t) \tag{3.3.48}$$

and

$$\int_{\Gamma_h(t)} \Pi_h z\,\mathrm{d}\sigma_h = \int_{\Gamma(t)} z\,\mathrm{d}\sigma.$$

We will write $\pi_h z = (\Pi_h z)^\ell$ for the lift of the Ritz projection.

The following bound is immediate:

Lemma 3.3.18. *For $z \in H^1(\Gamma(t))$,*

$$\|\pi_h z\|_{H^1(\Gamma(t))} \leq c\,\|z\|_{H^1(\Gamma(t))}\,, \qquad \|\pi_h z - z\|_{L^2(\Gamma(t))} \leq ch\,\|z\|_{H^1(\Gamma(t))}\,. \tag{3.3.49}$$

For $z \in H^2(\Gamma(t))$,

$$\|\pi_h z - z\|_{L^2(\Gamma(t))} + h\,\|\nabla_\Gamma(\pi_h z - z)\|_{L^2(\Gamma(t))} \leq ch^2\,\|z\|_{H^2(\Gamma(t))}\,. \tag{3.3.50}$$

Proof. We apply the techniques of Appendix A, combining the approximation property (Proposition 3.3.9) with the geometric estimates in Lemma 3.3.14.

For brevity we will only show the L^2 error estimate for a function $z \in H^1(\Gamma(t))$. We use an Aubin-Nitsche trick. Let ζ be the unique solution of

$$a(\zeta, \varphi) = m(z - \pi_h z - c_0, \varphi) \quad \text{for all } \varphi \in H^1(\Gamma(t)), \int_{\Gamma(t)} \zeta \, \mathrm{d}\sigma = 0,$$

with $c_0 = \frac{1}{|\Gamma(t)|} \int_{\Gamma(t)} z - \pi_h z \, \mathrm{d}\sigma$. Standard elliptic theory (Theorem A.2.5) tells us that

$$\|\zeta\|_{H^2(\Gamma(t))} \leq c \, \|z - \pi_h z\|_{L^2(\Gamma(t))} \tag{3.3.51}$$

Then, we obtain that

$$\begin{aligned} m(z - \pi_h z, z - \pi_h z) &= c_0^2 \, |\Gamma(t)|^2 + a(\zeta, z - \pi_h z) \\ &= c_0^2 \, |\Gamma(t)|^2 + a(\zeta - I_h \zeta, z - \pi_h z) + a(I_h \zeta, z - \pi_h z). \end{aligned} \tag{3.3.52}$$

First we see that

$$\begin{aligned} c_0 \, |\Gamma(t)| &= \int_{\Gamma(t)} z - \pi_h z \, \mathrm{d}\sigma = \int_{\Gamma(t)} z \, \mathrm{d}\sigma - \int_{\Gamma_h(t)} \Pi_h z \, \mu_h \, \mathrm{d}\sigma_h \\ &= \int_{\Gamma(t)} z \, \mathrm{d}\sigma - \int_{\Gamma_h(t)} \Pi_h z \, \mathrm{d}\sigma_h + \int_{\Gamma_h(t)} \Pi_h z (1 - \mu_h) \, \mathrm{d}\sigma_h \\ &= \int_{\Gamma_h(t)} \Pi_h z (1 - \mu_h) \, \mathrm{d}\sigma_h. \end{aligned}$$

Hence, we infer that

$$|c_0| \, |\Gamma(t)| \leq c h^2 \, \|\Pi_h z\|_{L^2(\Gamma_h(t))} \leq c h^2 \, \|z\|_{H^1(\Gamma(t))} \, . \tag{3.3.53}$$

For the second term of the right-hand side of (3.3.52), using the approximation property (3.3.29) and dual regularity (3.3.51) we see that

$$a(\zeta - I_h \zeta, z - \pi_h z) \leq c h \, \|\zeta\|_{H^2(\Gamma(t))} \, \|z\|_{H^1(\Gamma(t))} \leq c h \, \|z - \pi_h z\|_{L^2(\Gamma(t))} \, \|z\|_{H^1(\Gamma(t))} \, .$$

Finally, for the third term, since $I_h \zeta$ is the lift of a finite element function, using the geometric bound (3.3.42b) and the dual regularity result (3.3.51)

$$\begin{aligned} a(I_h \zeta, z - \pi_h z) &= a_h((I_h \zeta)^{-\ell}, \Pi_h z) - a(I_h \zeta, \pi_h z) \\ &\leq c h^2 \, \|\zeta\|_{H^2(\Gamma(t))} \, \|z\|_{H^1(\Gamma(t))} \leq c h^2 \, \|z - \pi_h z\|_{L^2(\Gamma(t))} \, \|z\|_{H^1(\Gamma(t))} \, . \end{aligned}$$

Combining these three estimates into (3.3.52), dividing by $\|z - \pi_h z\|_{L^2(\Gamma(t))}$, we have

$$\|z - \pi_h z\|_{L^2(\Gamma(t))} \leq ch \|z\|_{H^1(\Gamma(t))},$$

as required. □

Remark 3.3.19. This operator is the Ritz projection used by Du et al. (2011), but different to that used in other surface finite element analyses such as Dziuk and Elliott (2007b, 2013a), which use the operator $\mathcal{R}_h \colon H^2(\Gamma(t)) \to S_h^\ell(t)$ given as the unique solution of

$$a(\mathcal{R}_h z, \varphi_h) = a(z, \varphi_h) \quad \text{for all } \varphi_h \in S_h^\ell(t) \quad \text{and} \quad \int_{\Gamma(t)} \mathcal{R}_h z \, \mathrm{d}\sigma = 0.$$

Next we wish to show a stability bound for the Ritz projection in L^∞. First, we show a stability result for the Ritz projection into $W^{1,q}(\Gamma_h(t))$:

Theorem 3.3.20. *For $z \in H^2(\Gamma(t))$, the Ritz projection, $\pi_h z$, is bounded in $W^{1,q}$ for*

$$\begin{aligned} 1 \leq q \leq \infty \text{ if } n = 1, \\ 1 \leq q < \infty \text{ if } n = 2, \\ 1 \leq q \leq 6 \text{ if } n = 3. \end{aligned}$$

Furthermore, we have the bound

$$\|\pi_h z\|_{W^{1,q}(\Gamma(t))} \leq c \|z\|_{H^2(\Gamma(t))}. \tag{3.3.54}$$

Proof. First, we extend the result of Lemma 3.3.18 to the $W^{1,q}$-norm using a similar splitting argument and an inverse inequality (which is available since $\mathscr{T}_h(t)$ is quasi-uniform uniformly in time):

$$\begin{aligned} &\|\nabla_\Gamma(z - \pi_h z)\|_{L^q(\Gamma(t))} \\ &\quad \leq \|\nabla_\Gamma(z - I_h z)\|_{L^q(\Gamma(t))} + \|\nabla_\Gamma(I_h z - \pi_h z)\|_{L^q(\Gamma(t))} \\ &\quad \leq \|\nabla_\Gamma(z - I_h z)\|_{L^q(\Gamma(t))} + ch^{\min(0, n/q - n/2)} \|\nabla_\Gamma(I_h z - \pi_h z)\|_{L^2(\Gamma(t))}. \end{aligned}$$

From Proposition 3.3.9, we have

$$\|\nabla_\Gamma(z - I_h z)\|_{L^q(\Gamma(t))} \leq ch^{1+\min(0, n/q - n/2)} \|z\|_{H^2(\Gamma(t))}.$$

We also have that for $\varphi_h \in S_h^\ell(t)$, using (3.3.48),

$$\begin{aligned} a(I_h z - \pi_h z, \varphi_h) &= a(I_h z - z, \varphi_h) + a_h(\Pi_h z, \phi_h) - a(\pi_h z, \varphi_h) \\ &\leq ch\big(\|z\|_{H^2(\Gamma(t))} + \|\nabla_\Gamma \pi_h z\|_{L^2(\Gamma(t))} \big) \|\nabla_\Gamma \varphi_h\|_{L^2(\Gamma(t))} \,. \end{aligned}$$

Hence, we infer

$$\|\nabla_\Gamma (I_h z - \pi_h z)\|_{L^2(\Gamma(t))} \leq ch \|z\|_{H^2(\Gamma(t))} \,.$$

Combining these two bounds gives

$$\|\nabla_\Gamma (\pi_h z - z)\|_{L^q(\Gamma(t))} \leq ch^{1+\min(0,n/q-n/2)} \|z\|_{H^2(\Gamma(t))} \leq c \|z\|_{H^2(\Gamma(t))} \,,$$

for h small enough. Using (3.3.53), a Poincare inequality gives

$$\|\pi_h z - z\|_{L^q(\Gamma(t))} \leq c \|\nabla_\Gamma (\pi_h z - z)\|_{L^q(\Gamma(t))} + \left| \int_{\Gamma(t)} \pi_h z - z \,\mathrm{d}\sigma \right| \leq c \|z\|_{H^2(\Gamma(t))} \,.$$

Using the Sobolev embedding result (Lemma 3.2.1), this implies that

$$\|\pi_h z\|_{W^{1,q}(\Gamma_h(t))} \leq c \|z\|_{W^{1,q}(\Gamma(t))} + \|\pi_h z - z\|_{W^{1,q}(\Gamma(t))} \leq c \|z\|_{H^2(\Gamma(t))} \,. \qquad \square$$

Corollary 3.3.21. *The Ritz projection is bounded in L^∞ and we have the bound*

$$\|\Pi_h z\|_{L^\infty(\Gamma_h(t))} \leq \|\pi_h z\|_{L^\infty(\Gamma_h(t))} \leq c \|z\|_{H^2(\Gamma(t))} \,. \tag{3.3.55}$$

Proof. Choose q such that $q > n$ and such the previous result holds (any $1 \leq q \leq \infty$ for $n = 1$, $1 \leq q < \infty$ for $n = 2$ and $1 \leq q < 6$ for $n = 3$). We use a Sobolev embedding (Lemma 3.2.1), and the previous result to see

$$\|\pi_h z\|_{L^\infty(\Gamma(t))} \leq c \|\pi_h z\|_{W^{1,q}(\Gamma(t))} \leq c \|z\|_{H^2(\Gamma(t))} \,.$$

It is clear that

$$\|\Pi_h z\|_{L^\infty(\Gamma_h(t))} = \|\pi_h z\|_{L^\infty(\Gamma(t))} \,,$$

which completes the proof. $\square$

Since $\partial_h^\bullet \Pi_h z \neq \Pi_h \partial_h^\bullet z$, we also wish to have a bound on the discrete material derivative of this error for a function. We will assume that $z \in H^2(\Gamma(t))$ and $\partial^\bullet z \in H^2(\Gamma(t))$ for each t. Under this assumption, we may take a time derivative of

(3.3.48), so that for all $\phi_h \in S_h^T$ with lift $\varphi_h \in S_h^{\ell,T}$,

$$a_h(\partial_h^\bullet \Pi_h z, \phi_h) + b_h(V_h; \Pi_h z, \phi_h) = a(\partial_h^\bullet z, \varphi_h) + b(v_h; z, \varphi_h). \tag{3.3.56}$$

In fact using similar arguments to Lemma 3.2.5, we can construct a similar extension of a finite element function $\phi_h \in S_h(t)$ to a function $\widetilde{\phi}_h \in S_h^T$ by

$$\widetilde{\phi}_h(x,s) = \sum_{j=1}^N \gamma_j \phi_j^N(x,s) \quad \text{for } (x,s) \in \mathcal{G}_{h,T} \qquad \text{where } \phi_h(x) = \sum_{j=1}^N \gamma_j \phi_j^N(x,t).$$

Hence, we deduce (3.3.56) applies at each time $t \in (0,T)$ for $\phi_h \in S_h(t)$.

We start by proving two technical lemmas:

Lemma 3.3.22. *Given $z\colon \mathcal{G}_T \to \mathbb{R}$ with $z \in H^2(\Gamma(t))$ and $\partial^\bullet z \in H^2(\Gamma(t))$ for almost every time $t \in (0,T)$, then $\partial_h^\bullet \Pi_h z$ exists and we have the bound*

$$\left\| \nabla_{\Gamma_h} \left(\partial_h^\bullet \Pi_h z \right) \right\|_{L^2(\Gamma_h(t))} \leq c \big(\|z\|_{H^2(\Gamma(t))} + \|\partial^\bullet z\|_{H^2(\Gamma(t))} \big). \tag{3.3.57}$$

Proof. To show the bound, we start by rearranging (3.3.56) to obtain for $\phi_h \in S_h(t)$,

$$a_h(\partial_h^\bullet \Pi_h z, \phi_h) = a(\partial_h^\bullet z, \varphi_h) + \big(b(v_h; z, \varphi_h) - b_h(V_h; \Pi_h z, \varphi_h) \big).$$

Using a Young's inequality, (3.3.50) and (3.3.42d) gives

$$a_h(\partial_h^\bullet \Pi_h z, \phi_h) \leq c \big(\|\nabla_\Gamma \partial^\bullet z\|_{L^2(\Gamma(t))}^2 + \|z\|_{H^2(\Gamma(t))}^2 \big) + \frac{1}{2} \|\nabla_{\Gamma_h} \phi_h\|_{L^2(\Gamma_h(t))}^2 .$$

Applying this bound with $\phi_h = \partial_h^\bullet \Pi_h z$ gives the estimate (3.3.57). □

Lemma 3.3.23. *Define the function T_h on $S_h^\ell(t)$ by*

$$T_h(\varphi_h) := a(\partial_h^\bullet (\pi_h z - z), \varphi_h). \tag{3.3.58}$$

Then we have the bound

$$|T_h(\varphi_h)| \leq ch \left(\|z\|_{H^2(\Gamma(t))} + \|\partial^\bullet z\|_{H^2(\Gamma(t))} \right) \|\nabla_\Gamma \varphi_h\|_{L^2(\Gamma(t))} . \tag{3.3.59}$$

Furthermore, for any $\eta \in H^2(\Gamma(t))$, we have that

$$\begin{aligned} |T_h(\varphi_h)| \leq{}& ch \|z\|_{H^2(\Gamma(t))} \|\nabla_\Gamma(\varphi_h - \eta)\|_{L^2(\Gamma(t))} + ch^2 \|z\|_{H^2(\Gamma(t))} \|\eta\|_{H^2(\Gamma(t))} \\ &+ ch^2 \left(\|z\|_{H^2(\Gamma(t))} + \|\partial^\bullet z\|_{H^2(\Gamma(t))} \right) \|\nabla_\Gamma \varphi_h\|_{L^2(\Gamma(t))} . \end{aligned} \tag{3.3.60}$$

Proof. Using (3.3.48) and (3.3.56), we see for $\phi_h \in S_h(t)$, with lift $\varphi_h \in S_h^\ell(t)$,

$$\begin{aligned}
&a(\partial_h^\bullet z, \varphi_h) + b(v_h; z, \varphi_h) \\
&\quad = a_h(\partial_h^\bullet \Pi_h z, \phi_h) + b_h(V_h; \Pi_h z, \phi_h) \\
&\quad = \big(a_h(\partial_h^\bullet \Pi_h z, \phi_h) - a(\partial_h^\bullet \pi_h z, \varphi_h)\big) + \big(b_h(V_h; \Pi_h z, \phi_h) - b(v_h; \pi_h z, \varphi_h)\big) \\
&\qquad + a(\partial_h^\bullet \pi_h z, \varphi_h) + b(v_h; \pi_h z, \varphi_h).
\end{aligned}$$

Hence, we have that

$$\begin{aligned}
T_h(\varphi_h) &= a(\partial_h^\bullet \pi_h z, \varphi_h) - a(\partial_h^\bullet z, \varphi_h) \\
&= b(v_h; z - \pi_h z, \varphi_h) + \big(a(\partial_h^\bullet \pi_h z, \varphi_h) - a_h(\partial_h^\bullet \Pi_h z, \phi_h)\big) \\
&\qquad + \big(b(v_h; \pi_h z, \varphi_h) - b_h(V_h; \Pi_h z, \phi_h)\big).
\end{aligned}$$

Using our bound on the Ritz projection (3.3.50), and two geometric estimates (3.3.42d) and (3.3.44b), we have that

$$\begin{aligned}
|T_h(\varphi_h)| &\leq |b(v_h; z - \pi_h z, \varphi_h)| + |a(\partial_h^\bullet \pi_h z, \varphi_h) - a_h(\partial_h^\bullet \Pi_h z, \phi_h)| \\
&\qquad + |b(v_h; \pi_h z, \varphi_h) - b_h(V_h; \Pi_h z, \phi_h)| \\
&\leq ch \, \|z\|_{H^2(\Gamma(t))} \, \|\nabla_\Gamma \varphi_h\|_{L^2(\Gamma(t))} \\
&\qquad + ch^2 \big(\|\nabla_\Gamma \partial_h^\bullet \pi_h z\|_{L^2(\Gamma(t))} + \|\nabla_\Gamma \pi_h z\|_{L^2(\Gamma(t))} \big) \, \|\nabla_\Gamma \varphi_h\|_{L^2(\Gamma(t))} \\
&\leq ch \left(\|z\|_{H^2(\Gamma(t))} + \|\partial^\bullet z\|_{H^2(\Gamma(t))} \right) \|\nabla_\Gamma \varphi_h\|_{L^2(\Gamma(t))} .
\end{aligned}$$

We can improve this estimate by comparing v_h to the smooth velocity v and introducing a smooth function $\eta \in H^2(\Gamma(t))$. Then, we split the first term in $T_h(\varphi_h)$ into

$$b(v_h; \pi_h z - z, \varphi_h) = b(v_h - v; \pi_h z - z, \varphi_h) + b(v; \pi_h z - z, \varphi_h - \eta) + b(v; \pi_h z - z, \eta).$$

Using the smoothness of η, the final term, $b(v; \pi_h z - z, \eta)$, is bounded using an

integration by parts argument given by Dziuk and Elliott (2013a):

$$\begin{aligned}
b(v;\varphi,\eta) &= \int_{\Gamma(t)} \mathcal{B}(v)\nabla_\Gamma\varphi\cdot\nabla_\Gamma\eta\,\mathrm{d}\sigma \\
&= \sum_{i,j=1}^{n+1}\int_{\Gamma(t)} \mathcal{B}(v)_{ij}\,\underline{D}_j\varphi\,\underline{D}_i\eta\,\mathrm{d}\sigma \\
&= \sum_{i,j=1}^{n+1}\int_{\Gamma(t)} \underline{D}_j\big(\mathcal{B}(v)_{ij}\,\varphi\,\underline{D}_i\eta\big)\,\mathrm{d}\sigma - \int_{\Gamma(t)}\varphi\sum_{i,j=1}^{n+1}\underline{D}_j\big(\mathcal{B}(v)_{ij}\underline{D}_i\eta\big)\,\mathrm{d}\sigma \\
&= \int_{\Gamma(t)}\sum_{i,j=1}^{n+1} H\nu_j\mathcal{B}(v)_{ij}\,\varphi\,\underline{D}_i\eta\,\mathrm{d}\sigma - \int_{\Gamma(t)}\varphi\sum_{i,j=1}^{n+1}\underline{D}_j\big(\mathcal{B}(v)_{ij}\underline{D}_i\eta\big)\,\mathrm{d}\sigma.
\end{aligned}$$

Hence, we obtain

$$|b(v;\varphi,\eta)| \le c\,\|\varphi\|_{L^2(\Gamma(t))}\,\|\eta\|_{H^2(\Gamma(t))}\,.$$

Combining these calculations with (3.3.45) and (3.3.50), we get

$$\begin{aligned}
|b(v_h; z-\pi_h z,\varphi_h)| &\le ch\,\|\nabla_\Gamma(\pi_h z - z)\|_{L^2(\Gamma(t))}\,\|\nabla_\Gamma\varphi_h\|_{L^2(\Gamma(t))} \\
&\quad + c\,\|\nabla_\Gamma(\pi_h z - z)\|_{L^2(\Gamma(t))}\,\|\nabla_\Gamma\varphi_h - \eta\|_{L^2(\Gamma(t))} \\
&\quad + c\,\|\pi_h z - z\|_{L^2(\Gamma(t))}\,\|\eta\|_{H^2(\Gamma(t))} \\
&\le ch\,\|z\|_{H^2(\Gamma(t))}\,\|\nabla_\Gamma(\varphi_h-\eta)\|_{L^2(\Gamma(t))} \\
&\quad + ch^2\,\|z\|_{H^2(\Gamma(t))}\,\big(\,\|\nabla_\Gamma\varphi_h\|_{L^2(\Gamma(t))} + \|\eta\|_{H^2(\Gamma(t))}\,\big).
\end{aligned}$$

Hence, we have

$$\begin{aligned}
|T_h(\varphi_h)| &\le ch\,\|z\|_{H^2(\Gamma(t)}\,\|\nabla_\Gamma(\varphi_h-\eta)\|_{L^2(\Gamma(t))} + ch^2\,\|z\|_{H^2(\Gamma(t))}\,\|\eta\|_{H^2(\Gamma(t))} \\
&\quad + ch^2\left(\|z\|_{H^2(\Gamma(t))} + \|\partial^\bullet z\|_{H^2(\Gamma(t))}\right)\|\nabla_\Gamma\varphi_h\|_{L^2(\Gamma(t))}\,.
\end{aligned}$$

□

These results allow us to show an estimate for the difference between the material derivative of a function and its Ritz projection.

Lemma 3.3.24. *For $z\colon \mathcal{G}_T \to \mathbb{R}$ with $z, \partial^\bullet z \in H^2(\Gamma(t))$, we have*

$$\begin{aligned}
&\|\partial_h^\bullet(\pi_h z - z)\|_{L^2(\Gamma(t))} + h\,\|\nabla_\Gamma\partial_h^\bullet(\pi_h z - z)\|_{L^2(\Gamma(t))} \\
&\qquad \le ch^2\big(\,\|z\|_{H^2(\Gamma(t))} + \|\partial^\bullet z\|_{H^2(\Gamma(t))}\,\big).
\end{aligned} \tag{3.3.61}$$

Proof. We start by rewriting the error as

$$\begin{aligned} &a(\partial_h^\bullet(\pi_h z - z), \partial_h^\bullet(\pi_h z - z)) \\ &\quad = a(\partial_h^\bullet(\pi_h z - z), \partial_h^\bullet \pi_h z - I_h(\partial^\bullet z)) + a(\partial_h^\bullet(\pi_h z - z), I_h(\partial^\bullet z) - \partial^\bullet z) \\ &\qquad + a(\partial_h^\bullet(\pi_h z - z), \partial^\bullet z - \partial_h^\bullet z). \end{aligned} \tag{3.3.62}$$

We can bound the first term on the right-hand side using (3.3.59) by

$$\begin{aligned} |a(\partial_h^\bullet(\pi_h z - z), \partial_h^\bullet \pi_h z - I_h(\partial^\bullet z))| &= |T_h(\partial_h^\bullet \pi_h z - I_h(\partial^\bullet z))| \\ &\leq ch\big(\|\partial^\bullet z\|_{H^2(\Gamma(t))} + \|z\|_{H^2(\Gamma(t))} \big) \|\nabla_\Gamma(\partial_h^\bullet \pi_h z - I_h(\partial^\bullet z))\|_{L^2(\Gamma(t))} \\ &\leq ch\big(\|\partial^\bullet z\|_{H^2(\Gamma(t))} + \|z\|_{H^2(\Gamma(t))} \big) \|\nabla_\Gamma \partial_h^\bullet(\pi_h z - z)\|_{L^2(\Gamma(t))} \\ &\qquad + ch \|\nabla_\Gamma \partial_h^\bullet(\pi_h z - z)\|^2_{L^2(\Gamma(t))}. \end{aligned}$$

The second term is bounded using the approximation property (3.3.29):

$$|a(\partial_h^\bullet(\pi_h z - z), I_h(\partial^\bullet z) - \partial^\bullet z)| \leq ch \|\nabla_\Gamma \partial_h^\bullet(\pi_h z - z)\|_{L^2(\Gamma(t))} \|\partial^\bullet z\|_{H^2(\Gamma(t))}.$$

Finally, we use our estimate of the difference of material derivatives (3.3.46) to bound the third term:

$$|a(\partial_h^\bullet(\pi_h z - z), \partial^\bullet z - \partial_h^\bullet z)| \leq ch^2 \|\nabla_\Gamma \partial_h^\bullet(\pi_h z - z)\|_{L^2(\Gamma(t))} \|z\|_{H^2(\Gamma(t))}.$$

Combining these three bounds in (3.3.62), we get the desired gradient norm bound for h sufficiently small.

To show the L^2 bound, we use the Aubin-Nitsche trick. We start by writing $e = \partial_h^\bullet(\pi_h z - z)$, then e is in L^2 so can be set as the right-hand side for the dual problem: Find $\zeta \in H^1(\Gamma(t))$ such that

$$a(\varphi, \zeta) = m(e - c_0, \varphi) \quad \text{for all } \varphi \in H^1(\Gamma(t)), \text{ and } \int_{\Gamma(t)} \zeta \,\mathrm{d}\sigma = 0, \tag{3.3.63}$$

where $c_0 = \frac{1}{|\Gamma(t)|} \int_{\Gamma(t)} e \,\mathrm{d}\sigma$. Similarly to Theorem A.2.5, we know that (3.3.63) has a unique solution and satisfies the regularity result

$$\|\zeta\|_{H^2(\Gamma(t))} \leq c \|e\|_{L^2(\Gamma(t))}. \tag{3.3.64}$$

We note that from $\int_{\Gamma_h(t)} \Pi_h z \,\mathrm{d}\sigma_h = \int_{\Gamma(t)} z \,\mathrm{d}\sigma$, that

$$|\Gamma(t)|\,|c_0| = \int_{\Gamma(t)} \partial_h^\bullet(\pi_h z - z)\,\mathrm{d}\sigma = \frac{\mathrm{d}}{\mathrm{d}t}\int_{\Gamma(t)} \pi_h z - z \,\mathrm{d}\sigma - \int_{\Gamma(t)} (\pi_h z - z)\nabla_\Gamma \cdot v_h \,\mathrm{d}\sigma.$$

We remark that from (3.3.39) and (3.3.41d),

$$\begin{aligned}
&\frac{\mathrm{d}}{\mathrm{d}t}\int_{\Gamma(t)} \pi_h z - z \,\mathrm{d}\sigma \\
&\quad = \frac{\mathrm{d}}{\mathrm{d}t}\left(\int_{\Gamma(t)} \pi_h z \,\mathrm{d}\sigma - \int_{\Gamma_h(t)} \Pi_h z \,\mathrm{d}\sigma_h\right) = \frac{\mathrm{d}}{\mathrm{d}t}\left(\int_{\Gamma(t)} \pi_h z \left(1 - \frac{1}{\mu_h}\right) \mathrm{d}\sigma\right) \\
&\quad \le ch^2\big(\,\|\pi_h z\|_{L^2(\Gamma(t))} + \|\partial_h^\bullet \pi_h z\|_{L^2(\Gamma(t))}\,\big) \le ch^2\big(\,\|z\|_{H^2(\Gamma(t))} + \|\partial^\bullet z\|_{H^2(\Gamma(t))}\,\big)
\end{aligned}$$

and using (3.3.50), we infer

$$\int_{\Gamma(t)} (\pi_h z - z)\nabla_\Gamma \cdot v_h \,\mathrm{d}\sigma \le c\,\|\pi_h z - z\|_{L^2(\Gamma(t))} \le ch^2\,\|z\|_{H^2(\Gamma(t))}\,.$$

This implies

$$|c_0| \le ch^2\big(\,\|z\|_{H^2(\Gamma(t))} + \|\partial^\bullet z\|_{H^2(\Gamma(t))}\,\big).$$

These calculations lead to

$$m(e,e) - |\Gamma(t)|^2\, c_0^2 = a(\zeta, e) = a(\zeta - I_h\zeta, e) + T_h(I_h\zeta). \tag{3.3.65}$$

The first term on the right-hand side is bounded using the approximation property (3.3.29) and the gradient norm bound on e, together with the dual regularity result (3.3.64):

$$\begin{aligned}
|a(\zeta - I_h, e)| &\le \|\nabla_\Gamma(\zeta - I_h\zeta)\|_{L^2(\Gamma(t))}\,\|\nabla_\Gamma e\|_{L^2(\Gamma(t))} \\
&\le ch\,\|\zeta\|_{H^2(\Gamma(t))}\, ch\big(\,\|z\|_{H^2(\Gamma(t))} + \|\partial^\bullet z\|_{H^2(\Gamma(t))}\,\big) \\
&\le ch^2\,\|e\|_{L^2(\Gamma(t))}\,\big(\,\|z\|_{H^2(\Gamma(t))} + \|\partial^\bullet z\|_{H^2(\Gamma(t))}\,\big).
\end{aligned}$$

The second term is estimated using the improved bound (3.3.60) on $T_h(I_h\zeta)$ with $\eta = \zeta$. Applying the approximation (3.3.29) we see

$$\begin{aligned}
|T_h(I_h\zeta)| &\le ch^2\big(\,\|z\|_{H^2(\Gamma(t))} + \|\partial^\bullet z\|_{H^2(\Gamma(t))}\,\big)\,\|\zeta\|_{H^2(\Gamma(t))} \\
&\le ch^2\big(\,\|z\|_{H^2(\Gamma(t))} + \|\partial^\bullet z\|_{H^2(\Gamma(t))}\,\big)\,\|e\|_{L^2(\Gamma(t))}\,.
\end{aligned}$$

Applying these two bounds in (3.3.65) gives the desired result. □

3.4 Well-posedness of the continuous problem

We use this section to show some properties of the continuous scheme (3.2.19) based on the energy estimates coming from Theorem 3.3.6 along with further estimates and a pointwise in time and space bound on solutions. We will use these properties in later sections but they are also important results in their own right.

3.4.1 Improved bounds on the finite element scheme

In order to derive some improved bounds on $\partial_h^\bullet U_h$ and W_h, we will assume that $U_{h,0} = \Pi_h u_0$ with $u_0 \in H^2(\Gamma_0)$. It is clear that assumption (3.3.11) still holds in this case. In fact, we will make use of the bound

$$\int_{\Gamma_{h,0}} \varepsilon \left(|\nabla_{\Gamma_h} U_0|^2 + U_0^2 \right) + \frac{1}{\varepsilon} \psi(U_0) \, \mathrm{d}\sigma \leq c_\varepsilon \big(\|u_0\|^2_{H^2(\Gamma_0)} + \|u_0\|^4_{H^2(\Gamma_0)} \big). \tag{3.4.1}$$

This is not essential for well-posedness of the finite element method but will be used for the well-posedness results for the continuous problem.

First, we need a bound on $W_h|_{t=0}$:

Lemma 3.4.1. *Under the assumption that $u_0 \in H^2(\Gamma_0)$, the following bound holds for $W_h|_{t=0}$:*

$$\|W_h(0,\cdot)\|_{L^2(\Gamma_h(0))} \leq c_\varepsilon \big(\|u_0\|_{H^2(\Gamma_0)} + \|u_0\|^3_{H^2(\Gamma_0)} \big). \tag{3.4.2}$$

Proof. Since α, β are $C^1([0,T];\mathbb{R}^N)$ in time, we known that (3.3.13b) holds at time $t = 0$:

$$\varepsilon a_h(U_{h,0}, \phi_h) + \frac{1}{\varepsilon} m_h(\psi'(U_{h,0}), \phi_h) = m_h(W_h(0,\cdot), \phi_h) \quad \text{for all } \phi_h \in S_h^T.$$

We see that from the choice $U_{h,0} = \Pi_h u_0$, using Green's formula (A.2.9), we have

$$\begin{aligned} m_h(W_h(0,\cdot), W_h(0,\cdot)) &= \varepsilon a_h(U_{h,0}, W_h(0,\cdot)) + \frac{1}{\varepsilon} m_h(\psi'(U_{h,0}), W_h(0,\cdot)) \\ &= \varepsilon a(u_0, w_h(0,\cdot) + \frac{1}{\varepsilon} m_h(\psi'(U_{h,0}), W_h(0,\cdot)) \\ &= -\varepsilon m(-\Delta_\Gamma u_0, w_h(0,\cdot)) + \frac{1}{\varepsilon} m_h(\psi'(U_{h,0}), W_h(0,\cdot)) \\ &\leq c_\varepsilon \big(\|u_0\|_{H^2(\Gamma_0)} + \|u_0\|^3_{H^2(\Gamma_0)} \big) \, \|W_h(0,\cdot)\|_{L^2(\Gamma_h(0))} \, . \end{aligned}$$

In the last line we have used (3.3.26) and the Sobolev embedding of $H^1(\Gamma(t)) \hookrightarrow L^6(\Gamma(t))$ from Lemma 3.2.1. □

From Theorem 3.3.6, we see that $\beta \in C^1([0,T],\mathbb{R}^N)$ so $\partial_h^\bullet W_h$ exists. Hence, we may take the time derivative of (3.3.13b) to see, for $\phi_h \in S_h^T$, that

$$\begin{aligned}\varepsilon\big(a_h(\partial_h^\bullet U_h,\phi_h)+b_h(V_h;U_h,\phi_h)\big)+\frac{1}{\varepsilon}\big(m_h(\psi''(U_h)\partial_h^\bullet U_h,\phi_h)+g_h(V_h;\psi'(U_h),\phi_h)\big)\\ -\big(m_h(\partial_h^\bullet W_h,\phi_h)+g_h(V_h;W_h,\phi_h)\big)=0.\end{aligned} \tag{3.4.3}$$

Lemma 3.4.2. *Under the assumption that $u_0 \in H^2(\Gamma_0)$, we have the bound*

$$\begin{aligned}\varepsilon\int_0^T \|\partial_h^\bullet U_h\|^2_{L^2(\Gamma_h(t))}\,\mathrm{d}t+\sup_{t\in(0,T)}\|W_h\|^2_{L^2(\Gamma_h(t))}\\ \leq c_\varepsilon\big(\,\|u_0\|^2_{H^2(\Gamma_0)}+\|u_0\|^4_{H^2(\Gamma_0)}+\|u_0\|^6_{H^2(\Gamma_0)}\,\big).\end{aligned} \tag{3.4.4}$$

Proof. We start by testing (3.3.15) with $\varepsilon\partial_h^\bullet U_h$ and (3.4.3) with W_h to arrive at

$$\varepsilon m_h(\partial_h^\bullet U_h,\partial_h^\bullet U_h)+\varepsilon g_h(V_h;U_h,\partial_h^\bullet U_h)+\varepsilon a_h(W_h,\partial_h^\bullet U_h)=0 \tag{3.4.5}$$

and

$$\begin{aligned}\varepsilon\big(a_h(\partial_h^\bullet U_h,W_h)+b_h(V_h;U_h,W_h)\big)+\frac{1}{\varepsilon}\big(m_h(\psi''(U_h)\partial_h^\bullet U_h,W_h)\\ +g_h(V_h;\psi'(U_h),W_h)\big)-\big(m_h(\partial_h^\bullet W_h,W_h)+g_h(V_h;W_h,W_h)\big)=0.\end{aligned} \tag{3.4.6}$$

We remark that the transport formula (3.3.9) gives

$$m_h(\partial_h^\bullet W_h,W_h)+g_h(V_h;W_h,W_h)=\frac{1}{2}\frac{\mathrm{d}}{\mathrm{d}t}m_h(W_h,W_h)+\frac{1}{2}g_h(V_h;W_h,W_h).$$

Subtracting (3.4.6) from (3.4.5) gives

$$\begin{aligned}&\varepsilon m_h(\partial_h^\bullet U_h,\partial_h^\bullet U_h)+\frac{1}{2}\frac{\mathrm{d}}{\mathrm{d}t}m_h(W_h,W_h)\\ &\quad=-\varepsilon\big(g_h(V_h;\partial_h^\bullet U_h,U_h)+b_h(V_h;U_h,W_h)\big)\\ &\qquad+\frac{1}{\varepsilon}\big(m_h(\psi''(U_h)\partial_h^\bullet U_h,W_h)+g_h(V_h;\psi'(U_h),W_h)\big)-\frac{1}{2}g_h(V_h;W_h,W_h).\end{aligned} \tag{3.4.7}$$

Note that using a Hölder inequality, Young's inequality with ε, and the Sobolev

embedding (Lemma 3.3.8) we have

$$
\begin{aligned}
&\left|m_h(\psi''(U_h)\partial_h^\bullet U_h, W_h)\right| \\
&\quad= \left|\int_{\Gamma_h(t)} \psi''(U_h)\partial_h^\bullet U_h W_h \,\mathrm{d}\sigma_h\right| = \left|\int_{\Gamma_h(t)} (3U_h^2-1)\partial_h^\bullet U_h W_h \,\mathrm{d}\sigma_h\right| \\
&\quad\le 3\,\|U_h\|^2_{L^6(\Gamma_h(t))}\,\|\partial_h^\bullet U_h\|_{L^2(\Gamma_h(t))}\,\|W_h\|_{L^6(\Gamma_h(t))} + \|\partial_h^\bullet U_h\|_{L^2(\Gamma_h(t))}\,\|W_h\|_{L^2(\Gamma_h(t))} \\
&\quad\le 3\,\|U_h\|^2_{H^1(\Gamma_h(t))}\,\|\partial_h^\bullet U_h\|_{L^2(\Gamma_h(t))}\,\|W_h\|_{H^1(\Gamma_h(t))} + \|\partial_h^\bullet U_h\|_{L^2(\Gamma_h(t))}\,\|W_h\|_{L^2(\Gamma_h(t))} \\
&\quad\le \frac{\varepsilon}{4}\,\|\partial_h^\bullet U_h\|^2_{L^2(\Gamma_h(t))} + c_\varepsilon\big(\,\|U_h\|^2_{H^1(\Gamma_h(t))}\,\|W_h\|^2_{H^1(\Gamma_h(t))} + \|W_h\|^2_{L^2(\Gamma_h(t))}\,\big).
\end{aligned}
$$

Applying this result in (3.4.7), we have

$$
\begin{aligned}
&\varepsilon m_h(\partial_h^\bullet U_h, \partial_h^\bullet U_h) + \frac{\mathrm{d}}{\mathrm{d}t} m_h(W_h, W_h) \\
&\qquad\le c_\varepsilon\left(\|U_h\|^2_{H^1(\Gamma_h(t))} + \|W_h\|^2_{H^1(\Gamma_h(t))} + \|U_h\|^2_{H^1(\Gamma_h(t))}\,\|W_h\|^2_{H^1(\Gamma_h(t))}\right).
\end{aligned}
$$

Integrating in time using a Gronwall inequality gives us

$$
\begin{aligned}
&\varepsilon\int_0^T \|\partial_h^\bullet U_h\|^2_{L^2(\Gamma_h(t))}\,\mathrm{d}t + \sup_{t\in(0,T)}\|W_h\|^2_{L^2(\Gamma_h(t))} \\
&\qquad\le \|W_h(\cdot,0)\|^2_{L^2(\Gamma_h(t))} + c_\varepsilon\int_0^T\left(\|U_h\|^2_{H^1(\Gamma_h(t))} + \|W_h\|^2_{H^1(\Gamma_h(t))}\right)\mathrm{d}t \\
&\qquad\qquad + c_\varepsilon \sup_{t\in(0,T)}\|U_h\|^2_{H^1(\Gamma_h(t))}\int_0^T \|W_h\|^2_{H^1(\Gamma_h(t))}\,\mathrm{d}t.
\end{aligned}
$$

Applying the bounds from Theorem 3.3.6, Lemma 3.4.1 and (3.4.1) completes the proof. □

3.4.2 Existence

The idea of the existence proof is to show that the lift of the solutions to finite element scheme (3.3.13) converges, along a subsequence, to a solution of the continuous equations.

We suppose that $u_0 \in H^2(\Gamma_0)$ is a given function. This implies

$$
\int_{\Gamma_0} \varepsilon\big(\,|\nabla_\Gamma u_0|^2 + u_0^2\big) + \frac{1}{\varepsilon}\psi(u_0)\,\mathrm{d}\sigma \le c_\varepsilon\big(\,\|u_0\|^2_{H^2(\Gamma_0(t))} + \|u_0\|^4_{H^2(\Gamma_0(t))}\,\big) < +\infty. \tag{3.4.8}
$$

In this section, we will take $U_{h,0} = \Pi_h u_0$ with Π_h the Ritz projection defined in

(3.3.48). Since the Ritz projection is stable in H^1 we have that

$$\int_{\Gamma_{h,0}} \varepsilon \left(|\nabla_{\Gamma_h} U_0|^2 + |U_0|^2 \right) + \frac{1}{\varepsilon} \psi(U_0) \, \mathrm{d}\sigma_h < c \int_{\Gamma_0} \varepsilon \big(|\nabla_\Gamma u_0|^2 + u_0^2 \big) + \frac{1}{\varepsilon} \psi(u_0) \, \mathrm{d}\sigma.$$

This implies that the stability bound in Theorem 3.3.6 holds independently of h:

$$\begin{aligned} &\sup_{t \in (0,T)} \int_{\Gamma_h(t)} \varepsilon \big(|\nabla_{\Gamma_h} U_h|^2 + U_h^2 \big) + \frac{1}{\varepsilon} \psi(U_h) \, \mathrm{d}\sigma_h + \int_0^T \|W_h\|^2_{H^1(\Gamma_h(t))} \, \mathrm{d}t \\ &\qquad \leq c \int_{\Gamma_0} \varepsilon \big(|\nabla_\Gamma u_0|^2 + u_0^2 \big) + \frac{1}{\varepsilon} \psi(u_0) \, \mathrm{d}\sigma \leq c_\varepsilon \big(\|u_0\|^2_{H^2(\Gamma_0(t))} + \|u_0\|^4_{H^2(\Gamma_0(t))} \big). \end{aligned}$$

Furthermore, the stability bounds from Lemma 3.3.7 imply that we may transform this bound to $\{\Gamma(t)\}$ and bound the lifts $u_h = U_h^\ell$ and $w_h = W_h^\ell$ by

$$\begin{aligned} &\sup_{t \in (0,T)} \int_{\Gamma(t)} \varepsilon \big(|\nabla_\Gamma u_h|^2 + u_h^2 \big) + \frac{1}{\varepsilon} \psi(u_h) \, \mathrm{d}\sigma + \int_0^T \|w_h\|^2_{H^1(\Gamma(t))} \, \mathrm{d}t \\ &\quad \leq c \int_{\Gamma_0} \varepsilon \big(|\nabla_\Gamma u_0|^2 + u_0^2 \big) + \frac{1}{\varepsilon} \psi(u_0) \, \mathrm{d}\sigma < c_\varepsilon \big(\|u_0\|^2_{H^2(\Gamma_0(t))} + \|u_0\|^4_{H^2(\Gamma_0(t))} \big). \end{aligned}$$

Our assumption that $u_0 \in H^2(\Gamma_0)$ allows the use of the improved bounds in Lemma 3.4.2. Using similar lifting arguments we have

$$\int_0^T \|\partial^\bullet u_h\|^2_{L^2(\Gamma(t))} \, \mathrm{d}t \leq c_\varepsilon \left(\|u_0\|^2_{H^2(\Gamma_0)} + \|u_0\|^4_{H^2(\Gamma_0)} + \|u_0\|^6_{H^2(\Gamma_0)} \right).$$

This bound implies that u_h and w_h are uniformly bounded in the following norms:

$$\|u_h\|_{L^\infty_{H^1}} + \|u_h\|_{H^1(\mathcal{G}_T)} + \|w_h\|_{L^2_{H^1}}.$$

So, we may extract subsequences (for which we will still use the subscript h), and functions $\bar{u}$ and $\bar{w}$ with $\bar{u} \in L^\infty_{H^1} \cap H^1(\mathcal{G}_T)$, and $\bar{w} \in L^2_{H^1}$ such that

$$\begin{aligned} u_h &\rightharpoonup \bar{u} \quad \text{weakly in } H^1(\mathcal{G}_T) \\ w_h &\rightharpoonup \bar{w} \quad \text{weakly in } L^2_{H^1}. \end{aligned} \tag{3.4.9}$$

We remark that these results imply $\partial^\bullet \bar{u} \in L^2_{L^2}$ and $\partial^\bullet u_h \rightharpoonup \partial^\bullet \bar{u}$ weakly in $L^2_{L^2}$. Furthermore, from the compactness result (Proposition 3.2.7) we infer that:

$$u_h \to \bar{u} \quad \text{strongly in } L^2(\mathcal{G}_T) = L^2_{L^2}.$$

Hence, we may take a further subsequence (still denoted u_h) such that

$$u_h \to \bar{u} \quad \text{almost everywhere in } \mathcal{G}_T.$$

Using a Dominated Convergence Theorem-type argument (Robinson 2001, Lemma 8.3), since $\|\psi'(u_h)\|_{L^2(\mathcal{G}_T)} \le c\,\|u_h\|^3_{H^1(\mathcal{G}_T)}$ is bounded independently of h, we infer that

$$\psi'(u_h) \rightharpoonup \psi'(\bar{u}) \quad \text{weakly in } L^2_{L^2}. \tag{3.4.10}$$

We will show that $\bar{u}$ and $\bar{w}$ satisfy (3.2.19). For $\varphi \in L^2_{H^1}$, we write $\phi_h = \Pi_h \varphi$, where Π_h is the Ritz-projection (3.3.48), and $\varphi_h = \phi_h^\ell = \pi_h \varphi$. In addition to (3.3.48), we will use the following facts from Lemma 3.3.18:

$$\|\varphi_h\|_{H^1(\Gamma(t))} \le c\,\|\varphi\|_{H^1(\Gamma(t))} \qquad \text{and} \qquad \|\varphi_h - \varphi\|_{L^2(\Gamma(t))} \le ch\,\|\varphi\|_{H^1(\Gamma(t))}.$$

Using (3.3.13), we have

$$\begin{aligned} &m(\partial^\bullet \bar{u}, \varphi) + g(v; \bar{u}, \varphi) + a(w, \varphi) \\ &\quad = \big(m(\partial^\bullet \bar{u}, \varphi) - m_h(\partial_h^\bullet U_h, \phi_h)\big) + \big(g(v; \bar{u}, \varphi) - g_h(V_h; U_h, \phi_h)\big) \\ &\qquad + \big(a(w, \varphi) - a_h(W_h, \phi_h)\big). \end{aligned} \tag{3.4.11}$$

and

$$\begin{aligned} &\varepsilon a(\bar{u}, \varphi) + \frac{1}{\varepsilon} m(\psi'(\bar{u}), \varphi) - m(\bar{w}, \varphi) \\ &\quad = \varepsilon\big(a(\bar{u}, \varphi) - a_h(U_h, \phi_h)\big) + \frac{1}{\varepsilon}\big(m(\psi'(\bar{u}), \varphi) - m_h(\psi'(U_h), \phi_h)\big) \\ &\qquad - \big(m(\bar{w}, \varphi) - m_h(W_h, \phi_h)\big). \end{aligned} \tag{3.4.12}$$

We consider the right-hand sides of each of these equations term by term. We will denote by $c(h)$ a generic constant depending on h, which may also depend on ε, such that $c(h) \to 0$ as $h \to 0$.

- Using (3.3.46), (3.3.50) and (3.3.44a), we have

$$\begin{aligned} &|m(\partial^\bullet \bar{u}, \varphi) - m_h(\partial_h^\bullet U_h, \phi_h)| \\ &\quad \le |m(\partial^\bullet \bar{u}, \varphi) - m(\partial^\bullet u_h, \varphi)| + |m(\partial^\bullet u_h, \varphi) - m(\partial_h^\bullet u_h, \varphi)| \\ &\qquad + |m(\partial_h^\bullet u_h, \varphi) - m(\partial_h^\bullet u_h, \varphi_h)| + |m(\partial_h^\bullet u_h, \varphi_h) - m_h(\partial_h^\bullet U_h, \phi_h)| \\ &\quad \le |m(\partial^\bullet \bar{u} - \partial^\bullet u_h, \varphi)| \\ &\qquad + c(h)\big(\,\|\nabla_\Gamma u_h\|_{L^2(\Gamma(t))} + \|\partial_h^\bullet u_h\|_{L^2(\Gamma(t))}\,\big)\,\|\varphi\|_{H^1(\Gamma(t))}. \end{aligned}$$

- Using (3.3.45), (3.3.50) and (3.3.42c), we have

$$\begin{aligned}
&|g(v;\bar{u},\varphi) - g_h(V_h;U_h,\phi_h)| \\
&\quad \le |g(v;\bar{u},\varphi) - g(v;u_h,\varphi)| + |g(v;u_h,\varphi) - g(v_h;u_h,\varphi)| \\
&\qquad + |g(v_h;u_h,\varphi) - g(v_h;u_h,\varphi_h)| + |g(v_h;u_h,\varphi_h) - g_h(V_h;U_h,\phi_h)| \\
&\quad \le |g(v;\bar{u}-u_h,\varphi)| + c(h)\,\|u_h\|_{L^2(\Gamma(t))}\,\|\varphi\|_{H^1(\Gamma(t))}\,.
\end{aligned}$$

- Using (3.3.50), (3.3.42b) and (3.3.48), we have

$$|a(\bar{w},\varphi) - a_h(W_h,\phi_h)| = |a(\bar{w},\varphi) - a(w_h,\varphi)| = |a(\bar{w}-w_h,\varphi)|\,,$$

and

$$|a(\bar{u},\varphi) - a_h(U_h,\phi_h)| = |a(\bar{u},\varphi) - a(u_h,\varphi)| = |a(\bar{u}-u_h,\varphi)|\,.$$

- Using (3.3.50) and (3.3.43), we have

$$\begin{aligned}
&\big|m(\psi'(\bar{u}),\varphi) - m_h(\psi'(U_h),\phi_h)\big| \\
&\quad \le \big|m(\psi'(\bar{u}),\varphi) - m(\psi'(u_h),\varphi)\big| + \big|m(\psi'(u_h),\varphi) - m(\psi'(u_h),\varphi_h)\big| \\
&\qquad + \big|m(\psi'(u_h),\varphi_h) - m_h(\psi'(U_h),\phi_h)\big| \\
&\quad \le \big|m(\psi'(\bar{u}) - \psi'(u_h),\varphi)\big| + c(h)\,\big\|\psi'(u_h)\big\|_{L^2(\Gamma(t))}\,\|\varphi\|_{H^1(\Gamma(t))}\,.
\end{aligned}$$

- Using (3.3.50) and (3.3.42a), we have

$$\begin{aligned}
&|m(\bar{w},\varphi) - m_h(W_h,\phi_h)| \\
&\quad \le |m(\bar{w},\varphi) - m(w_h,\varphi)| + |m(w_h,\varphi) - m(w_h,\varphi_h)| \\
&\qquad + |m(w_h,\varphi_h) - m_h(W_h,\phi_h)| \\
&\quad \le |m(\bar{w}-w_h,\varphi)| + c(h)\,\|w_h\|_{L^2(\Gamma(t))}\,\|\varphi\|_{H^1(\Gamma(t))}\,.
\end{aligned}$$

From (3.4.11), this implies

$$\begin{aligned}
&\int_0^T m(\partial^\bullet \bar{u}, \varphi) + g(v; \bar{u}, \varphi) + a(\bar{w}, \varphi)\,\mathrm{d}t \\
&\quad = \int_0^T m(\partial^\bullet \bar{u}, \varphi) - m_h(\partial^\bullet u_h, \varphi_h) + \big(g(v; \bar{u}, \varphi) - g_h(V_h; U_h, \phi_h)\big) \\
&\qquad\qquad + \big(a(\bar{w}, \varphi) - a_h(W_h, \phi_h)\big)\,\mathrm{d}t \\
&\quad \leq \int_0^T m(\partial^\bullet \bar{u} - \partial^\bullet u_h, \varphi) + g(v; \bar{u} - u_h, \varphi) + a(\bar{w} - w_h, \varphi)\,\mathrm{d}t \\
&\qquad + c(h) \int_0^T \big(\|\partial_h^\bullet u_h\|_{L^2(\Gamma(t))} + \|u_h\|_{H^1(\Gamma(t))} + \|\nabla_\Gamma w_h\|_{L^2(\Gamma(t))} \big) \|\varphi\|_{H^1(\Gamma(t))}\,\mathrm{d}t.
\end{aligned}$$

Similarly, using (3.4.12), we obtain

$$\begin{aligned}
&\int_0^T \varepsilon a(\bar{u}, \varphi) + \frac{1}{\varepsilon} m(\psi'(\bar{u}), \varphi) - m(\bar{w}, \varphi)\,\mathrm{d}t \\
&\quad = \int_0^T \varepsilon\big(a(\bar{u}, \varphi) - a_h(U_h, \phi_h)\big) + \frac{1}{\varepsilon}\big(m(\psi'(\bar{u}), \varphi) - m_h(\psi'(U_h), \phi_h)\big) \\
&\qquad\qquad - \big(m(\bar{w}, \varphi) - m_h(W_h, \phi_h)\big)\,\mathrm{d}t \\
&\quad = \int_0^T \varepsilon a(\bar{u} - u_h, \varphi) + \frac{1}{\varepsilon} m(\psi'(\bar{u}) - \psi'(u_h), \varphi) - m(\bar{w} - w_h, \varphi)\,\mathrm{d}t \\
&\qquad + c(h) \int_0^T \big(\|u_h\|_{H^1(\Gamma(t))} + \|w_h\|_{L^2(\Gamma(t))} \big) \|\varphi\|_{H^1(\Gamma(t))}\,\mathrm{d}t.
\end{aligned}$$

We may send $h \to 0$ in the right-hand sides of both previous equations, and use the convergence results (3.4.9) and (3.4.10), so that for all $\varphi \in L^2_{H^1}$ we arrive at

$$\begin{aligned}
\int_0^T m(\partial^\bullet \bar{u}, \varphi) + g(v; \bar{u}, \varphi) + a(\bar{w}, \varphi)\,\mathrm{d}t = 0 \\
\int_0^T \varepsilon a(\bar{u}, \varphi) + \frac{1}{\varepsilon} m(\psi'(u), \varphi) - m(w, \varphi) = 0.
\end{aligned}$$

Finally, we use Lemma 3.2.10 to transform this equality into a almost everywhere in time equality so that the pair $\bar{u}, \bar{w}$ satisfy (3.2.19).

To show that $\bar{u}$ achieves the initial condition, we start by choosing $\varphi \in C^2(\bar{\mathcal{G}}_T)$ and continue with the notation $\varphi_h = \pi_h \varphi$. Using the discrete transport formula (3.3.35), the lift of the finite element solution u_h satisfies

$$\int_0^T m(u_h, \varphi_h)\dot{\alpha}\,\mathrm{d}t = -\int_0^T \big(m(\partial_h^\bullet u_h, \varphi_h) + m(u_h, \partial_h^\bullet \varphi_h) + g(v_h; u_h, \varphi_h)\big)\alpha\,\mathrm{d}t,$$

for all $\alpha \in C_c^\infty(0,T)$. Using similar limiting arguments as above, with the addition of (3.3.61), we obtain the identity

$$\int_0^T m(\bar{u},\varphi)\dot{\alpha}\,\mathrm{d}t = -\int_0^T \big(m(\partial^\bullet \bar{u},\varphi) + m(\bar{u},\partial^\bullet\varphi) + g(v;\bar{u},\varphi)\big)\alpha\,\mathrm{d}t.$$

In fact, by density of $C^2(\mathcal{G}_T)$ functions in $H^1(\mathcal{G}_T)$ (Hebey 2000, Theorem 2.4), we see that this equality holds for all $\varphi \in H^1(\mathcal{G}_T)$. This implies that $m(\bar{u},\varphi)$ is weakly differentiable as a function on $(0,T)$ with weak derivative $m(\partial^\bullet\bar{u},\varphi) + m(\bar{u},\partial^\bullet\varphi) + g(v;\bar{u},\varphi)$. Since $\bar{u},\varphi \in H^1(\mathcal{G}_T)$, this weak derivative is a function in $L^1(0,T)$, and hence we infer that $m(\bar{u},\varphi)$ is absolutely continuous on $[0,T]$ (Evans and Gariepy 1992, Section 4.9, Theorem 1). In particular, $\|\bar{u}\|_{L^2(\Gamma(t))}$ is absolutely continuous, which means that we can interpret $u(\cdot,0)$ as an $L^2(\Gamma_0)$ function. The absolute continuity of $m(u,\varphi)$ for $\varphi \in C^2(\mathcal{G}_T)$ also implies

$$\begin{aligned} &m\big(\bar{u}(\cdot,t),\varphi(\cdot,t)\big) - m\big(\bar{u}(\cdot,0),\varphi(\cdot,0)\big) \\ &\qquad = \int_0^t m(\partial^\bullet\bar{u},\varphi) + g(v;\bar{u},\varphi) + m(\bar{u},\partial^\bullet\varphi)\,\mathrm{d}s. \end{aligned} \tag{3.4.13}$$

Next, we choose $\varphi \in C^2(\mathcal{G}_T)$ with $\varphi(\cdot,T) = 0$. It is clear that $\varphi \in L^2_{H^1}$, hence we can use the limiting equation and (3.4.13) to see that

$$\int_0^T -m(\bar{u},\partial^\bullet\varphi) + a(\bar{w},\varphi)\,\mathrm{d}t = m(\bar{u}(\cdot,0),\varphi(\cdot,0)).$$

We can do the same in the finite element scheme for $\phi_h = \Pi_h\varphi$, using the transport formula (3.3.9):

$$\int_0^T -m_h(U_h,\partial_h^\bullet\phi_h) + a_h(W_h,\phi_h)\,\mathrm{d}t = m_h(\Pi_h u_0,\phi_h(\cdot,0)).$$

The above calculations show that we are able to take the limit $h \to 0$ (in the appropriate sense) to see that

$$\int_0^T -m(\bar{u},\partial^\bullet\varphi) + a(\bar{w},\varphi)\,\mathrm{d}t = m(u_0,\varphi(\cdot,0)).$$

Therefore, by comparing terms, we have shown that $\bar{u}(\cdot,0) = u_0$ almost everywhere in Γ_0 by the Fundamental Lemma of the Calculus of Variations.

Hence we have shown the following result:

Theorem 3.4.3. *Given $u_0 \in H^2(\Gamma_0)$ there exists a weak solution pair (u,w) of the*

Cahn-Hilliard equation in the sense of Definition 3.2.11. Furthermore the solution satisfies the energy bound

$$\begin{aligned}\sup_{t\in(0,T)}\int_{\Gamma(t)}\varepsilon\left(|\nabla_\Gamma u|^2+u^2\right)+\frac{1}{\varepsilon}\psi(u)\,\mathrm{d}\sigma+\int_0^T\|w\|^2_{H^1(\Gamma(t))}\,\mathrm{d}t\\ \leq c_\varepsilon\int_{\Gamma_0}\varepsilon\,|\nabla_\Gamma u_0|^2+\frac{1}{\varepsilon}\psi(u_0)\,\mathrm{d}\sigma.\end{aligned}\tag{3.4.14}$$

3.4.3 Uniqueness

To show the uniqueness result, we require an inverse Laplacian on $\Gamma(t)$. For $z\in L^2(\Gamma(t))$ with $\int_{\Gamma(t)}z\,\mathrm{d}\sigma=0$, we define $\mathcal{G}z$ the inverse Laplacian of z as the unique solution of

$$a(\mathcal{G}z,\varphi)=m(z,\varphi)\quad\text{ for all }\varphi\in H^1(\Gamma(t)),\text{ and }\int_{\Gamma(t)}\mathcal{G}z\,\mathrm{d}\sigma=0.\tag{3.4.15}$$

We will write

$$\|z\|_{-1}:=\|\nabla_\Gamma\mathcal{G}z\|_{L^2(\Gamma(t))}=a(\mathcal{G}z,\mathcal{G}z)^{\frac{1}{2}}.$$

and remark that

$$\|z\|^2_{-1}=m(\mathcal{G}z,z).$$

It is clear that if $z\in L^2(\Gamma(t))$ then $\mathcal{G}z\in H^1(\Gamma(t))$. We also have a similar result for the material derivative of $\mathcal{G}z$.

Lemma 3.4.4. *If $z\in H^1(\mathcal{G}_T)$, with $\int_{\Gamma(t)}z\,\mathrm{d}\sigma=0$, then $\mathcal{G}z\in H^1(\mathcal{G}_T)$.*

Proof. It is clear that $\mathcal{G}z\in L^2_{H^1}$ for $z\in L^2_{H^1}$. It is left to show $\partial^\bullet\mathcal{G}z\in L^2_{L^2}$. We start by taking a time derivative of (3.4.15) so that for $\xi\in H^1(\mathcal{G}_T)$:

$$a(\partial^\bullet\mathcal{G}z,\xi)+a(\mathcal{G}z,\partial^\bullet\xi)+b(v;\mathcal{G}z,\xi)=m(\partial^\bullet z,\xi)+m(z,\partial^\bullet\xi)+g(v;z,\xi).$$

From Lemma 3.2.5, given $\varphi\in H^1(\Gamma(t^*))$, we can construct $\widetilde{\varphi}\colon\mathcal{G}_T\to\mathbb{R}$, with $\widetilde{\varphi}\in H^1(\Gamma(t))$ for all $t\in[0,T]$ and $\partial^\bullet\widetilde{\varphi}=0$. Thus, we have that

$$a(\partial^\bullet\mathcal{G}z,\widetilde{\varphi})+b(v;\mathcal{G}z,\widetilde{\varphi})=m(\partial^\bullet z,\widetilde{\varphi})+g(v;z,\widetilde{\varphi})\quad\text{ for }t\in(0,T),$$

and, in particular, at $t=t^*$,

$$a(\partial^\bullet\mathcal{G}z,\varphi)+b(v;\mathcal{G}z,\varphi)=m(\partial^\bullet z,\varphi)+g(v;z,\varphi).$$

Also, we have that

$$m(\partial^\bullet z, 1) + g(v; z, 1) - b(v; \mathcal{G}z, 1) = \frac{\mathrm{d}}{\mathrm{d}t} \int_{\Gamma(t^*)} z \, \mathrm{d}\sigma = 0.$$

These calculations imply that $\partial^\bullet \mathcal{G}z$ solves the elliptic problem:

$$a(\partial^\bullet \mathcal{G}z, \varphi) = m(\partial^\bullet z, \varphi) + g(v; z, \varphi) - b(v; \mathcal{G}z, \varphi) \quad \text{for all } \varphi \in H^1(\Gamma(t^*)).$$

This implies that $\partial^\bullet \mathcal{G}z \in H^1(\Gamma(t^*))$ with the bound

$$\|\partial^\bullet \mathcal{G}z\|_{H^1(\Gamma(t^*))} \leq c \left(\|\partial^\bullet z\|_{L^2(\Gamma(t^*))} + \|z\|_{L^2(\Gamma(t^*))} + \|z\|_{-1} \right).$$

Integrating in time, we arrive at

$$\int_0^T \|\partial^\bullet \mathcal{G}z\|^2_{H^1(\Gamma(t))} \, \mathrm{d}t \leq c \int_0^T \|\partial^\bullet z\|^2_{L^2(\Gamma(t))} + \|z\|^2_{H^1(\Gamma(t))} \, \mathrm{d}t \leq c \, \|z\|^2_{H^1(\mathcal{G}_T)}. \qquad \square$$

Theorem 3.4.5. *There is at most one solution to* (3.2.19).

Proof. We suppose that (u_1, w_1) and (u_2, w_2) are solutions to (3.2.19). We will write $\eta^u = u_1 - u_2$ and $\eta^w = w_1 - w_2$. For $\varphi \in L^2_{H^1}$, we know that

$$m(\partial^\bullet \eta^u, \varphi) + g(v; \eta^u, \varphi) + a(\eta^w, \varphi) = 0 \tag{3.4.16a}$$

$$\varepsilon a(\eta^u, \varphi) + \frac{1}{\varepsilon}(\psi'(u_1) - \psi'(u_2), \varphi) - m(\eta^w, \varphi) = 0. \tag{3.4.16b}$$

Testing (3.4.16a) with $\varphi = 1$ tells us that

$$\int_{\Gamma(t)} \eta^u \, \mathrm{d}\sigma = \int_{\Gamma_0} \eta^u \, \mathrm{d}\sigma = 0,$$

Hence, since $\mathcal{G}\eta^u$ is well defined and $\mathcal{G}\eta^u \in H^1(\mathcal{G}_T)$, we may test the first equation with $\mathcal{G}\eta^u$, and apply (3.2.7), to obtain

$$\frac{\mathrm{d}}{\mathrm{d}t} m(\eta^u, \mathcal{G}\eta^u) + a(\eta^w, \mathcal{G}\eta^u) = m(\eta^u, \partial^\bullet \mathcal{G}\eta^u).$$

Using the definitions above, this is equivalent to

$$\frac{\mathrm{d}}{\mathrm{d}t} \|\eta^u\|^2_{-1} + m(\eta^w, \eta^u) = m(\eta^u, \partial^\bullet \mathcal{G}\eta^u). \tag{3.4.17}$$

Next, using the monotonicity of $z \mapsto z^3$, testing the second equation with η^u gives

$$\varepsilon a(\eta^u, \eta^u) - \frac{1}{\varepsilon} m(\eta^u, \eta^u) \leq m(\eta^w, \eta^u). \tag{3.4.18}$$

Taking the sum of (3.4.18) and (3.4.17), we obtain

$$\frac{\mathrm{d}}{\mathrm{d}t} \|\eta^u\|_{-1}^2 + \varepsilon \|\nabla_\Gamma \eta^u\|_{L^2(\Gamma(t))}^2 \leq \frac{1}{\varepsilon} m(\eta^u, \eta^u) + m(\eta^u, \partial^\bullet \mathcal{G}\eta^u).$$

For the first term on the right hand side, we see that

$$\frac{1}{\varepsilon} m(\eta^u, \eta^u) = \frac{1}{\varepsilon} a(\eta^u, \mathcal{G}\eta^u) \leq \frac{\varepsilon}{2} \|\nabla_\Gamma \eta^u\|_{L^2(\Gamma(t))}^2 + c_\varepsilon \|\eta^u\|_{-1}^2,$$

and for the second, we have

$$\begin{aligned} m(\eta^u, \partial^\bullet \mathcal{G}\eta^u) = a(\mathcal{G}\eta^u, \partial^\bullet \mathcal{G}\eta^u) &= \frac{1}{2}\frac{\mathrm{d}}{\mathrm{d}t} a(\mathcal{G}\eta^u, \mathcal{G}\eta^u) - \frac{1}{2} b(v; \mathcal{G}\eta^u, \mathcal{G}\eta^u) \\ &\leq \frac{1}{2}\frac{\mathrm{d}}{\mathrm{d}t} \|\eta^u\|_{-1}^2 + c \|\eta^u\|_{-1}^2. \end{aligned}$$

Combining these terms, we obtain the estimate

$$\frac{\mathrm{d}}{\mathrm{d}t} \|\eta^u\|_{-1}^2 + \varepsilon \|\nabla_\Gamma \eta^u\|_{L^2(\Gamma(t))}^2 \leq c_\varepsilon \|\eta^u\|_{-1}^2.$$

We next use a Gronwall inequality and integration in time to see

$$\sup_{t\in(0,T)} \|\eta^u\|_{-1}^2 + \varepsilon \int_0^T \|\nabla_\Gamma \eta^u\|_{L^2(\Gamma(t))}^2 \leq c_\varepsilon \|\eta^u|_{t=0}\|_{-1}^2 = 0.$$

Since $\int_{\Gamma(t)} \eta^u \,\mathrm{d}\sigma = 0$, we apply a Poincaré inequality to arrive at

$$\int_0^T \|\eta^u\|_{L^2(\Gamma(t))}^2 \,\mathrm{d}t \leq \int_0^T \|\nabla_\Gamma \eta^u\|_{L^2(\Gamma(t))}^2 \,\mathrm{d}t = 0.$$

This shows that $u_1 = u_2$.

Now, we know that $\eta^u = 0$, testing (3.4.16a) with η^w gives

$$m(\eta^w, \eta^w) = \varepsilon a(\eta^u, \eta^w) + \frac{1}{\varepsilon} m(\psi'(u_1) - \psi'(u_2), \eta^w) = 0.$$

This shows that $w_1 = w_2$. □

3.4.4 Regularity

In this section, we show that the solution enjoys H^2 regularity.

Theorem 3.4.6 (Regularity). *Let $u_0 \in H^2(\Gamma_0)$ and (u, w) be the solution pair of (3.2.19), then $u \in L^\infty_{H^2}$ and $w \in L^2_{H^2}$, with the bounds*

$$\varepsilon \sup_{t\in(0,T)} \|u\|^2_{H^2(\Gamma(t))} + \int_0^T \|w\|^2_{H^2(\Gamma(t))} \leq c_\varepsilon\big(\|u_0\|^2_{H^2(\Gamma_0)} + \|u_0\|^4_{H^2(\Gamma_0)} \big). \tag{3.4.19}$$

Proof. Using the improved estimates from Lemma 3.4.2, we have that

$$\begin{aligned} &\varepsilon \int_0^T \|\partial^\bullet u\|^2_{L^2(\Gamma(t))} + \sup_{t\in(0,T)} \|w\|^2_{L^2(\Gamma(t))} \\ &\quad \leq c_\varepsilon \|u_0\|^2_{H^2(\Gamma_0)} + c_\varepsilon \left(\int_{\Gamma_0} \varepsilon \left|\nabla_\Gamma u_0\right|^2 + \frac{1}{\varepsilon}\psi(u_0)\,\mathrm{d}\sigma \right) \\ &\qquad + \frac{c}{\varepsilon} \left(\int_{\Gamma_0} \varepsilon \left|\nabla_\Gamma u_0\right|^2 + \frac{1}{\varepsilon}\psi(u_0)\,\mathrm{d}\sigma \right)^2. \end{aligned} \tag{3.4.20}$$

Now, we can translate the fact that (u, w) are solutions of (3.2.19) into

$$\begin{aligned} \varepsilon a(u, \varphi) &= m(f_1, \varphi) \\ a(w, \varphi) &= m(f_2, \varphi) \quad \text{for all } \varphi \in H^1(\Gamma(t)), \end{aligned}$$

for $f_1 = w - \frac{1}{\varepsilon}\psi'(u)$ and $f_2 = \partial^\bullet u + u\nabla_\Gamma \cdot v$. Notice that

$$\int_{\Gamma(t)} f_1 \,\mathrm{d}\sigma = \int_{\Gamma(t)} f_2 \,\mathrm{d}\sigma = 0.$$

The above improved bounds combined with the bounds in Theorem 3.4.3 gives $f_1 \in L^\infty_{L^2}$ and $f_2 \in L^2_{L^2}$. Standard theory of elliptic partial differential equations (Theorem A.2.5) gives $u \in L^\infty_{H^2}$ and $w \in L^2_{H^2}$. The proof is completed by using the bounds in (3.4.14) and (3.4.20) on f_1 and f_2. □

3.5 Error analysis of finite element scheme

In this section, we show an error bound for the surface finite element method described in Section 3.3. The proof relies on decomposing the errors into errors between the smooth solution and Ritz projection and between the Ritz projection and discrete solution. In contrast to previous studies of partial differential equations on surfaces (Dziuk 1988; Dziuk and Elliott 2007a, 2013a), we show an error bound on

$\Gamma_h(t)$ instead of $\Gamma(t)$. This is required to deal with the non-linear term.

We will assume that u_0, u and w are bounded in the following norms

$$\|u_0\|^2_{H^2(\Gamma_0)} + \sup_{t\in(0,T)} \|u\|^2_{H^2(\Gamma(t))} + \int_0^T \|w\|^2_{H^2(\Gamma(t))} + \|\partial^\bullet u\|^2_{H^2(\Gamma(t))} \,\mathrm{d}t < +\infty. \tag{3.5.1}$$

Section 3.4.4 shows how to bound some of these terms. Again, we will assume that the initial condition of the finite element scheme is given by the Ritz projection:

$$U_{h,0} = \Pi_h u_0. \tag{3.5.2}$$

The error bound we will show is stated as follows:

Theorem 3.5.1. *Let u, w solve (3.2.14) and satisfy (3.5.1). Let U_h, W_h solve (3.3.13) with initial condition (3.5.2). We have that*

$$\varepsilon \sup_{t\in(0,T)} \left\| u^{-\ell} - U_h \right\|^2_{L^2(\Gamma_h(t))} + \int_0^T \left\| w^{-\ell} - W_h \right\|^2_{L^2(\Gamma_h(t))} \leq Ch^4, \tag{3.5.3}$$

with C given by

$$C = c_\varepsilon \|u_0\|^2_{H^2(\Gamma_0)} + c_\varepsilon \sup_{t\in(0,T)} \|u\|^2_{H^2(\Gamma(t))} + c_\varepsilon \int_0^T \left(\|\partial^\bullet u\|^2_{H^2(\Gamma(t))} + \|w\|^2_{H^2(\Gamma(t))} \right) \mathrm{d}t.$$

3.5.1 Pointwise bound on the discrete solution

In the following error analysis, a pointwise bound on the discrete solution uniformly in space and time will be extremely useful. This will allow us to convert the local Lipschitz property of ψ and ψ' into global results.

Lemma 3.5.2. *Let $F_h = W_h - \frac{1}{\varepsilon}\psi'(U_h)$, then $F_h \in L^\infty(0,T; L^2(\Gamma_h(t)))$ with the estimate*

$$\sup_{t\in(0,T)} \|F_h\|^2_{L^2(\Gamma_h(t))} \leq c_\varepsilon \big(\|u_0\|^2_{H^2(\Gamma_0)} + \|u_0\|^4_{H^2(\Gamma_0)} \big). \tag{3.5.4}$$

Furthermore, the mean value of F_h is zero:

$$\int_{\Gamma_h(t)} F_h \,\mathrm{d}\sigma_h = 0. \tag{3.5.5}$$

Proof. This follows immediately from Theorem 3.3.6 and Lemma 3.4.2 combined with a Sobolev inequality (Lemma 3.3.8) and (3.4.1). The mean value property follows since $\phi_h = 1$ is an admissible test function in (3.3.13b). □

Theorem 3.5.3. *The discrete solution U_h is bounded uniformly in space and time, independently of h, and we have the bound*

$$\sup_{t\in(0,T)} \|U_h\|^2_{L^\infty(\Gamma_h(t))} \leq c_\varepsilon\big(\|u_0\|^2_{H^2(\Gamma_0)} + \|u_0\|^4_{H^2(\Gamma_0)} \big). \tag{3.5.6}$$

Proof. We define $\widetilde{F}_h = F_h^\ell/\mu_h^\ell$, so that

$$\int_{\Gamma(t)} \widetilde{F}_h \,\mathrm{d}\sigma = \int_{\Gamma(t)} F_h^\ell \frac{1}{\mu_h^\ell} \,\mathrm{d}\sigma = \int_{\Gamma_h(t)} F_h \,\mathrm{d}\sigma_h = 0.$$

Let $\bar{u}\colon \mathcal{G}_T \to \mathbb{R}$ solve

$$-\varepsilon\Delta_\Gamma \bar{u} = \widetilde{F}_h \quad \text{on } \Gamma(t), \text{ and } \int_{\Gamma(t)} \bar{u} \,\mathrm{d}\sigma = \int_{\Gamma_h(t)} U_h \,\mathrm{d}\sigma_h \text{ for each } t \in (0,T).$$

Then it is clear that $\Pi_h \bar{u} = U_h$. Standard Elliptic theory (Theorem A.2.5) and the L^∞ bound on Π_h (3.3.55) gives that

$$\|U_h\|_{L^\infty(\Gamma_h(t))} = \|\Pi_h \bar{u}\|_{L^\infty(\Gamma_h(t))} \leq c\,\|\bar{u}\|_{H^2(\Gamma(t))} \leq c\left\|\widetilde{F}_h\right\|_{L^2(\Gamma(t))} \leq c\,\|F_h\|_{L^2(\Gamma_h(t))}.$$

We apply this inequality uniformly in time, with (3.5.4), to give the desired estimate. □

3.5.2 Splitting the error

We split the error into two parts using the Ritz projection Π_h from Section 3.3.5:

$$\begin{aligned} u^{-\ell} - U_h &= (u^{-\ell} - \Pi_h u) + (\Pi_h u - U_h) = \rho^u + \theta^u \\ w^{-\ell} - W_h &= (w^{-\ell} - \Pi_h w) + (\Pi_h w - W_h) = \rho^w + \theta^w. \end{aligned}$$

We note that from Lemma 3.3.18, we already have estimates for ρ^u and ρ^w and it is left to bound θ^u and θ^w. Notice that, the assumptions in (3.5.1) imply that $\theta^u \in S_h^T$ and $\theta^w \in \widetilde{S}_h^T$.

To derive equations for θ^u and θ^w, we start by rewriting (3.3.13a) using the

definition of Π_h and (3.2.15a) to obtain for $\phi_h \in S_h^T$ with lift $\varphi_h \in S_h^{\ell,T}$ that

$$\begin{aligned}
&\frac{\mathrm{d}}{\mathrm{d}t} m_h(\theta^u, \phi_h) + a_h(\theta^w, \phi_h) - m_h(\theta^u, \partial_h^\bullet \phi_h) \\
&\quad = \frac{\mathrm{d}}{\mathrm{d}t} m_h(\Pi_h u, \phi_h) + a_h(\Pi_h w, \phi_h) - m_h(\Pi_h u, \partial_h^\bullet \phi_h) \\
&\quad = \frac{\mathrm{d}}{\mathrm{d}t} m_h(\Pi_h u, \phi_h) + a(w, \varphi_h) - m_h(\Pi_h u, \partial_h^\bullet \phi_h) \\
&\quad = \frac{\mathrm{d}}{\mathrm{d}t} \big(m_h(\Pi_h u, \phi_h) - m(u, \varphi_h) \big) - \big(m_h(\Pi_h u, \partial_h^\bullet \phi_h) - m(u, \partial^\bullet \varphi_h) \big) \\
&\quad = \big(m_h(\partial_h^\bullet \Pi_h u, \phi_h) - m(\partial_h^\bullet u, \varphi_h) \big) + \big(g_h(V_h; \Pi_h u, \phi_h) - g(v_h; u, \varphi_h) \big) \\
&\qquad + m(u, \partial^\bullet \varphi_h - \partial_h^\bullet \varphi_h) \\
&\quad =: E_1(\phi_h) + E_2(\phi_h) + E_3(\phi_h).
\end{aligned} \tag{3.5.7}$$

Next, we rewrite (3.3.13b) using (3.2.15b) this time to see for $\phi_h \in \widetilde{S}_h^T$ with lift $\varphi_h \in \widetilde{S}_h^{\ell,T}$ that

$$\begin{aligned}
&\varepsilon a_h(\theta^u, \phi_h) + \frac{1}{\varepsilon} m_h(\psi'(\Pi_h u) - \psi'(U_h), \phi_h) - m_h(\theta^w, \phi_h) \\
&\quad = \varepsilon a_h(\Pi_h u, \phi_h) + \frac{1}{\varepsilon} m_h(\psi'(\Pi_h u), \phi_h) - m_h(\Pi_h w, \phi_h) \\
&\quad = \varepsilon a(u, \varphi_h) + \frac{1}{\varepsilon} m_h(\psi'(\Pi_h u), \phi_h) - m_h(\Pi_h w, \phi_h) \\
&\quad = \frac{1}{\varepsilon} \big(m_h(\psi'(\Pi_h u), \phi_h) - m(\psi'(u), \varphi_h) \big) - \big(m_h(\Pi_h w, \phi_h) - m(w, \varphi_h) \big) \\
&\quad =: E_4(\phi_h) + E_5(\phi_h).
\end{aligned} \tag{3.5.8}$$

The quantities $E_j(\phi_h)$, for $j = 1, \dots, 5$, are consistency terms involving the approximation properties of the finite element spaces and the geometric perturbation.

Lemma 3.5.4. *For $\phi_h \in S_h^T$ we have*

$$|E_1(\phi_h)| \le c h^2 \big(\|\partial^\bullet u\|_{H^2(\Gamma(t))} + \|u\|_{H^2(\Gamma(t))} \big) \|\phi_h\|_{L^2(\Gamma_h(t))} \tag{3.5.9}$$

$$|E_2(\phi_h)| \le c h^2 \|u\|_{H^2(\Gamma(t))} \|\phi_h\|_{H^1(\Gamma_h(t))} \tag{3.5.10}$$

$$|E_3(\phi_h)| \le c h^2 \|u\|_{L^2(\Gamma(t))} \|\phi_h\|_{H^1(\Gamma_h(t))}, \tag{3.5.11}$$

and for $\phi_h \in \widetilde{S}_h^T$:

$$|E_4(\phi_h)| \le c \frac{h^2}{\varepsilon} \|u\|_{H^2(\Gamma(t))} \|\phi_h\|_{L^2(\Gamma_h(t))} \tag{3.5.12}$$

$$|E_5(\phi_h)| \le c h^2 \|w\|_{H^2(\Gamma(t))} \|\phi_h\|_{L^2(\Gamma_h(t))}. \tag{3.5.13}$$

Proof. The proof is a combination of the geometric bounds from Section 3.3.4 and the bounds of Π_h from Lemmas 3.3.18 and 3.3.24. We will show each in turn:

- For (3.5.9), we use the bound on the Ritz projection (3.3.61) and the geometric bounds (3.3.44a) and (3.3.46) to see that

$$\begin{aligned}
&|m_h(\partial_h^\bullet \Pi_h u, \phi_h) - m(\partial_h^\bullet u, \varphi_h)| \\
&\quad \leq |m_h(\partial_h^\bullet \Pi_h u, \phi_h) - m(\partial_h^\bullet \pi_h u, \varphi_h)| + |m(\partial_h^\bullet(\pi_h u - u), \varphi_h)| \\
&\quad \leq ch^2 \big(\|u\|_{H^2(\Gamma(t))} + \|\partial^\bullet u\|_{H^2(\Gamma(t))} \big) \|\phi_h\|_{L^2(\Gamma_h(t))}
\end{aligned}$$

- For (3.5.10), we use the bound on the Ritz projection (3.3.50) and (3.3.42c) to see that

$$\begin{aligned}
&|g_h(V_h; \Pi_h u, \phi_h) - g(v_h; u, \varphi_h)| \\
&\quad \leq |g_h(V_h; \Pi_h u, \phi_h) - g(v_h; \pi_h u, \varphi_h)| + |g(v_h; \pi_h u - u, \varphi_h)| \\
&\quad \leq ch^2 \|u\|_{H^2(\Gamma(t))} \|\phi_h\|_{L^2(\Gamma(t))} .
\end{aligned}$$

- For (3.5.11), we simply use the bound on the material derivative (3.3.46) and the stability of the lifting process (3.3.26) to see that

$$\begin{aligned}
m(u, \partial^\bullet \varphi_h - \partial_h^\bullet \varphi_h) &\leq \|u\|_{L^2(\Gamma(t))} \|\partial^\bullet \varphi_h - \partial_h^\bullet \varphi_h\|_{L^2(\Gamma(t))} \\
&\leq ch^2 \|u\|_{L^2(\Gamma(t))} \|\nabla_{\Gamma_h} \phi_h\|_{L^2(\Gamma_h(t))} .
\end{aligned}$$

- For (3.5.12), we use the L^2 bound on the Ritz projection (3.3.50), the geometric bound (3.3.42a), the L^∞-stability bound on Π_h (3.3.55), and the local Lipschitz property of ψ to see that

$$\begin{aligned}
&\big|m_h(\psi'(\Pi_h u), \phi_h) - m(\psi'(u), \varphi)\big| \\
&\quad \leq \big|m_h(\psi'(\Pi_h u), \phi_h) - m(\psi'(\pi_h u), \varphi_h)\big| + \big|m(\psi'(\pi_h u) - \psi'(u), \varphi_h)\big| \\
&\quad \leq ch^2 \big(\big\|\psi'(\Pi_h u)\big\|_{L^2(\Gamma_h(t))} + c_L \|u\|_{H^2(\Gamma(t))} \big) \|\phi_h\|_{L^2(\Gamma_h(t))} \\
&\quad \leq ch^2 \|u\|_{H^2(\Gamma(t))} \|\phi_h\|_{L^2(\Gamma_h(t))} .
\end{aligned}$$

  We have written c_L for the Lipschitz constant of ψ'.

- For (3.5.13), we again use the L^2 bound on the Ritz projection (3.3.50) and

the geometric bound (3.3.42a) to see that

$$\begin{aligned}
&|m_h(\Pi_h w, \phi_h) - m(w, \varphi_h)| \\
&\quad \leq |m_h(\Pi_h w, \phi_h) - m(\pi_h w, \varphi_h)| + |m(\pi_h w - w, \varphi_h)| \\
&\quad \leq ch^2 \|w\|_{H^2(\Gamma(t))} \|\phi_h\|_{L^2(\Gamma(t))}.
\end{aligned}$$

□

3.5.3 Error bounds

In this section, we derive bounds on θ^u and θ^w based on the error equations derived in the previous section and natural energy methods for the partial differential equation system go on to show the final error estimate.

To bound θ^u and θ^w we start by testing (3.5.7) with $\varepsilon\theta^u$ and (3.5.8) with θ^w and subtract to see that

$$\begin{aligned}
&\varepsilon \frac{\mathrm{d}}{\mathrm{d}t} m_h(\theta^u, \theta^u) + m_h(\theta^w, \theta^w) \\
&\quad = \varepsilon m_h(\theta^u, \partial_h^\bullet \theta^u) + \frac{1}{\varepsilon} m_h(\psi'(\Pi_h u) - \psi'(U_h), \theta^w) \\
&\qquad + E_1(\varepsilon\theta^u) + E_2(\varepsilon\theta^u) + E_3(\varepsilon\theta^u) - E_4(\theta^w) - E_5(\theta^w).
\end{aligned}$$

The transport lemma (3.3.9) tells us that

$$m_h(\theta^u, \partial_h^\bullet \theta^u) = \frac{1}{2}\frac{\mathrm{d}}{\mathrm{d}t} m_h(\theta^u, \theta^u) - \frac{1}{2} g_h(V_h; \theta^u, \theta^u).$$

Applying Lemma 3.5.4, with the local Lipschitz property of ψ', this result gives that

$$\begin{aligned}
&\frac{\varepsilon}{2}\frac{\mathrm{d}}{\mathrm{d}t} m_h(\theta^u, \theta^u) + m_h(\theta^w, \theta^w) \\
&\quad \leq c\frac{\varepsilon}{2} \|\theta^u\|^2_{L^2(\Gamma_h(t))} + \frac{1}{\varepsilon} \|\theta^u\|_{L^2(\Gamma_h(t))} \|\theta^w\|_{L^2(\Gamma_h(t))} \\
&\qquad + c\varepsilon h^2 \big(\|\partial^\bullet u\|_{H^2(\Gamma(t))} + \|u\|_{H^2(\Gamma(t))} \big) \|\theta^u\|_{L^2(\Gamma_h(t))} \\
&\qquad + \frac{ch^2}{\varepsilon} \big(\|u\|_{H^2(\Gamma(t))} + \|w\|_{H^2(\Gamma(t))} \big) \|\theta^w\|_{L^2(\Gamma_h(t))} \\
&\qquad + c\varepsilon h^2 \|u\|_{H^2(\Gamma(t))} \|\nabla_{\Gamma_h} \theta^u\|_{L^2(\Gamma_h(t))}.
\end{aligned} \tag{3.5.14}$$

We apply a Young's inequality to find that

$$\begin{aligned}
&\varepsilon\frac{\mathrm{d}}{\mathrm{d}t}\left\|\theta^u\right\|^2_{L^2(\Gamma_h(t))}+\left\|\theta^w\right\|^2_{L^2(\Gamma_h(t))}\\
&\quad\leq\frac{1}{\varepsilon^2}\left\|\theta^u\right\|^2_{L^2(\Gamma_h(t))}+c\varepsilon\left\|\nabla_{\Gamma_h}\theta^u\right\|^2_{L^2(\Gamma_h(t))}\\
&\qquad+\frac{ch^4}{\varepsilon^2}\big(\left\|\partial^\bullet u\right\|^2_{H^2(\Gamma(t))}+\left\|u\right\|^2_{H^2(\Gamma(t))}+\left\|w\right\|^2_{H^2(\Gamma(t))}\big).
\end{aligned}\tag{3.5.15}$$

Next, in order to bound the $\nabla_{\Gamma_h}\theta^u$ term in the previous equation, we test (3.5.8) with θ^u. Using Lemmas 3.3.18 and 3.5.4 and the L^∞ bound on u and U_h, we have for some $\delta>0$,

$$\begin{aligned}
\varepsilon a_h(\theta^u,\theta^u)&=m(\theta^w,\theta^u)-\frac{1}{\varepsilon}m_h(\psi'(\Pi_h u)-\psi'(U_h),\theta^u)+E_4(\theta^u)+E_5(\theta^u)\\
&\leq c\frac{1}{\varepsilon}\left\|\theta^u\right\|^2_{L^2(\Gamma_h(t))}+\left\|\theta^w\right\|_{L^2(\Gamma_h(t))}\left\|\theta^u\right\|_{L^2(\Gamma_h(t))}\\
&\qquad+c\frac{h^2}{\varepsilon}\big(\left\|u\right\|_{H^2(\Gamma(t))}+\left\|w\right\|_{H^2(\Gamma(t))}\big)\left\|\theta^u\right\|_{L^2(\Gamma_h(t))}\\
&\leq c\frac{1}{\varepsilon}\left\|\theta^u\right\|^2_{L^2(\Gamma_h(t))}+\delta\left\|\theta^w\right\|^2_{L^2(\Gamma(t))}\\
&\qquad+c\frac{h^4}{\varepsilon^2}\big(\left\|u\right\|^2_{H^2(\Gamma(t))}+\left\|w\right\|^2_{H^2(\Gamma(t))}\big).
\end{aligned}\tag{3.5.16}$$

Applying this bound in the right-hand side of (3.5.15), we may choose δ small enough so that

$$\begin{aligned}
&\varepsilon\frac{\mathrm{d}}{\mathrm{d}t}\left\|\theta^u\right\|^2_{L^2(\Gamma_h(t))}+\left\|\theta^w\right\|^2_{L^2(\Gamma_h(t))}\\
&\quad\leq c\frac{1}{\varepsilon}\left\|\theta^u\right\|^2_{L^2(\Gamma_h(t))}+c\frac{h^4}{\varepsilon^2}\big(\left\|\partial^\bullet u\right\|^2_{H^2(\Gamma(t))}+\left\|u\right\|^2_{H^2(\Gamma(t))}+\left\|w\right\|^2_{H^2(\Gamma(t))}\big).
\end{aligned}\tag{3.5.17}$$

We recall from (3.5.2): $U_{h,0}=\Pi_h u_0$, hence we have that $\theta^u|_{t=0}=\Pi_h u_0-U_{h,0}=0$. Applying a Gronwall inequality and integrating in time gives the following bounds on θ^u and θ^w:

$$\varepsilon\sup_{t\in(0,T)}\left\|\theta^u\right\|^2_{L^2(\Gamma_h(t))}+\int_0^T\left\|\theta^w\right\|^2_{L^2(\Gamma_h(t))}\,\mathrm{d}t\leq Ch^4,\tag{3.5.18}$$

with $C=C(u,w,\varepsilon,T)$ given by

$$C=c_\varepsilon\int_0^T\big(\left\|\partial^\bullet u\right\|^2_{H^2(\Gamma(t))}+\left\|u\right\|^2_{H^2(\Gamma(t))}+\left\|w\right\|^2_{H^2(\Gamma(t))}\big)\,\mathrm{d}t.$$

Proof of Theorem 3.5.1. The previous bound can then be combined with the bounds

on ρ^u and ρ^w from Lemma 3.3.18 to give the result:

$$\begin{aligned}
&\varepsilon \sup_{t\in(0,T)} \left\|u^{-\ell} - U_h\right\|^2_{L^2(\Gamma_h(t))} + \int_0^T \left\|w^{-\ell} - W_h\right\|^2_{L^2(\Gamma_h(t))} \,\mathrm{d}t \\
&\quad \leq \varepsilon \sup_{t\in(0,T)} \|\rho^u\|^2_{L^2(\Gamma_h(t))} + \int_0^T \|\rho^u\|^2_{L^2(\Gamma_h(t))} \,\mathrm{d}t \\
&\qquad + \varepsilon \sup_{t\in(0,T)} \|\theta^u\|^2_{L^2(\Gamma_h(t))} + \int_0^T \|\theta^u\|^2_{L^2(\Gamma_h(t))} \,\mathrm{d}t \\
&\quad \leq ch^4 \left(\varepsilon \sup_{t\in(0,T)} \|u\|^2_{H^2(\Gamma(t))} + \int_0^T \|w\|^2_{H^2(\Gamma(t))} \,\mathrm{d}t \right) \\
&\qquad + c_\varepsilon h^4 \int_0^T \left(\|\partial^\bullet u\|^2_{H^2(\Gamma(t))} + \|u\|^2_{H^2(\Gamma(t))} + \|w\|^2_{H^2(\Gamma(t))} \right) \mathrm{d}t. \qquad \square
\end{aligned}$$

3.6 Numerical results

The above finite element method discretised in time using semi-implicit time stepping. Given U_0 and a partition of time $0 = t_0, t_1, \ldots, t_M = T$, for $k = 0, \ldots, M-1$, we find (U_{k+1}, W_{k+1}) as the solution the matrix system

$$\begin{aligned}
\mathcal{M}(t_{k+1})U_{k+1} + (t_{k+1} - t_k)\mathcal{S}(t_{k+1})W_{k+1} &= \mathcal{M}(t_k)U_k \\
\varepsilon\mathcal{S}(t_{k+1})U_{k+1} - \mathcal{M}(t_{k+1})W_{k+1} &= -\frac{1}{\varepsilon}\Psi(U_k).
\end{aligned}$$

Full analysis of the fully discrete problem is left to future work. Based on ideas from Dziuk and Elliott (2012), we expect stability subject to $\tau < \varepsilon$ and convergence rate order $\tau + h^2$ for the discrete version of the norms in Theorem 3.5.1.

The method was implemented using the ALBERTA finite element toolbox (Schmidt et al. 2005) and the full block linear system solved using a direct solver.

3.6.1 Fourth-order linear problem

We start by showing the derived orders of convergence can be achieved for a fourth order linear problem. We calculate with $\psi \equiv 0$ and choose $\varepsilon = 0.1$. We couple $\tau \approx h^2$ to ensure we see the full order of convergence. The surface is given by $\Gamma(t) = \{x \in \mathbb{R}^3 : \Phi(x,t) = 0\}$ with

$$\Phi(x,t) = \frac{x_1^2}{a(t)} + x_2^2 + x_3^2 - 1. \tag{3.6.1}$$

We have chosen $a(t) = 1.0 + 0.25\sin(10\pi t)$ and solve for $t \in (0, 0.1)$. The exact solution is given by $u(x,t) = e^{-6t}x_1x_2$, where right hand side f is calculated from

$$f = u_t + v \cdot \nabla u + u\nabla_\Gamma \cdot v + \varepsilon\Delta_\Gamma^2 u.$$

The convergence is shown in Table 3.1 for the errors in the L^2 norm. The experimental order of convergence (eoc) is calculated via the formula (A.7.1). The results for the H^1 norm are not shown here, however we observe first order convergence in h.

h	$\left\|u^{-\ell} - U_h\right\|_{L^2(\Gamma_h(T))}$	(eoc)
$5.564983 \cdot 10^{-1}$	$9.424750 \cdot 10^{-3}$	—
$2.866409 \cdot 10^{-1}$	$3.001764 \cdot 10^{-3}$	1.724571
$1.443332 \cdot 10^{-1}$	$8.068147 \cdot 10^{-4}$	1.914955
$7.229393 \cdot 10^{-2}$	$2.033971 \cdot 10^{-4}$	1.993007

h	$\left\|w^{-\ell} - W_h\right\|_{L^2(\Gamma_h(T))}$	(eoc)
$5.564983 \cdot 10^{-1}$	$4.796888 \cdot 10^{-3}$	—
$2.866409 \cdot 10^{-1}$	$1.432177 \cdot 10^{-3}$	1.821993
$1.443332 \cdot 10^{-1}$	$3.824468 \cdot 10^{-4}$	1.924429
$7.229393 \cdot 10^{-2}$	$9.651516 \cdot 10^{-5}$	1.991496

Table 3.1: Error table of the solution of a fourth-order linear problem with surface defined by (3.6.1).

3.6.2 Cahn-Hilliard equation on a periodically evolving surface

In this example, we consider the same surface as above but now with the full nonlinearity as considered in the above analysis over the time interval $t \in (0, 0.8)$.

The initial condition for the simulations was the interpolant of a small perturbation about zero given by

$$u_0(x,y,z) = 0.1\cos(2\pi x)\cos(2\pi y)\cos(2\pi z).$$

We present two plots to show the behaviour of the numerical solution. First, in Figure 3.6.1, we see that for short times we have good convergence of the solution. The second, Figure 3.6.2, demonstrates that the energy does not decrease

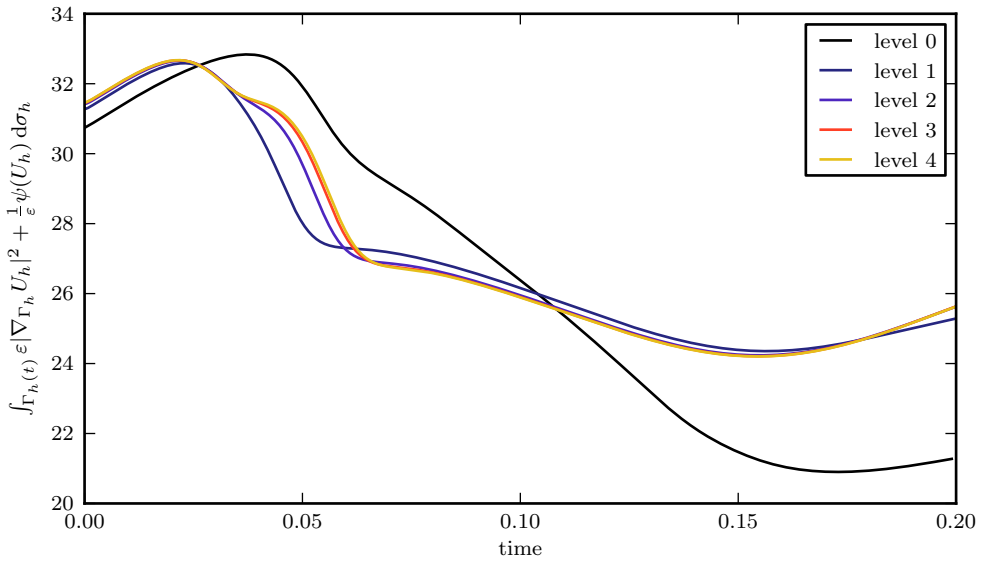

Figure 3.6.1: A plot of the Ginzburg-Landau energy over five levels of refinement.

monotonically along solutions. Running for a longer time suggests that the solution converges to a time periodic solution. We show a plot of the solution at level 2 at different times in Figure 3.6.3. The system is solved with a fixed time step of 10^{-4}.

3.6.3 Examples on other surfaces

We show the flexibility of the method with two other examples with larger surface deformation. In both cases the initial condition is taken to be a small random perturbation about zero.

First, we take a surface given by the level set function

$$\Phi(x,t) = x_1^2 + x_2^2 + a(t)^2 G(x_3^2/L(t)) - a(t)^2, \tag{3.6.2}$$

where

$$\begin{aligned} G(s) &= 200s(s - 199/100) \\ a(t) &= 0.1 + 0.05\sin(2\pi t) \\ L(t) &= 1 + 0.2\sin(4\pi t). \end{aligned}$$

In addition, we will prescribe a tangential velocity so that we will consider points

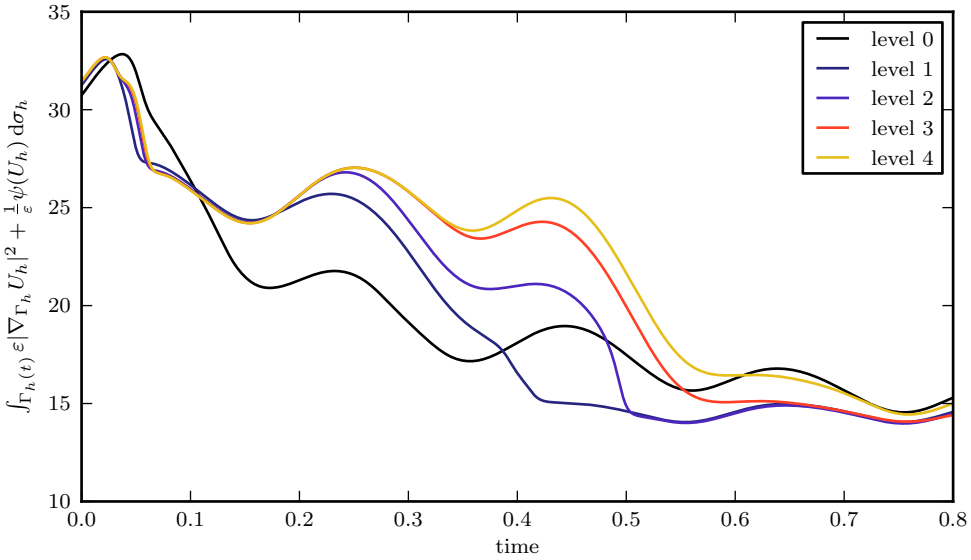

Figure 3.6.2: A plot of the Ginzburg-Landau energy over five levels of refinement over a longer time interval.

moving according to

$$X(t) = \left(X_1(0)\frac{a(t)}{a(0)}, X_2(0)\frac{a(t)}{a(0)}, X_3(0)\frac{L(t)}{L(0)} \right).$$

We plot the solution at different times in Figure 3.6.4. In particular, we notice that under this flow the nodes remain uniformly distributed.

Secondly, we consider a surface given in parametric form by

$$\begin{aligned} X(t) = \Big(& 2X_1(0) + t(1.5\tan^{-1}(1000X_1(0) + 0.5))X_1(0), \\ & R\big(t, |X_1(0)|, \sqrt{X_2(0)^2 + X_3(0)^2}\big)X_2(0), \\ & R\big(t, |X_1(0)|, \sqrt{X_2(0)^2 + X_3(0)^2}\big)X_3(0)\Big), \end{aligned} \tag{3.6.3}$$

where

$$R(t, r_1, r_2) = \exp(-2t)r_2 + (1 - \exp(-2t)((1 - r_1)^2(0.05 + r_1^2 + r_1^2\sqrt{1 - r_1^2})).$$

We plot the mesh and solution at different times in Figure 3.6.5.

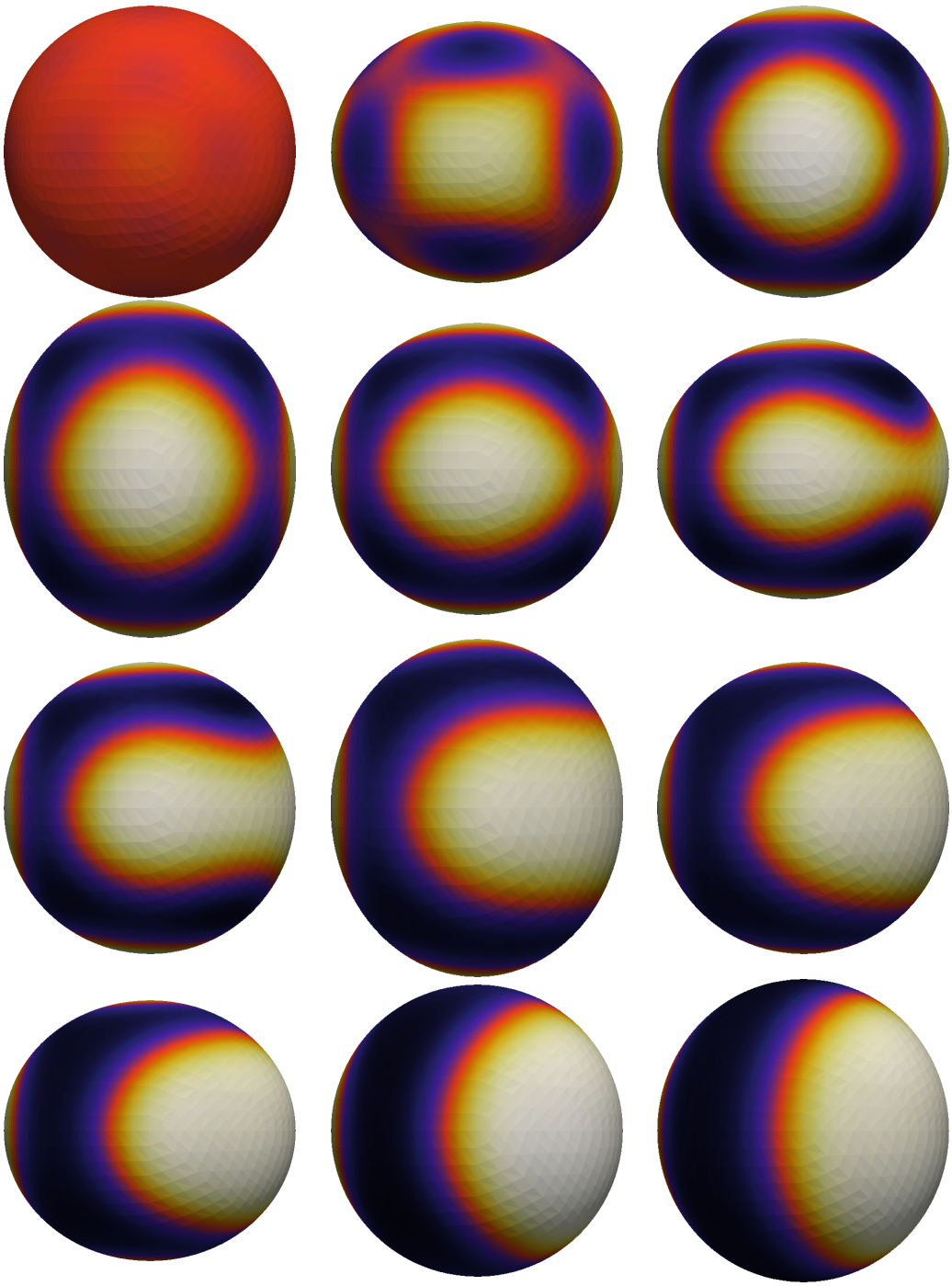

Figure 3.6.3: Plot of the solution of the Cahn-Hilliard equation at level two for time $t = 0.0, 0.05, 0.1, 0.15, 0.2, 0.25, 0.3, 0.35, 0.4, 0.45, 0.5, 1.0$. The colour scheme represents values between -1 and 1.

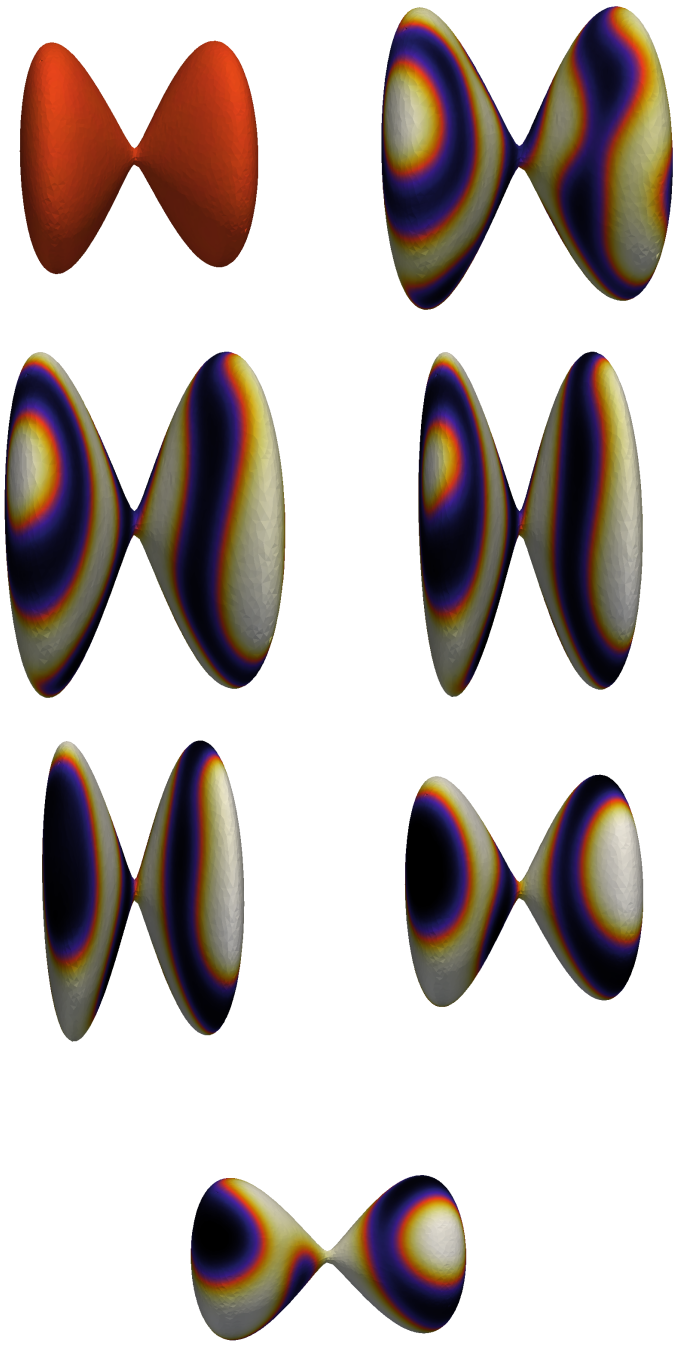

Figure 3.6.4: Plot of the solution on the surface defined by (3.6.2) at times $t = 0, 0.1, 0.2, 0.3, 0.4, 0.5, 0.6$.

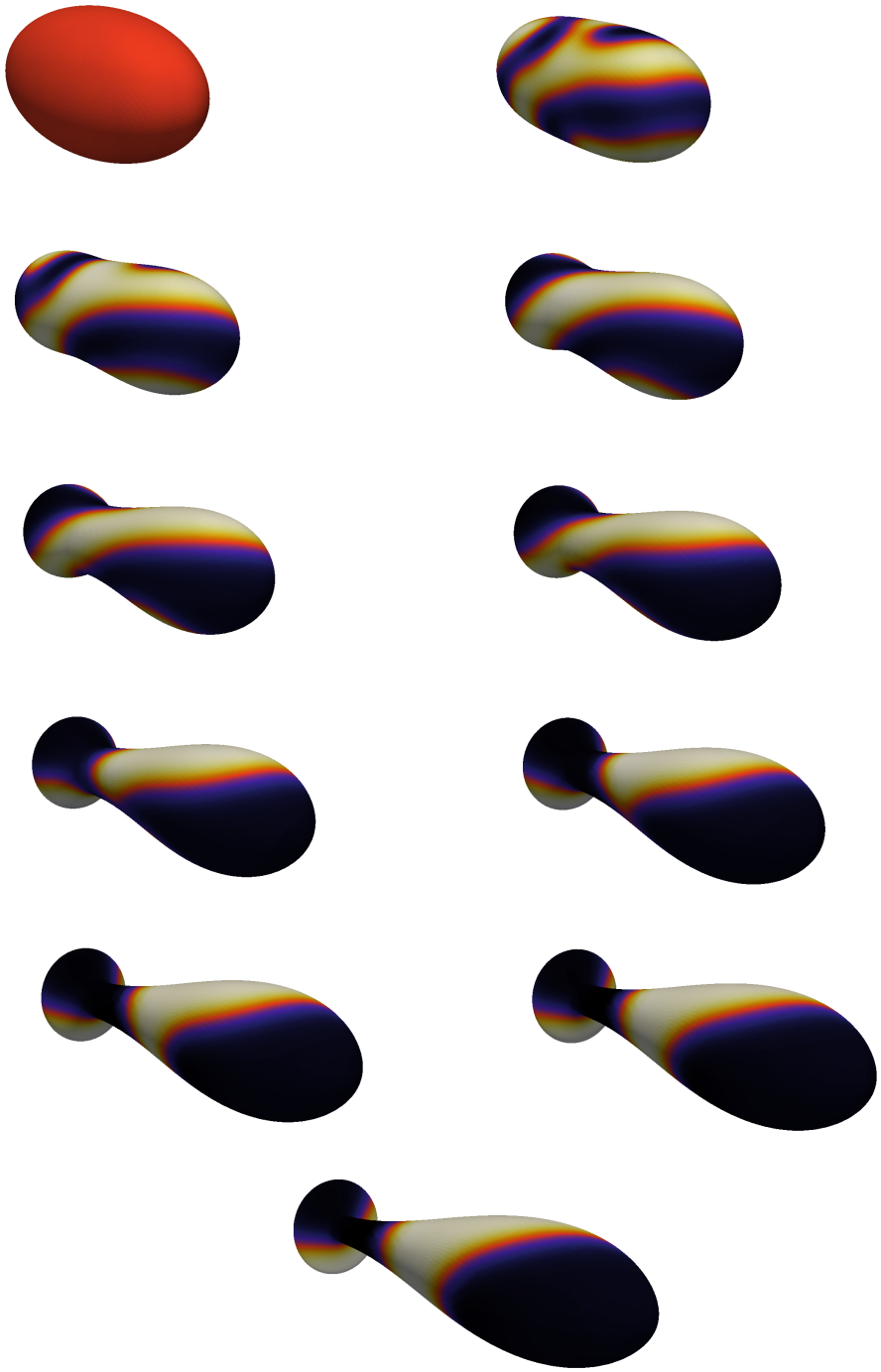

Figure 3.6.5: Plot of the solution on the surface defined by (3.6.3) at times $t = 0, 0.1, 0.2, 0.3, 0.4, 0.5, 0.6, 0.7, 0.8, 0.9, 1.0$. This example has a large surface deformation, which leads to degenerate triangles. However, the method is still stable enough to continue the calculations.

Chapter 4

Unfitted finite element methods for surface partial differential equations

4.1 Introduction

For the final method that we present, we assume that we are given an implicit representation of a surface as a solution to a geometric equation via a level set or phase field method. The methods described in the previous chapters all are based on the idea of using a polyhedral approximation of the surface as the computational domain. They rely on the assumption that the approximation consists of a quasi-uniform triangulation, which in practice may be difficult to construct. In particular, in the context of evolving surfaces, meshes can lose their quality and re-meshing may be required, see Eilks and Elliott (2008); Elliott and Stinner (2013) for example. Here, in this chapter, we propose using the implicit representation combined with a volumetric finite element space to avoid such difficulties. We aim to ensure that our methods also behave optimally efficiently and accurately with respect to the dimension of the surface.

We propose two different unfitted finite element methods to solve a Poisson equation: Let Γ be a smooth n-dimensional hypersurface in $\mathbb{R}^{n+1}$ and $f \in L^2(\Gamma)$; we seek solutions $u\colon \Gamma \to \mathbb{R}$ of

$$-\Delta_\Gamma u + u = f \quad \text{on } \Gamma. \tag{4.1.1}$$

Both methods use a bulk regular triangulation of an ambient domain and

perform calculations on an approximation of either the surface or a narrow band around the surface. In general, the induced mesh, the restriction of the outer mesh to the computational domain, will not be regular. We study these methods analytically and computationally.

4.1.1 Unfitted finite element methods for surface partial differential equations

This work builds on the previous studies of Olshanskii et al. (2009) and Deckelnick et al. (2010). The methods for the Poisson equation presented in this chapter can be seen as the same as those mentioned except we exchange the tangential, or projected, gradient for the full gradient; this overcomes the degeneracy often faced by implicit methods. Our methods also have similarities to the closest point method; see Ruuth and Merriman (2008) for example. The methods in this chapter can be related to phase field methods (Rätz and Voigt 2006) with the smooth profile of the phase field variable replaced by either a Dirac-delta function located on an approximation of the surface or the characteristic function of a narrow band about the surface.

This method presented here could easily be combined with unfitted finite element methods for elliptic problems in bulk domains presented by Barrett and Elliott (1984) to solve the coupled bulk-surface problem from Chapter 2. Many of the analytic tools in this chapter could be used to give a similar convergence result also.

4.1.2 Outline of chapter

We start this chapter by describing, mathematically, the computational domains used in this chapter and some basic properties and how these approximate the surface. In the third section, we describe and analyse both the sharp interface and narrow band methods for calculating solutions to a Poisson equation on a surface. Next, we present numerical experiments showing the convergence and efficiency of the methods for the Poisson equation. The chapter concludes with suggestions of future work in which we hope to solve a partial differential equation posed on an evolving surface.

4.2 Preliminaries

In this chapter, we will use the notation from Appendix A. In particular, there exists a narrow band $U := \{x \in \mathbb{R}^{n+1} : |d(x)| < \delta_\Gamma\}$ as the domain of the closest

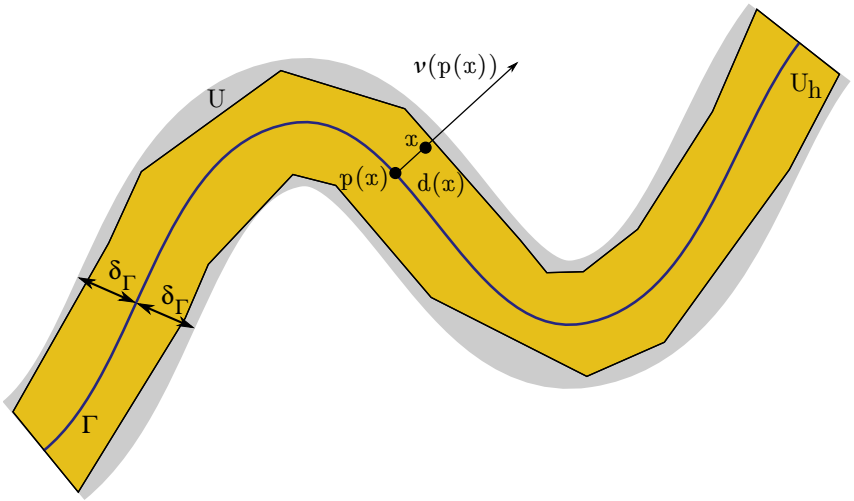

Figure 4.2.1: A sketch of a section of the polyhedral narrow band U_h about the surface.

point operator $p\colon U \to \Gamma$ given by

$$x = p(x) + d(x)\nu(p(x)) \quad \text{for } x \in U. \tag{4.2.1}$$

This allows the choice of extension of a function $z\colon \Gamma \to \mathbb{R}$ defined implicitly by

$$z^e(x) := z(p(x)) \quad \text{for } x \in U. \tag{4.2.2}$$

This notation represents that z is extended constantly in the normal direction to the surface. Denoting by $\nu(x) = \nabla d(x)$ and by $\mathcal{H}(x) = \nabla^2 d(x)$ the Hessian of d, we can calculate

$$\nabla z^e(x) = (\mathrm{Id} - d(x)\mathcal{H}(x))\nabla_\Gamma z(p(x)) \quad \text{for } x \in U, \tag{4.2.3}$$

and

$$\begin{aligned} &z^e_{x_i,x_j}(x) \\ &= \sum_{k,l=1}^{n+1} \underline{D}_l \underline{D}_k z(p(x))(\delta_{ik} - \nu_i(x)\nu_k(x) - d(x)\mathcal{H}_{ik}(x))(\delta_{jl} - \nu_j(x)\nu_l(x) - d(x)\mathcal{H}_{jl}(x)) \\ &\quad - \sum_{k=1}^{n+1} \underline{D}_k z(p(x))(\nu_i(x)\mathcal{H}_{jk}(x) + \nu_j(x)\mathcal{H}_{ik}(x) + d(x)\mathcal{H}_{ik,x_j}(x)) \end{aligned} \tag{4.2.4}$$

for $x \in U$ and $i, j = 1, \ldots, n+1$.

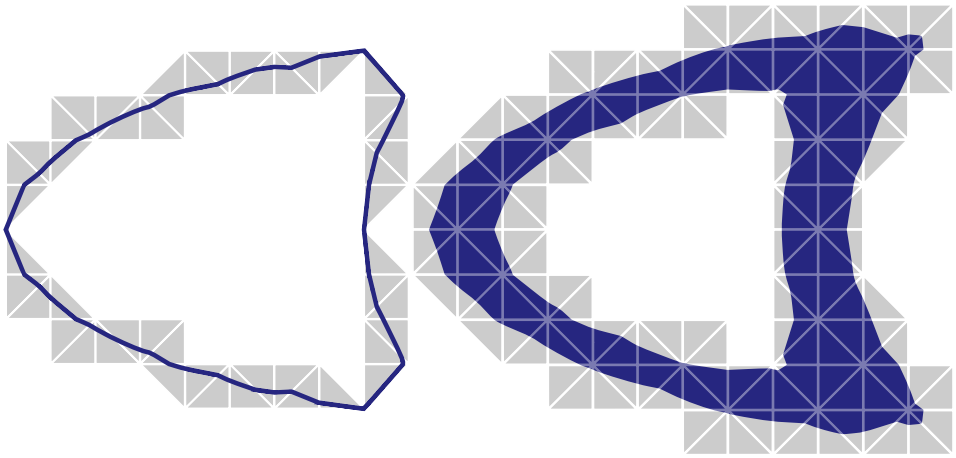

Figure 4.2.2: An example of the computational domains Γ_h and D_h.

For the remainder of this chapter, we will use a polyhedral domain $U_h \subset U$; see Figure 4.2.1 for example. Let $\mathscr{T}_h$ be a regular triangulation (Definition A.3.1) of U_h consisting of closed simplices T. We denote by $h := \max_{T \in \mathscr{T}_h} h(T)$, where $h(T) = \operatorname{diam}(T)$. We will write X_h for the finite element space of piecewise linear functions over U_h:

$$X_h := \{\phi_h \in C^0(\bar{U}_h) : \phi_h|_T \in P_1(T), T \in \mathscr{T}_h\},$$

and by $I_h \colon C^0(\bar{U}_h) \to X_h$ the usual Lagrange interpolation operator. We have

$$\|f - I_h f\|_{W^{k,p}(T)} \leq c h(T)^{2-k} \|f\|_{W^{2,p}(T)} \qquad \text{for } T \in \mathscr{T}_h, \tag{4.2.5}$$

for $k = 0, 1$ and $1 \leq p \leq \infty$. In particular, for the distance function we have

$$\|d - I_h d\|_{L^\infty(U_h)} + h \|\nabla(d - I_h d)\|_{L^\infty(U_h)} \leq c h^2. \tag{4.2.6}$$

Let us next define our computational domains by

$$\Gamma_h := \{x \in U_h : I_h d(x) = 0\}$$
$$D_h := \{x \in U_h : |I_h d(x)| < h\},$$

as approximations of the given hypersurface Γ; see Figure 4.2.2 for example. We will denote by ν_h the unit normal to Γ_h, which can be extended to U_h by

$$\nu_h(x) = \frac{\nabla I_h d(x)}{|\nabla I_h d(x)|} \qquad \text{for } x \in U_h.$$

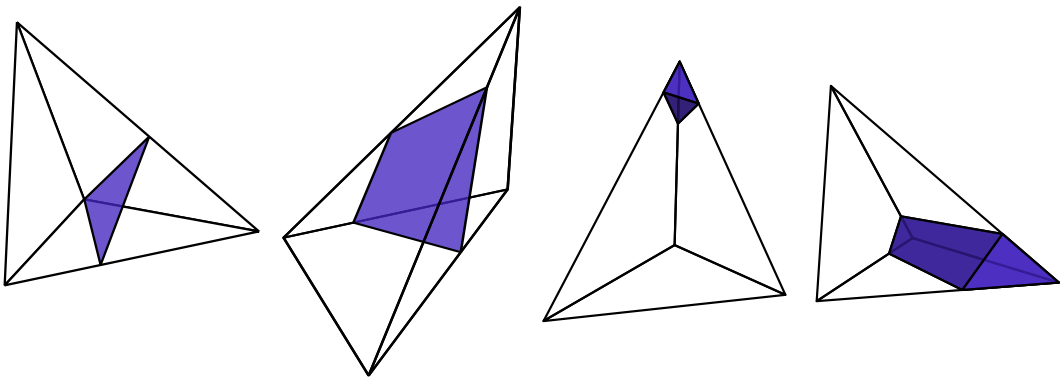

Figure 4.2.3: Examples of intersections of $\Gamma_h \cap T$ (left two plots) and $D_h \cap T$ (right two images).

Note that Γ_h is a polygon whose facets are line segments if $n = 1$ and polyhedral surface whose facets consist of triangles or quadrilaterals if $n = 2$. The corresponding decomposition of Γ_h is in general not shape-regular and can have arbitrarily small elements. Similarly, D_h is composed of various polygons if $n = 1$ and polyhedra if $n = 2$. Examples of different possible intersections of $T \cap \Gamma_h$ or $T \cap D_h$ are given in Figure 4.2.3.

Furthermore, we introduce $F_h \colon U_h \to \mathbb{R}^{n+1}$ by

$$F_h(x) := p(x) + I_h d(x)\nu(p(x)) \quad \text{for } x \in U_h.$$

Since the decomposition (4.2.1) is unique, we can immediately see that

$$p(F_h(x)) = p(x) \quad \text{and} \quad d(F_h(x)) = I_h d(x) \quad \text{for } x \in U_h. \tag{4.2.7}$$

In view of (4.2.1), we can write

$$F_h(x) = x + \eta_h(x)\nu(x) \quad \text{for } x \in U_h, \quad \text{where } \eta_h(x) = I_h d(x) - d(x), \tag{4.2.8}$$

and, for $i, j = 1, \dots, n+1$,

$$\partial_{x_j}(F_h(x))_i = \delta_{ij} + (\eta_h(x))_{x_j}\nu_i(x) + \eta_h(x)\mathcal{H}_{ij}(x) \quad \text{for } x \in U_h. \tag{4.2.9}$$

We infer from (4.2.6) that F_h is bi-Lipschitz (Lipschitz with Lipschitz inverse) for small h and that

$$\|F_h - \mathrm{Id}\|_{L^\infty(U_h)} + h\,\|\nabla F_h - \mathrm{Id}\|_{L^\infty(U_h)} \le ch^2. \tag{4.2.10}$$

Note that in particular, we have

$$F_h(\Gamma_h) = \Gamma \quad \text{and} \quad F_h(D_h) = D^h := \{x \in U_h : |d(x)| < h\}.$$

Given a function $\phi_h \colon \Gamma_h \to \mathbb{R}$, we denote by $\phi_h^\ell(p(x)) := \phi_h(F_h^{-1}(x))$ the lift of ϕ_h. We see that

$$(\phi_h^\ell)^e(x) = \phi_h^\ell(p(x)) = \phi_h(F_h^{-1}(p(x))) = \phi_h(x) \quad \text{for } x \in \Gamma_h, \tag{4.2.11}$$

since $F_h(x) = p(x)$ for $x \in \Gamma_h$. Finally, we denote by μ_h the quotient of measures on Γ and Γ_h so that $\mathrm{d}\sigma = \mu_h \, \mathrm{d}\sigma_h$. The proof of the equivalent result (A.5.2) can be easily adapted to show:

$$\sup_{\Gamma_h} |1 - \mu_h| \leq ch^2. \tag{4.2.12}$$

Using the properties of F_h together with the coarea formula and (4.2.3, 4.2.4) one can prove the following result on the equivalence of certain norms.

Lemma 4.2.1. *There exist constants $c_1, c_2 > 0$, which are independent of h, such that for all $z \in H^1(\Gamma)$,*

$$c_1 \|z^e\|_{L^2(\Gamma_h)} \leq \|z\|_{L^2(\Gamma)} \leq c_2 \|z^e\|_{L^2(\Gamma_h)} \tag{4.2.13a}$$

$$c_1 \frac{1}{\sqrt{h}} \|z^e\|_{L^2(D_h)} \leq \|z\|_{L^2(\Gamma)} \leq c_2 \frac{1}{\sqrt{h}} \|z^e\|_{L^2(D_h)} \tag{4.2.13b}$$

$$c_1 \|\nabla z^e\|_{L^2(\Gamma_h)} \leq \|\nabla_\Gamma z\|_{L^2(\Gamma)} \leq c_2 \|\nabla z^e\|_{L^2(\Gamma_h)} \tag{4.2.13c}$$

$$c_1 \frac{1}{\sqrt{h}} \|\nabla z^e\|_{L^2(D_h)} \leq \|\nabla_\Gamma z\|_{L^2(\Gamma)} \leq c_2 \frac{1}{\sqrt{h}} \|\nabla z^e\|_{L^2(D_h)}. \tag{4.2.13d}$$

If, in addition, $z \in H^2(\Gamma)$, then

$$c_1 \frac{1}{\sqrt{h}} \left\|\nabla^2 z^e\right\|_{L^2(D_h)} \leq \|z\|_{H^2(\Gamma)}. \tag{4.2.14}$$

Proof. This follows a similar proof as (A.5.2).

For the sharp interface norms, we use the identity:

$$\int_{\Gamma_h} (z^e)^2 \mu_h \, \mathrm{d}\sigma_h = \int_\Gamma z^2 \, \mathrm{d}\sigma.$$

By (4.2.3):

$$\int_{\Gamma_h} |\nabla z^e|^2 \, \mu_h \, \mathrm{d}\sigma_h = \int_\Gamma |(\mathrm{Id} - d\mathcal{H})\nabla_\Gamma z|^2 \, \mathrm{d}\sigma.$$

For the narrow band integrals, following the result of Olshanskii et al. (2009, Lemma 3.2),

define:

$$\lambda(x) := \prod_{j=1}^{n} (1 - d(x)\kappa_j(x)) \quad \text{for } x \in U_h,$$

where κ_j is an extension of a principal curvature of Γ given by:

$$\kappa_j(x) = \frac{\kappa_j(p(x))}{1 + d(x)\kappa_j(p(x))} \quad \text{for } x \in U_h \quad \text{and } j = 1, \dots, n.$$

Then, using (4.2.1), we have

$$\int_{D_h} (z^e)^2 \lambda \, \mathrm{d}x = \int_{-h}^{h} \int_{\Gamma} z^e (p + r\nu(p))^2 \, \mathrm{d}\sigma(p) \, \mathrm{d}r.$$

The bounds are then completed using (4.2.6) and (4.2.12). □

Our approximations will be based on a weak form of (4.1.1): Find $u \in H^1(\Gamma)$ such that

$$a(u, \varphi) = l(\varphi) \quad \text{for all } \varphi \in H^1(\Gamma), \tag{4.2.15}$$

where

$$a(w, \varphi) = \int_{\Gamma} \nabla_\Gamma w \cdot \nabla_\Gamma \varphi + w\varphi \, \mathrm{d}\sigma \quad \text{and} \quad l(\varphi) = \int_{\Gamma} f\varphi \, \mathrm{d}\sigma.$$

We recall from Theorem A.2.5 that for every $f \in L^2(\Gamma)$ there exists a unique solution $u \in H^2(\Gamma)$ of (4.2.15), which satisfies the bound

$$\|u\|_{H^2(\Gamma)} \leq c \|f\|_{L^2(\Gamma)}. \tag{4.2.16}$$

We finish this section with an abstract error estimate, similar to Lemma A.4.1, which we shall use later in order to analyse our schemes. Let V_h be a finite-dimensional space and $V^e := \{v^e : v \in H^1(\Gamma)\}$. Suppose that $a_h \colon (V_h + V^e) \times (V_h + V^e) \to \mathbb{R}$ is a symmetric positive semi-definite bilinear form, which is in addition positive definite on $V_h \times V_h$. Furthermore, let $l_h \colon V_h \to \mathbb{R}$ be linear. Then the approximate problem,

$$a_h(u_h, v_h) = l_h(v_h) \quad \text{for all } v_h \in V_h, \tag{4.2.17}$$

has a unique solution $u_h \in V_h$. Introducing the energy norm,

$$\|v\|_h := \sqrt{a_h(v, v)} \quad \text{for } v \in V_h + V^e,$$

we have by Strang's second lemma

$$\|u^e - u_h\|_h \leq 2 \inf_{v_h \in V_h} \|u^e - v_h\|_h + \sup_{\phi_h \in V_h} \frac{|a_h(u^e, \phi_h) - l_h(\phi_h)|}{\|\phi_h\|_h}. \tag{4.2.18}$$

In the following section, we shall present three different choices of a_h and l_h (two new methods plus that of Olshanskii et al. (2009)) along with the corresponding analysis of the resulting schemes.

4.3 Description and analysis of the methods

4.3.1 Method 1: Sharp interface method

We define

$$\widetilde{\mathscr{T}_h^I} := \{T \in \mathscr{T}_h : \mathscr{H}^n(T \cap \Gamma_h) > 0\}.$$

Let us observe that if $T \in \mathscr{T}_h$ satisfies $\mathscr{H}^n(T \cap \Gamma_h) > 0$, for $\mathscr{H}^n$ the n-dimensional Hausdorff measure, the following two cases can occur:

(a) $\text{int}(T) \cap \Gamma_h \neq \emptyset$, in which case $\mathscr{H}^n(\partial T \cap \Gamma_h) = 0$;

(b) $T \cap \Gamma_h = \partial T \cap \Gamma_h$, in which case $T \cap \Gamma_h$ is the face between two elements.

In case (b), we make a fixed, but arbitrary, choice of one of the two elements to be included and remove the other. We define our computational triangulation $\mathscr{T}_h^I$ by

$$\mathscr{T}_h^I := \left\{ T \in \widetilde{\mathscr{T}_h^I} : T \text{ has not been disregarded because of (b)} \right\}.$$

We may therefore conclude that there exists a set $N \subset \Gamma_h$, consisting of the intersection of the boundary of elements with Γ_h, with $\mathscr{H}^n(N) = 0$ such that every $x \in \Gamma_h \setminus N$ belongs to exactly one $T \in \mathscr{T}_h^I$. We then define

$$U_h^I := \bigcup_{T \in \mathscr{T}_h^I} T.$$

Clearly, $U_h^I \subseteq U_h$ provided that h is small enough. An example of this construction over four levels of refinement is given in Figure 4.3.1.

We define the finite element space V_h by

$$V_h := \{\phi_h \in C^0(U_h^I) : \phi_h|_T \in P_1(T) \text{ for each } T \in \mathscr{T}_h^I\}.$$

Note that for $\phi_h \in V_h$, $\nabla \phi_h$ is uniquely defined on $\Gamma_h \setminus N$ in view of the definition $\mathscr{T}_h^I$.

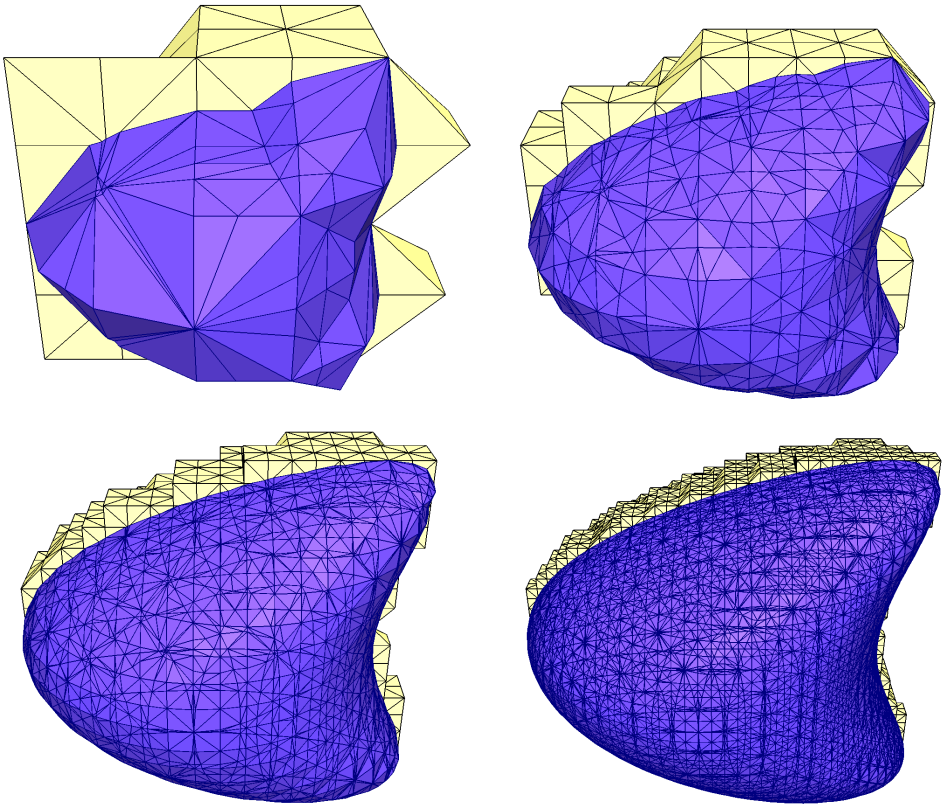

Figure 4.3.1: The computational domain for the sharp interface method using the level set function $\Phi(x, y, z) = (x - z^2)^2 + y^2 + z^2 - 1$. The blue half of the surface shows the induced triangulation on Γ_h and the off white section shows the underlying triangulation $\mathscr{T}_h^I$.

The finite element problem is (4.2.17): Find $u_h \in V_h$ such that

$$a_h(u_h, \phi_h) = l_h(\phi_h) \quad \text{for all } \phi_h \in V_h, \tag{4.3.1}$$

with

$$a_h(w_h, \phi_h) = \int_{\Gamma_h} \nabla w_h \cdot \nabla \phi_h + w_h \phi_h \, \mathrm{d}\sigma_h \quad \text{and} \quad l_h(\phi_h) = \int_{\Gamma_h} f^e \phi_h \, \mathrm{d}\sigma_h.$$

In order to verify that the symmetric bilinear form a_h is positive definite on $V_h \times V_h$ we note that $a_h(\phi_h, \phi_h) = 0$ implies that

$$\int_{\Gamma_h \cap T} |\nabla \phi_h|^2 + \phi_h^2 \, \mathrm{d}\sigma_h = 0 \quad \text{for all } T \in \mathscr{T}_h^I.$$

Since $\mathscr{H}^n(T \cap \Gamma_h) > 0$ for $T \in \mathscr{T}_h^I$, we infer that $\nabla \phi_h|_{T \cap \Gamma_h} = 0$ and $\phi_h|_{T \cap \Gamma_h} = 0$. The first equality implies that, since ϕ_h is piecewise linear, it takes a constant value on T and from the second, since ϕ_h is continuous on T, this value is 0. We deduce that $\phi_h = 0$ on T, for each $T \in \mathscr{T}_h^I$, hence $\phi_h = 0$ in U_h^I. The approximate problem (4.3.1) has a unique solution $u_h \in V_h$ which satisfies

$$\|u_h\|_h = \left(\|\nabla u_h\|^2_{L^2(\Gamma_h)} + \|u_h\|^2_{L^2(\Gamma_h)} \right)^{\frac{1}{2}} \leq c \, \|f\|_{L^2(\Gamma)} .$$

We require an interpolation estimate on Γ_h. Since $z \in H^2(\Gamma)$ we have $z^e \in C^0(U_h)$ so that $I_h z^e$ is well-defined.

Lemma 4.3.1. *Let $z \in H^2(\Gamma)$. Then*

$$\|z^e - I_h z^e\|_{L^2(\Gamma_h)} + h \, \|\nabla (z^e - I_h z^e)\|_{L^2(\Gamma_h)} \leq c h^2 \, \|z\|_{H^2(\Gamma)} . \tag{4.3.2}$$

Proof. We first observe that Theorem 3.7 in Olshanskii et al. (2009) yields

$$\|z^e - I_h z^e\|_{L^2(\Gamma_h)} + h \, \|\nabla_{\Gamma_h} (z^e - I_h z^e)\|_{L^2(\Gamma_h)} \leq c h^2 \, \|z\|_{H^2(\Gamma)} . \tag{4.3.3}$$

Hence, it remains to bound $\|\nabla (z^e - I_h z^e) \cdot \nu_h\|_{L^2(\Gamma_h)}$. To do so, we start by consid-

ering an element $T \in \mathscr{T}_h^I$. We see that

$$\begin{aligned}
&\int_{T\cap\Gamma_h} |\nabla(z^e - I_h z^e)\cdot\nu_h|^2 \,\mathrm{d}\sigma_h \\
&\quad\le 2\int_{T\cap\Gamma_h} |\nabla z^e\cdot\nu_h|^2 \,\mathrm{d}\sigma_h + 2\int_{T\cap\Gamma_h} |\nabla(I_h z^e)\cdot\nu_h|^2 \,\mathrm{d}\sigma_h \\
&\quad\le 2\int_{T\cap\Gamma_h} |\nabla z^e\cdot(\nu_h-\nu)|^2 \,\mathrm{d}\sigma_h + ch(T)^{-1}\int_T |\nabla(I_h z^e)\cdot\nu_h|^2 \,\mathrm{d}x =: I_1 + I_2,
\end{aligned}$$

since $\nabla z^e\cdot\nu = 0$ in U_h and $\mathscr{H}^n(T\cap\Gamma_h) \le ch(T)^{-1}\mathscr{H}^{n+1}(T)$. Note that by (4.2.6), we have

$$\|\nu-\nu_h\|_{L^\infty(T)} = \left\|\nabla d - \frac{\nabla I_h d}{|\nabla I_h d|}\right\|_{L^\infty(T)} \le ch(T) \tag{4.3.4}$$

so that

$$I_1 \le ch^2\int_{T\cap\Gamma_h} |\nabla z^e|^2 \,\mathrm{d}\sigma_h.$$

Furthermore, recalling (4.3.4) and (4.2.5) implies that

$$I_2 \le ch(T)^{-1}\int_T \left(|\nabla(I_h z^e - z^e)|^2 + |\nabla z^e\cdot(\nu_h-\nu)|^2\right)\mathrm{d}x \le ch\,\|z^e\|^2_{H^2(T)}.$$

We use the bounds for I_1 and I_2, then sum over all elements $T \in \mathscr{T}_h^I$ and apply Lemma 4.2.1 to see that

$$\int_{\Gamma_h} |\nabla(z^e - I_h z^e)\cdot\nu_h|^2 \,\mathrm{d}\sigma_h \le ch^2\,\|\nabla z^e\|^2_{L^2(\Gamma_h)} + ch\,\|z^e\|^2_{H^2(D_{2h})} \le ch^2\,\|z\|^2_{H^2(\Gamma)},$$

since $T \in D_{2h}$ for all $T \in \mathscr{T}_h^I$. □

Theorem 4.3.2. *Let u solve the Poisson equation (4.2.15) and let u_h be the solution of the finite element scheme (4.3.1). Then*

$$\|u^e - u_h\|_{L^2(\Gamma_h)} + h\,\|\nabla(u^e-u_h)\|_{L^2(\Gamma_h)} \le ch^2\,\|u\|_{H^2(\Gamma)}. \tag{4.3.5}$$

Proof. In view of the definition of $\|\cdot\|_h$, the Strang Lemma (4.2.18) and the approx-

imation property (Lemma 4.3.1), we have, for $e_h := u^e - u_h$,

$$\begin{aligned}
&\left(\|e_h\|^2_{L^2(\Gamma_h)} + \|\nabla e_h\|^2_{L^2(\Gamma_h)}\right)^{\frac{1}{2}} \\
&\quad \le 2\left(\|u^e - I_h u^e\|^2_{L^2(\Gamma_h)} + \|\nabla(u^e - I_h u^e)\|^2_{L^2(\Gamma_h)}\right)^{\frac{1}{2}} + \sup_{\phi_h \in V_h} \frac{|a_h(u^e, \phi_h) - l_h(\phi_h)|}{\|\phi_h\|_h} \\
&\quad \le ch\,\|u\|_{H^2(\Gamma)} + \sup_{\phi_h \in V_h} \frac{|a_h(u^e, \phi_h) - l_h(\phi_h)|}{\|\phi_h\|_h}.
\end{aligned}$$

In order to estimate the second term, we choose an arbitrary $\phi_h \in V_h$ and denote by $\varphi_h = \phi_h^\ell \in H^1(\Gamma)$ the corresponding lift. Then

$$a_h(u^e, \phi_h) - l_h(\phi_h) = \big(a_h(u^e, \phi_h) - a(u, \varphi_h)\big) + \big(l(\varphi_h) - l_h(\phi_h)\big) =: I_1 + I_2.$$

Using the transformation rule, (4.2.4) and (4.2.11) we obtain

$$\begin{aligned}
\int_\Gamma \nabla_\Gamma u \cdot \nabla_\Gamma \varphi_h + u\varphi_h \,\mathrm{d}\sigma &= \int_{\Gamma_h} \big((\nabla_\Gamma u) \circ p \cdot (\nabla_\Gamma \varphi_h) \circ p + (u \circ p)(\varphi_h \circ p)\big)\mu_h \,\mathrm{d}\sigma_h \\
&= \int_{\Gamma_h} \big((\mathrm{Id} - d\mathcal{H})^{-2}\nabla u^e \cdot \nabla \phi_h + u^e \varphi_h\big)\mu_h \,\mathrm{d}\sigma_h,
\end{aligned}$$

so that by (4.2.6) and (4.2.12)

$$\begin{aligned}
|I_1| &\le \int_{\Gamma_h} \left|(\mu_h(\mathrm{Id} - d\mathcal{H})^{-2} - \mathrm{Id})\nabla u^e \cdot \nabla \phi_h\right| \,\mathrm{d}\sigma_h + \int_{\Gamma_h} |(\mu_h - 1)u^e \phi_h| \,\mathrm{d}\sigma_h \\
&\le ch^2 \,\|u^e\|_h \,\|\phi_h\|_h \,.
\end{aligned}$$

Similarly, we can bound I_2 using (4.2.12) by

$$|I_2| \le \int_{\Gamma_h} |\mu_h - 1|\, f^e \phi_h \,\mathrm{d}\sigma_h \le ch^2 \,\|f\|_{L^2(\Gamma)} \,\|\phi_h\|_h \,.$$

As a result, we obtain

$$\sup_{\phi_h \in V_h} \frac{|a_h(u^e, \phi_h) - l_h(\phi_h)|}{\|\phi_h\|_h} \le ch^2 \,\|f\|_{L^2(\Gamma)} \,, \tag{4.3.6}$$

so that we have in conclusion

$$\|e_h\|_{L^2(\Gamma_h)} + \|\nabla e_h\|_{L^2(\Gamma_h)} \le ch \,\|f\|_{L^2(\Gamma)} \,. \tag{4.3.7}$$

In order to improve the L^2 error bound, we employ the usual Aubin-Nitsche

argument. Denote by $w \in H^2(\Gamma)$ the unique solution of the dual problem:

$$a(\varphi, w) = \int_\Gamma e_h^\ell \varphi \, \mathrm{d}\sigma \quad \text{for all } \varphi \in H^1(\Gamma),$$

which satisfies

$$\|w\|_{H^2(\Gamma)} \leq c \left\| e_h^\ell \right\|_{L^2(\Gamma)}. \tag{4.3.8}$$

We have

$$\begin{aligned} \left\| e_h^\ell \right\|_{L^2(\Gamma)}^2 &= a(e_h^\ell, w) \\ &= \big(a(e_h^\ell, w) - a_h(e_h, w^e)\big) + a_h(e_h, w^e - I_h w^e) \\ &\qquad + \big(a_h(u^e, I_h w^e) - l_h(I_h w^e)\big) \\ &=: I_1 + I_2 + I_3. \end{aligned} \tag{4.3.9}$$

As above, we deduce together with the energy norm bound (4.3.7) and the equivalence of norms (Lemma 4.2.1),

$$|I_1| \leq ch^2 \|e_h\|_h \|w^e\|_h \leq ch^3 \|f\|_{L^2(\Gamma)} \|w\|_{H^1(\Gamma)}.$$

Next, the finite element equation (4.3.1) and (4.3.7) imply

$$|I_2| \leq \|e_h\|_h \|w^e - I_h w^e\|_h \leq ch^2 \|f\|_{L^2(\Gamma)} \|w\|_{H^2(\Gamma)}.$$

Finally, our estimate of $\|d\|_{L^\infty(\Gamma_h)}$, (4.3.6), (4.3.1) and Lemma 4.2.1 yield

$$|I_3| \leq ch^2 \|f\|_{L^2(\Gamma)} \|I_h w^e\|_h \leq ch^2 \|f\|_{L^2(\Gamma)} \|w\|_{H^2(\Gamma)}.$$

Inserting the above estimates into (4.3.9) and recalling (4.3.8) we obtain

$$\left\| e_h^\ell \right\|_{L^2(\Gamma)} \leq ch^2 \|f\|_{L^2(\Gamma)},$$

which together with Lemma 4.2.1 gives the error bound in the L^2 norm. □

4.3.2 The sharp interface method of Olshanskii et al. (2009)

For completeness we include the original sharp interface method of Olshanskii et al. (2009). We compare the solution of our sharp interface method to this to see the effect of using full gradients.

The same geometric construction as in the previous section is used leading

to a triangulation $\mathscr{T}_h^I$ of a domain U_h^I about the surface Γ_h. We use the zero level set of $I_h d$ as the induced mesh Γ_h. The difference in the methods follows from our choice of full gradients in the bilinear for a_h. This method uses the same right-hand side l_h, but, instead, the bilinear form

$$a_h(w_h, \phi_h) = \int_{\Gamma_h} \nabla_{\Gamma_h} w_h \cdot \nabla_{\Gamma_h} \phi_h + w_h \phi_h \, \mathrm{d}\sigma_h,$$

where the tangential gradient ∇_{Γ_h} is calculated using the projection operator P_h so that

$$\nabla_{\Gamma_h} \phi_h := P_h \nabla \phi_h, \qquad P_h(x) := \mathrm{Id} - \nu_h(x) \otimes \nu_h(x) \quad \text{for } x \in \Gamma_h.$$

To ensure that this method is well-posed solutions are sought in the finite element space

$$W_h = \{\phi_h \in C(\Gamma_h) : \text{ there exists } \widetilde{\phi}_h \in V_h \text{ with } \widetilde{\phi}_h|_{\Gamma_h} = \phi_h\}.$$

This is an identification of the quotient space V_h with the equivalence of finite element functions equal in the norm induced by a_h. In realisations of the two sharp interface methods, the choice of W_h instead of V_h does not change the implementation since conjugate gradient iteration solves the resulting system of linear equations by considering the traces of the nodal basis of V_h as a spanning set for W_h.

The finite element method is: Find $u_h \in W_h$ such that

$$a_h(u_h, \phi_h) = l_h(\phi_h) \quad \text{for all } \phi_h \in W_h. \tag{4.3.10}$$

It is clear that a_h is positive definite over W_h hence there exists a unique solution to (4.3.10). Furthermore, the interpolation result (4.3.3) in Lemma 4.3.1 along with the reasoning in Theorem 4.3.2 give the following error estimate presented by Olshanskii et al. (2009):

Theorem 4.3.3. *Let u be the solution of (4.2.15) and u_h the solution of the finite element scheme (4.3.10); then*

$$\|u^e - u_h\|_{L^2(\Gamma_h)} + h \|\nabla_{\Gamma_h}(u^e - u_h)\|_{L^2(\Gamma_h)} \leq ch^2 \|u\|_{H^2(\Gamma)}. \tag{4.3.11}$$

Furthermore, analysis of the resulting linear algebraic system has been performed by Olshanskii and Reusken (2010). The authors show, in the case of a curve in two dimensions, that the (effective) spectral condition number of the diagonally scaled mass matrix and the diagonally scaled stiffness matrix behave like $h^{-3} |\log h|$ and $h^{-2} |\log h|$, respectively.

4.3.3 Method 2: Narrow-band method

Let us define the narrow-band triangulation by

$$\mathscr{T}_h^B := \{T \in \mathscr{T}_h : \mathscr{H}^{n+1}(T \cap D_h) > 0\}.$$

and the narrow band domain by

$$U_h^B := \bigcup_{T \in \mathscr{T}_h^B} T.$$

We define a finite element space V_h on the triangulation $\mathscr{T}_h^B$ by

$$V_h := \{\phi_h \in C^0(U_h^B) : \phi_h|_T \in P_1(T) \text{ for each } T \in \mathscr{T}_h^B\}.$$

The second finite element scheme is (4.2.17): Find $u_h \in V_h$ such that

$$a_h(u_h, \phi_h) = l_h(\phi_h) \quad \text{for all } \phi_h \in V_h, \tag{4.3.12}$$

with

$$a_h(w_h, \phi_h) = \frac{1}{2h}\int_{D_h} \nabla w_h \cdot \nabla \phi_h + w_h \phi_h \,\mathrm{d}x, \quad l_h(\phi_h) = \frac{1}{2h}\int_{D_h} f^e \phi_h \,\mathrm{d}x.$$

It is not difficult to verify that a_h is positive definite on $V_h \times V_h$. Hence the finite element scheme (4.3.12) has a unique solution $u_h \in V_h$ which satisfies

$$\|u_h\|_h = \left(\frac{1}{2h}\int_{D_h} |\nabla u_h|^2 + u_h^2 \,\mathrm{d}x\right)^{\frac{1}{2}} \leq c\,\|f\|_{L^2(\Gamma)}\,. \tag{4.3.13}$$

Remark 4.3.4. The choice of global scaling $\frac{1}{2h}$ in front of the integrals above is chosen to arrive at the appropriate scaling in the following error analysis. It is chosen so that the $\|\cdot\|_h$-norm behaves as the $H^1(\Gamma)$-norm.

The space V_h comes equipped with the following approximation property:

Lemma 4.3.5. *Let $z \in H^2(\Gamma)$; then*

$$\frac{1}{\sqrt{h}}\,\|z^e - I_h z^e\|_{L^2(D_h)} + \sqrt{h}\,\|\nabla(z^e - I_h z^e)\|_{L^2(D_h)} \leq ch^2\,\|z\|_{H^2(\Gamma)}\,. \tag{4.3.14}$$

Proof. We infer from our basic interpolation estimate (4.2.5) that

$$\begin{aligned}
&\frac{1}{h}\left\|z^e - I_h z^e\right\|^2_{L^2(D_h)} + h\left\|\nabla(z^e - I_h z^e)\right\|^2_{L^2(D_h)} \\
&\quad\le \sum_{T\in\mathscr{T}_h^B}\left(\frac{1}{h}\left\|z^e - I_h z^e\right\|^2_{L^2(T)} + h\left\|\nabla(z^e - I_h z^e)\right\|^2_{L^2(T)}\right) \\
&\quad\le ch^3 \sum_{T\in\mathscr{T}_h^B}\left\|z^e\right\|^2_{H^2(T)} \le ch^3\left\|z^e\right\|^2_{H^2(D_{3h})} \le ch^4\left\|z\right\|^2_{H^2(\Gamma)}.
\end{aligned}$$

□

We use the same framework as above to show an error bound. We remark briefly, that this bound is optimal in the energy norm but not in the L^2 norm.

Theorem 4.3.6. *Let u be the solution of (4.2.15) and let u_h be the solution of the finite element scheme (4.3.12), then*

$$\left(\frac{1}{2h}\int_{D_h} |\nabla(u^e - u_h)|^2 + |u^e - u_h|^2 \,\mathrm{d}x\right)^{\frac{1}{2}} \le ch\left\|f\right\|_{L^2(\Gamma)}. \tag{4.3.15}$$

Proof. Let us write $e_h := u^e - u_h$. We observe from (4.2.18) and (4.3.14) that

$$\left(\frac{1}{2h}\int_{D_h} |\nabla e_h|^2 + e_h^2 \,\mathrm{d}x\right)^{\frac{1}{2}} \le ch\left\|u\right\|_{H^2(\Gamma)} + \sup_{\phi_h\in V_h}\frac{|a_h(u^e,\phi_h) - l_h(\phi_h)|}{\left\|\phi_h\right\|_h}. \tag{4.3.16}$$

In order to estimate the second term we derive from (4.2.4) that

$$-\Delta u^e + u^e = f^e + R, \tag{4.3.17}$$

where

$$|R(x)| \le c\,|d(x)|\left(\,|\nabla_\Gamma u(p(x))| + \left|\nabla^2_\Gamma u(p(x))\right|\,\right) \quad \text{for } x\in U. \tag{4.3.18}$$

We multiply (4.3.17) by $\phi_h\circ F_h^{-1}$, $\phi_h\in V_h$, and integrate over D^h. Since $\dfrac{\partial u^e}{\partial\nu} = 0$ on ∂D^h, we obtain

$$\int_{D^h}\nabla u^e\cdot\nabla(\phi_h\circ F_h^{-1})\,\mathrm{d}x + \int_{D^h} u^e\phi_h\circ F_h^{-1}\,\mathrm{d}x = \int_{D^h} f^e\phi_h\circ F_h^{-1}\,\mathrm{d}x + \int_{D_h} R\phi_h\circ F_h^{-1}\,\mathrm{d}x.$$

Observing that $\nabla(\phi_h\circ F_h^{-1}) = [(DF_h)^{-\mathrm{t}}\circ F_h^{-1}]\nabla\phi_h\circ F_h^{-1}$ we deduce from the

transformation rule

$$\begin{aligned}\int_{D_h} \nabla u^e \circ F_h \cdot (DF_h)^{-\mathrm{t}} \nabla \phi_h \, |\det DF_h| \, \mathrm{d}x + \int_{D_h} u^e \circ F_h \phi_h \, |\det DF_h| \, \mathrm{d}x \\ = \int_{D_h} f^e \circ F_h \phi_h \, |\det DF_h| \, \mathrm{d}x + \int_{D_h} R \circ F_h \phi_h \, |\det DF_h| \, \mathrm{d}x.\end{aligned} \tag{4.3.19}$$

Recalling the definition of u^e, (4.2.7) and (4.2.8), we have

$$u^e(x) = u(p(x)) = u(p(F_h(x))) = u^e(F_h(x)) \tag{4.3.20}$$

and hence, using (4.2.9), we obtain

$$\begin{aligned}\nabla u^e(x) &= \nabla u^e(F_h(x)) + \big(\nabla u^e(F_h(x)) \cdot \nu(x)\big)\nabla \eta_h(x) + \eta_h(x)\mathcal{H}(x)\nabla u^e(F_h(x)) \\ &= (\mathrm{Id} - \eta_h \mathcal{H}(x))\nabla u^e(F_h(x)),\end{aligned}$$

since $\nabla u^e(F_h(x)) \cdot \nu(x) = (\mathrm{Id} - d(x)\mathcal{H}(x))\nabla_\Gamma u(p(x)) \cdot \nabla(d(x)) = 0$. As a result we derive

$$\nabla u^e(F_h(x)) = \big(\mathrm{Id} - \eta_h \mathcal{H}(x)\big)^{-1} \nabla u^e(x).$$

Hence we see that

$$a_h(u^e, \phi_h) - l_h(\phi_h) = \langle R_h, \phi_h \rangle, \tag{4.3.21}$$

where

$$\begin{aligned}&\langle R_h, \phi_h \rangle \\ &\quad = \frac{1}{2h} \int_{D_h} \Big((\mathrm{Id} + \eta_h \mathcal{H}(x))^{-1} \nabla u^e(x) \cdot (DF_h)^{-\mathrm{t}} \nabla \phi_h \, |\det DF_h| - \nabla u^e \cdot \nabla \phi_h \Big) \, \mathrm{d}x \\ &\qquad + \frac{1}{2h} \int_{D_h} (f^e \phi_h - u^e \phi_h)(|\det DF_h| - 1) \, \mathrm{d}x + \frac{1}{2h} \int_{D_h} R \circ F_h \phi_h \, |\det DF_h| \, \mathrm{d}x.\end{aligned}$$

Inserting this expression into (4.3.21) and recalling (4.2.6), (4.2.10) and (4.3.18) as

well as Lemma 4.2.1, we infer that, for all $\phi \in V_h$,

$$
\begin{aligned}
&|a_h(u^e, \phi_h) - l_h(\phi_h)| \\
&\quad \leq c \int_{D_h} \left(|\nabla u^e| \, |\phi_h| + |u^e| \, |\phi_h| + |f^e| \, |\phi_h| \right) \mathrm{d}x \\
&\qquad + c \left(\int_{D_h} |R \circ F_h|^2 \, \mathrm{d}x \right)^{\frac{1}{2}} \left(\int_{D_h} |\phi_h|^2 \, \mathrm{d}x \right)^{\frac{1}{2}} \\
&\quad \leq ch \left(\|u\|_{H^1(\Gamma)} + \|f\|_{L^2(\Gamma)} + \left(\frac{1}{2h} \int_{D^h} |R|^2 \, \mathrm{d}x \right)^{\frac{1}{2}} \right) \|\phi_h\|_h \\
&\quad \leq ch \big(\|u\|_{H^2(\Gamma)} + \|f\|_{L^2(\Gamma)} \big) \, \|\phi_h\|_h \\
&\quad \leq ch \, \|f\|_{L^2(\Gamma)} \, \|\phi_h\|_h \, .
\end{aligned}
$$

Inserting this estimate into (4.3.16) we complete the proof of the theorem. □

We remark that our narrow-band method has similarities with the h-narrow band method of Deckelnick et al. (2010). The main difference is that we use full instead of projected gradients in our discrete bilinear forms. The difference means that our discrete problem is not degenerate. Our method also has control over the normal derivative of the error away from the surface, hence our method produces solutions which are almost constant in the normal direction.

4.4 Numerical Experiments

4.4.1 Notes on implementation

Assembly of the matrices is nonstandard in that the method requires integration over partial elements. To do so we subdivide the integration areas in simplices using the Triangle (Shewchuk 1996, 2005) and Tetgen (Si 2006) packages. In each case, the linear system is solved with the conjugate gradient method until the residual is reduced by a factor of 10^{-8} in comparison to its initial value in the ℓ^2 norm. Due to the lack of shape-regularity of Γ_h and D_h, the matrix systems are ill conditioned and so we used a Jacobi preconditioner in order to speed up the convergence of our iterative solver.

In practice, we will take U_h to be a subset of a cube-shaped domain. The triangulation $\mathscr{T}_h$ will be computed by adaptively refining only those elements which intersect the computational domain, either Γ_h or D_h; see Figure 4.4.1 for an example.

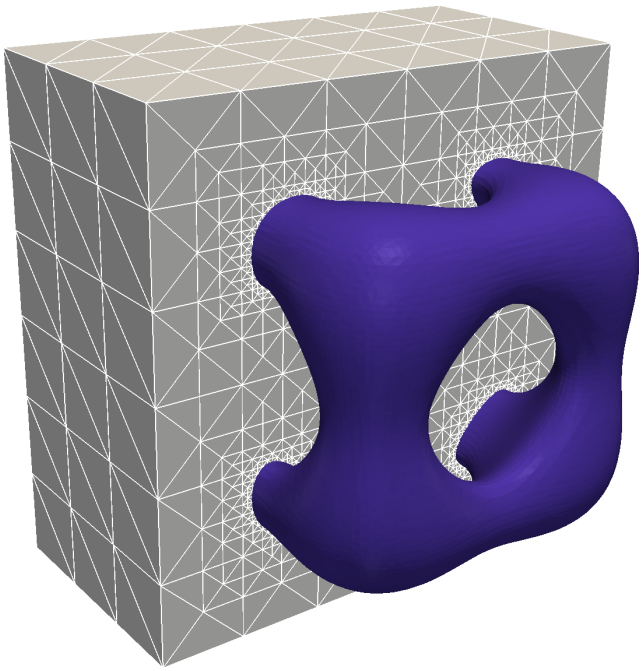

Figure 4.4.1: The above plot shows an example of this construction. The grey elements represent part of the underlying triangulation and the blue surface is Γ_h.

4.4.2 Numerical results

For each of our new methods, we present numerical simulations that demonstrate the convergence of each. The experimental order of convergence is calculated via formula (A.7.1). We also compare the results of our sharp interface method against the method of Olshanskii et al. (2009) for one of the examples. As well as the error in various norms, we include the number of degrees of freedom (dofs) of the linear system (the dimension of V_h), the number of elements in $\mathscr{T}_h^I$ or $\mathscr{T}_h^B$ and the number of conjugate gradient iterations required to solve the system.

Example one: sphere

The first example is on a sphere. We start with $\Phi(x, y, z) = \sqrt{x^2 + y^2 + z^2} - 1$. We take the right-hand side so that the exact solution is given by $u(x, y, z) = \cos(2\pi x)\cos(2\pi y)\cos(2\pi z)$.

Example two: torus

The second example is on a torus. We start with $\Phi(x, y, z) = (\sqrt{x^2 + y^2} - R)^2 + z^2 - r^2$ with $R = 1.0, r = 0.6$.

We parameterise the torus by

$$x = (R - r\cos\theta)\cos\varphi, \quad y = (R - r\cos\theta)\cos\varphi, \quad z = r\sin\theta, \quad \text{for } \theta, \varphi \in (-\pi, \pi),$$

and take f so that the exact solution is

$$u(\theta, \varphi) = \cos(3\varphi)\sin(3\theta + \varphi).$$

Example three: from Dziuk (1988)

The third example is taken from Dziuk (1988). We start with $\Phi(x, y, z) = (x - z^2)^2 + y^2 + z^2 - 1$. We remark that this is not a distance function, however this method only requires the zero level-set of the level-set function, so no adjustments are required. We take the right hand side so that the exact solution is given by $u(x, y, z) = xy$.

Discussion

For the sharp interface method, the results of Examples one, two and three are shown in Tables 4.1, 4.2 and 4.4. A plot of the solution is shown on two different meshes above the table of errors. In all three examples, we see the order of convergence expected from the analysis and the error is of a similar magnitude as for the surface finite element method for the same number of degrees of freedom (Section A.7.2). Furthermore, we see that the number of conjugate gradient solver iterations approximately doubles between mesh refinements: This is again similar to the results for the surface finite element method.

For the second example, we compare the results of the sharp interface method (Table 4.2) with the method from Olshanskii et al. (2009) (Table 4.3). These two methods produce similar results. The error in the L^2 norm produced by the method of Olshanskii et al. (2009) is slightly smaller than in method one, although it takes slightly more conjugate gradient iterations to solve the system of linear equations. The main difference comes from the fact that method one uses full gradients, so the error estimate from Theorem 4.3.2 provides control of the normal derivative of the solution away from the surface. In fact, the method of Olshanskii et al. (2009) does not converge to the true solution in the norm $\|\nabla(u^e - u_h)\|_{L^2(\Gamma_h)}$; see Figure 4.3a for an example.

For the narrow band method, the results of Examples one and two are shown in Tables 4.5 and 4.6. A plot of the solution on two different meshes is shown in Figure 4.4.2. In both examples, we see faster convergence than shown in the analysis.

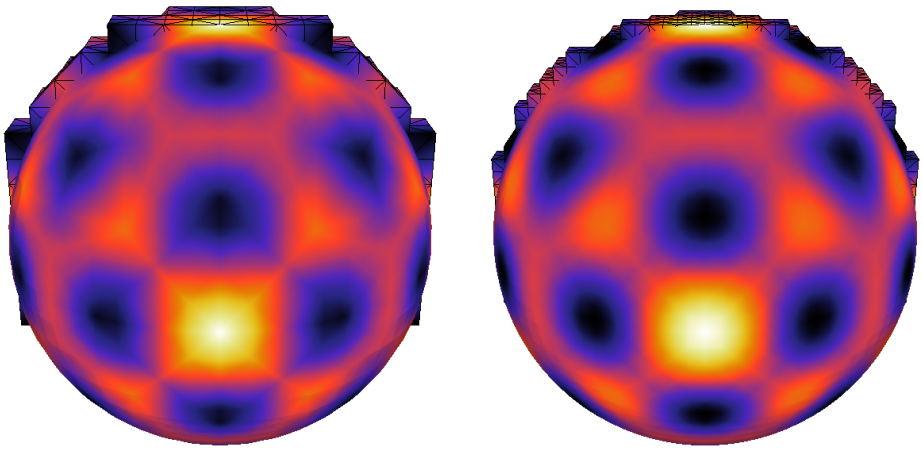

h	$\|u^e - u_h\|_{L^2(\Gamma_h)}$	eoc	$\|\nabla(u^e - u_h)\|_{L^2(\Gamma_h)}$	eoc
$\sqrt{3}$	$4.04068 \cdot 10^{+1}$	—	$1.52194 \cdot 10^{+1}$	—
$2^{-1}\sqrt{3}$	$1.01375 \cdot 10^{+1}$	1.99490	9.47772	0.68330
$2^{-2}\sqrt{3}$	$3.76636 \cdot 10^{-1}$	4.75039	5.86936	0.69134
$2^{-3}\sqrt{3}$	$1.90326 \cdot 10^{-1}$	0.98470	4.31727	0.44308
$2^{-4}\sqrt{3}$	$5.21416 \cdot 10^{-2}$	1.86797	2.27205	0.92612
$2^{-5}\sqrt{3}$	$1.27837 \cdot 10^{-2}$	2.02813	1.12561	1.01329
$2^{-6}\sqrt{3}$	$3.26099 \cdot 10^{-3}$	1.97092	$5.69978 \cdot 10^{-1}$	0.98173
$2^{-7}\sqrt{3}$	$8.07000 \cdot 10^{-4}$	2.01467	$2.83520 \cdot 10^{-1}$	1.00746
$2^{-8}\sqrt{3}$	$2.02104 \cdot 10^{-4}$	1.99747	$1.41880 \cdot 10^{-1}$	0.99878

h	dofs	elements	cg iterations
$\sqrt{3}$	15	24	4
$2^{-1}\sqrt{3}$	118	288	22
$2^{-2}\sqrt{3}$	406	1 152	38
$2^{-3}\sqrt{3}$	1 846	5 280	69
$2^{-4}\sqrt{3}$	7 606	21 888	110
$2^{-5}\sqrt{3}$	30 406	87 936	171
$2^{-6}\sqrt{3}$	121 894	352 704	237
$2^{-7}\sqrt{3}$	487 318	1 410 960	438
$2^{-8}\sqrt{3}$	1 947 570	5 639 424	804

Table 4.1: Result for the sharp interface method on a sphere.

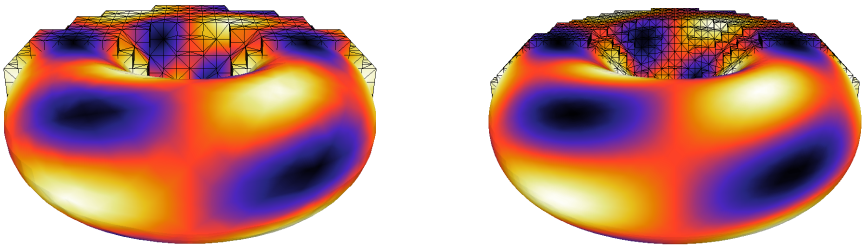

h	$\|u^e - u_h\|_{L^2(\Gamma_h)}$	eoc	$\|\nabla(u^e - u_h)\|_{L^2(\Gamma_h)}$	eoc
$\sqrt{3}$	6.03053	—	$1.45014 \cdot 10^{+1}$	—
$2^{-1}\sqrt{3}$	1.67739	1.84607	$1.13951 \cdot 10^{+1}$	0.34778
$2^{-2}\sqrt{3}$	$7.10825 \cdot 10^{-1}$	1.23865	7.95596	0.51831
$2^{-3}\sqrt{3}$	$1.90004 \cdot 10^{-1}$	1.90346	4.07793	0.96420
$2^{-4}\sqrt{3}$	$4.73865 \cdot 10^{-2}$	2.00348	2.04879	0.99306
$2^{-5}\sqrt{3}$	$1.19721 \cdot 10^{-2}$	1.98480	1.03454	0.98578
$2^{-6}\sqrt{3}$	$3.01376 \cdot 10^{-3}$	1.99004	$5.17692 \cdot 10^{-1}$	0.99882
$2^{-7}\sqrt{3}$	$7.52514 \cdot 10^{-4}$	2.00177	$2.58691 \cdot 10^{-1}$	1.00086

h	dofs	elements	cg iterations
$\sqrt{3}$	55	140	24
$2^{-1}\sqrt{3}$	217	688	38
$2^{-2}\sqrt{3}$	912	2 608	69
$2^{-3}\sqrt{3}$	3 404	9 984	128
$2^{-4}\sqrt{3}$	14 080	41 008	240
$2^{-5}\sqrt{3}$	56 944	165 616	359
$2^{-6}\sqrt{3}$	226 592	659 056	641
$2^{-7}\sqrt{3}$	903 664	2 626 880	1 249

Table 4.2: Result for the sharp interface on a torus.

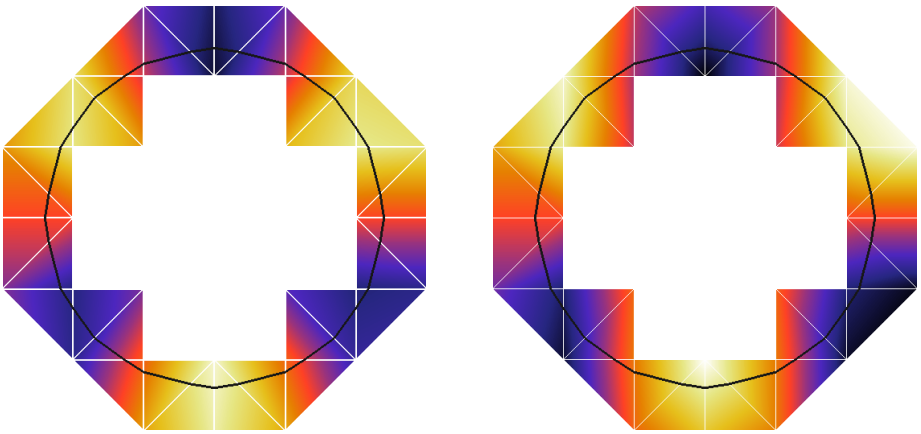

(a) Plots of the solution to example two using method one (left) and the method of Olshanskii et al. (2009) (right). The solution has been clipped to show the cross section of the torus. The black line is the approximation of the surface Γ_h and the triangulation shown in white. This demonstrates the reduced normal errors from using the full gradient.

h	$\|u^e - u_h\|_{L^2(\Gamma_h)}$	eoc	$\|\nabla_{\Gamma_h}(u^e - u_h)\|_{L^2(\Gamma_h)}$	eoc
$\sqrt{3}$	6.13634	—	$1.34194 \cdot 10^{+1}$	—
$2^{-1}\sqrt{3}$	1.61226	1.92829	$1.06768 \cdot 10^{+1}$	0.32984
$2^{-2}\sqrt{3}$	$5.80174 \cdot 10^{-1}$	1.47453	6.93654	0.62219
$2^{-3}\sqrt{3}$	$1.34881 \cdot 10^{-1}$	2.10480	3.31260	1.06625
$2^{-4}\sqrt{3}$	$3.32886 \cdot 10^{-2}$	2.01859	1.65770	0.99878
$2^{-5}\sqrt{3}$	$8.41979 \cdot 10^{-3}$	1.98317	$8.35673 \cdot 10^{-1}$	0.98817
$2^{-6}\sqrt{3}$	$2.09973 \cdot 10^{-3}$	2.00358	$4.16491 \cdot 10^{-1}$	1.00465
$2^{-7}\sqrt{3}$	$5.22559 \cdot 10^{-4}$	2.00654	$2.07738 \cdot 10^{-1}$	1.00352

h	dofs	elements	cg iterations
$\sqrt{3}$	55	140	28
$2^{-1}\sqrt{3}$	217	688	44
$2^{-2}\sqrt{3}$	912	2 608	90
$2^{-3}\sqrt{3}$	3 404	9 984	163
$2^{-4}\sqrt{3}$	14 080	41 008	278
$2^{-5}\sqrt{3}$	56 944	165 616	583
$2^{-6}\sqrt{3}$	226 592	659 056	1 077
$2^{-7}\sqrt{3}$	903 664	2 626 880	2 080

(b) Result for the method of Olshanskii et al. (2009) on a torus.

Table 4.3: A comparison of results between the two sharp interface methods.

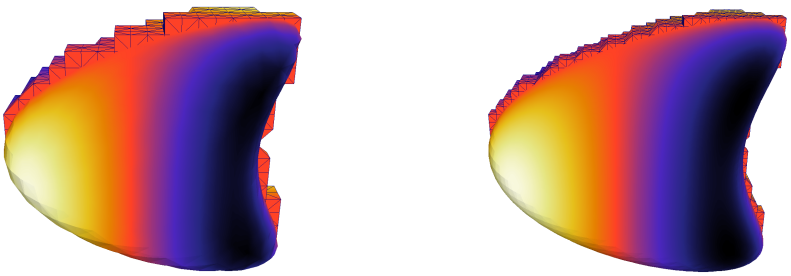

h	$\|u^e - u_h\|_{L^2(\Gamma_h)}$	eoc	$\|\nabla(u^e - u_h)\|_{L^2(\Gamma_h)}$	eoc
$\sqrt{3}$	$5.15752 \cdot 10^{-1}$	—	1.54322	—
$2^{-1}\sqrt{3}$	$3.31237 \cdot 10^{-1}$	0.63881	1.15310	0.42043
$2^{-2}\sqrt{3}$	$9.97842 \cdot 10^{-2}$	1.73098	$6.46853 \cdot 10^{-1}$	0.83401
$2^{-3}\sqrt{3}$	$2.57329 \cdot 10^{-2}$	1.95520	$3.41718 \cdot 10^{-1}$	0.92063
$2^{-4}\sqrt{3}$	$6.59538 \cdot 10^{-3}$	1.96409	$1.71480 \cdot 10^{-1}$	0.99477
$2^{-5}\sqrt{3}$	$1.64586 \cdot 10^{-3}$	2.00261	$8.55564 \cdot 10^{-2}$	1.00309
$2^{-6}\sqrt{3}$	$4.10269 \cdot 10^{-4}$	2.00420	$4.28811 \cdot 10^{-2}$	0.99653
$2^{-7}\sqrt{3}$	$1.02735 \cdot 10^{-4}$	1.99764	$2.14321 \cdot 10^{-2}$	1.00057

h	dofs	elements	cg iterations
$\sqrt{3}$	16	24	16
$2^{-1}\sqrt{3}$	102	256	25
$2^{-2}\sqrt{3}$	430	1 248	53
$2^{-3}\sqrt{3}$	1 948	5 664	103
$2^{-4}\sqrt{3}$	8 068	23 512	196
$2^{-5}\sqrt{3}$	32 388	94 480	298
$2^{-6}\sqrt{3}$	130 036	379 272	585
$2^{-7}\sqrt{3}$	520 232	1 516 800	1 151

Table 4.4: Result for sharp interface method on Dziuk surface.

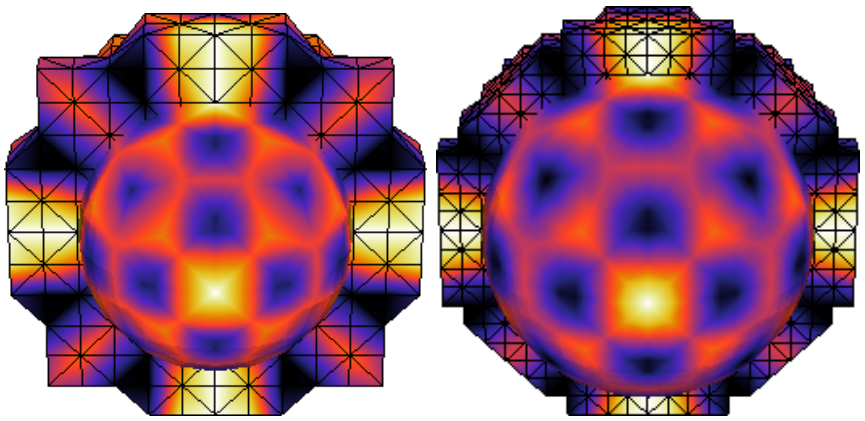

(a) Example one: Γ = sphere

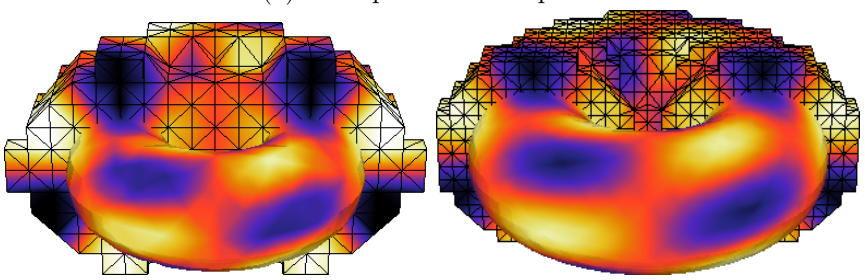

(b) Example one: Γ = torus

Figure 4.4.2: Plots of the solutions of method two the narrow band unfitted finite element method at various mesh sizes.

In fact the errors are similar to the sharp interface methods for each mesh size, although the latter requires slightly more degrees of freedom. Furthermore, we see the number of conjugate gradient solver iterations approximately doubles between mesh refinements. In comparison to the method of Deckelnick et al. (2010), we also have control over the normal derivative of the error away from the surface. This also affects the L^2 error in the narrow band where we see second-order convergence whereas the method of Deckelnick et al. (2010) exhibits only first-order convergence in the $L^2(D_h)$ norm.

4.5 A hybrid method for equations on evolving surfaces

We conclude this chapter with a note on the future direction of our work on of these methods. We will take our notation from Chapter 3. We wish to solve partial differential equations on evolving surfaces and take as our example an advection-

diffusion equation: Find $u\colon \mathcal{G}_T \to \mathbb{R}$ such that

$$\partial^\bullet u + u\nabla_\Gamma \cdot v - \Delta_\Gamma u = f. \tag{4.5.1}$$

In order to motivate our thoughts, we fix $t^* \in (0,T)$ and calculate for sufficiently smooth function φ, defined on a narrow band about $\Gamma(t^*)$,

$$\begin{aligned}\frac{\mathrm{d}}{\mathrm{d}t}\int_{\Gamma(t)} u\varphi \,\mathrm{d}\sigma\bigg|_{t=t^*} &= \int_{\Gamma(t^*)} \partial^\bullet(u\varphi) + u\varphi\nabla_\Gamma\cdot v \,\mathrm{d}\sigma \\ &= \int_{\Gamma(t^*)} \varphi\partial^\bullet u + uv\cdot\varphi + u\varphi\nabla_\Gamma\cdot v\,\mathrm{d}\sigma = \int_{\Gamma(t^*)} \varphi\Delta_\Gamma u + uv\cdot\nabla\varphi + \varphi f\,\mathrm{d}\sigma.\end{aligned}$$

Note that φ does not depend on t. In conclusion, we obtain

$$\frac{\mathrm{d}}{\mathrm{d}t}\int_{\Gamma(t)} u\varphi\,\mathrm{d}\sigma\bigg|_{t=t_*} + \int_{\Gamma(t^*)} \nabla_\Gamma u\cdot\nabla_\Gamma\varphi\,\mathrm{d}\sigma = \int_{\Gamma(t^*)} uv\cdot\nabla\varphi\,\mathrm{d}\sigma + \int_{\Gamma(t^*)} f\varphi\,\mathrm{d}\sigma. \tag{4.5.2}$$

The idea is to combine the sharp interface method for the lower order terms with the narrow band method for the diffusion terms using an implicit Euler time stepping method. One can show that for a sufficiently small time step, $\tau\|v\|_{L^\infty(\mathcal{G}_T)} < h$, the previous sharp interface is contained within the new narrow band. This will imply that the method conserves mass.

One further difficulty to overcome is that the advection term can lead to spurious oscillations in the normal direction to the surface, since we have no diffusion in that direction. A possible remedy is to add streamline diffusion in the normal direction to the surface. In our case, numerical results suggest that this penalty term does not affect the accuracy of the method so may be taken arbitrarily large.

h	$(\frac{1}{2h}\,\|u^e-u_h\|^2_{L^2(D_h)})^{\frac{1}{2}}$	(eoc)	$(\frac{1}{2h}\,\|\nabla(u^e-u_h)\|^2_{L^2(D_h)})^{\frac{1}{2}}$	(eoc)
$\sqrt{3}$	4.78338	—	$1.84002 \cdot 10^{+1}$	—
$2^{-1}\sqrt{3}$	3.79113	0.33540	$1.10972 \cdot 10^{+1}$	0.72953
$2^{-2}\sqrt{3}$	$6.00857 \cdot 10^{-1}$	2.65753	6.56763	0.75675
$2^{-3}\sqrt{3}$	$2.39769 \cdot 10^{-1}$	1.32538	4.70945	0.47981
$2^{-4}\sqrt{3}$	$6.91536 \cdot 10^{-2}$	1.79377	2.42830	0.95561
$2^{-5}\sqrt{3}$	$1.47734 \cdot 10^{-2}$	2.22680	1.22329	0.98918
$2^{-6}\sqrt{3}$	$3.73584 \cdot 10^{-3}$	1.98350	$6.14259 \cdot 10^{-1}$	0.99385
$2^{-7}\sqrt{3}$	$9.70899 \cdot 10^{-4}$	1.94404	$3.07116 \cdot 10^{-1}$	1.00006

h	$\|u^e-u_h\|_{L^2(\Gamma_h)}$	(eoc)	$\|\nabla(u^e-u_h)\|_{L^2(\Gamma_h)}$	(eoc)
$\sqrt{3}$	2.57553	—	$1.13034 \cdot 10^{+1}$	—
$2^{-1}\sqrt{3}$	3.72889	−0.53388	$1.10432 \cdot 10^{+1}$	0.03360
$2^{-2}\sqrt{3}$	$4.73667 \cdot 10^{-1}$	2.97680	6.27874	0.81461
$2^{-3}\sqrt{3}$	$1.88299 \cdot 10^{-1}$	1.33085	4.72643	0.40972
$2^{-4}\sqrt{3}$	$5.33564 \cdot 10^{-2}$	1.81929	2.48230	0.92907
$2^{-5}\sqrt{3}$	$1.23057 \cdot 10^{-2}$	2.11633	1.20011	1.04851
$2^{-6}\sqrt{3}$	$3.54650 \cdot 10^{-3}$	1.79486	$6.02231 \cdot 10^{-1}$	0.99478
$2^{-7}\sqrt{3}$	$9.48127 \cdot 10^{-4}$	1.90324	$2.97786 \cdot 10^{-1}$	1.01604

h	dofs	elements	cg iterations
$\sqrt{3}$	221	816	20
$2^{-1}\sqrt{3}$	493	1 968	26
$2^{-2}\sqrt{3}$	1 274	5 712	45
$2^{-3}\sqrt{3}$	4 718	22 464	46
$2^{-4}\sqrt{3}$	18 662	87 936	134
$2^{-5}\sqrt{3}$	73 934	350 784	254
$2^{-6}\sqrt{3}$	298 886	1 411 824	488
$2^{-7}\sqrt{3}$	1 194 280	5 649 024	869

Table 4.5: Result for the narrow band method on a sphere.

h	$(\frac{1}{2h}\,\|u^e-u_h\|^2_{L^2(D_h)})^{\frac{1}{2}}$	(eoc)	$(\frac{1}{2h}\,\|\nabla(u^e-u_h)\|^2_{L^2(D_h)})^{\frac{1}{2}}$	(eoc)
$\sqrt{3}$	7.40091	—	$1.87130 \cdot 10^{+1}$	—
$2^{-1}\sqrt{3}$	2.68743	1.46148	$1.14673 \cdot 10^{+1}$	0.70652
$2^{-2}\sqrt{3}$	1.19776	1.16589	8.91224	0.36367
$2^{-3}\sqrt{3}$	$4.06532 \cdot 10^{-1}$	1.55890	5.17295	0.78480
$2^{-4}\sqrt{3}$	$9.66548 \cdot 10^{-2}$	2.07246	2.60175	0.99150
$2^{-5}\sqrt{3}$	$2.22761 \cdot 10^{-2}$	2.11734	1.30693	0.99330
$2^{-6}\sqrt{3}$	$5.35416 \cdot 10^{-3}$	2.05676	$6.54438 \cdot 10^{-1}$	0.99785

h	$\|u^e-u_h\|_{L^2(\Gamma_h)}$	(eoc)	$\|\nabla(u^e-u_h)\|_{L^2(\Gamma_h)}$	(eoc)
$\sqrt{3}$	2.49823	—	$1.61819 \cdot 10^{+1}$	—
$2^{-1}\sqrt{3}$	1.62953	0.61645	$1.27498 \cdot 10^{+1}$	0.34391
$2^{-2}\sqrt{3}$	$7.13768 \cdot 10^{-1}$	1.19093	9.34296	0.44852
$2^{-3}\sqrt{3}$	$2.35902 \cdot 10^{-1}$	1.59727	4.98524	0.90622
$2^{-4}\sqrt{3}$	$7.26544 \cdot 10^{-2}$	1.69907	2.37468	1.06993
$2^{-5}\sqrt{3}$	$1.99335 \cdot 10^{-2}$	1.86586	1.12826	1.07363
$2^{-6}\sqrt{3}$	$5.14142 \cdot 10^{-3}$	1.95496	$5.49913 \cdot 10^{-1}$	1.03682

h	dofs	elements	cg iterations
$\sqrt{3}$	273	1 012	31
$2^{-1}\sqrt{3}$	659	2 736	34
$2^{-2}\sqrt{3}$	2 165	10 208	54
$2^{-3}\sqrt{3}$	8 820	42 080	134
$2^{-4}\sqrt{3}$	35 060	167 504	241
$2^{-5}\sqrt{3}$	138 568	657 472	436
$2^{-6}\sqrt{3}$	562 868	2 668 224	826

Table 4.6: Result for the narrow band method on a torus.

Appendix A

The surface finite element method

A.1 Introduction

In this appendix, we recall results for the surface finite element method. We will analyse the method for solving a Poisson equation on an arbitrary surface. We start by describing in detail the assumptions on the surface and how we make sense of the Poisson equation via a weak formulation. We then describe the surface finite element method and go on to show optimal order error estimates. We conclude this chapter with some numerical examples and some discussion of how to implement this method.

We will consider the surface Poisson equation, which is also known as the Laplace-Beltrami equation. We seek solutions $u\colon \Gamma \to \mathbb{R}$ of

$$-\Delta_\Gamma u + cu = f \quad \text{on } \Gamma. \tag{A.1.1}$$

We will assume that $f \in L^2(\Gamma)$ is given and the constant $c > 0$ or $c = 0$ and $\int_\Gamma f \,\mathrm{d}\sigma = 0$.

We will look to approximate this problem using the surface finite element method. Most of the work of this chapter is taken from the work of Dziuk (1988). Further explanation of some of the results are given in Dziuk and Elliott (2013b). We take our notation from Deckelnick et al. (2005) and Dziuk and Elliott (2013b).

A.2 Surface notation

We will assume that Γ is a C^3 compact, connected, orientable, n-dimensional hypersurface, embedded in $\mathbb{R}^{n+1}$ for $n = 1, 2$, or 3.

Definition A.2.1 (Hypersurface). Let $k \in \mathbb{N}$. A subset $\Gamma \subset \mathbb{R}^{n+1}$ is called a C^k-hypersurface, if for each point $x_0 \in \Gamma$ there exists an open set $U \subset \mathbb{R}^{n+1}$ containing x_0 and a function $\phi \in C^k(U)$ such that

$$U \cap \Gamma = \{x \in U : \phi(x) = 0\} \qquad \text{and} \qquad \nabla\phi \neq 0 \quad \text{for all } x \in U \cap \Gamma.$$

We will assume that Γ is the boundary of a connected domain Ω, so it can be described as the zero level set of an oriented distance function d given by

$$d(x) := \begin{cases} -\min\{|x-y| : y \in \Gamma\} & \text{for } x \in \Omega \\ 0 & \text{for } x \in \Gamma \\ \min\{|x-y| : y \in \Gamma\} & \text{otherwise.} \end{cases} \tag{A.2.1}$$

This assumption implies Γ has no boundary. We will use this assumption throughout this thesis but it is not a restriction on the methods developed.

This allows us to define the unit normal to Γ by $\nu := \nabla d$ (by assumption, $|\nabla d| = 1$ in a neighbourhood of Γ), the extended Weingarten map, or shape operator, by $\mathcal{H} := \nabla_\Gamma \nu$. We define the mean curvature of Γ by $H := \operatorname{trace} \mathcal{H}$. This is equivalent to

$$H(x) = \nabla_\Gamma \cdot \nu(x) = \Delta d(x) \quad \text{for } x \in \Gamma.$$

Note that this definition varies from the standard definition of mean curvature by a factor n. As an example, we consider a sphere of radius R centred at x_0: $\Gamma = \{x \in \mathbb{R}^{n+1} : |x - x_0| = R\}$ and the choice $d(x) = |x - x_0| - R$. The normal $\nu = \nabla d = (x - x_0)/R$ is outward pointing and the mean curvature is given by $H = n/R$.

In order to explore the properties of d, we define a narrow band U about Γ by $U = \{x \in \mathbb{R}^{n+1} : |d(x)| < \delta_\Gamma\}$, where δ_Γ is constructed through the following procedure. Let r by the maximal ratio of geodesic distance to Euclidean distance for any two points on Γ:

$$r := \sup_{x,y \in \Gamma, x \neq y} \frac{L_\Gamma(x,y)}{|x-y|}$$

where L_Γ is the geodesic distance

$$L_\Gamma(x,y) := \inf\left\{\int_0^1 \left|\gamma'(t)\right| \,\mathrm{d}t : \gamma \in W^{1,1}([0,1];\Gamma), \gamma(0)=x, \gamma(1)=y\right\}.$$

Since Γ is a C^2 hypersurface, we can define $M := \max_{y\in\Gamma} |\nabla \nu(y)|$. Notice that $r \geq 1$ and $M \geq 0$. We choose $\delta_\Gamma > 0$ so that $\delta_\Gamma r M < 1$.

Lemma A.2.2. *The distance function d is in $C^2(U)$. For every $x \in U$, there exists a unique point $p(x) \in \Gamma$ such that*

$$x = p(x) + d(x)\nu(p(x)) \quad \text{for } x \in U. \tag{A.2.2}$$

Furthermore, we have

$$\nabla d(x) = \nu(p(x)), \quad \text{in particular } |\nabla d(x)| = 1 \quad \text{for } x \in U. \tag{A.2.3}$$

Proof. The proof is taken from Gilbarg and Trudinger (2001, Lemma 14.16).

We consider the mapping $\Phi\colon \Gamma \times (-\delta_\Gamma, \delta_\Gamma) \to U$ given by

$$\Phi(p,d) := p + d\nu(p).$$

We claim Φ is a bijection onto U. We first show that Φ is onto. Let $x \in U$; since Γ is compact there exists a point $p \in \Gamma$ with $|x-p| = \min_{y\in\Gamma} |x-y|$. Clearly, $x-p$ is perpendicular to the tangent space of Γ at p, so $x - p = d\nu(p)$, with

$$d = |x-p| = \min_{y\in\Gamma} |x-y| = |d(x)| < \delta_\Gamma,$$

hence, $x = \Phi(p,d)$. Next to show that Φ is injective, suppose that

$$p_1 + d_1\nu(p_1) = p_2 + d_2\nu(p_2) = x,$$

with $(p_j, d_j) \in \Gamma \times (-\delta_\Gamma, \delta_\Gamma)$. Then,

$$d(x) = d(p_j + d_j\nu(p_j)) = d_j \quad \text{for } j = 1,2,$$

so $d_1 = d_2 = d(x)$. Next, fix $\varepsilon > 0$ such that $\delta_\Gamma r M(1+\varepsilon) < 1$ and choose a curve $\gamma \in W^{1,1}([0,1];\Gamma)$ with

$$\gamma(0) = p_1, \gamma(1) = p_2 \text{ and } \int_0^1 \left|\gamma'(t)\right| \,\mathrm{d}t \leq (1+\varepsilon) L_\Gamma(p_1,p_2).$$

Then, we have

$$\begin{aligned}
|p_1 - p_2| &= |d(x)|\,|\nu(p_1) - \nu(p_2)| \\
&= |d(x)| \left| \int_0^1 \nabla\nu(\gamma(t))\gamma'(t)\,\mathrm{d}t \right| \\
&\leq \delta_\Gamma \int_0^1 |\nabla\nu(\gamma(t))| \left|\gamma'(t)\right| \,\mathrm{d}t \\
&\leq \delta_\Gamma M \int_0^1 \left|\gamma'(t)\right| \,\mathrm{d}t \\
&\leq \delta_\Gamma M(1+\varepsilon) L_\Gamma(p_1, p_2) \\
&\leq \delta_\Gamma r M(1+\varepsilon)\,|p_1 - p_2|\,.
\end{aligned}$$

From which, we infer $p_1 = p_2$. Hence Φ is a bijection and so, for every $x \in U$, there exists a unique $p = p(x) \in \Gamma$ satisfying (A.2.2).

Furthermore, choosing local coordinates for Γ and applying the Inverse Function Theorem to Φ implies that $p, d \in C^1(U)$. Next, fix $x \in U$. For small $\varepsilon > 0$ we also have $x + \varepsilon\nu(p(x)) \in U$ and

$$x + \varepsilon\nu(p(x)) = p(x) + (d(x) + \varepsilon)\nu(p(x)).$$

Since Φ is one-to-one, considering d evaluated at each side, we infer that $d(x + \varepsilon\nu(p(x))) = d(x) + \varepsilon$. Rearranging, we obtain:

$$\frac{d(x + \varepsilon\nu(p(x))) - d(x)}{\varepsilon} = 1,$$

so that the limit $\varepsilon \to 0$ yields

$$1 = \nabla d(x) \cdot \nu(p(x)) \leq |\nabla d(x)|\,|\nu(p(x))| \leq 1$$

because d is Lipschitz with constant 1. Hence, (A.2.3) holds. Since ν is differentiable in a neighbourhood of Γ and $p \in C^1(U)$, this relation implies in addition that $d \in C^2(U)$. □

Remark A.2.3.

- The width of the band δ_Γ only depends locally on the curvature of Γ.
- The first equation (A.2.2) defines an operator $p\colon U \to \mathbb{R}$ which we will call either the closest point operator or normal projection operator.

- The second equation (A.2.3) allows us to extend ν by

$$\nu(x) := \nabla d(x) = \nu(p(x)) \quad \text{for all } x \in U.$$

Given a function $\eta\colon \Gamma \to \mathbb{R}$, we define its tangential gradient by

$$\nabla_\Gamma \eta := \nabla \widetilde{\eta} - (\nabla \widetilde{\eta} \cdot \nu)\nu, \tag{A.2.4}$$

where $\nabla\widetilde{\eta}$ is the gradient of an arbitrary smooth extension of η to U with respect to the ambient coordinates in $\mathbb{R}^{n+1}$. It can be shown that this definition is independent of the extension $\widetilde{\eta}$ since it only depends on values of η on the surface.

Lemma A.2.4. *The tangential gradient $\nabla_\Gamma\eta$ only depends on the values of η on Γ.*

Proof. It is enough to show that if $\eta = 0$ on Γ then $\nabla_\Gamma\eta = 0$. Fix $x \in \Gamma$ and choose a path $\gamma\colon (-\varepsilon, \varepsilon) \to \Gamma$ such that $\gamma(0) = x$ and $\gamma'(0) = \nabla_\Gamma\eta(x)$. Since $\eta(\gamma(s)) = 0$ for $s \in (-\varepsilon, \varepsilon)$, we have

$$\begin{aligned} 0 &= \frac{\mathrm{d}}{\mathrm{d}s}\eta(\gamma(s))\bigg|_{s=0} = \nabla\eta(x) \cdot \gamma'(0) \\ &= (\nabla_\Gamma\eta(x) + \nabla\eta(x) \cdot \nu(x)\nu(x)) \cdot \nabla_\Gamma\eta(x) = |\nabla_\Gamma\eta(x)|^2 . \end{aligned}$$

□

The tangential gradient is a vector-valued function and we will denote its $n+1$ components by

$$\nabla_\Gamma\eta = (\underline{D}_1\eta, \ldots, \underline{D}_{n+1}\eta) \in \mathbb{R}^{n+1}. \tag{A.2.5}$$

Hence, the surface divergence of a vector field $v\colon \Gamma \to \mathbb{R}^{n+1}$ is

$$\nabla_\Gamma \cdot v := \sum_{j=1}^{n+1} \underline{D}_j v_j. \tag{A.2.6}$$

This gives a natural definition of the Laplace-Beltrami operator (the surface Laplacian) as

$$\Delta_\Gamma\eta := \nabla_\Gamma \cdot \nabla_\Gamma\eta = \sum_{j=1}^{n+1} \underline{D}_j\underline{D}_j\eta. \tag{A.2.7}$$

We will write integration on Γ with respect to the surface measure $\mathrm{d}\sigma$. The integration by parts formula (Dziuk and Elliott 2013b, Theorem 2.10) is given by

$$\int_\Gamma \underline{D}_j\eta \,\mathrm{d}\sigma = -\int_\Gamma H\nu_i\eta \,\mathrm{d}\sigma. \tag{A.2.8}$$

Combined with a product rule this gives a Green's formula on surfaces (Dziuk and Elliott 2013b, Theorem 2.14)

$$\int_\Gamma -\Delta_\Gamma \eta \, \varphi \, \mathrm{d}\sigma = \int_\Gamma \nabla_\Gamma \eta \cdot \nabla_\Gamma \varphi \, \mathrm{d}\sigma. \tag{A.2.9}$$

For more facts on surface derivatives and integrals see Gilbarg and Trudinger (2001, Chapters 14 and 16) and Dziuk and Elliott (2013b).

We will consider the solution of partial differential equations on surfaces in a weak sense. This involves the use of weak derivatives and surface Sobolev spaces (Wloka 1987; Hebey 2000). We say $\eta \colon \Gamma \to \mathbb{R}$, $\eta \in L^1_{\mathrm{loc}}(\Gamma)$ is weakly differentiable if there exists $\xi \in (L^1_{\mathrm{loc}}(\Gamma))^{n+1}$ such that

$$\int_\Gamma \eta \underline{D}_j \varphi \, \mathrm{d}\sigma = -\int_\Gamma \xi_j \varphi \, \mathrm{d}\sigma \quad \text{for } j = 1, \ldots, n+1, \text{ and for all } \varphi \in C^1(\Gamma).$$

In such a case we say that $\underline{D}_j \eta = \xi$ weakly. We define $W^{s,p}(\Gamma)$ as follows:

$$W^{s,p}(\Gamma) = \left\{ \eta \in L^p(\Gamma) : \underline{D}^\alpha \eta \in L^p(\Gamma) \text{ for all } |\alpha| \leq s \right\},$$

where $\alpha = (\alpha_1, \ldots, \alpha_{n+1})$ is a multi-index and the tangential derivatives $\underline{D}^\alpha = \underline{D}_1^{\alpha_1} \ldots \underline{D}_{n+1}^{\alpha_{n+1}}$ are to be considered in the weak sense. This definition requires Γ to be $C^{l,\kappa}$ with $l + \kappa \geq 1$ and $s \leq l + \kappa$ if $l + \kappa \in \mathbb{N}$, $s < l + \kappa$ if $l + \kappa \notin \mathbb{N}$. We equip this space with the norm

$$\|\eta\|_{W^{s,p}(\Gamma)} := \left(\int_\Gamma \sum_{|\alpha| \leq s} |\underline{D}^\alpha \eta|^p \, \mathrm{d}\sigma \right)^{\frac{1}{p}},$$

for $1 \leq p < \infty$ with the obvious extension if $p = \infty$. We will write $H^s(\Gamma) = W^{s,2}(\Gamma)$ with inner product

$$(\eta, \varphi)_{H^s(\Gamma)} := \int_\Gamma \sum_{|\alpha| \leq s} \underline{D}^\alpha \eta \underline{D}^\alpha \varphi \, \mathrm{d}\sigma.$$

It is clear that $W^{s,p}(\Gamma)$ is a Banach space and $H^s(\Gamma)$ is a Hilbert space.

The above theory allows us to define a weak formulation of (A.1.1): Find $u \in H^1(\Gamma)$ such that

$$\int_\Gamma \nabla_\Gamma u \cdot \nabla_\Gamma \varphi + cu\varphi \, \mathrm{d}\sigma = \int_\Gamma f\varphi \, \mathrm{d}\sigma, \qquad \left(\int_\Gamma u \, \mathrm{d}\sigma = 0, \text{ if } c = 0 \right). \tag{A.2.10}$$

Using standard techniques, one may show the following well-posedness result:

Theorem A.2.5. *There exists a unique solution $u \in H^1(\Gamma)$ to (A.2.10). Moreover, if Γ is C^3, then $u \in H^2(\Gamma)$ with the bound*

$$\|u\|_{H^2(\Gamma)} \leq c \|f\|_{L^2(\Gamma)} . \tag{A.2.11}$$

Proof. Existence and uniqueness follow from standard Lax-Milgram techniques (Evans 1998). The regularity result is shown in Aubin (1982, Theorem 4.7) for the case of smooth surfaces, which can be generalised to a result on C^3 surfaces. □

Throughout this thesis, we will use abstract notation to describe the weak formulations of partial differential equations. This allows us to write any analysis in a clean and consistent manner, reducing long equations into simple results from functional analysis. To this end, we introduce a bilinear form $a\colon H^1(\Gamma)\times H^1(\Gamma) \to \mathbb{R}$ and a linear form $l\colon H^1(\Gamma) \to \mathbb{R}$ by

$$a(w,\varphi) := \int_\Gamma \nabla_\Gamma w \cdot \nabla_\Gamma \varphi \,\mathrm{d}\sigma \tag{A.2.12}$$

$$l(\varphi) := \int_\Gamma f\varphi \,\mathrm{d}\sigma. \tag{A.2.13}$$

With this notation, (A.2.10) becomes: Find $u \in H^1(\Gamma)$ such that

$$a(u,\varphi) = l(\varphi) \quad \text{for all } \varphi \in H^1(\Gamma), \quad \left(\int_\Gamma u \,\mathrm{d}\sigma = 0, \text{ if } c = 0\right).$$

A.3 Finite element scheme

In this section, we will set out the surface finite element method as described in Dziuk (1988). To keep the presentation clear, we will avoid discussions of more complex variants listed in the introduction chapter.

A.3.1 Triangulated surfaces

The first stage of the method is to construct a polyhedral approximation Γ_h of Γ. We restrict the nodes $\{X_j\}_{j=1}^N$ of Γ_h to lie on Γ. In practice, there are two steps to construct such a triangulation. First a coarse, or macro, triangulation is defined, often constructed by hand. This will have a few, large elements but be sufficiently fine so as to capture essential aspects of the geometry. In particular, Γ_h must lie in U. Then this triangulation is refined using some strategy (for example, bisectional refinement) to make finer triangles. To ensure that this refined triangulation still satisfies our assumptions above, all new nodes are projected onto the surface using

the closest point operator (A.2.2). See Figure A.3.1 for an example using regular refinement and Figure A.3.2 for the results of a local refinement rule.

We take a triangulation $\mathscr{T}_h$ of Γ_h consisting of closed simplices, either line segments ($n = 1$), triangles ($n = 2$) or tetrahedra ($n = 3$). We define h to be the maximum diameter of elements in $\mathscr{T}_h$:

$$h := \max\{\operatorname{diam}(E) : E \in \mathscr{T}_h\}. \tag{A.3.1}$$

We will assume that $\mathscr{T}_h$ is a quasi-uniform triangulation:

Definition A.3.1 (Quasi-uniform triangulation). Let $\{\Gamma_h\}$ be a family of polyhedral approximations of Γ indexed by $h > 0$, each with triangulation $\mathscr{T}_h$. The family $\{\mathscr{T}_h\}$ is said to be quasi-uniform if there exists $\rho > 0$ such that

$$\min\{\operatorname{diam} B_E : E \in \mathscr{T}_h\} \geq \rho h \operatorname{diam} \Gamma$$

for all h, where B_E is the largest ball contained in E.

We say a triangulation $\mathscr{T}_h$ of Γ_h is quasi-uniform if it is part of a quasi-uniform family of triangulations $\{\mathscr{T}_h\}$ of a family of triangulated surfaces $\{\Gamma_h\}$.

The fact the nodes of Γ_h lie on Γ and the regularity of $\mathscr{T}_h$ ensure that Γ_h can be considered as an interpolant of Γ and we may use a Bramble-Hilbert Lemma (Brenner and Scott 2002) to estimate any geometric errors.

The interpolated surface Γ_h is Lipschitz, so we can define $H^1(\Gamma_h)$ with integration on Γ_h with respect to a discrete surface measure $\mathrm{d}\sigma_h$. We define the gradient of a function $\eta_h \colon \Gamma_h \to \mathbb{R}$ element-wise by

$$\nabla_{\Gamma_h} \eta_h|_E := \nabla \widetilde{\eta}_h - (\nabla \widetilde{\eta}_h \cdot \nu_h)\nu_h, \tag{A.3.2}$$

for each $E \in \mathscr{T}_h$ with outward pointing normal ν_h. Here, $\widetilde{\eta}_h$ is some arbitrary extension of η_h away from Γ_h. As with the continuous case, we will write $\nabla_{\Gamma_h} \eta_h = P_h \nabla \eta_h$, with $P_h(x) := \mathrm{Id} - \nu_h(x) \otimes \nu_h(x)$, for $x \in \Gamma_h$.

Given a triangulation $\mathscr{T}_h$ of the discrete surface Γ_h, we next define our surface finite element space which we denote S_h. We take a continuous piecewise linear finite element space on Γ_h. Precisely, this is

$$S_h := \{\phi_h \in C(\Gamma_h) : \phi_h|_E \in P_1(E), \text{ for all } E \in \mathscr{T}_h\}, \tag{A.3.3}$$

where $P_1(\omega)$ denotes the space of affine functions on ω.

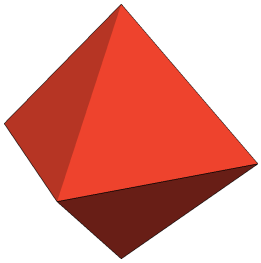

(a) no global refinements (macro triangulation)

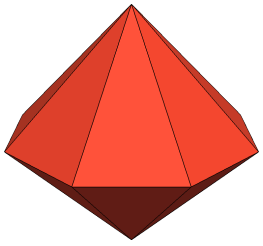

(b) 1 global refinement

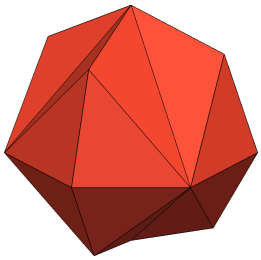

(c) 2 global refinements

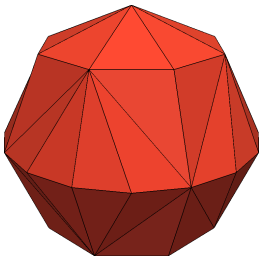

(d) 3 global refinements

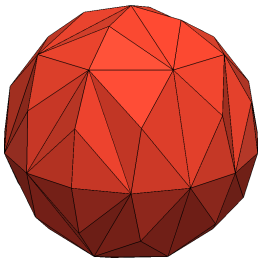

(e) 4 global refinements

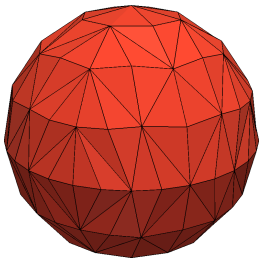

(f) 5 global refinements

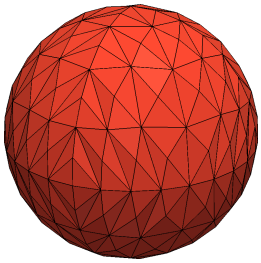

(g) 6 global refinements

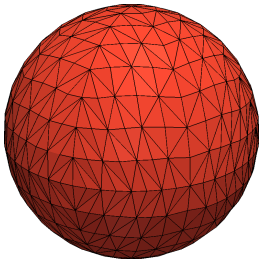

(h) 7 global refinements

Figure A.3.1: The above figures show examples of a sphere going through successive global refinements. Between each triangulation each triangle is split in two using a bisectional refinement and any new nodes are projected to the surface. See Schmidt et al. (2005) for details.

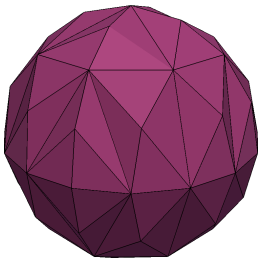

(a) no local refinements (macro triangulation plus 4 global refinements)

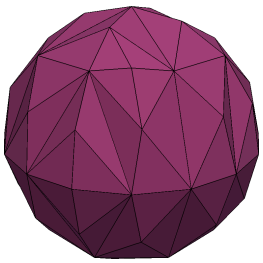

(b) 1 local refinement

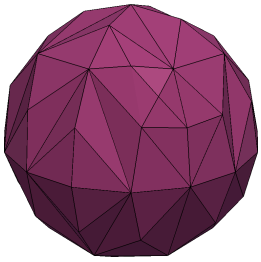

(c) 2 local refinements

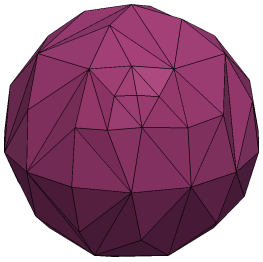

(d) 3 local refinements

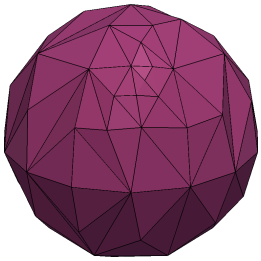

(e) 4 local refinements

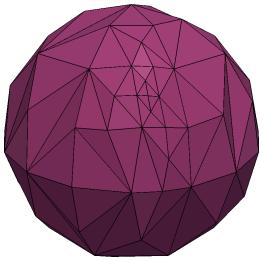

(f) 5 local refinements

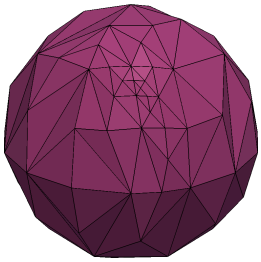

(g) 6 local refinements

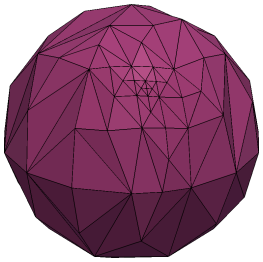

(h) 7 local refinements

Figure A.3.2: The above figures show examples of a sphere going through successive local refinements. Between triangulations one element is marked for refinement then a conforming bisectional refinement algorithm is used refining some neighbouring elements of the marked triangle to ensure the resulting triangulation is still conforming. Again, see Schmidt et al. (2005) for details.

A.3.2 Discrete equations

The finite element method is defined by the problem: Find $U_h \in S_h$ such that

$$\int_{\Gamma_h} \nabla_{\Gamma_h} U_h \cdot \nabla_{\Gamma_h} \phi_h + c\, U_h \phi_h \,\mathrm{d}\sigma_h = \int_{\Gamma_h} \widetilde{f} \phi_h \,\mathrm{d}\sigma_h \quad \text{for all } \phi_h \in S_h, \qquad \left(\int_{\Gamma_h} U_h \,\mathrm{d}\sigma_h = 0 \text{ if } c = 0 \right). \tag{A.3.4}$$

Here $\widetilde{f} \in L^2(\Gamma_h)$ is some approximation of f which we assume satisfies:

$$\left\| \widetilde{f} \right\|_{L^2(\Gamma_h)} \leq c \, \|f\|_{L^2(\Gamma)} \qquad \left(\text{and } \int_{\Gamma_h} \widetilde{f} \,\mathrm{d}\sigma_h = 0 \text{ if } c = 0 \right). \tag{A.3.5}$$

Theorem A.3.2 (Well-posedness)**.** *There exists a unique solution U_h to the finite element method* (A.3.4) *that satisfies the bound*

$$\|U_h\|_{H^1(\Gamma_h)} \leq c \, \|f\|_{L^2(\Gamma)} . \tag{A.3.6}$$

Proof. The proof follows a very similar route to Theorem A.2.5. We use the usual Lax-Milgram techniques to show existence and uniqueness of a solution using a Poincaré inequality to ensure the bilinear form is coercive in the case $c = 0$. The bound follows by testing (A.3.4) and using the assumption (A.3.5). □

We will also define the abstract bilinear forms, $a_h \colon S_h \times S_h \to \mathbb{R}$ and $l_h \colon S_h \to \mathbb{R}$, to describe (A.3.4) as discrete counterparts to (A.2.12, A.2.13) by

$$a_h(W_h, \phi_h) := \int_{\Gamma_h} \nabla_{\Gamma_h} W_h \cdot \nabla_{\Gamma_h} \phi_h + c W_h \phi_h \,\mathrm{d}\sigma_h \tag{A.3.7}$$

$$l_h(\phi_h) := \int_{\Gamma_h} \widetilde{f} \phi_h \,\mathrm{d}\sigma_h. \tag{A.3.8}$$

This lets us to rewrite (A.3.4) as: Find $U_h \in S_h$ such that

$$a_h(U_h, \phi_h) = l_{\Gamma_h}(\phi_h) \quad \text{for all } \phi_h \in S_h.$$

A.3.3 Isoparametric finite elements

One may also use a higher-order approximation of the surface, equal to a higher-order to finite element space. This leads to so-called isoparametric finite element methods.

Under the assumption of higher regularity of Γ, we start by constructing an initial polyhedral approximation, as above, $\Gamma_h^{(1)}$, with triangulation $\mathscr{T}_h^{(1)}$. For each

element $E \in \mathscr{T}_h^{(1)}$, $p|_E$ maps to a unique "curved element" $e = p(E)$ on Γ. We denote by p_k the Lagrangian interpolation of p over E of order k. We can consider a kth order polynomial approximation of e over E using $p_k(E) = E^{(k)}$. We define the union of all such polynomially curved elements $\{E^{(k)} : E \in \mathscr{T}_h^{(1)}\} =: \mathscr{T}_h^{(k)}$ to be a triangulation of a kth order approximation $\Gamma_h^{(k)}$ of Γ.

We define a kth order finite element space $S_h^{(k)}$ by

$$S_h^{(k)} := \{\phi_h \in C(\Gamma_h) : \phi_h|_{E^{(k)}} \circ (p_k)^{-1} \in P_k(E) \text{ for all } E^{(k)} \in \mathscr{T}_h^{(k)}\},$$

where $P_k(\omega)$ is the space of piecewise polynomial functions of degree k over ω.

The finite element method is to solve (A.3.4) over $S_h^{(k)}$: Find $U_h^{(k)} \in S_h^{(k)}$ such that

$$\int_{\Gamma_h} \nabla_{\Gamma_h^{(k)}} U_h^{(k)} \cdot \nabla_{\Gamma_h} \phi_h + c\, U_h^{(k)} \phi_h \,\mathrm{d}\sigma_h = \int_{\Gamma_h^{(k)}} \widetilde{f} \phi_h \,\mathrm{d}\sigma_h \quad \text{for all } \phi_h \in S_h^{(k)}, \left(\int_{\Gamma_h^{(k)}} U_h^{(k)} \,\mathrm{d}\sigma_h = 0 \text{ if } c = 0 \right). \tag{A.3.9}$$

Similarly to the results in the rest of this chapter, this higher order approximation leads to the following error bound:

Theorem A.3.3 (Higher order error bound)**.** *Let $u \in H^{k+1}(\Gamma)$ be the solution of (A.1.1) and $U_h^{(k)} \in S_h^{(k)}$ be the solution of (A.3.9) with lift $u_h^{(k)} = (U_h^{(k)})^\ell$. Then, we have the estimate*

$$\left\| u - u_h^{(k)} \right\|_{L^2(\Gamma)} + h \left\| \nabla_\Gamma (u - u_h^{(k)}) \right\|_{L^2(\Gamma)} \leq c h^{k+1} \left(\|u\|_{H^{k+1}(\Gamma)} + \|f\|_{L^2(\Gamma)} \right). \tag{A.3.10}$$

The proof of this result can be found in Demlow (2009). We will not give the details here.

A.4 Abstract error analysis

In order to derive error estimates for the surface finite element method, we must estimate the errors from two effects. First, as with planar domains, we must estimate the error by restricting the test and solution spaces to finite-dimensional approximations of $H^1(\Gamma)$. This is often called the interpolation error since it is usually bounded using results from interpolation theory. Secondly, we have introduced a further error to the planar case; since $S_h \not\subseteq H^1(\Gamma)$. The second errors are called

variational crimes; see Brenner and Scott (2002, Chapter 8) or Strang and Fix (2008, Chapter 4) for a more general overview of variational crimes.

We treat this abstractly using two lemmas. Both results can be used for the finite element analysis of methods with variational crimes. The first is a generalisation of Céa's Lemma (often called the Strang Lemma) and the second is a slight variation on the classical Aubin-Nitsche trick. The extra terms in each represent the residual of the discrete solution in the continuous equations; in the case of Galerkin orthogonality these terms will evaluate to zero.

Let $V_h \subseteq V$ and let a be a bilinear form and l be a linear form on V. Further, let a_h, l_h be bilinear and linear forms on V_h. We will assume that each pair satisfies the assumptions of the Lax-Milgram theorem. Suppose that $u \in V$ and $u_h \in V_h$ satisfy

$$a(u, \varphi) = l(\varphi) \quad \text{for all } \varphi \in V \tag{A.4.1a}$$

$$a_h(u_h, \varphi_h) = l_h(\varphi_h) \quad \text{for all } \varphi_h \in V_h. \tag{A.4.1b}$$

We will write $\|\cdot\|_a$ for the norm induced by the bilinear form a:

$$\|\eta\|_a := a(\eta, \eta)^{\frac{1}{2}}, \quad \text{for } \eta \in V.$$

Lemma A.4.1 (Strang Lemma)**.** *Let the above assumptions hold. Define $F_h \colon V_h \to \mathbb{R}$ by*

$$F_h(\phi_h) := a(u - u_h, \phi_h), \tag{A.4.2}$$

then

$$\|u - u_h\|_a \leq 2 \inf_{v_h \in V_h} \|u - v_h\|_a + \sup_{w_h \in V_h \setminus \{0\}} \frac{F_h(w_h)}{\|w_h\|_a}. \tag{A.4.3}$$

Proof. For any $v_h \in V_h$,

$$\begin{aligned}
\|u - u_h\|_a &\leq \|u - v_h\|_a + \|v_h - u_h\|_a \\
&= \|u - v_h\|_a + a(v_h - u_h, v_h - u_h)^{\frac{1}{2}} \\
&\leq \|u - v_h\|_a + \sup_{w_h \in V_h \setminus \{0\}} \frac{a(v_h - u_h, w_h)}{\|w_h\|_a} \\
&\leq 2 \|u - v_h\|_a + \sup_{w_h \in V_h \setminus \{0\}} \frac{a(u - u_h, w_h)}{\|w_h\|_a}.
\end{aligned}$$

□

Next, we suppose that we have a further Hilbert space $(H, \langle \cdot, \cdot \rangle_H)$ and a Banach space $(Z, \|\cdot\|_Z)$ with $Z \subset V \subset H$ with each inclusion continuous. This

implies that for $\zeta \in H$, the functional

$$\chi_\zeta(\varphi) = \langle \zeta, \varphi \rangle_H,$$

is a bounded linear functional on V with

$$|\chi_\zeta(\varphi)| \leq \|\zeta\|_H \|\varphi\|_H \leq c \|\zeta\|_H \|\varphi\|_V .$$

Hence, there exists a unique solution $z \in V$ of

$$a(\varphi, z) = \chi_\zeta(\varphi) \quad \text{for all } \varphi \in V. \tag{A.4.4}$$

We assume that the solution $z \in Z$ and satisfies the bound

$$\|z\|_Z \leq c \|\zeta\|_H . \tag{A.4.5}$$

Further, we assume that for all $v \in Z$ there exists $v_h^* \in V_h$ satisfying

$$\|v - v_h^*\|_a \leq ch \|v\|_Z . \tag{A.4.6}$$

Lemma A.4.2 (Abstract Aubin-Nitsche)**.** *Let the above assumptions hold and let $e \in V$. Define $F_h \colon V_h \to \mathbb{R}$ by*

$$F_h(\phi_h) = a(e, \phi_h), \tag{A.4.7}$$

then

$$\|e\|_H \leq ch \|e\|_a + \sup_{\phi_h \in V_h \setminus \{0\}} \frac{F_h(\phi_h)}{\|\phi_h\|_a}. \tag{A.4.8}$$

Proof. Since $e \in V \subset H$, from our assumptions (A.4.4) and (A.4.5), there exists a unique $z \in Z$ such that

$$a(\varphi, z) = \chi_e(\varphi) \quad \text{for all } \varphi \in V,$$

and

$$\|z\|_Z \leq c \|e\|_H .$$

Further, by the assumption (A.4.6), we know there exists $z_h^* \in V_h$ with

$$\|z - z_h^*\|_a \leq ch \|z\|_Z .$$

Then, we calculate

$$\begin{aligned}
\|e\|_H^2 &= \langle e, e\rangle_H \\
&= a(e, z) \\
&= a(e, z - z_h^*) + a(e, z_h^*) \\
&\leq \left(ch \|e\|_a + \sup_{\phi_h \in V_h \setminus \{0\}} \frac{a(e, \phi_h)}{\|\phi_h\|_a} \right) \|z\|_Z \\
&\leq \left(ch \|e\|_a + \sup_{\phi_h \in V_h \setminus \{0\}} \frac{a(e, \phi_h)}{\|\phi_h\|_a} \right) \|e\|_H .
\end{aligned}$$

Dividing by $\|e\|_H$ gives the result. □

A.5 Domain perturbation

In this section, we will look to bound any errors in our finite element method coming from the domain approximation. To do this, we will use some standard interpolation results to show in what sense the two surfaces are 'close' and then interpret this in a more geometric sense. This geometric interpretation is sufficient to bound the errors arising from the variation crime.

Lemma A.5.1 (Surface interpolation)**.** *Let d be the signed distance function to Γ and ν and ν_h the unit normal vector fields to Γ and Γ_h, respectively. Then*

$$\|d\|_{L^\infty(\Gamma_h)} \leq ch^2 \tag{A.5.1a}$$

$$\|\nu_j - (\nu_h)_j\|_{L^\infty(\Gamma_h)} \leq ch \quad \text{for } j = 1, \ldots, n+1. \tag{A.5.1b}$$

Proof. Both results follow from standard interpolation theory (Brenner and Scott 2002, Chapter 4). Since the nodes of Γ_h lie on Γ, standard Lagrange interpolation yields $I_h d = 0$ on Γ_h, hence we have that

$$\|d\|_{L^\infty(\Gamma_h)} = \|d - I_h d\|_{L^\infty(\Gamma_h)} \leq ch^2 \|d\|_{W^{1,\infty}(\Gamma_h)} \leq ch^2.$$

The second result follows since $\nu_j - (\nu_h)_j = \partial_{x_j} d$. □

The next result interprets these bounds in a more geometric setting

Lemma A.5.2 (Geometric interpretation)**.** *Let μ_h denote the quotient of measures*

on Γ *and* Γ_h *so that* $\mathrm{d}\sigma = \mu_h \,\mathrm{d}\sigma_h$*, then*

$$\sup_{\Gamma_h} |1 - \mu_h| \leq ch^2. \tag{A.5.2}$$

Let $\mathcal{Q}_h = \frac{1}{\mu_h}(\mathrm{Id} - d\mathcal{H})PP_hP(\mathrm{Id} - d\mathcal{H})$*; then*

$$\sup_{\Gamma_h} |P - \mathcal{Q}_h| \leq ch^2. \tag{A.5.3}$$

Proof. This proof is given by Dziuk and Elliott (2007a), although the original result is from the original work of Dziuk (1988).

To simplify the presentation, we will consider a single element $E \in \mathscr{T}_h$ in a two-dimensional surface, with an associated curved element $e = p(E)$. We will assume further that $E \subset \mathbb{R}^2 \times \{0\}$.

For $x = (x_1, x_2, 0) \in E$, we have by (A.2.2) that the map p satisfies

$$p_{i,x_j} = \delta_{ji} - \nu_j\nu_i - d\mathcal{H}_{ij}.$$

Furthermore, our simplifications imply that $\mathrm{d}\sigma_h = \mathrm{d}x_1\,\mathrm{d}x_2$ and $\mathrm{d}\sigma = |p_{x_1} \times p_{x_2}|\,\mathrm{d}x_1\,\mathrm{d}x_2$, so we have that

$$\mu_h = |p_{x_1} \times p_{x_2}|\,.$$

To derive the estimate (A.5.2), we observe from (A.5.1a) that

$$p_{i,x_j} = \delta_{ji} - \nu_j\nu_i - d\mathcal{H}_{ij} = P_{ji} + O(h^2).$$

This implies, with e_j written for the jth standard basis function in $\mathbb{R}^3$, that

$$\begin{aligned} p_{x_1} \times p_{x_2} &= (e_1 - \nu_1\nu - d\nu_{x_1}) \times (e_2 - \nu_2\nu - d\nu_{x_2}) \\ &= (e_1 - \nu_1\nu) \times (e_2 - \nu_2\nu) + O(h^2) \\ &= e_3 - \nu_2 e_1 \times \nu - \nu_1\nu \times e_2 + O(h^2) \\ &= \nu_3\nu + O(h^2), \end{aligned}$$

and that

$$|p_{x_1} \times p_{x_2}|^2 = |\nu_3\nu|^2 + O(h^2) = 1 - \nu_1^2 - \nu_2^2 + O(h^2).$$

Hence, from (A.5.1b),

$$|1-\mu_h| = |1-|p_{x_1}\times p_{x_2}|| = \frac{\left|1-|p_{x_1}\times p_{x_2}|^2\right|}{1+|p_{x_1}\times p_{x_2}|} = \frac{\nu_1^2+\nu_2^2+O(h^2)}{1+|p_{x_1}\times p_{x_2}|} \leq ch^2.$$

To show the second bound, we note that

$$P - \frac{1}{\mu_h}(\mathrm{Id}-d\mathcal{H})PP_hP(\mathrm{Id}-d\mathcal{H}) = P - PP_hP + O(h^2) = (P\nu_h)\otimes(P\nu_h) + O(h^2).$$

We use the fact that $\nu_h = e_3$ to get

$$|P\nu_h| = |\nu_h - (\nu\cdot\nu_h)\nu_h| = |e_3 - \nu_3\nu| = \sqrt{1-\nu_1^2-\nu_2^2} = O(h).$$

Hence (A.5.3) is shown. □

A.6 Error bounds

In this section we will prove an error bound for the surface finite element method. The idea is to combine the abstract lemmas from Section A.4 with the geometric estimates from Section A.5. The final part to bring these together is that we need to construct some way to transform our finite element space S_h into the abstract space $V_h \subset V$. We do this using a lifting procedure.

We define the lift operator for functions on Γ_h using the closest point operator (A.2.2). We remark that $p|_{\Gamma_h}$ is a homeomorphism onto Γ. For a function $\eta_h\colon \Gamma_h \to \mathbb{R}$, we define its lift, $\eta_h^\ell\colon \Gamma \to \mathbb{R}$, implicitly by

$$\eta_h^\ell(p(x)) := \eta_h(x) \quad \text{for } x\in\Gamma_h. \tag{A.6.1}$$

We can also define an inverse lift operator for a function $\eta\colon \Gamma\to\mathbb{R}$

$$\eta^{-\ell}(x) := \eta(p(x)) \quad \text{for } x\in\Gamma_h. \tag{A.6.2}$$

We will write $\eta^e(x) := \eta(p(x))$, for $x\in U$, for the extension of η to U using (A.6.2) so that $\eta^{-\ell} = \eta^e|_{\Gamma_h}$.

Lemma A.6.1. *Let $E\in\mathscr{T}_h$ and $e = p(E)\subset\Gamma$. There exist constants $c_1, c_2 > 0$, independent of E and h, such that for all $\eta_h\colon\Gamma_h\to\mathbb{R}$, such that the following*

quantities exist, we have

$$c_1 \left\| \eta_h^\ell \right\|_{L^2(e)} \leq \|\eta_h\|_{L^2(E)} \leq c_2 \left\| \eta_h^\ell \right\|_{L^2(e)} \tag{A.6.3a}$$

$$c_1 \left\| \nabla_\Gamma \eta_h^\ell \right\|_{L^2(e)} \leq \|\nabla_{\Gamma_h} \eta_h\|_{L^2(E)} \leq c_2 \left\| \nabla_\Gamma \eta_h^\ell \right\|_{L^2(e)} \tag{A.6.3b}$$

$$\left\| \nabla^2_{\Gamma_h} \eta_h \right\|_{L^2(E)} \leq c_2 \big(\|\eta\|_{H^2(e)} + h \|\nabla_\Gamma \eta\|_{L^2(e)} \big). \tag{A.6.3c}$$

Proof. This comes from writing

$$\int_{\Gamma_h} \eta_h^2 \, \mu_h \, \mathrm{d}\sigma_h = \int_\Gamma (\eta_h^\ell)^2 \, \mathrm{d}\sigma,$$

and

$$\nabla_{\Gamma_h} \eta_h = P_h (P - d\mathcal{H}) \nabla \eta_h^\ell = P_h (\mathrm{Id} - d\mathcal{H}) \nabla_\Gamma \eta_h^\ell,$$

and applying the results of Lemma A.5.2. □

For an arbitrary test function ϕ_h, we will denote its lift by $\varphi_h = \phi_h^\ell$. Similarly, we will use lower case letters for lifted versions of upper case-named finite element functions: $u_h = U_h^\ell, w_h = W_h^\ell$.

We will write S_h^ℓ for the space of lifted finite element functions:

$$S_h^\ell = \{ \varphi_h = \phi_h^\ell : \phi_h \in S_h \}.$$

We remark that Lemma A.6.1 implies $S_h^\ell \subseteq H^1(\Gamma)$. The space of lifted finite element functions comes with the following approximation property:

Proposition A.6.2 (Approximation property)**.** *Let $z \in H^2(\Gamma)$. The lift of the nodal interpolant of z, for which we will write $I_h z \in S_h^\ell$, is a well defined function in S_h^ℓ and satisfies the following bound:*

$$\|z - I_h z\|_{H^1(\Gamma)} \leq ch \|z\|_{H^2(\Gamma)}. \tag{A.6.4}$$

Proof. This proof is taken from Dziuk (1988).

From Sobolev embedding, z is continuous, and so that linear (nodal) interpolant $\widetilde{I}_h z \in S_h$ is well defined by

$$\widetilde{I}_h z(X_j) = z(X_j) \quad \text{for } j = 1, \ldots, N, \quad \text{and} \quad \widetilde{I}_h z \in P_1(E) \quad \text{for all } E \in \mathscr{T}_h.$$

Standard interpolation theory (Ciarlet 1978; Brenner and Scott 2002) gives that

$$\left\| z^{-\ell} - \widetilde{I}_h z^{-\ell} \right\|_{H^1(E)} \leq ch \left\| \nabla^2_{\Gamma_h} z^{-\ell} \right\|_{H^2(E)} \qquad \text{for each } E \in \mathscr{T}_h.$$

We define $I_h z = (\widetilde{I}_h z)^\ell$. The stability of the lifting process (Lemma A.6.1) implies

$$\begin{aligned} \|z - I_h z\|_{H^1(\Gamma)} &\leq c \left\| z^{-\ell} - \widetilde{I}_h z^{-\ell} \right\|_{H^1(\Gamma_h)} \\ &\leq ch \left(\sum_{E \in \mathscr{T}_h} \left\| \nabla^2_{\Gamma_h} z^{-\ell} \right\|^2_{L^2(E)} \right)^{\frac{1}{2}} \\ &\leq ch \big(\|z\|_{H^2(\Gamma)} + h \|\nabla_\Gamma z\|_{L^2(\Gamma)} \big). \end{aligned}$$

□

This answers the question about the first type of errors. The results from Section A.5 allow us to bound the second.

Lemma A.6.3 (Geometric bound)**.** *Let $W_h, \phi_h \in S_h$ with lifts $w_h, \varphi_h \in S_h^\ell$; then*

$$|a(w_h, \varphi_h) - a_h(W_h, \phi_h)| \leq ch^2 \|\nabla_\Gamma w_h\|_{L^2(\Gamma)} \|\nabla_\Gamma \varphi_h\|_{L^2(\Gamma)}. \tag{A.6.5}$$

Proof. We start by bounding the lower-order terms. Using (A.5.2), we infer that

$$\begin{aligned} \left| \int_\Gamma w_h \varphi_h \, \mathrm{d}\sigma - \int_{\Gamma_h} W_h \phi_h \, \mathrm{d}\sigma_h \right| &= \left| \int_\Gamma w_h \varphi_h \left(1 - \frac{1}{\mu_h^\ell} \right) \mathrm{d}\sigma \right| \\ &\leq \sup_\Gamma \left| 1 - \frac{1}{\mu_h^\ell} \right| \|w_h\|_{L^2(\Gamma)} \|\varphi_h\|_{L^2(\Gamma)} \\ &\leq c \sup_{\Gamma_h} |1 - \mu_h| \, \|w_h\|_{L^2(\Gamma)} \|\varphi_h\|_{L^2(\Gamma)} \\ &\leq ch^2 \|w_h\|_{L^2(\Gamma)} \|\varphi_h\|_{L^2(\Gamma)}. \end{aligned}$$

Next, we see since $P\mathcal{H} = \mathcal{H}P = \mathcal{H}$ that

$$\nabla_{\Gamma_h} W_h = P_h(P - d\mathcal{H})\nabla w_h = P_h(\mathrm{Id} - d\mathcal{H})\nabla_\Gamma w_h.$$

Hence, since P and $\mathcal{H}$ are symmetric, we obtain the identity

$$\begin{aligned}
&\int_{\Gamma_h} \nabla_{\Gamma_h} W_h \cdot \nabla_{\Gamma_h} \phi_h \,\mathrm{d}\sigma_h \\
&\quad = \int_\Gamma P_h(\mathrm{Id} - d\mathcal{H})\nabla_\Gamma w_h \cdot P_h(\mathrm{Id} - d\mathcal{H})\nabla_\Gamma \varphi_h \frac{1}{\mu_h^\ell} \,\mathrm{d}\sigma \\
&\quad = \int_\Gamma \frac{1}{\mu_h^\ell}(\mathrm{Id} - d\mathcal{H})PP_hP(\mathrm{Id} - d\mathcal{H})\nabla_\Gamma w_h \cdot \nabla_\Gamma \varphi_h \,\mathrm{d}\sigma \\
&\quad = \int_\Gamma \mathcal{Q}_h^\ell \nabla_\Gamma w_h \cdot \nabla_\Gamma \varphi_h \,\mathrm{d}\sigma.
\end{aligned} \tag{A.6.6}$$

This implies, using (A.5.3), that

$$\begin{aligned}
&\left| \int_\Gamma \nabla_\Gamma w_h \cdot \nabla_\Gamma \varphi_h \,\mathrm{d}\sigma - \int_{\Gamma_h} \nabla_{\Gamma_h} W_h \cdot \nabla_{\Gamma_h} \phi_h \,\mathrm{d}\sigma_h \right| \\
&\quad = \left| \int_\Gamma \nabla_\Gamma w_h \cdot \nabla_\Gamma \varphi_h \,\mathrm{d}\sigma - \int_\Gamma \frac{1}{\mu_h}(P - d\mathcal{H})P_h(P - d\mathcal{H})\nabla_\Gamma w_h \cdot \nabla_\Gamma \varphi_h \mu_h \,\mathrm{d}\sigma \right| \\
&\quad = \left| \int_\Gamma (P - \mathcal{Q}_h^\ell)\nabla_\Gamma w_h \cdot \nabla_\Gamma \varphi_h \,\mathrm{d}\sigma \right| \\
&\quad \leq \sup_\Gamma \left| P - \mathcal{Q}_h^\ell \right| \|\nabla_\Gamma w_h\|_{L^2(\Gamma)} \|\nabla_\Gamma \varphi_h\|_{L^2(\Gamma)} \\
&\quad \leq \sup_{\Gamma_h} |P - \mathcal{Q}_h| \, \|\nabla_\Gamma w_h\|_{L^2(\Gamma)} \|\nabla_\Gamma \varphi_h\|_{L^2(\Gamma)} \\
&\quad \leq ch^2 \|\nabla_\Gamma w_h\|_{L^2(\Gamma)} \|\nabla_\Gamma \varphi_h\|_{L^2(\Gamma)} .
\end{aligned}$$

□

We have not specified the $\widetilde{f}$ which occurs in the bilinear form l_h. We consider two possible choices:

Lemma A.6.4. *Let $\phi_h \in S_h$ with lift $\varphi_h \in S_h^\ell$. If $\widetilde{f} = f^{-\ell}$, then*

$$|l(\varphi_h) - l_h(\phi_h)| \leq ch^2 \|f\|_{L^2(\Gamma)} . \tag{A.6.7}$$

Alternatively, if $\widetilde{f} = f\mu_h$, then

$$|l(\varphi_h) - l_h(\phi_h)| = 0. \tag{A.6.8}$$

Proof. Both results follow in a similar fashion to the bound of the lower order term in the previous lemma. □

Remark A.6.5. Neither of these choices are fully practical for $f \in L^2(\Gamma)$ and would have to be approximated by some quadrature rules. We do not wish to study these errors in this thesis and will assume that these terms can be calculated exactly. In

the following numerical examples, we will use $\widetilde{f} = \widetilde{I}_h f$ for some smoother examples of f.

Theorem A.6.6 (Error bounds)**.** *Let $u \in H^2(\Gamma)$ be the solution of (A.1.1) and let $U_h \in S_h$ be the solution of (A.3.4) with lift $u_h = U_h^\ell$. Let either of the results from A.6.4 hold. Then, we have the estimate*

$$\|u - u_h\|_{L^2(\Gamma)} + h \|\nabla_\Gamma (u - u_h)\|_{L^2(\Gamma)} \leq ch^2 \|f\|_{L^2(\Gamma)}. \tag{A.6.9}$$

Proof. This proof follows by applying the abstract lemma. We consider $V = H^1(\Gamma)$ and the finite element space $V_h = S_h^\ell$. The abstract notation for the continuous problem fits exactly for a and l. We apply the result with

$$\begin{aligned} a_h(w_h, \varphi_h) &:= \int_{\Gamma_h} \nabla_{\Gamma_h} W_h \cdot \nabla_{\Gamma_h} \phi_h + W_h \phi_h \, \mathrm{d}\sigma_h \\ l_h(\varphi_h) &:= \int_{\Gamma_h} \widetilde{f} \phi_h \, \mathrm{d}\sigma_h, \end{aligned}$$

with $w_h = W_h^\ell$ and $\varphi_h = \phi_h^\ell$.

For $F_h(\varphi_h) = a(u - u_h, \varphi_h)$ using the geometric bounds from Lemmas A.6.3 and A.6.4, along with the stability bound (A.3.6), we have

$$\begin{aligned} F_h(\varphi_h) &= a(u - u_h, \varphi_h) = l(\varphi_h) - a(u_h, \varphi_h) \\ &= \big(l(\varphi_h) - l_h(\phi_h)\big) + \big(a_h(U_h, \phi_h) - a(u_h, \varphi_h)\big) \\ &\leq ch^2 \|f\|_{L^2(\Gamma)} \|\varphi_h\|_{H^1(\Gamma)} + ch^2 \|U_h\|_{H^1(\Gamma_h)} \|\varphi_h\|_{H^1(\Gamma)} \\ &\leq ch^2 \|f\|_{L^2(\Gamma)} \|\varphi_h\|_{H^1(\Gamma)}. \end{aligned} \tag{A.6.10}$$

The Strang Lemma (Lemma A.4.1) tells us that

$$\|u - u_h\|_{H^1(\Gamma)} \leq c \inf_{v_h \in S_h^\ell} \|u - v_h\|_{H^1(\Gamma)} + c \sup_{\varphi_h \in S_h^\ell \setminus \{0\}} \frac{F_h(\varphi_h)}{\|\varphi_h\|_{H^1(\Gamma)}}.$$

The first term is bounded by the approximation property (Proposition A.6.2) to give

$$\inf_{v_h \in S_h^\ell} \|u - v_h\|_{H^1(\Gamma)} \leq \|u - I_h u\|_{H^1(\Gamma)} \leq ch \|u\|_{H^2(\Gamma)} \leq ch \|f\|_{L^2(\Gamma)}.$$

Combing with (A.6.10) we have shown that

$$\|u - u_h\|_{H^1(\Gamma)} \leq ch \|f\|_{L^2(\Gamma)}. \tag{A.6.11}$$

To show the improved L^2 estimate, we consider the abstract Aubin-Nitsche lemma, with $H = L^2(\Gamma)$ and $Z = H^2(\Gamma)$. The regularity result (A.2.11) gives us the dual regularity result and the approximation property (A.6.4) gives us (A.4.6). Hence (A.4.8), with $e = u - u_h$, tells us that

$$\|u - u_h\|_{L^2(\Gamma)} \leq ch \|u - u_h\|_{H^1(\Gamma)} + \sup_{\varphi_h \in S_h^\ell \setminus \{0\}} \frac{F_h(\varphi_h)}{\|\varphi_h\|_{H^1(\Gamma)}}$$

The first term is bounded using the H^1 norm bound (A.6.11):

$$ch \|u - u_h\|_{H^1(\Gamma)} \leq ch^2 \|f\|_{L^2(\Gamma)} .$$

Again, combining with (A.6.10) we have shown

$$\|u - u_h\|_{L^2(\Gamma)} \leq ch^2 \|f\|_{L^2(\Gamma)} . \qquad \square$$

A.7 Numerical results

We conclude this section with numerical evidence for the result from Theorem A.6.6. We also include some other indicators of the efficiency of this method in comparison with the other methods presented in this thesis.

A.7.1 Details of implementation

All methods in this thesis (unless otherwise specified) were implemented using the Distributed and Unified Numerics Environment (DUNE) (Bastian, Blatt, Dedner, Engwer, Klöfkorn, Ohlberger and Sander 2008b; Bastian, Blatt, Dedner, Engwer, Klöfkorn, Kornhuber, Ohlberger and Sander 2008a). DUNE is a "generic grid interface for parallel and adaptive scientific computing" written in C++. This means that DUNE provides an interface (set of libraries) for using different grid managers on which finite element codes can be based. In this thesis we use the ALBERTA (Schmidt et al. 2005) and ALUGrid (Burri, Dedner, Klöfkorn and Ohlberger 2006) interfaces. Both grid managers have a bisectional refinement and coarsening algorithms implemented and ALUGrid also runs in parallel for three dimensional meshes. Implementation of the routines for assembling the matrices were written using the DUNE-FEM modules (Dedner, Klöfkorn, Nolte and Ohlberger 2010) and the resulting systems were solved using the DUNE-FEM interface to the DUNE-ISTL module (Blatt and Bastian 2007; Bastian and Blatt 2008). The DUNE-ISTL module provides optimised implementations of preconditioned methods such as the conjugate

gradient method, generalised minimal residual method, and the biconjugate gradient stabilised method which when linked to a parallel grid manager can all be run in parallel also.

Surface macro triangulations were either created by hand or using the CGAL 3D surface mesh generation routines (Rineau and Yvinec 2013). Visualisation is performed with ParaView (Henderson 2012) or matplotlib (Hunter 2007, 2012) for planar images and graphs.

A.7.2 Numerical examples

We will consider three examples of surfaces in this section: a sphere, a torus and the Dziuk surface (taken from Dziuk 1988). On each surface, we will solve

$$-\Delta_\Gamma u + u = f,$$

with an appropriate right-hand side to produce and exact solution which we can calculate by hand. In each case we calculate f using an extension $\widetilde{u}$ of u to ambient coordinates applying the formula

$$f = -(P\nabla)\cdot(P\nabla)\widetilde{u} + \widetilde{u} = -\sum_{i,j,k=1}^{n+1}(\delta_{ik}-\nu_i\nu_k)\partial_{x_k}\big((\delta_{ij}-\nu_i\nu_j)\partial_{x_j}\widetilde{u}\big) + \widetilde{u}.$$

On the sphere, we calculate a right-hand side f so that

$$u(x,y,z) = \cos(2\pi x)\cos(2\pi y)\cos(2\pi z).$$

We parameterise the torus by

$$x = (R - r\cos\theta)\cos\varphi, \quad y = (R - r\cos\theta)\cos\varphi, \quad z = r\sin\theta, \quad \text{for } \theta,\varphi \in (-\pi,\pi).$$

and take the exact solution

$$u(\theta,\varphi) = \cos(3\varphi)\sin(3\theta+\varphi).$$

Finally, on the Dziuk surface, we take a right hand side f such that the exact solution is

$$u(x,y,z) = xy.$$

In this case we solve the system of linear equations using a Jacobi precondi-

tioned conjugate gradient method. We start from a macro triangulation and perform successive global refinements to construct a sequence of meshes. At each mesh size, we calculate the mesh size h_i, the number of elements $|\mathscr{T}_{h_i}|$, the number of degrees of freedom (i.e. number of nodes). We then solve the finite element scheme on that mesh computing the number of conjugate gradient iterations and the errors $\|u^e - U_{h_i}\|_{L^2(\Gamma_{h_i})}$ and $\left\|\nabla_{\Gamma_{h_i}}(u^e - U_{h_i})\right\|_{L^2(\Gamma_{h_i})}$. Given an error E_i and E_{i-1} at two different mesh sizes h_i and h_{i-1}, we calculate the experimental order of convergence (eoc) by

$$(\text{eoc})_i = \frac{\log(E_i/E_{i-1})}{\log(h_i/h_{i-1})}. \tag{A.7.1}$$

We remark that in all three examples we observe that error reduces as order $O(h)$ in the H^1 semi-norm and as $O(h^2)$ in the L^2 norm, which agrees with the theoretical results from Theorem A.6.6. We also see that the number of conjugate gradient iterations roughly doubles between each mesh refinement, so that the number of solver iterations scales with the number of degrees of freedom.

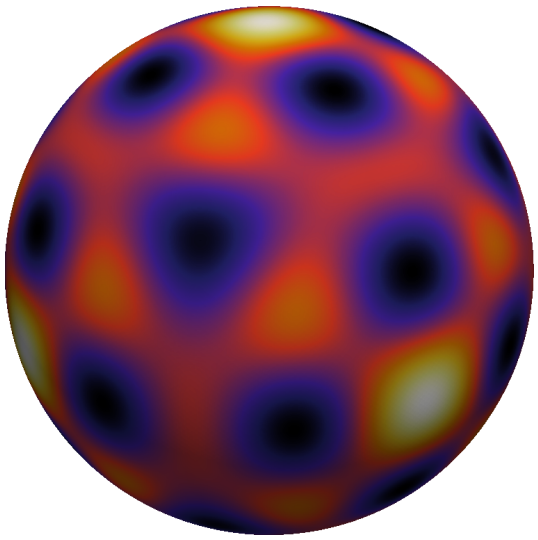

(a) Solution plotted on Γ

h	L^2 error	(eoc)	H^1 error	(eoc)
1.15470	$1.55366 \cdot 10^{+2}$	—	$1.56072 \cdot 10^{+2}$	—
$6.50115 \cdot 10^{-1}$	$1.44636 \cdot 10^{+1}$	4.132932	$1.65080 \cdot 10^{+1}$	3.910672
$3.37267 \cdot 10^{-1}$	$5.02331 \cdot 10^{-1}$	5.120010	6.61163	1.394257
$1.70294 \cdot 10^{-1}$	$1.37203 \cdot 10^{-1}$	1.899174	3.65870	0.865916
$8.53594 \cdot 10^{-2}$	$3.58699 \cdot 10^{-2}$	1.942448	1.87968	0.964310
$4.27064 \cdot 10^{-2}$	$9.09338 \cdot 10^{-3}$	1.981673	$9.46985 \cdot 10^{-1}$	0.989967
$2.13565 \cdot 10^{-2}$	$2.28281 \cdot 10^{-3}$	1.994451	$4.74475 \cdot 10^{-1}$	0.997232
$1.06787 \cdot 10^{-2}$	$5.71398 \cdot 10^{-4}$	1.998364	$2.37370 \cdot 10^{-1}$	0.999255

h	elements	degrees of freedom	solver iter.
1.15470	24	14	10
$6.50115 \cdot 10^{-1}$	96	50	18
$3.37267 \cdot 10^{-1}$	384	194	28
$1.70294 \cdot 10^{-1}$	1 536	770	49
$8.53594 \cdot 10^{-2}$	6 144	3 074	92
$4.27064 \cdot 10^{-2}$	24 576	12 290	176
$2.13565 \cdot 10^{-2}$	98 304	49 154	333
$1.06787 \cdot 10^{-2}$	393 216	196 610	634

(b) Error table with experimental orders of convergence

Table A.1: Results for surface finite element method on a sphere.

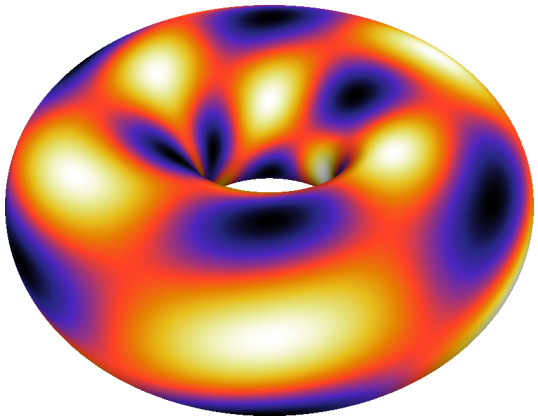

(a) Solution plotted on Γ

h	L^2 error	(eoc)	H^1 error	(eoc)
1.60000	4.36707	—	$1.44124 \cdot 10^{+1}$	—
$9.82540 \cdot 10^{-1}$	1.57587	2.090335	$1.07070 \cdot 10^{+1}$	0.609476
$5.41335 \cdot 10^{-1}$	$5.66160 \cdot 10^{-1}$	1.717298	6.49553	0.838418
$2.77856 \cdot 10^{-1}$	$1.66560 \cdot 10^{-1}$	1.834542	3.48553	0.933365
$1.39856 \cdot 10^{-1}$	$4.37702 \cdot 10^{-2}$	1.946719	1.77833	0.980270
$7.00447 \cdot 10^{-2}$	$1.10891 \cdot 10^{-2}$	1.985583	$8.93811 \cdot 10^{-1}$	0.994875
$3.50370 \cdot 10^{-2}$	$2.78139 \cdot 10^{-3}$	1.996469	$4.47462 \cdot 10^{-1}$	0.998807
$1.75203 \cdot 10^{-2}$	$6.95862 \cdot 10^{-4}$	1.999229	$2.23790 \cdot 10^{-1}$	0.999768

h	elements	degrees of freedom	solver iter.
1.60000	72	36	18
$9.82540 \cdot 10^{-1}$	288	144	22
$5.41335 \cdot 10^{-1}$	1 152	576	46
$2.77856 \cdot 10^{-1}$	4 608	2 304	92
$1.39856 \cdot 10^{-1}$	18 432	9 216	185
$7.00447 \cdot 10^{-2}$	73 728	36 864	371
$3.50370 \cdot 10^{-2}$	294 912	147 456	741
$1.75203 \cdot 10^{-2}$	1 179 648	589 824	1 476

(b) Error table with experimental orders of convergence

Table A.2: Results for surface finite element method on a torus.

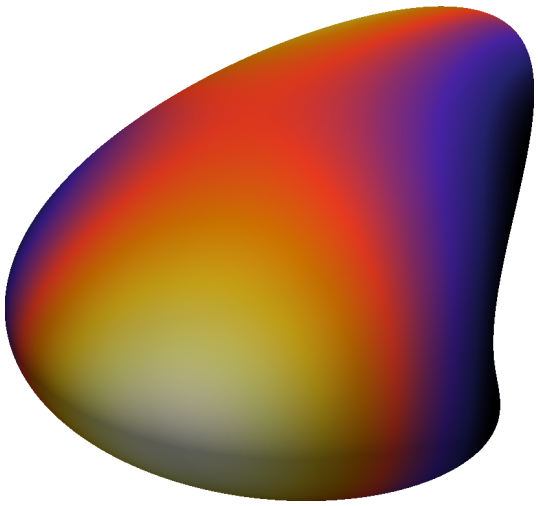

(a) Solution plotted on the Dziuk surface.

h	L^2 error	(eoc)	H^1 error	(eoc)
$8.71611 \cdot 10^{-1}$	$1.43162 \cdot 10^{-1}$	—	$8.37901 \cdot 10^{-1}$	—
$4.59489 \cdot 10^{-1}$	$3.80698 \cdot 10^{-2}$	2.068880	$5.00657 \cdot 10^{-1}$	0.804367
$2.68889 \cdot 10^{-1}$	$1.86128 \cdot 10^{-2}$	1.335480	$2.88469 \cdot 10^{-1}$	1.028960
$1.66861 \cdot 10^{-1}$	$7.69758 \cdot 10^{-3}$	1.850501	$1.57142 \cdot 10^{-1}$	1.273087
$9.01149 \cdot 10^{-2}$	$2.52516 \cdot 10^{-3}$	1.809196	$8.08140 \cdot 10^{-2}$	1.079412
$4.62581 \cdot 10^{-2}$	$7.07302 \cdot 10^{-4}$	1.908381	$4.06707 \cdot 10^{-2}$	1.029682
$2.32896 \cdot 10^{-2}$	$1.82492 \cdot 10^{-4}$	1.974195	$2.03642 \cdot 10^{-2}$	1.008015

h	elements	degrees of freedom	solver iter.
$8.71611 \cdot 10^{-1}$	92	48	19
$4.59489 \cdot 10^{-1}$	368	186	33
$2.68889 \cdot 10^{-1}$	1 472	738	57
$1.66861 \cdot 10^{-1}$	5 888	2 946	107
$9.01149 \cdot 10^{-2}$	23 552	11 778	211
$4.62581 \cdot 10^{-2}$	94 208	47 106	417
$2.32896 \cdot 10^{-2}$	376 832	188 418	828

(b) Error table with experimental orders of convergence

Table A.3: Results for surface finite element method on Γ = Dziuk surface.

Bibliography[1]

David Adalsteinsson and James A. Sethian. Transport and diffusion of material quantities on propagating interfaces via level set methods. *Journal of Computational Physics*, 185(1):271–288, 2003.

ALBERTA. An adaptive hierarchical finite element toolbox (Version 2.0.1) [Computer Software]. Available at `http://www.alberta-fem.de`, 2007.

Pierre Alliez, Laurent Rineau, Stéphane Tayeb, Jane Tournois, and Mariette Yvinec. 3D mesh generation. In *CGAL User and Reference Manual*. CGAL Editorial Board, 4.0 edition, 2012.

ALUGrid. Adaptive, Load-balanced, and Unstructured Grid Library (Git master branch, accessed 2 Dec 2012) [Computer Software]. Available at `http://aam.mathematik.uni-freiburg.de/IAM/Research/alugrid`, 2013.

Thierry Aubin. *Nonlinear analysis on manifolds, Monge-Ampère equations*. Springer-Verlag, New York, 1982.

Ruth E. Baker, Eamonn A. Gaffney, and Philip K. Maini. Partial differential equations for self-organization in cellular and developmental biology. *Nonlinearity*, 21 (11):R251–R290, 2008.

Eberhard Bänsch and Klaus Deckelnick. Optimal error estimates for the Stokes and Navier-Stokes equations with slip-boundary condition. *Mathematical Modelling and Numerical Analysis*, 33(5):923–938, 1999.

Raquel Barreira. *Numerical solution of nonlinear partial differential equations on triangulated surfaces*. DPhil thesis, University of Sussex, 2009.

[1]The URLs cited in this work were correct at the time of submission. The author makes no undertaking that the citations remain live or are accurate or appropriate.

Raquel Barreira, Charles M. Elliott, and Anotida Madzvamuse. The surface finite element method for pattern formation on evolving biological surfaces. *Journal of Mathematical Biology*, 63:1095–1119, 2011.

John W. Barrett and Charles M. Elliott. A finite element method on a fixed mesh for the Stefan problem with convection in a saturated porous medium. In K. W. Morton and M. J. Baines, editors, *Numerical Methods for Fluid Dynamics*, pages 389–409, London, 1982. Academic Press.

John W. Barrett and Charles M. Elliott. A finite-element method for solving elliptic equations with Neumann data on a curved boundary using unfitted meshes. *IMA Journal of Numerical Analysis*, 4(3):309–325, 1984.

John W. Barrett and Charles M. Elliott. Fixed mesh finite element approximations to a free boundary problem for an elliptic equation with an oblique derivative boundary condition. *Computers & Mathematics with Applications*, 11(4):335–345, 1985.

John W. Barrett and Charles M. Elliott. A practical finite element approximation of a semi-definite Neumann problem on a curved domain. *Numerische Mathematik*, 51(1):23–36, 1987a.

John W. Barrett and Charles M. Elliott. Fitted and unfitted finite-element methods for elliptic equations with smooth interfaces. *IMA Journal of Numerical Analysis*, 7(3):283–300, 1987b.

John W. Barrett and Charles M. Elliott. Finite-element approximation of elliptic equations with a Neumann or Robin condition on a curved boundary. *IMA Journal of Numerical Analysis*, 8(3):321–342, 1988.

John W. Barrett, Harald Garcke, and Robert Nürnberg. On sharp interface limits of Allen–Cahn/Cahn–Hilliard variational inequalities. *Discrete and Continuous Dynamical Systems - Series S*, 1(1):1–14, 2008a.

John W. Barrett, Harald Garcke, and Robert Nürnberg. Parametric approximation of Willmore flow and related geometric evolution equations. *SIAM Journal on Scientific Computing*, 31(1):225–253, 2008b.

John W. Barrett, Harald Garcke, and Robert Nürnberg. A variational formulation of anisotropic geometric evolution equations in higher dimensions. *Numerische Mathematik*, 109(1):1–44, 2008c.

John W. Barrett, Harald Garcke, and Robert Nürnberg. On the parametric finite element approximation of evolving hypersurfaces in $\mathbb{R}^3$. *Journal of Computational Physics*, 227(9):4281–4307, 2008d.

Peter Bastian and Markus Blatt. On the generic parallelisation of iterative solvers for the finite element method. *International Journal Computational Science and Engineering*, 4(1):56–69, 2008.

Peter Bastian and Christian Engwer. An unfitted finite element method using discontinuous Galerkin. *International Journal for Numerical Methods in Engineering*, 79(12):1557–1576, 2009.

Peter Bastian, Markus Blatt, Andreas Dedner, Christian Engwer, Robert Klöfkorn, Ralf Kornhuber, Mario Ohlberger, and Oliver Sander. A generic grid interface for parallel and adaptive scientific computing. Part II: implementation and tests in DUNE. *Computing*, 82(2–3):121–138, 2008a.

Peter Bastian, Markus Blatt, Andreas Dedner, Christian Engwer, Robert Klöfkorn, Mario Ohlberger, and Oliver Sander. A generic grid interface for parallel and adaptive scientific computing. Part I: abstract framework. *Computing*, 82(2–3): 103–119, 2008b.

John R. Baumgardner and Paul O. Frederickson. Icosahedral discretization of the two-sphere. *SIAM Journal on Numerical Analysis*, 22(6):1107–1115, 1985.

Michael Bergdorf, Ivo F. Sbalzarini, and Petros Koumoutsakos. A Lagrangian particle method for reaction-diffusion systems on deforming surfaces. *Journal of Mathematical Biology*, 61:649–663, 2010.

Marsha J. Berger, Donna A. Calhoun, Christiane Helzel, and Randall J. LeVeque. Logically rectangular finite volume methods with adaptive refinement on the sphere. *Philosophical Transactions of the Royal Society A: Mathematical, Physical and Engineering Sciences*, 367(1907):4483–4496, 2009.

Christine Bernardi. Optimal finite-element interpolation on curved domains. *SIAM Journal on Numerical Analysis*, 26(5):1212–1240, 1989.

Marcelo Bertalmío, Li-Tien Cheng, Stanley Osher, and Guillermo Sapiro. Variational problems and partial differential equations on implicit surfaces. *Journal of Computational Physics*, 174(2):759–780, 2001.

Markus Blatt and Peter Bastian. The iterative solver template library. In *Proceedings of the 8th international conference on Applied parallel computing: state of the art in scientific computing*, PARA'06, pages 666–675, Berlin / Heidelberg, 2007. Springer-Verlag.

James F. Blowey and Charles M. Elliott. The Cahn-Hilliard gradient theory for phase separation with non-smooth free energy Part I: Mathematical analysis. *European Journal of Applied Mathematics*, 2(03):233–280, 1991.

James F. Blowey and Charles M. Elliott. The Cahn-Hilliard gradient theory for phase separation with non-smooth free energy Part II: Numerical analysis. *European Journal of Applied Mathematics*, 3(02):147–179, 1992.

Michael R. Booty and Mchael Siegel. A hybrid numerical method for interfacial fluid flow with soluble surfactant. *Journal of Computational Physics*, 229(10): 3864–3883, 2010.

Dieter Bothe and Jan Prüss. Stability of equilibria for two-phase flows with soluble surfactant. *The Quarterly Journal of Mechanics and Applied Mathematics*, 63(2): 177–199, 2010.

Dieter Bothe, Jan Prüss, and Gieri Simonett. Well-posedness of a two-phase flow with soluble surfactant. In Haim Brezis, Michel Chipot, and Joachim Escher, editors, *Nonlinear Elliptic and Parabolic Problems*, volume 64 of *Progress in Nonlinear Differential Equations and Their Applications*, pages 37–61. Birkhuser Basel, 2005.

Susan C. Brenner and L. Ridgway Scott. *The Mathematical Theory of Finite Element Methods*. Springer, New York, 2002.

Martin Burger. Finite element approximation of elliptic partial differential equations on implicit surfaces. *Computing and Visualization in Science*, 12(3):87–100, 2009.

Adrian Burri, Andreas Dedner, Robert Klöfkorn, and Mario Ohlberger. An efficient implementation of an adaptive and parallel grid in DUNE. In Egon Krause, Yurii Shokin, Michael Resch, and Nina Shokina, editors, *Computational Science and High Performance Computing II*, volume 91 of *Notes on Numerical Fluid Mechanics and Multidisciplinary Design*, pages 67–82. Springer, Berlin / Heidelberg, 2006.

Gunduz Caginalp. Stefan and Hele-Shaw type models as asymptotic limits of the phase-field equations. *Physical Review A*, 39(11):5887–5896, 1989.

John W. Cahn and John E. Hilliard. Free energy of a nonuniform system. I. Interfacial free energy. *The Journal of Chemical Physics*, 28(2):258–267, 1958.

John W. Cahn, Paul C. Fife, and Oliver Penrose. A phase-field model for diffusion-induced grain-boundary motion. *Acta Materialia*, 45(10):4397–4413, 1997.

Donna A. Calhoun and Christiane Helzel. A finite volume method for solving parabolic equations on logically Cartesian curved surface meshes. *SIAM Journal on Scientific Computing*, 31(6):4066–4099, 2010.

Mark A. J. Chaplain, Mahadevan Ganesh, and Ivan G. Graham. Spatio-temporal pattern formation on spherical surfaces: numerical simulation and application to solid tumour growth. *Journal of Mathematical Biology*, 42(5):387–423, 2001.

A.Y. Chernyshenko and M.A. Olshanskii. Non-degenerate Eulerian finite element method for solving PDEs on surfaces. *Russian Journal of Numerical Analysis and Mathematical Modelling*, 28(2):101–124, 2013.

Philippe G. Ciarlet. *The finite element method for elliptic problems*. North-Holland Pub. Co., Amsterdam, 1978.

Philippe G. Ciarlet and Pierre-Arnaud Raviart. Interpolation theory over curved elements, with applications to finite element methods. *Computer Methods in Applied Mechanics and Engineering*, 1(2):217–249, 1972a.

Philippe G. Ciarlet and Pierre-Arnaud Raviart. The combined effect of curved boundaries and numerical integration in isoparametric finite element methods. In A. K. Aziz, editor, *The Mathematical Foundation of Finite Element Method with Applications to Partial Differential Equations*. Academic Press, New York, 1972b.

Ulrich Clarenz, Udo Diewald, Gerhard Dziuk, and Martin Rumpf. A finite element method for surface restoration with smooth boundary conditions. *Computer Aided Geometric Design*, 21(5):427–455, 2004.

Edmund J. Crampin, Eamonn A. Gaffney, and Philip K. Maini. Reaction and diffusion on growing domains: Scenarios for robust pattern formation. *Bulletin of Mathematical Biology*, 61(6):1093–1120, 1999.

Klaus Deckelnick, Charles M. Elliott, and Vanessa Styles. Numerical diffusion-induced grain boundary motion. *Interfaces and Free Boundaries*, 3(4):393–414, 2001.

Klaus Deckelnick, Gerhard Dziuk, and Charles M. Elliott. Computation of geometric partial differential equations and mean curvature flow. *Acta Numerica*, 14:139–232, 2005.

Klaus Deckelnick, Andreas Günther, and Michael Hinze. Finite element approximation of Dirichlet boundary control for elliptic PDEs on two- and three-dimensional curved domains. *SIAM Journal on Control and Optimization*, 48(4):2798–2819, 2009.

Klaus Deckelnick, Gerhard Dziuk, Charles M. Elliott, and Claus-Justus Heine. An h-narrow band finite-element method for elliptic equations on implicit surfaces. *IMA Journal of Numerical Analysis*, 30(2):351–376, 2010.

Andreas Dedner, Robert Klöfkorn, Martin Nolte, and Mario Ohlberger. A generic interface for parallel and adaptive discretization schemes: abstraction principles and the Dune-Fem module. *Computing*, 90(3-4):165–196, 2010.

Andreas Dedner, Pravin Madhavan, and Björn Stinner. Analysis of the discontinuous Galerkin method for elliptic problems on surfaces. *IMA Journal of Numerical Analysis*, [online] Available at `http://dx.doi.org/10.1093/imanum/drs033`, 2013.

Raymond Defay and Ilya Prigogine. *Surface tension and adsorption*. Wiley, New York, 1966.

Alan Demlow. Higher-order finite element methods and pointwise error estimates for elliptic problems on surface. *SIAM Journal on Numerical Analysis*, 47(2): 805–827, 2009.

Alan Demlow and Gerhard Dziuk. An adaptive finite element method for the Laplace-Beltrami operator on implicitly defined surfaces. *SIAM Journal on Numerical Analysis*, 45(1):421–442, 2007.

Alan Demlow and Maxim A. Olshanskii. An adaptive surface finite element method based on volume meshes. *SIAM Journal on Numerical Analysis*, 50(3):1624–1647, 2012.

Distributed and Unified Numerics Environment. (Version 2.1) [Computer Software]. Available at `http://www.dune-project.org`, 2012.

Qiang Du, Lili Ju, and Li Tian. Finite element approximation of the Cahn-Hilliard equation on surfaces. *Computer Methods in Applied Mechanics and Engineering*, 200(29–32):2458–2470, 2011.

François Dubois. Discrete vector potential representation of a divergence-free vector field in three-dimensional domains: Numerical analysis of a model problem. *SIAM Journal on Numerical Analysis*, 27(5):1103–1141, 1990.

DUNE-FEM. (Git master branch, accessed 18 Feb 2013) [Computer Software]. Available at `http://dune.mathematik.uni-freiburg.de`, 2013.

Gerhard Dziuk. Finite elements for the Beltrami operator on arbitrary surfaces. In Stefan Hildebrandt and Rolf Leis, editors, *Partial Differential Equations and Calculus of Variations*, volume 1357 of *Lecture Notes in Mathematics*, pages 142–155. Springer-Verlag, Berlin, 1988.

Gerhard Dziuk and Ulrich Clarenz. Numerical methods for conformally parametrized surfaces. Talk at CPDw04 – Interphase 2003: Numerical Methods for Free Boundary Problems, Newton Institute, Cambridge, 2003.

Gerhard Dziuk and Charles M. Elliott. Finite elements on evolving surfaces. *IMA Journal of Numerical Analysis*, 27(2):262–292, 2007a.

Gerhard Dziuk and Charles M. Elliott. Surface finite elements for parabolic equations. *Journal of Computational Mathemtatics*, 25(4):385–407, 2007b.

Gerhard Dziuk and Charles M. Elliott. Eulerian finite element method for parabolic PDEs on implicit surfaces. *Interfaces and Free Boundaries*, 10(1):119–138, 2008.

Gerhard Dziuk and Charles M. Elliott. An Eulerian approach to transport and diffusion on evolving implicit surfaces. *Computing and Visualization in Science*, 13(1):17–28, 2010.

Gerhard Dziuk and Charles M. Elliott. A fully discrete evolving surface finite element method. *SIAM Journal on Numerical Analysis*, 50(5):2677–2694, 2012.

Gerhard Dziuk and Charles M. Elliott. L^2-estimates for the evolving surface finite element method. *Mathematics of Computation*, 82:1–24, 2013a.

Gerhard Dziuk and Charles M. Elliott. Finite element methods for surface PDEs. *Acta Numerica*, 22:289–396, 2013b.

Gerhard Dziuk, Dietmar Kröner, and Thomas Müller. Scalar conservation laws on moving hypersurfaces. Technical report, Freiburg, 2012a.

Gerhard Dziuk, Christian Lubich, and Dhia Mansor. Runga-Kutta time discretization of parabolic differential equations on evolving surfaces. *IMA Journal of Numerical Analysis*, 32(2):394–416, 2012b.

Carston Eilks and Charles M. Elliott. Numerical simulation of dealloying by surface dissolution via the evolving surface finite element method. *Journal of Computational Physics*, 227(23):9727–9741, 2008.

Charles M. Elliott. The Cahn-Hilliard model for the kinetics of phase separation. In José F. Rodrigues, editor, *Mathematical Models for Phase Change Problems*, volume 88 of *International Series of Numerical Mathematics*, pages 35–73. Birkhäuser, Basel, 1989.

Charles M. Elliott and Donald. A. French. Numerical studies of the Cahn-Hilliard Equation for phase separation. *IMA Journal of Applied Mathematics*, 38(2):97–128, 1987.

Charles M. Elliott and Donald. A. French. A non-conforming finite element method for the two dimensional Cahn-Hilliard equation. *SIAM Journal on Numerical Analysis*, 26(4):884–903, 1989.

Charles M. Elliott and Thomas Ranner. Finite element analysis for a coupled bulk-surface partial differential equation. *IMA Journal of Numerical Analysis*, 33(2): 377–402, 2013.

Charles M. Elliott and Zheng Songmu. On the Cahn-Hilliard equation. *Archive for Rational Mechanics and Analysis*, 96(4):339–357, 1986.

Charles M. Elliott and Björn Stinner. Modeling and computation of two phase geometric biomembranes using surface finite elements. *Journal of Computational Physics*, 229(18):6585–6612, 2010a.

Charles M. Elliott and Björn Stinner. A surface phase field model for two-phase biological membranes. *SIAM Journal on Applied Mathematics*, 70(8):2904–2928, 2010b.

Charles M. Elliott and Björn Stinner. Computation of two-phase biomembranes with phase dependent material parameters using surface finite elements. *Communications in Computational Physics*, 13:325–360, 2013.

Charles M. Elliott and Vanessa Styles. An ALE ESFEM for solving PDEs on evolving surfaces. *Milan Journal of Mathematics*, 80(2):469–501, 2012.

Charles M. Elliott, Donald. A. French, and Fabio A. Milner. A second order splitting method for the Cahn-Hilliard equation. *Numerische Mathematik*, 54(5):575–590, 1989.

Charles M. Elliott, Björn Stinner, Vanessa Styles, and Richard Welford. Numerical computation of advection and diffusion on evolving diffuse interfaces. *IMA Journal of Numerical Analysis*, 31(3):786–812, 2011.

Charles M. Elliott, Björn Stinner, and Chandrasekhar Venkataraman. Modelling cell motility and chemotaxis with evolving surface finite elements. *Journal of The Royal Society Interface*, 9(76):3027–3044, 2012.

Christian Engwer and Felix Heimann. DUNE-UDG: A cut-cell framework for unfitted discontinuous Galerkin methods. In Andreas Dedner, Bernd Flemisch, and Robert Klöfkorn, editors, *Advances in DUNE*, pages 89–100. Springer, Berlin / Heidelberg, 2012.

Jonah Erlebacher, Michael J. Aziz, Alain Karma, Nikolay Dimitrov, and Karl Sieradzki. Evolution of nanoporosity in delloying. *Nature*, 410:450–453, 2001.

Lawrence C. Evans. *Partial differential equations*. American Mathematical Society, Providence, R.I., 1998.

Lawrence C. Evans and Ronald F. Gariepy. *Measure theory and fine properties of functions*. CRC Press, Inc., Boca Raton, Florida, 1992.

Sashikumaar Ganesan and Lutz Tobiska. A coupled arbitrary Lagrangian-Eulerian and Lagrangian method for computation of free surface flows with insoluble surfactants. *Journal of Computational Physics*, 228(8):2859–2873, 2009.

Sashikumaar Ganesan, Andreas Hahn, Kristin Held, and Lutz Tobiska. An accurate numerical method for computation of two-phase flows with surfactants. In J. Eberharsteiner et. al, editor, *European congress on computational methods in applied sciences and engineering (ECCOMAS)*, 2012.

Harald Garcke, Kei Fong Lam, and Björn Stinner. Diffuse interface modelling of soluble surfactants in two-phase flow. *arXiv preprint arXiv:1303.2559*, 2013.

Alfred Gierer and Hans Meinhardt. A theory of biological pattern formation. *Kybernetik*, 12(1):30–39, 1972.

David Gilbarg and Neil S. Trudinger. *Elliptic partial differential equations of second order*. Springer, Berlin, 2001.

Jon Goerke. Pulmonary surfactant: functions and molecular composition. *Biochimica et Biophysica Acta (BBA) – Molecular Basis of Disease*, 1408(2–3):79–89, 1998.

Harold P. Grace. Dispersion phenomena in high viscosity immiscible fluid systems and application of static mixers as dispersion devices in such systems. *Chemical Engineering Communications*, 14(3–6):225–277, 1982.

John B. Greer. An improvement of a recent Eulerian method for solving PDEs on general geometries. *Journal of Scientific Computing*, 29(3):321–352, 2006.

John B. Greer, Andrea L. Bertozzi, and Guillermo Sapiro. Fourth order partial differential equations on general geometries. *Journal of Computational Physics*, 216(1):216–246, 2006.

Pierre Grisvard. *Elliptic Problems in Nonsmooth Domains*. Cambridge University Press, Cambridge, 2011.

Anita Hansbo and Peter Hansbo. An unfitted finite element method, based on Nitsche's method, for elliptic interface problems. *Computer Methods in Applied Mechanics and Engineering*, 191(47–48):5537–5552, 2002.

Philip Hartman. *Ordinary differential equations*. SIAM, Philadelphia, PA, 2002.

Emmanuel Hebey. *Nonlinear analysis on manifolds: Soblev spaces and inequalities*. Courant Institute of Mathematical Sciences, New York, NY, 2000.

Claus-Justus Heine. Isoparametric finite element approximation of curvature on hypersurfaces. Technical report, Freiburg, 2005.

Amy Henderson. ParaView: Parallel visualization application (Version 3.14.1-1ubuntu1) [Computer Software]. Available at `http://www.paraview.org`, 2012.

John D. Hunter. Matplotlib: A 2D graphics environment. *Computing In Science & Engineering*, 9(3):90–95, 2007.

John D. Hunter. matplotlib (Version 1.1.1 rc1+git20120423-0ubuntu1) [Computer Software]. Available at `http://matplotlib.org`, 2012.

Ilse Ipsen and Rizwana Rehman. Perturbation bounds for determinants and characteristic polynomials. *SIAM Journal on Matrix Analysis and Applications*, 30 (2):762–776, 2008.

Ashley J. James and John S. Lowengrub. A surfactant-conserving volume-of-fluid method for interfacial flows with insoluble surfactant. *Journal of Computational Physics*, 201(2):685–722, 2004.

Lili Ju and Qiang Du. A finite volume method on general surfaces and its error estimates. *Journal of Mathematical Analysis and Applications*, 352(2):645–668, 2009.

Lili Ju, Li Tian, and Desheng Wang. A posteriori error estimates for finite volume approximations of elliptic equations on general surfaces. *Computer Methods in Applied Mechanics and Engineering*, 198(5–8):716–726, 2009.

David Kay, Vanessa Styles, and Richard Welford. Finite element approximation of a Cahn-Hilliard-Navier-Stokes system. *Interfaces and Free Boundaries*, 10(1): 15–43, 2008.

Yong-Il Kwon and Jeffrey J. Derby. Modeling the coupled effects of interfacial and bulk phenomena during solution crystal growth. *Journal of Crystal Growth*, 230 (1–2):328–335, 2001.

Olga A. Ladyzhenskaia and Nina N. Uraltseva. *Linear and quasilinear elliptic equations. Translated by Scripta Technica. Translation editor: Leon Ehrenpreis*. Academic Press, New York, 1968.

Ming-Chih Lai, Yu-Hau Tseng, and Huaxiong Huang. An immersed boundary method for interfacial flows with insoluble surfactant. *Journal of Computational Physics*, 227(15):7279–7293, 2008.

Julien Lefevre and Jean-Francois Mangin. A reaction-diffusion model of the human brain development. In *Biomedical Imaging: From Nano to Macro, 2010 IEEE International Symposium on*, pages 77 –80, 2010.

Michel Lenoir. Optimal isoparametric finite elements and error estimates for domains involving curved boundaries. *SIAM Journal on Numerical Analysis*, 23(3): 562–580, 1986.

Y. Li and J. Kim. A comparison study of phase-field models for an immiscible binary mixture with surfactant. *The European Physical Journal B*, 85(10):1–9, 2012.

John S. Lowengrub, Jian-Jun Xu, and Axel Voigt. Surface phase separation and flow in a simple model of multicomponent drops and vesicles. *FDMP: Fluid Dynamics & Materials Processing*, 3(1):1–20, 2007.

Christian Lubich and Dhia Mansour. Variational discretization of linear wave equations on evolving surfaces. Technical report, Tubingen, 2012.

Christian Lubich, Dhia Mansour, and Chandrasekhar Venkataraman. Backward difference time discretization of parabolic differential equations on evolving surfaces. *IMA Journal of Numerical Analysis*, [online] Available at `http://dx.doi.org/10.1093/imanum/drs044`, 2013.

Colin B. Macdonald and Steven J. Ruuth. Level set equations on surfaces via the closest point method. *Journal of Scientific Computing*, 35(2–3):219–240, 2008.

Colin B. Macdonald and Steven J. Ruuth. The implicit closest point method for the numerical solution of partial differential equations on surfaces. *SIAM Journal on Scientific Computing*, 31(6):4330–4350, 2009.

Colin B. Macdonald, Jeremy Brandman, and Steven J. Ruuth. Solving eigenvalue problems on curved surfaces using the closest point method. *Journal of Computational Physics*, 230(22):7944–7956, 2011.

Davide Marenduzzo and Enzo Orlandini. Phase separation dynamics on curved surfaces. *Soft Matter*, 9(4):1178–1187, 2013.

Thomas März and Colin B. Macdonald. Calculus on surfaces with general closest point functions. *SIAM Journal on Numerical Analysis*, 50(6):3303–3328, 2012.

Emile S. Medvedev and Alexei A. Stuchebrukhov. Proton diffusion along biological membranes. *Journal of Physics: Condensed Matter*, 23(23):234103, 2011.

Moritz Mercker, Mariya Ptashnyk, Jens Kühnle, Dirk Hartmann, Matthias Weiss, and Willi Jäger. A multiscale approach to curvature modulated sorting in biological membranes. *Journal of Theoretical Biology*, 301(0):67–82, 2012.

Norman R. Morrow and Geoffrey Mason. Recovery of oil by spontaneous imbibition. *Current Opinion in Colloid & Interface Science*, 6(4):321–337, 2001.

Jean-Claude Nedelec. Curved finite element methods for the solution of singular integral equations on surfaces in $\mathbb{R}^3$. *Computer Methods in Applied Mechanics and Engineering*, 8(1):61–80, 1976.

Matthew P. Neilson, John A. Mackenzie, Steven D. Webb, and Robert H. Insall. Modeling cell movement and chemotaxis using pseduopod-based feedback. *SIAM Journal on Scientific Computing*, 33(3):1035–1057, 2011.

Igor L. Novak, Fei Gao, Yung-Sze Choi, Diana Resasco, James C. Schaff, and Boris M. Slepchenko. Diffusion on a curved surface coupled to diffusion in the

volume: Application to cell biology. *Journal of Computational Physics*, 226(2): 1271–1290, 2007.

L. A. Oganesyan and L. A. Rukhovets. *Variational-Difference Methods for Solving Elliptic Equations (Russian)*. Publ. House of Armenian Acad. Sci., Erevan, 1979.

Maxim A. Olshanskii and Arnold Reusken. A finite element method for surface PDEs: Matrix properties. *Numerische Mathematik*, 114(3):491–520, 2010.

Maxim A. Olshanskii, Arnold Reusken, and Jörg Grande. A finite element method for elliptic equations on surfaces. *SIAM Journal on Numerical Analysis*, 47(5): 3339–3358, 2009.

Maxim A. Olshanskii, Arnold Reusken, and Xiamin Xu. On surface meshes induced by level set functions. Technical report, IGMP report 347, RWTH Aachen, 2012.

Maxim A. Olshanskii, Arnold Reusken, and Xiamin Xu. A stabilized finite element method for advection-diffusion equations on surfaces. *arXiv preprint arXiv:1301.3741*, 2013.

Stanley Osher and Ron Fedkiw. *Level set methods and dynamic implicit surfaces*, volume 153. Springer, New York, 2002.

Charles S. Peskin. Flow patterns around heart valves: A numerical method. *Journal of Computational Physics*, 10(2):252–271, 1972.

Ramón G. Plaza, Faustino Sánchez-Garduño, Pablo Padilla, Rafael A. Barrio, and Philip K. Maini. The effect of growth and curvature on pattern formation. *Journal of Dynamics and Differential Equations*, 16(4):1093–1121, 2004.

Andreas Rätz and Matthias Röger. Turing instabilities in a mathematical model for signaling networks. *Journal of Mathematical Biology*, 65(6–7):1215–1244, 2012.

Andreas Rätz and Axel Voigt. PDE's on surfaces—a diffuse interface approach. *Communications in Mathematical Sciences*, 4(3):575–590, 2006.

Laurent Rineau and Mariette Yvinec. 3D Surface Mesh Generation. In *CGAL User and Reference Manual*. CGAL Editorial Board, 4.2 edition, 2013.

James C. Robinson. *Infinite-Dimensional Dynamical Systems*. Cambridge University Press, Cambridge, 2001.

Steven J. Ruuth and Barry Merriman. A simple embedding method for solving partial differential equations on surfaces. *Journal of Computational Physics*, 227 (3):1943–1961, 2008.

Karl H. Schellbach. Probleme der Variationsrechnung. *Journal für die reine und angewandte Mathematik*, 1851(41):293–363, 1851.

Alfred Schmidt, Kunibert G. Siebert, Daniel Köster, and Claus-Justus Heine. *Design of adaptive finite element software: The finite element toolbox ALBERTA*. Springer-Verlag, Berlin / Heidelberg, 2005.

Jürgen Schnakenberg. Simple chemical reaction systems with limit cycle behaviour. *Journal of Theoretical Biology*, 81(3):389–400, 1979.

Oliver Schoenborn and Rashmi C. Desai. Kinetics of Phase Ordering on Curved Surfaces. *Journal of Statistical Physics*, 95(5–6):949–979, 1999.

Peter Schwartz, David Adalsteinsson, Phillip Colella, Adam Paul Arkin, and Matthew Onsum. Numerical computation of diffusion on a surface. *Proceedings of the National Acadamy of Sciences, USA*, 102(32):11151–11156, 2005.

L. Ridgway Scott. *Finite element techniques for curved boundaries*. PhD thesis, Massachusetts Institute of Technology, Cambridge, MA, 1973.

James A. Sethian. *Level set methods and fast marching methods*. Cambridge University Press, Cambridge, 1999.

Jonathan R. Shewchuk. Triangle: Engineering a 2D quality mesh generator and Delaunay triangulator. In Ming C. Lin and Dinesh Manocha, editors, *Applied Computational Geometry Towards Geometric Engineering*, volume 1148 of *Lecture Notes in Computer Science*, pages 203–222. Springer, Berlin / Heidelberg, 1996.

Jonathan R. Shewchuk. Triangle: A two-dimensional quality mesh generator and Delaunay triangulator (Version 1.6). Available at `http://www.cs.cmu.edu/~quake/triangle.html`, 2005.

Hang Si. Tetgen: A quality tetrahedral nesh generator and 3D Delaunay triangulator (Version 1.4.1) [Computer software]. Available at `http://tetgen.org`, 2006.

Gilbert Strang and George J. Fix. *An analysis of the finite element method*. Wellesley-Cambridge Press, Wellesley, MA, second edition, 2008.

Knut Erik Teigen, Xiangrong Li, John S. Lowengrub, Fan Wang, and Axel Voigt. A diffuse-interface approach for modeling transport, diffusion and adsorption/desorption of material quantities on a deformable interface. *Communications in mathematical sciences*, 7(4):1009–1037, 2009.

Vidar Thomée. *Galerkin finite element methods for parabolic problems*. Springer, 2006.

Alan M. Turing. The chemical basis of morphogenesis. *Philosophical Transactions of the Royal Society of London, Series B: Biological Sciences*, 237(641):37–72, 1952.

Carmen Varea, Jose L. Aragón, and Rafael A. Barrio. Turing patterns on a sphere. *Physical Review E*, 60(4):4588–4592, 1999.

Morten Vierling. Control-constrained parabolic optimal control problems on evolving surfaces - theory and variational discretization. *arXiv preprint arXiv:1106.0622v4*, 2011.

Joseph Wloka. *Partial Differential Equations*. Cambridge University Press, Cambridge, 1987.

Jian-Jun Xu and Hong-Kai Zhao. An Eulerian formulation for solving partial differential equations along a moving interface. *Journal of Scientific Computing*, 19 (1–3):573–594, 2003.

Jian-Jun Xu, Zhilin Li, John S. Lowengrub, and Hongkai Zhao. A level-set method for interfacial flows with surfactant. *Journal of Computational Physics*, 212(2): 590–616, 2006.

Jian-Jun Xu, Yin Yang, and John S. Lowengrub. A level-set continuum method for two-phase flows with insoluble surfactant. *Journal of Computational Physics*, 231 (17):5897–5909, 2012.

Milos Zlamal. Curved elements in the finite element method. I. *SIAM Journal on Numerical Analysis*, 10(1):229–240, 1973.

Milos Zlamal. Curved elements in the finite element method. II. *SIAM Journal on Numerical Analysis*, 11(2):347–362, 1974.